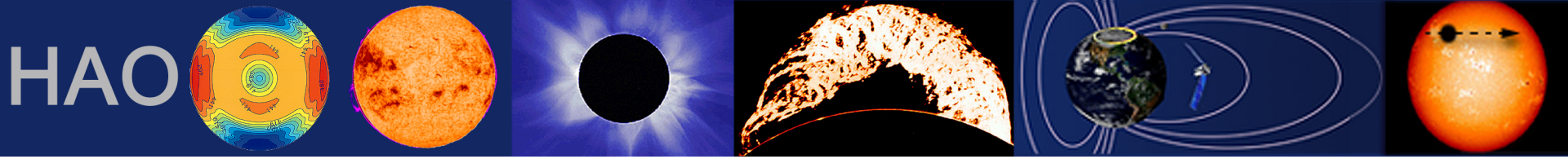

Solar Polarization Measurements: Instruments and Techniques

Bruce W. Lites
High Altitude Observatory
National Center for Atmospheric Research

Solar Spectropolarimetry and Diagnostic Techniques
Estes Park, Colorado, USA
24 - 28 September 2018

A copy of the powerpoint files for the course will be placed online at:

http://download.hao.ucar.edu/pub/lites/estespark/instrumentation_spectropolHAO2018.pptx/

You will also find there a PDF copy.

Outline

I. Motivation for Measurement of Solar Polarization
II. Describing the Polarization of Light
III. Modification of Polarization by Optical Devices
IV. Requirements for Solar Polarization Measurements
V. Approaches to Solar Polarimetry
VI. Spectral Discriminators
VII. Detectors for Solar Polarimetry
VIII. Polarization Calibration Techniques
IX. Modern Solar Polarimeters – Ground-based
X. Space-based Polarimeters

I. Polarized Light: Definitions and Concepts

References:

Jefferies, J., Lites, B. W., and Skumanich, A. 1989, "Transfer of Line Radiation in a Magnetic Field", *ApJ* 343, pp.920-935. The development in this section follows closely this paper, and most of the sign and notation conventions are adopted here.

Rees, D. E.,1987, "A Gentle Introduction to Polarized Radiative Transfer", in *Numerical Radiative Transfer*, ed. W. Kalkofen, Cambridge: Cambridge University Press. This work provides a good introduction to the subject and some basic insight into more advanced treatments involving scattering and non-LTE polarized transfer.

del Toro Iniesta, J. C., 2003, *Introduction to Spectropolarimetry*, Cambridge: Cambridge University Press. A recent book providing a general overview of polarized light, measurement techniques, and polarized transfer.

Born, M. and Wolf, E., 1980, *Principles of Optics*, New York: Pergamon. This is the classic text on optics and light.

Landi degl'Innocenti, E., 1992, "Magnetic Field Measurements", in *Solar Observations, Techniques and Interpretation*, ed. F. Sánchez, M. Collados, and M. Vásquez, pp. 71-143. A nice introduction to the field from the master.

Landi degl'Innocenti, E. and Landolfi, M., 2004, "Polarization in Spectral Lines", Kluwer Academic Press, Dordrecht. A new book with, I suspect, all the details you would ever want to know.

Resources:

- **"Polarization of Light: From Basics to Instruments" Presentation by N. Manset, CFHT:** http://www.cfht.hawaii.edu/~manset/PolarizationLightIntro.ppt

- **Meadowlark Optics Brochure:**

https://www.meadowlark.com/store/catalog/Polarizers_Oct_18_2012.pdf

- **Fundamentals of Optics:** F. A. Jenkins & F. E. White 1957, Mc Graw-Hill, New York

- **The Sun: An Introduction:** M. Stix, 2004 Springer, Berlin (corrected 2nd edition)

- Polarizing Optics:

http://pe2bz.philpem.me.uk/Lights/-%20Laser/Info-902-LaserCourse/c06-10/mod06_10.htm

REFERENCES

Babcock, H. W. 1961, ApJ, 133, 572

Borrero, J. M., & Kobel, P. 2013, A&A, 550, A98

Buehler, D., Lagg, A., & Solanki, S. K. 2013, A&A, 555, A33

Harvey, J. W., Branston, D., Henney, C. J., Keller, C. U., & SOLIS and GONG Teams. 2007, ApJ, 659, L177

Howard, R., & Labonte, B. J. 1981, Sol. Phys., 74, 131

Hyder, C. L. 1965, ApJ, 141, 272

Ishikawa, R., & Tsuneta, S. 2009, A&A, 495, 607

Ito, H., Tsuneta, S., Shiota, D., Tokumaru, M., & Fujiki, K. 2010, ApJ, 719, 131

Judge, P. G., Elmore, D. F., Lites, B. W., Keller, C. U., & Rimmele, T. 2004, Applied Optics, 43, 3817

Keller, C. U., Schüssler, M., Vögler, A., & Zakharov, V. 2004, ApJ, 607, L59

Kleint, L., Berdyugina, S. V., Shapiro, A. I., & Bianda, M. 2010, A&A, 524, A37

Kosugi, T., Matsuzaki, K., Sakao, T., Shimizu, T., Sone, Y., Tachikawa, S., Hashimoto, T., Minesugi, K., Ohnishi, A., Yamada, T., Tsuneta, S., Hara, H., Ichimoto, K., Suematsu, Y., Shimojo, M., Watanabe, T., Shimada, S., Davis, J. M., Hill, L. D., Owens, J. K., Title, A. M., Culhane, J. L., Harra, L. K., Doschek, G. A., & Golub, L. 2007, Sol. Phys., 243, 3

Leighton, R. B. 1964, ApJ, 140, 1547

Lites, B. W. 1987, Applied Optics, 26, 3838

—. 2002, ApJ, 573, 431

—. 2011, ApJ, 737, 52

Lites, B. W., Akin, D. L., Card, G., Cruz, T., Duncan, D. W., Edwards, C. G., Elmore, D. F., Hoffmann, C., Katsukawa, Y., Katz, N., Kubo, M., Ichimoto, K., Shimizu, T., Shine, R. A., Streander, K. V., Suematsu, A., Tarbell, T. D., Title, A. M., & Tsuneta, S. 2013, Sol. Phys., 283, 579

Lites, B. W., & Ichimoto, K. 2013, Sol. Phys., 283, 601

Lites, B. W., Kubo, M., Socas-Navarro, H., Berger, T., Frank, Z., Shine, R., Tarbell, T., Title, A., Ichimoto, K., Katsukawa, Y., Tsuneta, S., Suematsu, Y., Shimizu, T., & Nagata, S. 2008, ApJ, 672, 1237

Lites, B. W., Leka, K. D., Skumanich, A., Martinez Pillet, V., & Shimizu, T. 1996, ApJ, 460, 1019

Orozco Suárez, D., & Katsukawa, Y. 2012, ApJ, 746, 182

Sánchez Almeida, J. 2003, A&A, 411, 615

Schüssler, M., & Vögler, A. 2008, A&A, 481, L5

Shchukina, N., & Trujillo Bueno, J. 2003, in Astronomical Society of the Pacific Conference Series, Vol. 307, Solar Polarization, ed. J. Trujillo-Bueno & J. Sanchez Almeida, 336

Shimizu, T., Nagata, S., Tsuneta, S., Tarbell, T., Edwards, C., Shine, R., Hoffmann, C., Thomas, E., Sour, S., Rehse, R., Ito, O., Kashiwagi, Y., Tabata, M., Kodeki, K., Nagase, M., Matsuzaki, K., Kobayashi, K., Ichimoto, K., & Suematsu, Y. 2008, Sol. Phys., 249, 221

Shiota, D., Tsuneta, S., Shimojo, M., Sako, N., Orozco Suárez, D., & Ishikawa, R. 2012, ApJ, 753, 157

Spruit, H. C. 1976, Sol. Phys., 50, 269

Steiner, O., & Rezaei, R. 2012, in Astronomical Society of the Pacific Conference Series, Vol. 456, Fifth Hinode Science Meeting, ed. L. Golub, I. De Moortel, & T. Shimizu, 3

Steiner, O., Rezaei, R., Schlichenmaier, R., Schaffenberger, W., & Wedemeyer-Böhm, S. 2009, in Astronomical Society of the Pacific Conference Series, Vol. 415, The Second Hinode Science Meeting: Beyond Discovery-Toward Understanding, ed. B. Lites, M. Cheung, T. Magara, J. Mariska, & K. Reeves, 67

Stenflo, J. O. 2011, A&A, 529, A42

—. 2013, A&A Rev., 21, 66

Tsuneta, S., Ichimoto, K., Katsukawa, Y., Nagata, S., Otsubo, M., Shimizu, T., Suematsu, Y., Nakagiri, M., Noguchi, M., Tarbell, T., Title, A., Shine, R., Rosenberg, W., Hoffmann, C., Jurcevich, B., Kushner, G., Levay, M., Lites, B., Elmore, D., Matsushita, T., Kawaguchi, N., Saito, H., Mikami, I., Hill, L. D., & Owens, J. K. 2008, Sol. Phys., 249, 167

Ulrich, R. K., & Tran, T. 2013, ApJ, 768, 189

Waldmeier, M. 1960, ZAp, 49, 176

Wang, Y.-M., Nash, A. G., & Sheeley, Jr., N. R. 1989, ApJ, 347, 529

I. Motivation for Measurement of Solar Polarization

Why Measure Polarization from the Sun?

- **Infer magnetic fields**

- **Coronagraphs: isolate scattered coronal radiation from instrumental/terrestrial scattered light**

- **Physics of interaction of polarized light with atomic systems**

Polarization Measurements

Zeeman Effect

Inferred Vector Magnetic Field

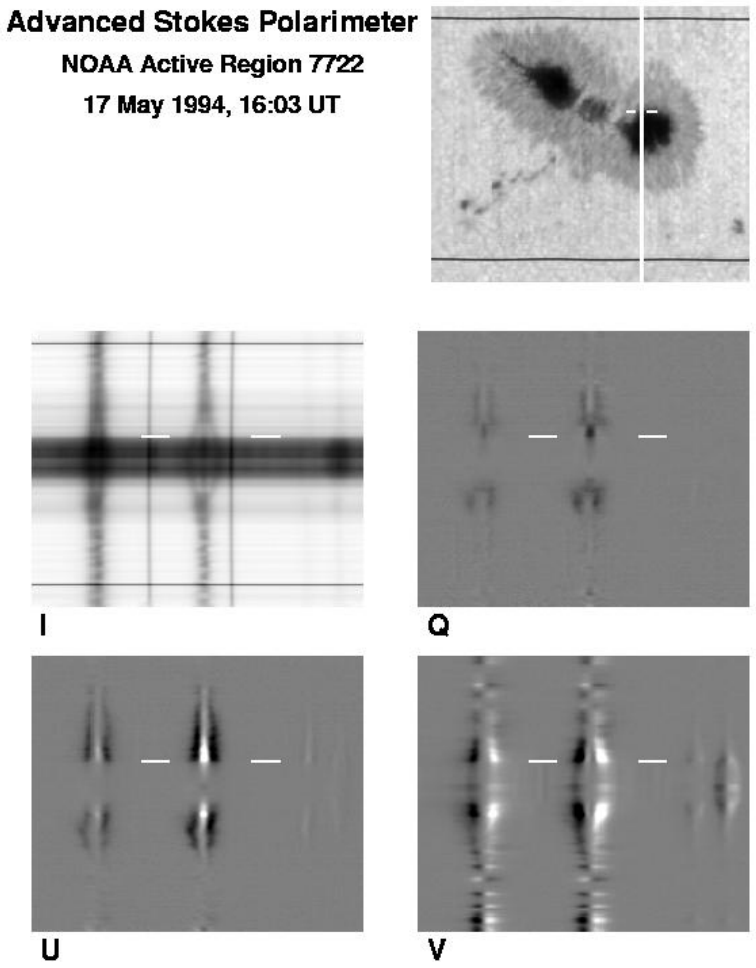

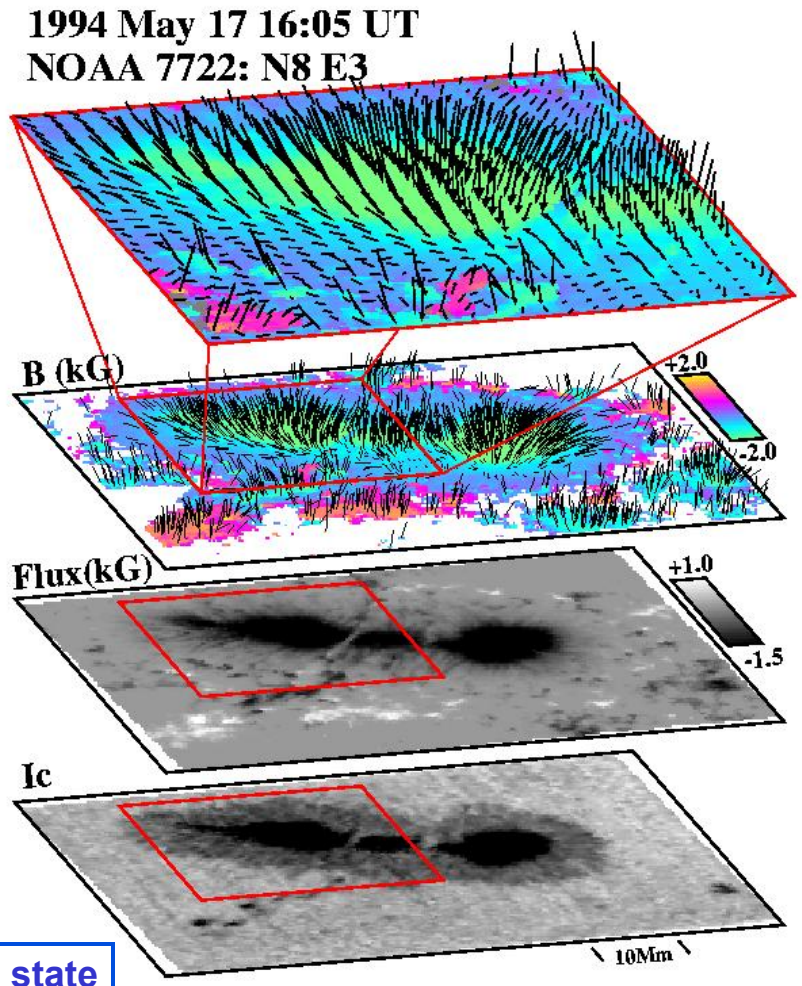

The Stokes 4-vector $\{I, Q, U, V\}^T$ describes the complete state of polarization of light

Scattering from a Classical linear oscillator

- Three orthogonal, *uncorrelated* linear oscillators
- Each oscillator reacts to oscillating electric field of single photons
- Oscillator along line-of-sight does not contribute to observed signal

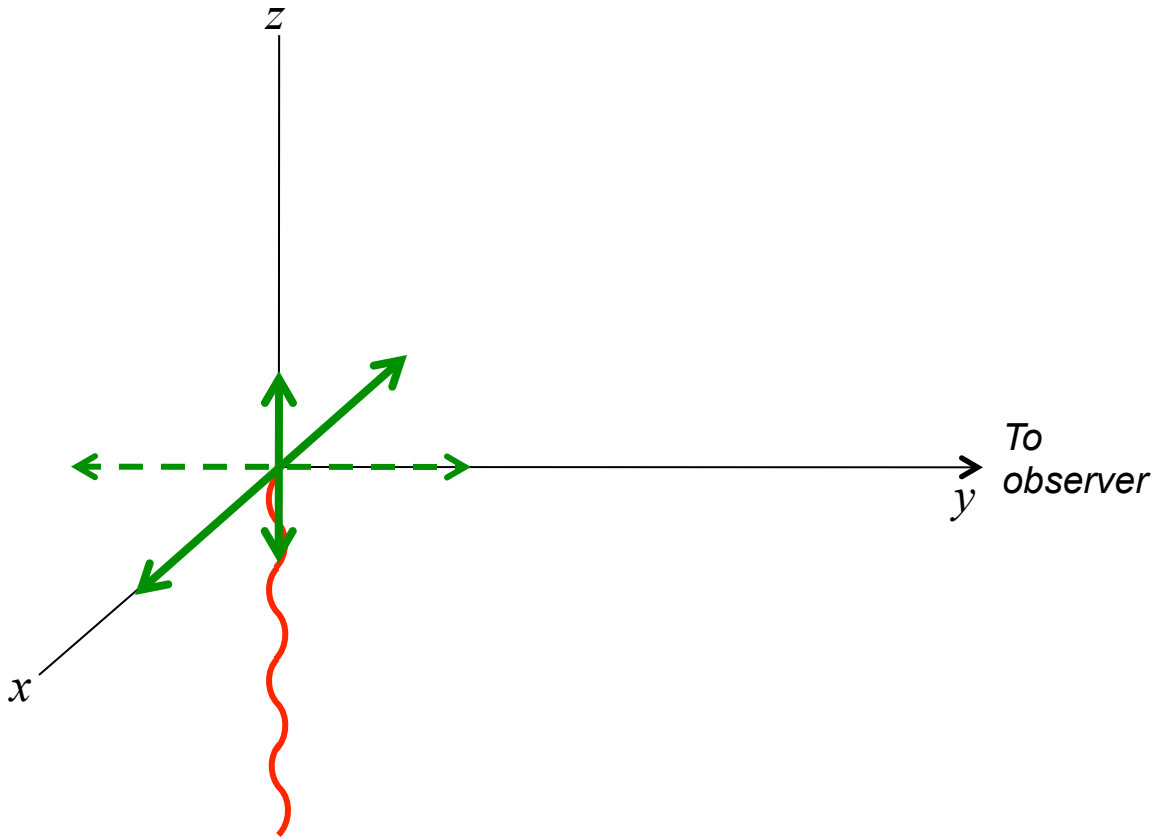

Scattering polarization: electrons scattering white light from the photosphere results in polarization that aids detection of faint coronal structure.

From Space: white light, no polarization detection

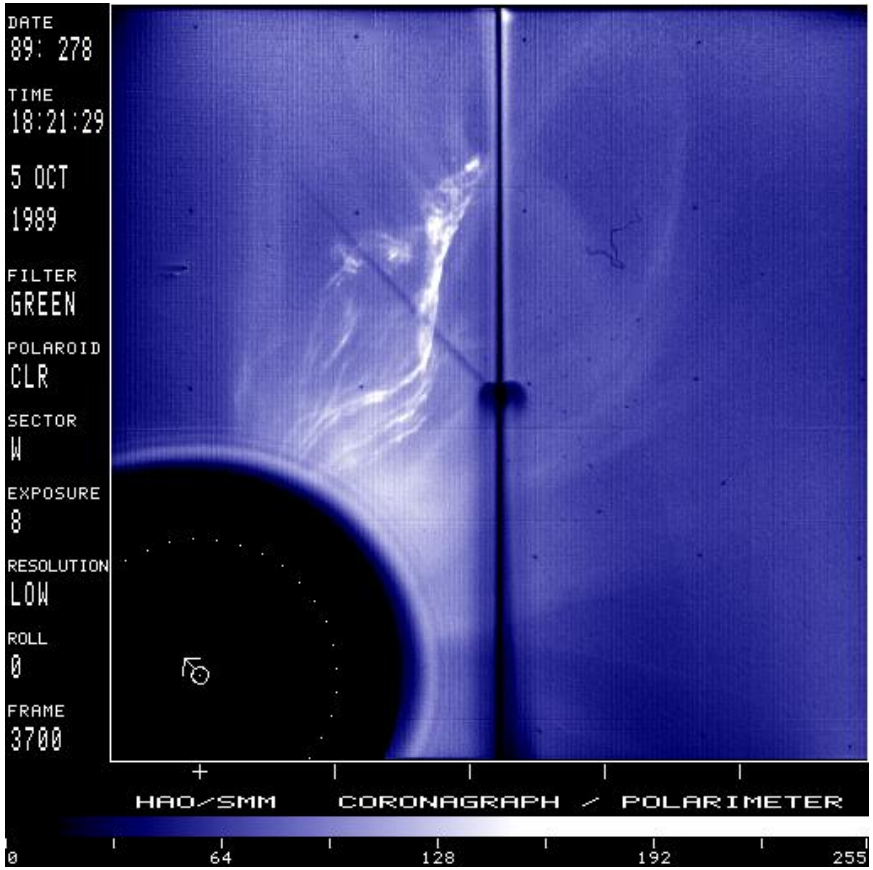

From Ground: white light,with polarization detection

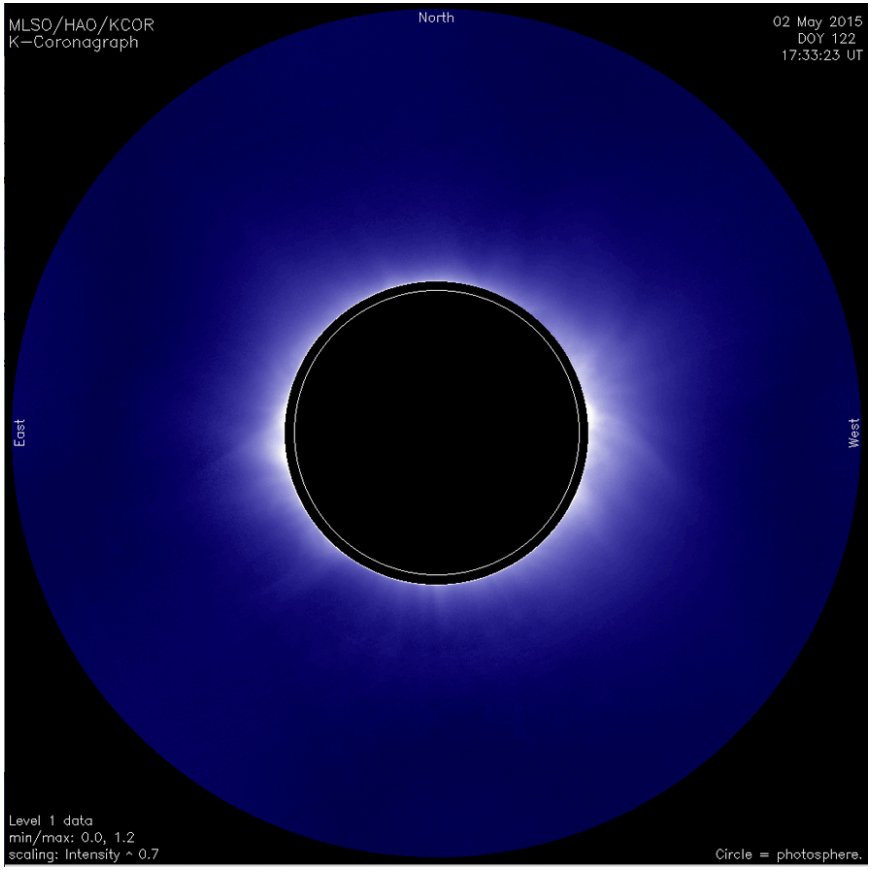

II. Describing Polarization of Radiation

Propagating Light Wave: The Electric Vector

Light is a **TRANSVERSE** electromagnetic wave

- Alternating electric and magnetic fields
- Choose to describe in terms of the E-field

Define the electromagnetic wave along the z-direction by its time-space variation of the electric vector E:

$$\mathbf{E}(z,t) = \mathbf{E}_0 e^{i(\omega t - \mathbf{k}\bullet\mathbf{z})}$$

E-field *complex* amplitudes $\tilde{a}_x, \tilde{a}_y$ in the orthogonal x- and y-directions:

x-component amplitude x-component phase

$$E_x(t) = a_x e^{i(\omega t - \varepsilon_x - kz)} \hat{x} = \tilde{a}_x \hat{x}$$

$$E_y(t) = a_y e^{i(\omega t - \varepsilon_y - kz)} \hat{y} = \tilde{a}_y \hat{y}$$

Example: electric vectors of a wave polarized at 45° to the x-axis

$$E_x(t) = a_x e^{i(\omega t - \varepsilon_x - kz)} \hat{x} = \tilde{a}_x \hat{x}$$

$$E_y(t) = a_y e^{i(\omega t - \varepsilon_y - kz)} \hat{y} = \tilde{a}_y \hat{y}$$

Equal amplitudes: $a_x = a_y$

Equal phases: $\varepsilon_x = \varepsilon_y$

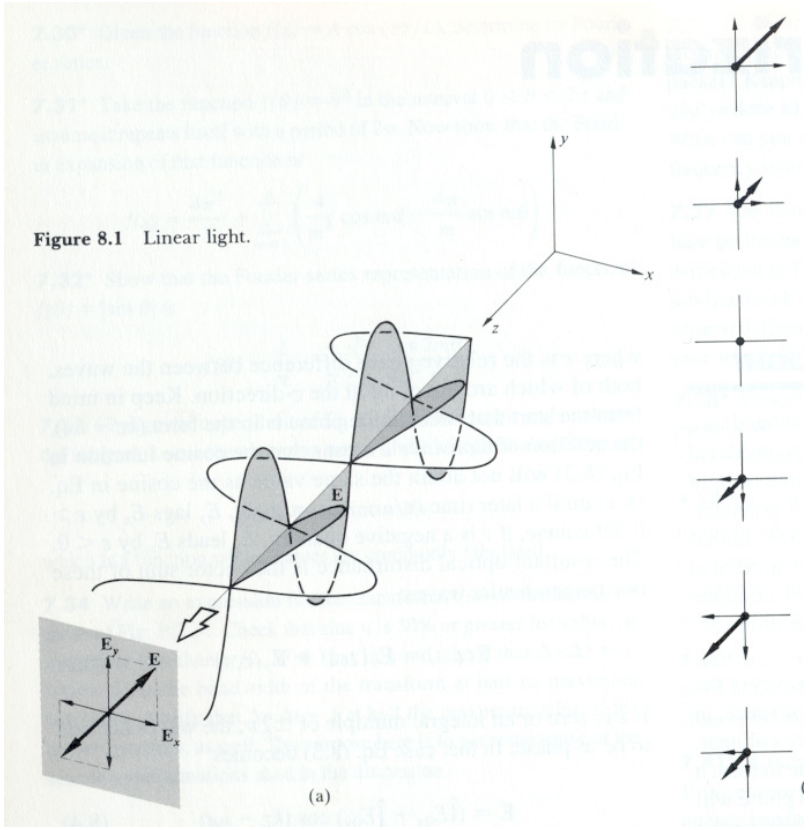

- Right-handed coordinate system
- Light propagates along z, with electric vectors in the plane x-y
- Produces *eliptically-polarized* light at the observation plane
- Observer views light from +z
- As right-handed spiral moves toward +z, the electric field vector at the observation plane rotates clockwise

$$\mathbf{E}(z,t) = \mathbf{E}_0 e^{i(\omega t - \mathbf{k}\bullet\mathbf{z})}$$

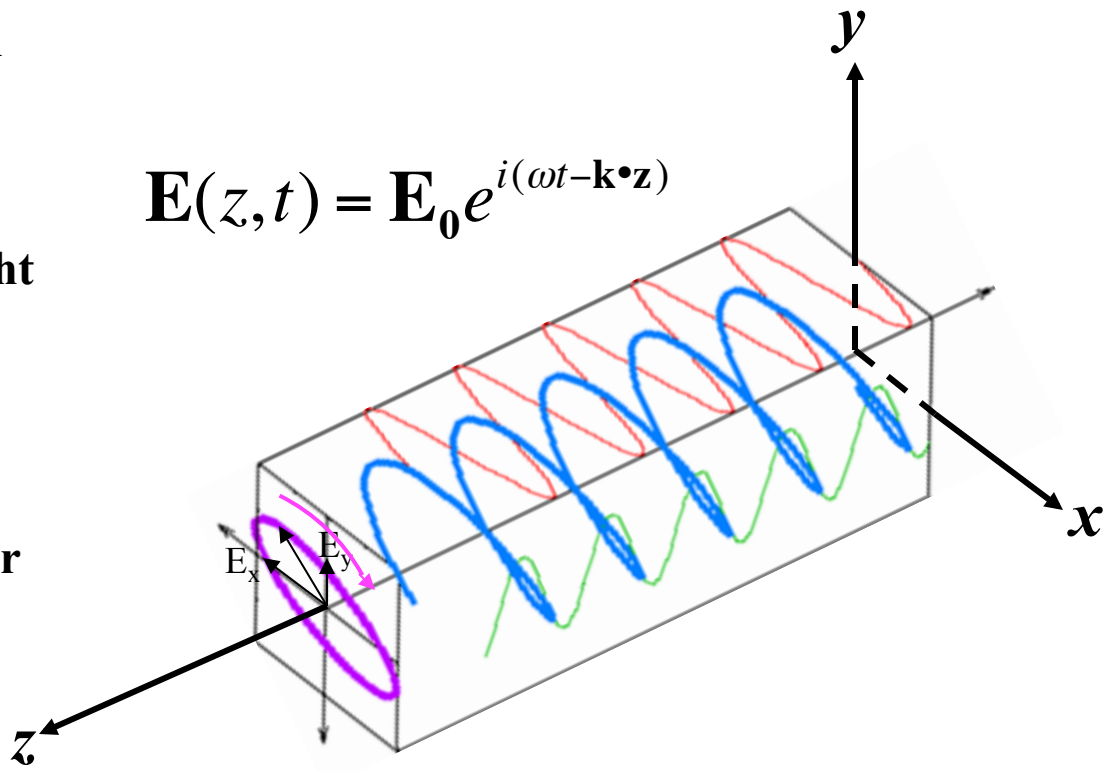

Standard Optical Convention: Right circularly polarized light is seen to have electric vector rotating clockwise as viewed by the detector (against the direction of propagation)

Electric vectors:

$$E_x(t) = a_x e^{i(\omega t - \varepsilon_x - kz)}\hat{x} = \tilde{a}_x \hat{x}$$

$$E_y(t) = a_y e^{i(\omega t - \varepsilon_y - kz)}\hat{y} = \tilde{a}_y \hat{y}$$

An animated view of a special case of elliptical polarization: Circular Polarization

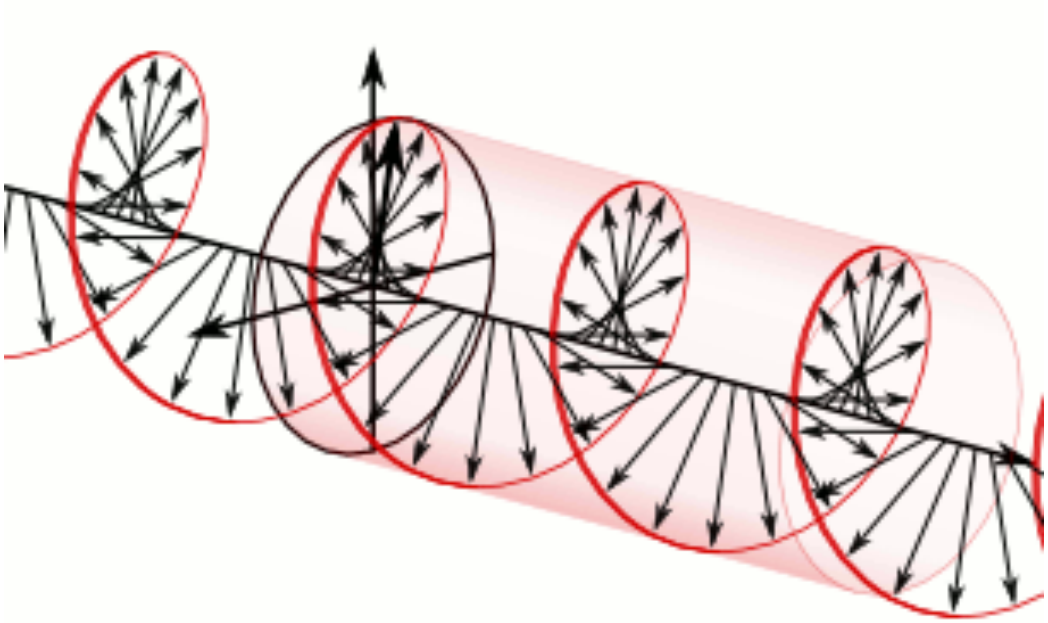

$$E_x(t) = a_x e^{i(\omega t - \varepsilon_x - kz)} \hat{x} = \tilde{a}_x \hat{x}$$

Equal amplitudes: $a_x = a_y$

$$E_y(t) = a_y e^{i(\omega t - \varepsilon_y - kz)} \hat{y} = \tilde{a}_y \hat{y}$$

Phases: $\varepsilon_x = \varepsilon_y + \pi/2$

Review of Vector Notation, Matrix Multiplication

Stokes Vector

$$\mathbf{I} = \begin{pmatrix} I \\ Q \\ U \\ V \end{pmatrix}$$

Transpose of Stokes Vector

$$\mathbf{I}^T = [IQUV]$$

Mueller Matrix **M**

$$\mathbf{M} = \begin{bmatrix} m_{11} & m_{12} & m_{13} & m_{14} \\ m_{21} & m_{22} & m_{23} & m_{24} \\ m_{31} & m_{32} & m_{33} & m_{34} \\ m_{41} & m_{42} & m_{43} & m_{44} \end{bmatrix}$$

Multiply rows of **M** by components of **I** to get elements of **I'**

$$\mathbf{I'} = \mathbf{MI} = \begin{bmatrix} m_{11} & m_{12} & m_{13} & m_{14} \\ m_{21} & m_{22} & m_{23} & m_{24} \\ m_{31} & m_{32} & m_{33} & m_{34} \\ m_{41} & m_{42} & m_{43} & m_{44} \end{bmatrix} \begin{pmatrix} I \\ Q \\ U \\ V \end{pmatrix}$$

$$U' = m_{31}I + m_{32}Q + m_{33}U + m_{34}V$$

Description of the state of polarization: the Stokes vector $\{I,Q,U,V\}^T$

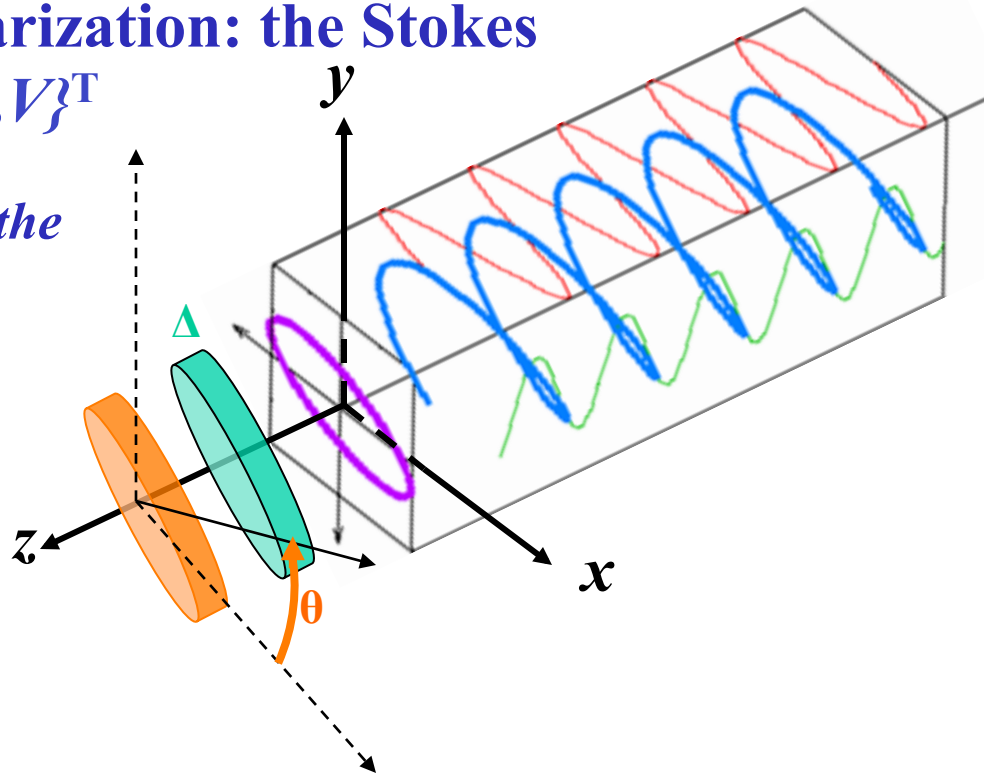

FIRST: an operational description of the Stokes vector using idealized lab measurements:

Consider a polarization device inserted in the beam that first may contain an element that retards the phase of E_y by Δ radians relative to E_x

then a linear polarizer at angle θ measured counter-clockwise from the x-axis.

The electric vector exiting this device, as measured along the θ-direction at the plane of observation becomes:

$$E_\theta(\Delta,t) = E_x(t)\cos\theta + E_y(t)e^{-i\Delta}\sin\theta$$

where E_x and E_y are the complex amplitudes prior to passing through the optics (the "compensator") in the beam

Description of the state of polarization: the Stokes vector $\{I,Q,U,V\}^T$

A "measurement" is an intensity measurement at the output of this device, averaged over a time long compared to the period of the wave:

$$I = \langle E(t,\theta,\delta)E^*(t,\theta,\delta)\rangle \qquad (< > = \text{time average})$$

(In fact, solar light is not a single wave, but a superposition of wave packets, each of which has a randomly-distributed phase)

Measurements defining the LINEAR polarization Stokes parameters Q, U:

For *Q, U* pick Δ=0 (no retarder) and four linear polarization measurements equally spaced by 45°: θ= [0, π/4, π/2, 3π/4] denoted by the symbols [↔ ⤢ ↕ ⤡].

Measurements defining the CIRCULAR polarization Stokes parameter V:

For circularly-polarized light *V*, the measurement is done with a quarter-wave linear retarder (Δ= π/2) and two positions of the polarizer (θ= [π/4, 3π/4]), the amplitude of the output linear signal being the amount of right- and left-circularly polarized light (denoted by symbols ↻ and ↺).

Description of the state of polarization: the Stokes vector $\{I,Q,U,V\}^T$

Denote the phase difference between the electric vectors along the x- and y-axes as

$$\delta = \varepsilon_x - \varepsilon_y$$

The operational definition of the Stokes parameters are then as follows:

$$I = I_{\leftrightarrow} + I_{\updownarrow} = I_{\nearrow} + I_{\searrow} = \langle a_x^2 \rangle + \langle a_y^2 \rangle$$

$$Q = I_{\leftrightarrow} - I_{\updownarrow} = \langle a_x^2 \rangle - \langle a_y^2 \rangle$$

$$U = I_{\nearrow} - I_{\searrow} = 2\langle a_x\, a_y \cos\delta \rangle$$

$$V = I_{\circlearrowright} - I_{\circlearrowleft} = 2\langle a_x\, a_y \sin\delta \rangle$$

Exercise II.1

Use the definition of the complex x- and y-components of the electric vector

$$E_x(t) = a_x e^{i(\omega t - \varepsilon_x - kz)}\hat{x} = \tilde{a}_x \hat{x}$$

$$E_y(t) = a_y e^{i(\omega t - \varepsilon_y - kz)}\hat{y} = \tilde{a}_y \hat{y}$$

and the expression for the output from the "polarization analyzer" (retarder along y-axis with retardation Δ, followed by a linear polarizer at angle θ measured counter-clockwise from the +x direction)

$$E_\theta(\Delta, t) = E_x(t)\cos\theta + E_y(t)e^{-i\Delta}\sin\theta$$

to derive the operational definition of the Stokes parameters:

$I = \langle a_x^2 \rangle + \langle a_y^2 \rangle$

$Q = \langle a_x^2 \rangle - \langle a_y^2 \rangle$

$U = 2\langle a_x\, a_y \cos\delta \rangle$

$V = 2\langle a_x\, a_y \sin\delta \rangle$

Stokes vectors for linearly polarized light

+Q

$\theta = 0$

$$\begin{pmatrix} 1 \\ 1 \\ 0 \\ 0 \end{pmatrix}$$

-Q

$\theta = \pi/2$

$$\begin{pmatrix} 1 \\ -1 \\ 0 \\ 0 \end{pmatrix}$$

+U

$\theta = \pi/4$

$$\begin{pmatrix} 1 \\ 0 \\ 1 \\ 0 \end{pmatrix}$$

-U

$\theta = -\pi/4$

$$\begin{pmatrix} 1 \\ 0 \\ -1 \\ 0 \end{pmatrix}$$

Stokes vectors for circularly-polarized light

+V

Right Circular Polarization

$$\begin{pmatrix} 1 \\ 0 \\ 0 \\ 1 \end{pmatrix}$$

-V

Left Circular Polarization

$$\begin{pmatrix} 1 \\ 0 \\ 0 \\ -1 \end{pmatrix}$$

Partially- and Totally-Polarized Light

Stokes Vector $I = \begin{pmatrix} I \\ Q \\ U \\ V \end{pmatrix}$

Totally-polarized: $I = \sqrt{Q^2 + U^2 + V^2}$

Partially-polarized: $I > \sqrt{Q^2 + U^2 + V^2}$

Un-polarized: $Q = U = V = 0$

To summarize the sign conventions:

Right-handed circular polarization
Electric vector circulates *clockwise*
***sin* δ > 0**
***V* > 0**

Left-handed circular polarization
Electric vector circulates *counterclockwise*
***sin* δ < 0**
***V* < 0**

- **The Stokes vector $\{I,Q,U,V\}^{T}$ is a complete description of the state of polarization for *intensity* (i.e., energy, *not* the electric field).**
- **It is capable of describing *partially polarized light*: $P = \left(Q^2 + U^2 + V^2\right)^{1/2} / I \leq 1$ Partial polarization arises commonly in optical systems, where optical elements may de-polarize light.**
- **It *cannot describe physical optics phenomena*, such as interference of polarized radiation, because such phenomena involve both the amplitudes and phases of the electric field vector.**
  - For such problems, one must work with the ***Jones vector*** representation of polarization of radiation, a formulation that carries all the phase information. But the **Jones vector representation can only describe fully polarized light (P=1).**
  - Since nearly all optical astronomical measurements are intensity measurements, the **Stokes representation of the polarization is preferred.**

The Coherency Matrix Formulation: Deriving the Stokes Vector using Jones Vectors

The coherency matrix formulation of the Stokes vector representation provides a more rigorous definition of the state of polarization than does the intuitive, operational definition given above. Consider the representation of the electric vector described by the Jones vector e, wherein the amplitudes and phases of two orthogonal components of the electric vector are described by a complex vector in 2-space:

$$e = \begin{pmatrix} a_x e^{-i\theta_x} \\ a_y e^{-i\theta_y} \end{pmatrix}$$

$$\delta = \theta_x - \theta_y$$

[suppressing here the time and propagation factors $e^{i(\omega t - kz)}$]

Then the coherency matrix, or polarization tensor, can be defined for the average properties (<>) of the wavefront such that it provides the amplitudes (diagonal terms) and the phase relationship (off-diagonals) for the electric vector:

$$\mathbf{J} = \langle \mathbf{e}\mathbf{e}^{+} \rangle = \begin{bmatrix} \langle e_x e_x^{*} \rangle & \langle e_x e_y^{*} \rangle \\ \langle e_y e_x^{*} \rangle & \langle e_y e_y^{*} \rangle \end{bmatrix} = \begin{bmatrix} a_x^2 & a_x a_y e^{-i\delta} \\ a_x a_y e^{i\delta} & a_y^2 \end{bmatrix}$$

[transpose complex conjugate]

Now we define an orthogonal basis for J in terms of the Pauli matrices:

$$\boldsymbol{\sigma}_0 = \begin{pmatrix} 1 & 0 \\ 0 & 1 \end{pmatrix}, \boldsymbol{\sigma}_1 = \begin{pmatrix} 1 & 0 \\ 0 & -1 \end{pmatrix}, \boldsymbol{\sigma}_2 = \begin{pmatrix} 0 & 1 \\ 1 & 0 \end{pmatrix}, \boldsymbol{\sigma}_3 = \begin{pmatrix} 0 & -i \\ i & 0 \end{pmatrix}$$

J is expanded in terms of these elements, with linear coefficients S_j:

$$\mathbf{J} = \frac{1}{2}\sum_0^3 S_j \boldsymbol{\sigma}_\mathbf{j}$$

and these S_j may be identified with the Stokes parameters:

$$I = Trace\left(\boldsymbol{\sigma}_0 \mathbf{J}\right)$$
$$Q = Trace\left(\boldsymbol{\sigma}_1 \mathbf{J}\right)$$
$$U = Trace\left(\boldsymbol{\sigma}_2 \mathbf{J}\right)$$
$$V = Trace\left(\boldsymbol{\sigma}_3 \mathbf{J}\right)$$

Exercise II.2

Use the identification of the Stokes parameters in terms of the Pauli matrices and the coherency matrix, show the equivalence of the Stokes parameters so derived to the operational definition of the Stokes parameters:

$$I = \langle a_x^2 \rangle + \langle a_y^2 \rangle$$

$$Q = \langle a_x^2 \rangle - \langle a_y^2 \rangle$$

$$U = 2\langle a_x\, a_y \cos\delta \rangle$$

$$V = 2\langle a_x\, a_y \sin\delta \rangle$$

Mueller Matrices: Representing the Effects of Optics

When an optical element alters the state of polarization of a light beam passing through it, the action upon the Stokes vector may be described by a 4x4 Mueller matrix:

$$\mathbf{I}' = \begin{pmatrix} I' \\ Q' \\ U' \\ V' \end{pmatrix} = \begin{pmatrix} M_{11} & M_{12} & M_{13} & M_{14} \\ M_{21} & M_{22} & M_{23} & M_{24} \\ M_{31} & M_{32} & M_{33} & M_{34} \\ M_{41} & M_{42} & M_{43} & M_{44} \end{pmatrix} \begin{pmatrix} I \\ Q \\ U \\ V \end{pmatrix} = \mathbf{MI}$$

According to the definitions of the Stokes vector, a perfect linear polarizer oriented so as to transmit polarized light in the horizontal (↔ , x-direction):

$$\mathbf{M}_{\mathbf{lin}}(\theta = 0) = \frac{1}{2} \begin{pmatrix} 1 & 1 & 0 & 0 \\ 1 & 1 & 0 & 0 \\ 0 & 0 & 0 & 0 \\ 0 & 0 & 0 & 0 \end{pmatrix}$$

A rotation of the coordinate frame through an angle χ may be represented by the following rotation matrix R as applied to a Stokes vector:

$$\mathbf{R} = \begin{pmatrix} 1 & 0 & 0 & 0 \\ 0 & \cos 2\chi & \sin 2\chi & 0 \\ 0 & -\sin 2\chi & \cos 2\chi & 0 \\ 0 & 0 & 0 & 1 \end{pmatrix}$$

The angle χ is doubled in the rotation matrix because *Q,U* complete a full cycle of variation from positive to negative to positive again in π radians. That is, a rotation of the frame from orientation along a beam polarized in the +*Q* direction by $\pi/4$ will lead to +*U* polarized radiation.

Put another way, the rotational orientation of the linear polarizer is ambiguous by π radians. *This is the essence of the "180° azimuth ambiguity" for the magnetic field vector as inferred from the polarization of light.* There is no way to infer experimentally the actual orientation of the linear polarizer from its effect upon the light it transmits, it will always be ambiguous by π radians.

If we wish to determine the Mueller matrix $\mathbf{M}_G^R$ of an optical element G rotated by an angle χ from its measured matrix $\mathbf{M}_G$, we must first rotate the incoming Stokes vector into the new reference frame, apply $\mathbf{M}_G$ in the new frame, then rotate back to the original frame to get the resultant Stokes vector:

$$\mathbf{I}' = \mathbf{R}^{-1}\mathbf{M}_G\mathbf{R}\mathbf{I} = \mathbf{M}_G^R\mathbf{I}$$

Where of course:

$$\mathbf{R}^{-1}(\chi) = \mathbf{R}(-\chi)$$

Consider a linear retarder, i.e. one in which vertical (y-) electric field oscillations lag oscillations in the horizontal (x-) electric field by Δ radians. It has a Mueller matrix:

$$\mathbf{M}_{ret} = \begin{pmatrix} 1 & 0 & 0 & 0 \\ 0 & 1 & 0 & 0 \\ 0 & 0 & \cos\Delta & \sin\Delta \\ 0 & 0 & -\sin\Delta & \cos\Delta \end{pmatrix}$$

Mueller Calculus (Linear Algebra)

The action of a sequence of optical elements upon an input Stokes vector I may be represented by the successive multiplication of the Mueller matrix of that element:

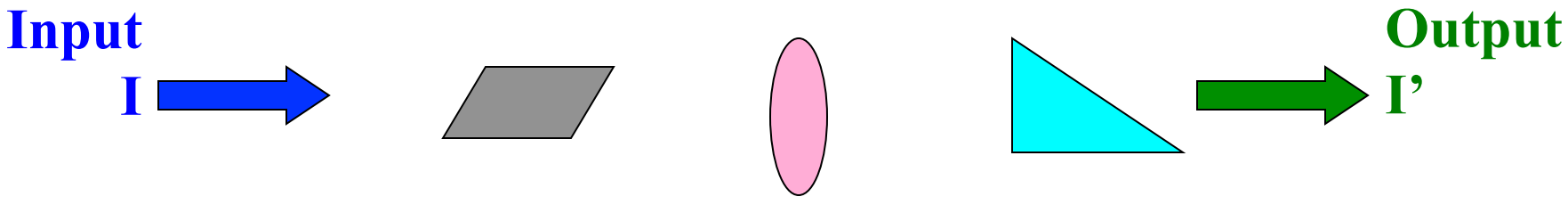

$$\mathbf{I'} = \mathbf{M_3\, M_2\, M_1\, I}$$

When rotated through an angle θ the retarder has the following Mueller matrix:

$$\mathbf{M}_{\mathbf{ret}}^{\theta} = \begin{pmatrix} 1 & 0 & 0 & 0 \\ 0 & \cos^2 2\theta + \sin^2 2\theta \cos\Delta & \cos 2\theta \sin 2\theta (1-\cos\Delta) & -\sin 2\theta \sin\Delta \\ 0 & \cos 2\theta \sin 2\theta (1-\cos\Delta) & \sin^2 2\theta + \cos^2 2\theta \cos\Delta & \cos 2\theta \sin\Delta \\ 0 & \sin 2\theta \sin\Delta & -\cos 2\theta \sin\Delta & \cos\Delta \end{pmatrix}$$

Consider an optical device designed to produce circular polarization. First we illuminate a linear polarizer oriented with its transmission axis so as to produce pure Stokes Q. We follow this by a ¼-wave retarder (Δ=π/2) rotated at θ=π/4, and examine the output Stokes Vector:

$$\mathbf{I}^{\mathbf{out}} = \mathbf{M}_{\mathbf{ret}}^{\pi/4}\mathbf{M}_{\mathbf{lin}}^{\mathbf{0}} \begin{pmatrix} I \\ Q \\ U \\ V \end{pmatrix} = \frac{1}{2}\begin{pmatrix} 1 & 0 & 0 & 0 \\ 0 & 0 & 0 & -1 \\ 0 & 0 & 1 & 0 \\ 0 & 1 & 0 & 1 \end{pmatrix}\begin{pmatrix} 1 & 1 & 0 & 0 \\ 1 & 1 & 0 & 0 \\ 0 & 0 & 0 & 0 \\ 0 & 0 & 0 & 0 \end{pmatrix}\begin{pmatrix} I \\ Q \\ U \\ V \end{pmatrix}$$

$$= \frac{1}{2}\begin{pmatrix} 1 & 0 & 0 & 0 \\ 0 & 0 & 0 & -1 \\ 0 & 0 & 1 & 0 \\ 0 & 1 & 0 & 1 \end{pmatrix}\begin{pmatrix} I+Q \\ I+Q \\ 0 \\ 0 \end{pmatrix} = \frac{1}{2}\begin{pmatrix} I+Q \\ 0 \\ 0 \\ I+Q \end{pmatrix}$$

Therefore this device produces pure circularly polarized light. Some observations about Mueller matrices:

•One may measure the polarizing properties of all the optical elements in an optical system, then reconstruct the net polarizing properties of the system as a product of these matrices.

•In general, Mueller matrices *do not commute!* Reversing the order of polarizing optics in the beam may result in an entirely different polarization. Consider reversing the order of the elements in the previous device. The last element is a linear polarizer, and hence the output will be pure linear polarization (+*Q*), not pure circular polarization (+*V*)

•Since the first column of the Mueller matrix, when acting on unpolarized light ($\{I,0,0,0\}^T$) must give a valid Stokes vector, we have: $M_{11} \geq \sqrt{M_{21}^2 + M_{31}^2 + M_{41}^2}$

Exercise II.3. Use the rotation matrix for angle θ and the Mueller matrix representation of a linear retarder of retardance Δ to derive the Mueller matrix of a rotated linear retarder:

$$\mathbf{M}_{\mathbf{ret}}^{\theta} = \begin{pmatrix} 1 & 0 & 0 & 0 \\ 0 & \cos^2 2\theta + \sin^2 2\theta \cos\Delta & \cos 2\theta \sin 2\theta (1-\cos\Delta) & -\sin 2\theta \sin\Delta \\ 0 & \cos 2\theta \sin 2\theta (1-\cos\Delta) & \sin^2 2\theta + \cos^2 2\theta \cos\Delta & \cos 2\theta \sin\Delta \\ 0 & \sin 2\theta \sin\Delta & -\cos 2\theta \sin\Delta & \cos\Delta \end{pmatrix}$$

A Cautionary Note

Sign conventions in polarimetry differ:

•I use here the Optical convention for the sense of circular polarization (electric vector as viewed by the detector). The particle physics definition is opposite, and is used in some works.

Some authors (i.e. del Toro Iniesta, Rees) use the opposite sign for the time exponential in describing the electric field (-*iωt*) which leads to different signs of quantities (e.g. in the Pauli matrices). ***This is a matter of convention only, it has no physical implications.***

Furthermore, there are *sign errors that do cause physical differences* "sprinkled richly" throughout the literature on this subject. If you need a reference without sign errors, always consult the works of Landi degl' Innocenti!

III. Modification of Polarization by Optical Devices

Stack of Plates Polarizers - 1

- Reflection from glass plate is partially polarized, favoring polarization perpendicular to the plane of incidence
- **Snell's law of refraction:** $\dfrac{\sin\phi}{\sin\phi'} = n$
- When angle between reflected and refracted ray = π/2, reflected ray must be completely polarized perpendicular to the plane of incidence: **Brewster's angle of incidence ϕ_B**:

$$\phi_B = \frac{\pi}{2} - \phi'$$

$$n = \frac{\sin\phi_B}{\cos\phi_B} = \tan\phi_B$$

- Stack of glass plates: each reflection removes more of the transmitted polarization perpendicular to the plane of incidence

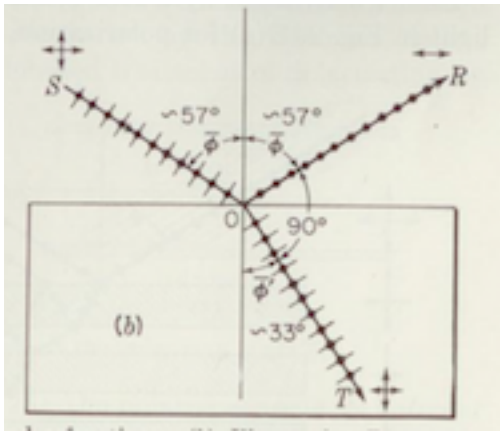

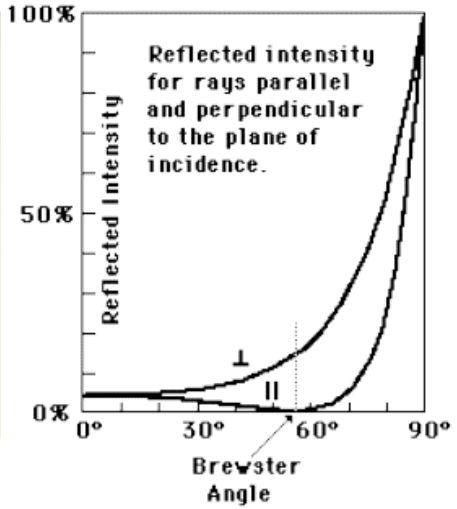

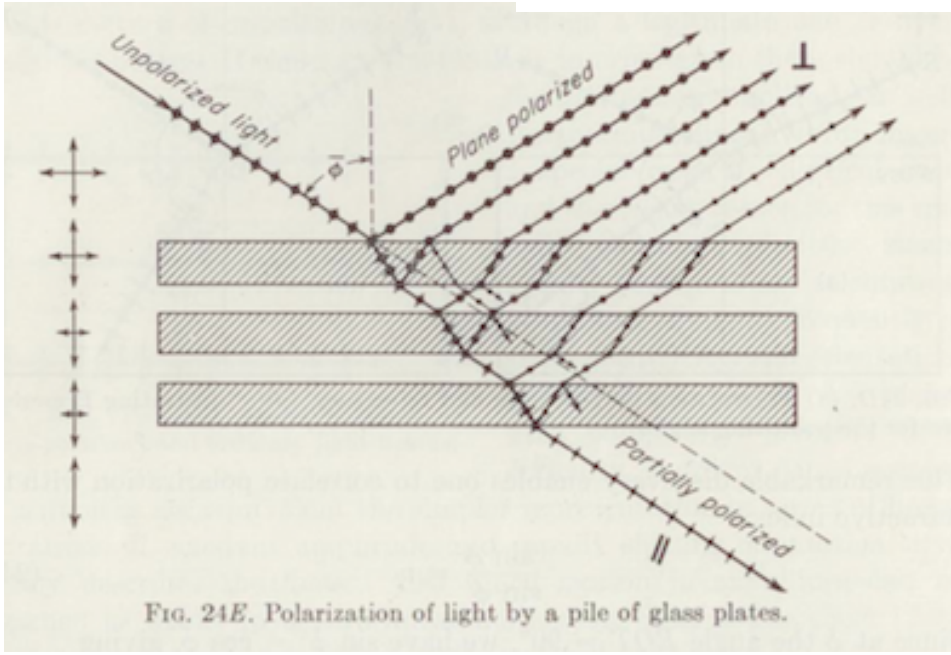

Fig. 21E. Polarization of light by a pile of glass plates.

Illustrations from Jenkins & White 1957, pp. 491,492

Stack of Plates Polarizers – 2: Dielectric Coatings

- **Reflections from dielectric coatings can be made to polarize like a stack of glass plates**
- **Coatings are very thin, so multiple reflected waves are not spatially-displaced**
- **High efficiency for both reflected and transmitted beams (depending on λ)**
- **Useful in production of polarizing beam splitters:**

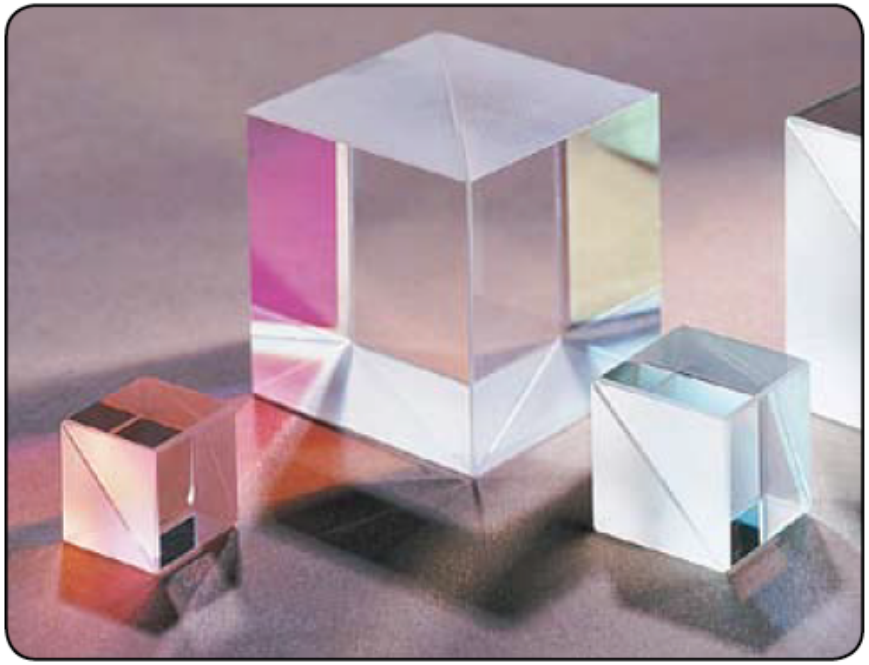

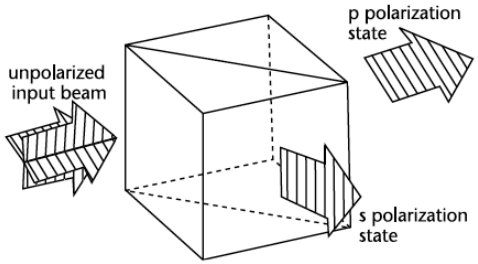

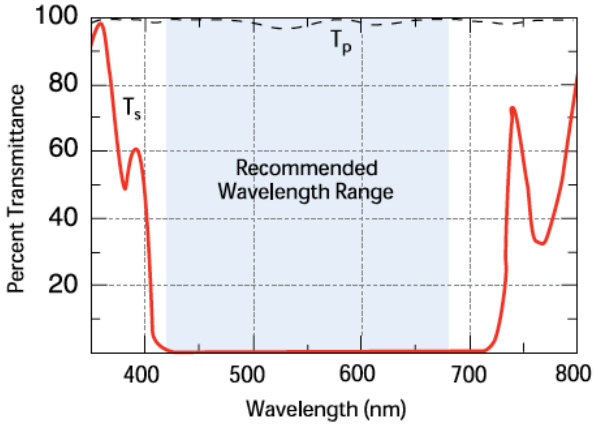

Illustrations from Meadolark Optics Catalog

Diattenuation − 1 (Linear Polarizers)

- **Diattenuation (*aka Dichroism)*:** occurs in materials that have anisotropic refractive index, whereby one direction of polarization is absorbed preferentially
- **Complex refractive index *n*, complex wavenumber *k*:**

$$n_{complex} = n + i\kappa \qquad n,\ \kappa \text{ real}$$

$$k = \frac{2\pi n_{complex}}{\lambda_0}$$

- Electric vector propagating in medium with complex refractive index:

$$\mathbf{E}(z,t) = \mathrm{Re}\left[\mathbf{E_0} e^{i(\omega t - \mathbf{k}\bullet\mathbf{z})}\right] = \mathrm{Re}\left[\mathbf{E_0} e^{i(\omega t - 2\pi(n+i\kappa)z/\lambda_0)}\right]$$

$$= e^{2\pi\kappa z/\lambda_0}\,\mathrm{Re}\left[\mathbf{E_0} e^{i(\omega t - 2\pi n\mathbf{z}/\lambda_0)}\right]$$

- Complex component of index of refraction leads to **attenuation** for $\kappa<0$
- **Examples of diattenuation: wire grid polarizers, certain crystals, polymer polarizers**

Diattenuation - 2: Wire Grid Polarizers

- Grid of parallel electrical conductors with transmitting space between them
- Currents may move along conducting wires, so reflection of light with electric vector parallel to wires
- Highest efficiency polarizing when spacing of wires $d \leq \lambda/2$
- Transmission of light polarized perpendicularly to the wires
- Mainly effective at infrared wavelengths because of difficulty of producing finely-spaced wires

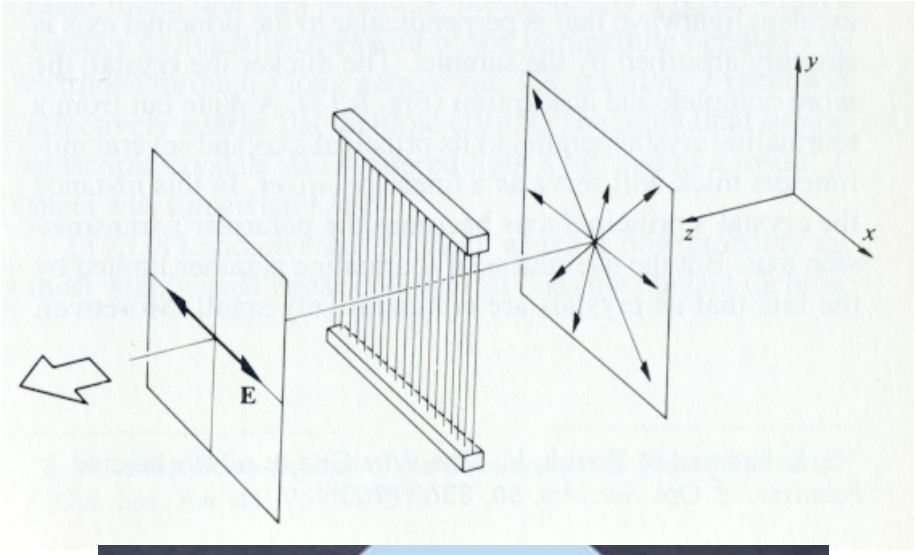

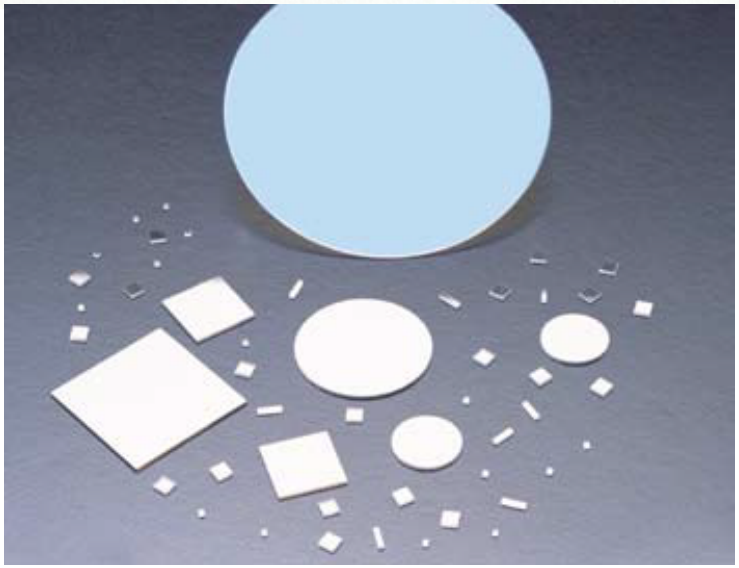

Lower illustration from Meadolark Optics Catalog

Diattenuation - 3 – Some Crystals

Some crystalline structures preferentially absorb one state of polarization, i.e. tourmaline:

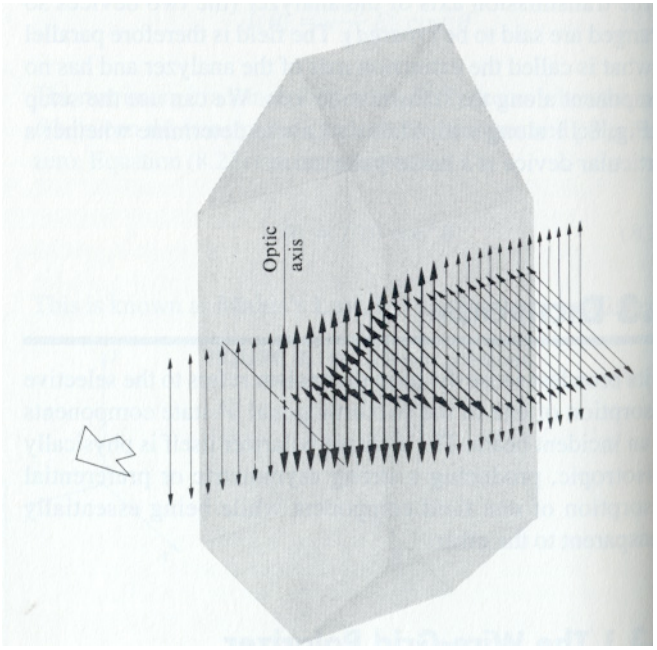

Diattenuation - 4 – Polymer Materials

- **Polyvinyl alcohol has elongated molecules**
- **Inclusion of iodine atoms increases electrical conductivity**
- **Sheet of material stretched in one dimension, leading to a material acting similarly to the wire grid polarizer**

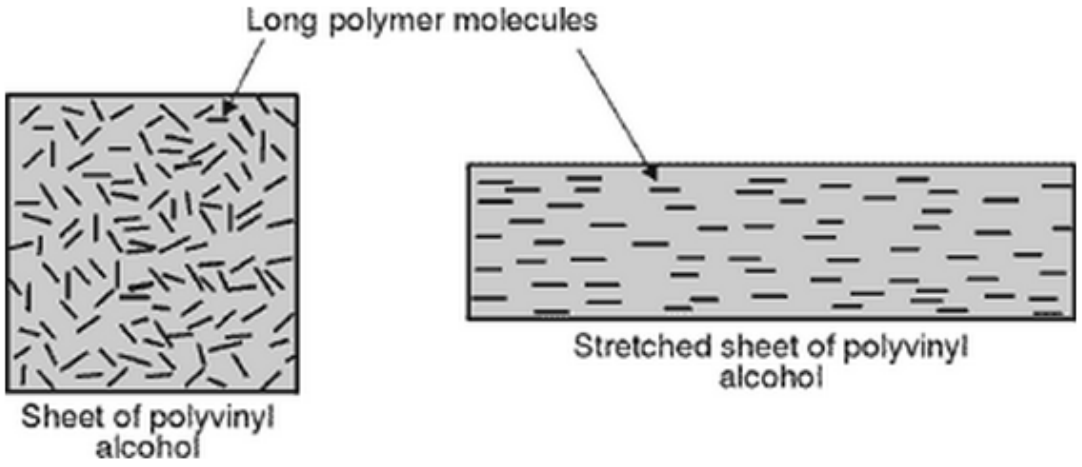

Birefringence – 1: Crystals and Other Materials

- **Birefringence** arises when the propagation properties within a medium are **anisotropic**
- Anisotropy of the index of refraction: **different propagation speeds along different axes**
- Classical analog is the response to incoming radiation of an electron that is bound to the crystalline lattice by differing "spring" constants along differing axes:

- The speed of propagation along each axis is $[c/n_x, c/n_y, c/n_z]$
- Most commonly deal with **uniaxial** crystals where n along only one axis differs from n along the other two axes
- **Optic axis** of the crystal: rotation of crystal about this axis results in no change of its optical properties
- Orthogonal linear polarizations (perpendicular to optic axis) propagate at same speed along the optic axis

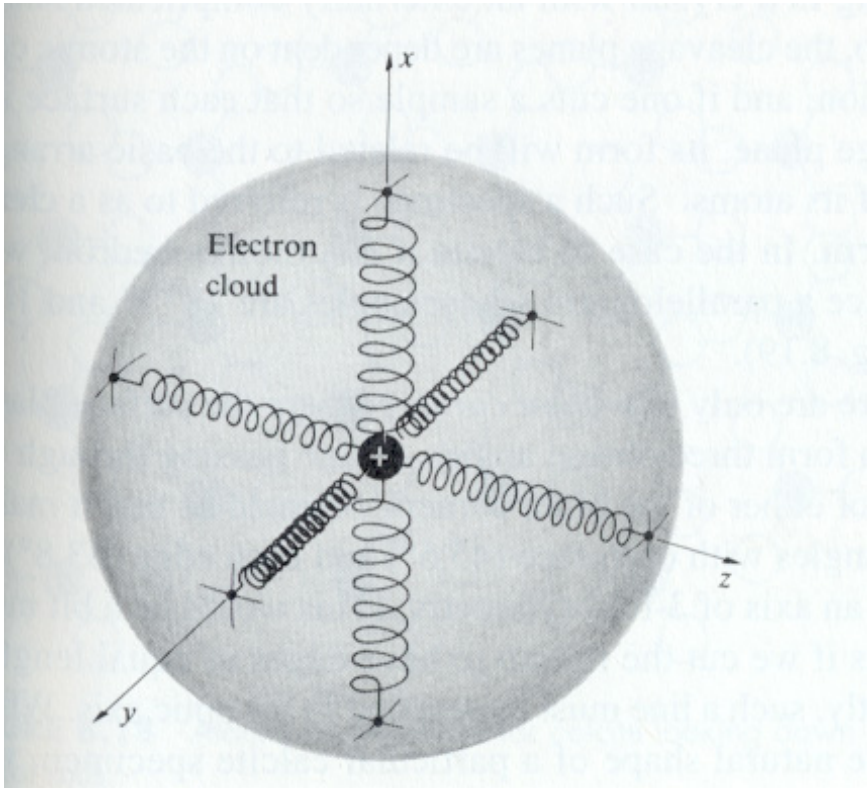

Birefringence – 2: Double Refraction

- **Double refraction** occurs in uniaxial crystals when orthogonal linear polarizations propagate differently

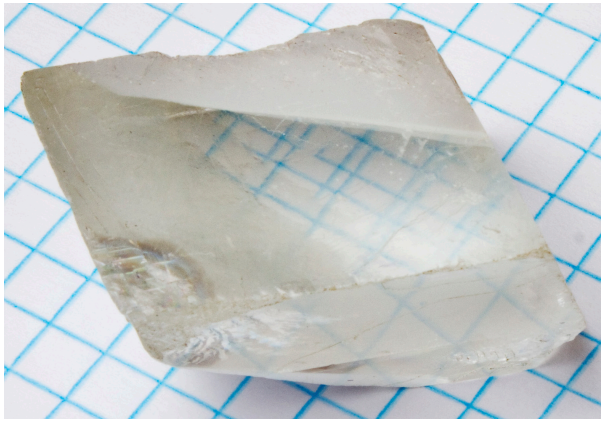

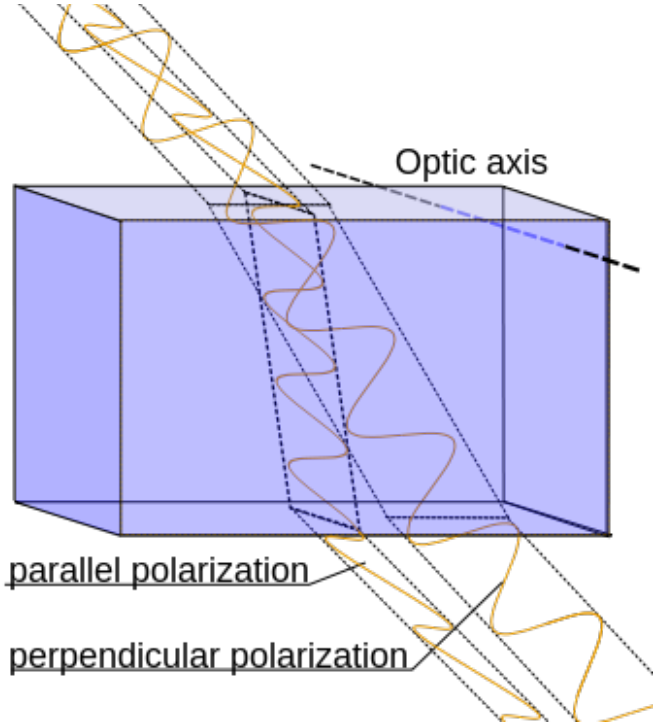

Light polarized perpendicular to the optic axis (***ordinary*** or ***o-ray***):

- Larger index of refraction n_o in calcite
- Lower propagation speed in calcite
- More optical refraction

Calcite and Polarizers

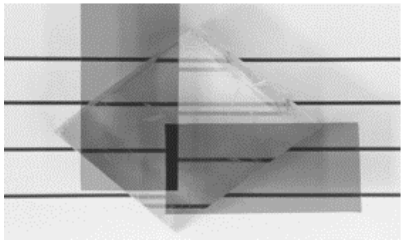

Light polarized parallel to the optic axis (***extraordinary*** or ***e-ray***):

- Smaller index of refraction n_e in calcite
- Higher propagation speed in calcite
- Less optical refraction

Birefringence – 3: Classes of Uniaxial Crystals

- Wavefronts propagating from the source *P* within the crystal propagate at different speeds depending upon their polarization

- In calcite, $n_o > n_e$, [1.658>1.486 at 5893 Å] "negative optical sign"
- In quartz, $n_o < n_e$, [1.5443<1.5534 at 5893 Å] "positive optical sign"

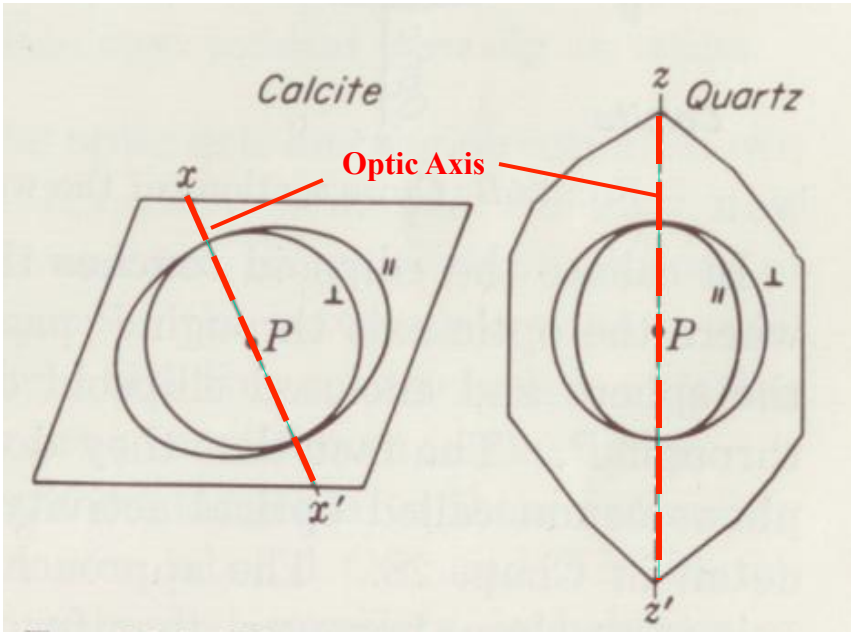

Illustration from Jenkins & White 1957

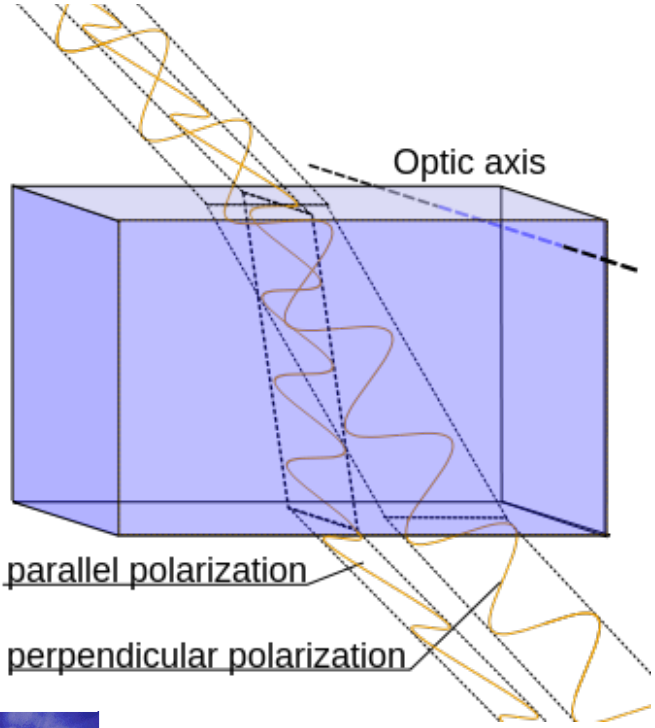

Illustration of double refraction on previous slide: for QUARTZ (positive optical sign), NOT CALCITE!

Birefringence – 4: Uses of Uniaxial Crystals

Many different optical devices can be constructed from uniaxial crystals:

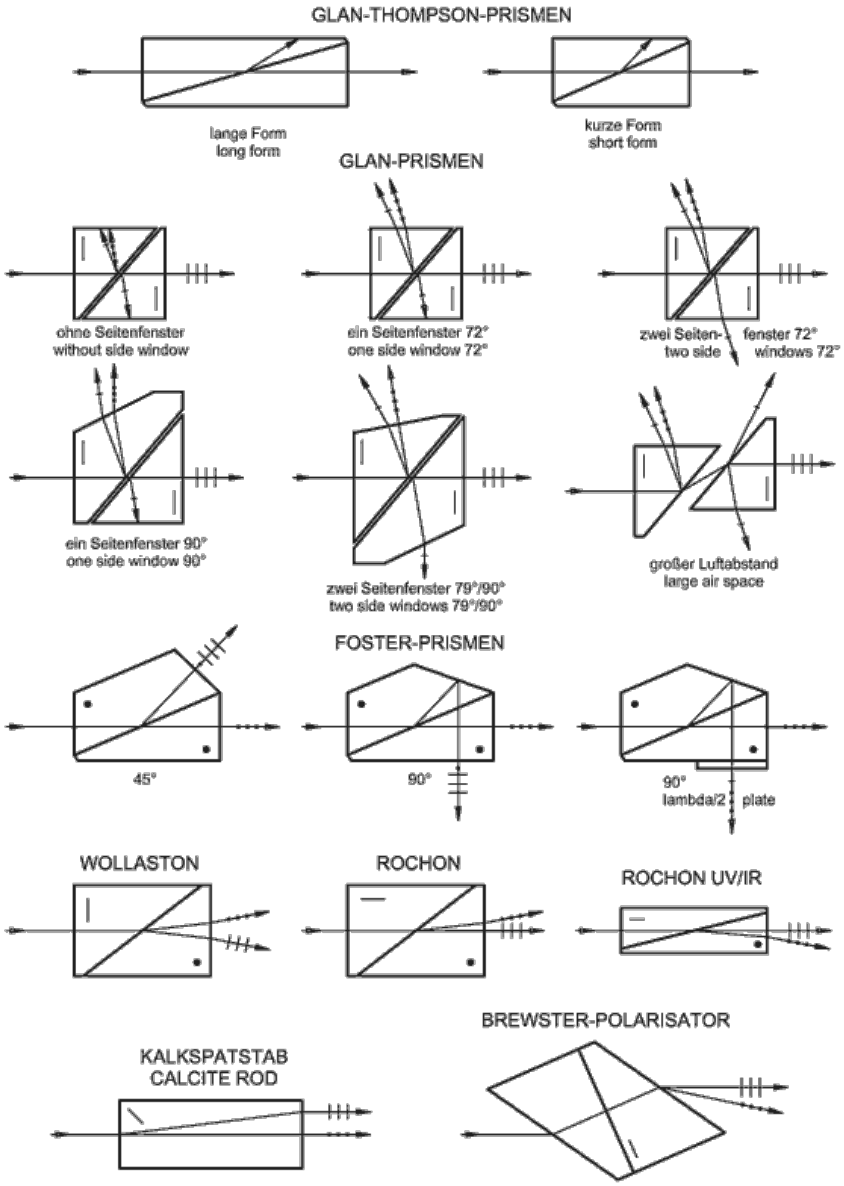

Diagram from Halle catalog: http://www.b-halle.de/EN/Catalog/Polarizers/Different_Types_of_Polarizing_Prisms.php

Linear Retarders – 1

- For extraordinary rays propagating perpendicular to the optic axis of a birefringent material, linear polarizations along and perpendicular to the optic axis travel through the medium at differing speeds
- On exit of the material, one polarization is said to be retarded relative to the other; i.e. the phase of the wave fronts of the two polarizations will differ:

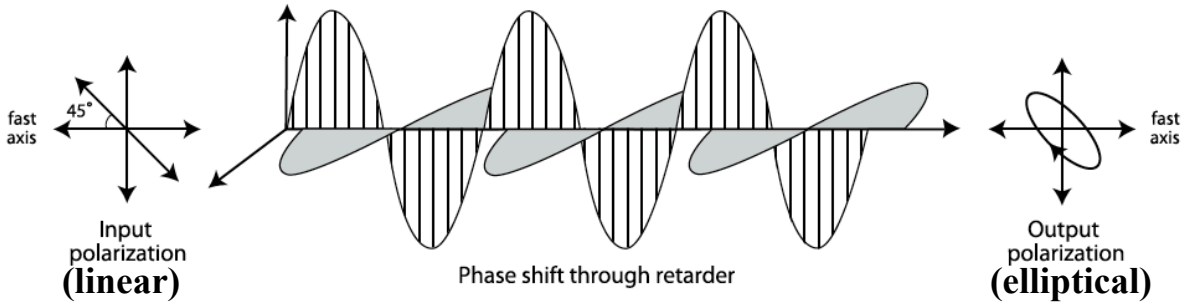

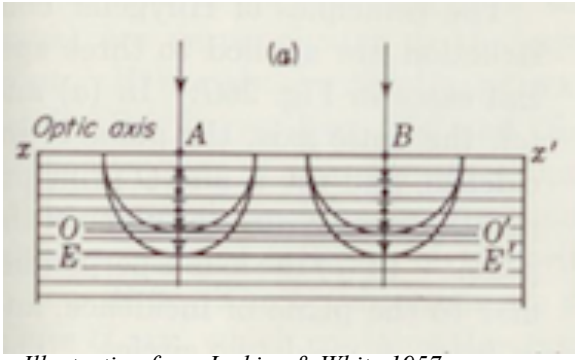

Illustration from Jenkins & White 1957

- Retardation (in waves): $r = d(|n_e - n_o|)/\lambda$ (d is thickness, λ is wavelength)
- **Retardation is enormously useful!** Retarders help us analyze and manipulate elliptical polarization, construct filters in frequency, and many other things.

Linear Retarders – 2: Crystalline Retarders

Crystalline birefringent retarders: example – quartz

- To achieve λ/4 waves retardance at the Na D-line:

$$d = \lambda/[4|(n_e - n_o)] = 5.893 \times 10^{-5}/[4(1.5534\text{-}1.5443)] \text{ cm} = \textbf{16 microns!}$$

- Difficult to cut crystals so thin! This is called a **zero order retarder**
- **Multiple Order Retarders:** if the desired fractional wave retardation is Δ waves, one can use a crystal retarding (N + Δ) waves total:
  - Ease of fabrication, but…
  - Retardation depends strongly on angle
  - Much stronger dependence of retardation on temperature than zero order
- **Compound Zero Order Retarders:** sandwich two multiple order retarders together, but having optic axes perpendicular to one another
  - Net retardance is difference of the retardance of the two elements
  - Same temperature sensitivity of retardance as zero order retarder, but….
  - Retardation depends strongly on angle

Linear Retarders – 3: Polymer Retarders

Polymer birefringent retarders:

- Most polymer materials are birefringent because spatial ordering of long molecules causes anisotropic optical behavior
- Typically material is stretched to obtain alignment – slow axis parallel to stretch direction
- Fractional wave retardance achieved with reasonable thickness – zero order
- Slow dependence of retardance on wavelength
- Large angle of acceptance
- Usually laminated to rigid substrate to achieve good optical quality

Uses of Retarders – 1: Quarter Wave Retarder

1. **Circular Polarizer:** Generate circularly-polarized light from unpolarized light

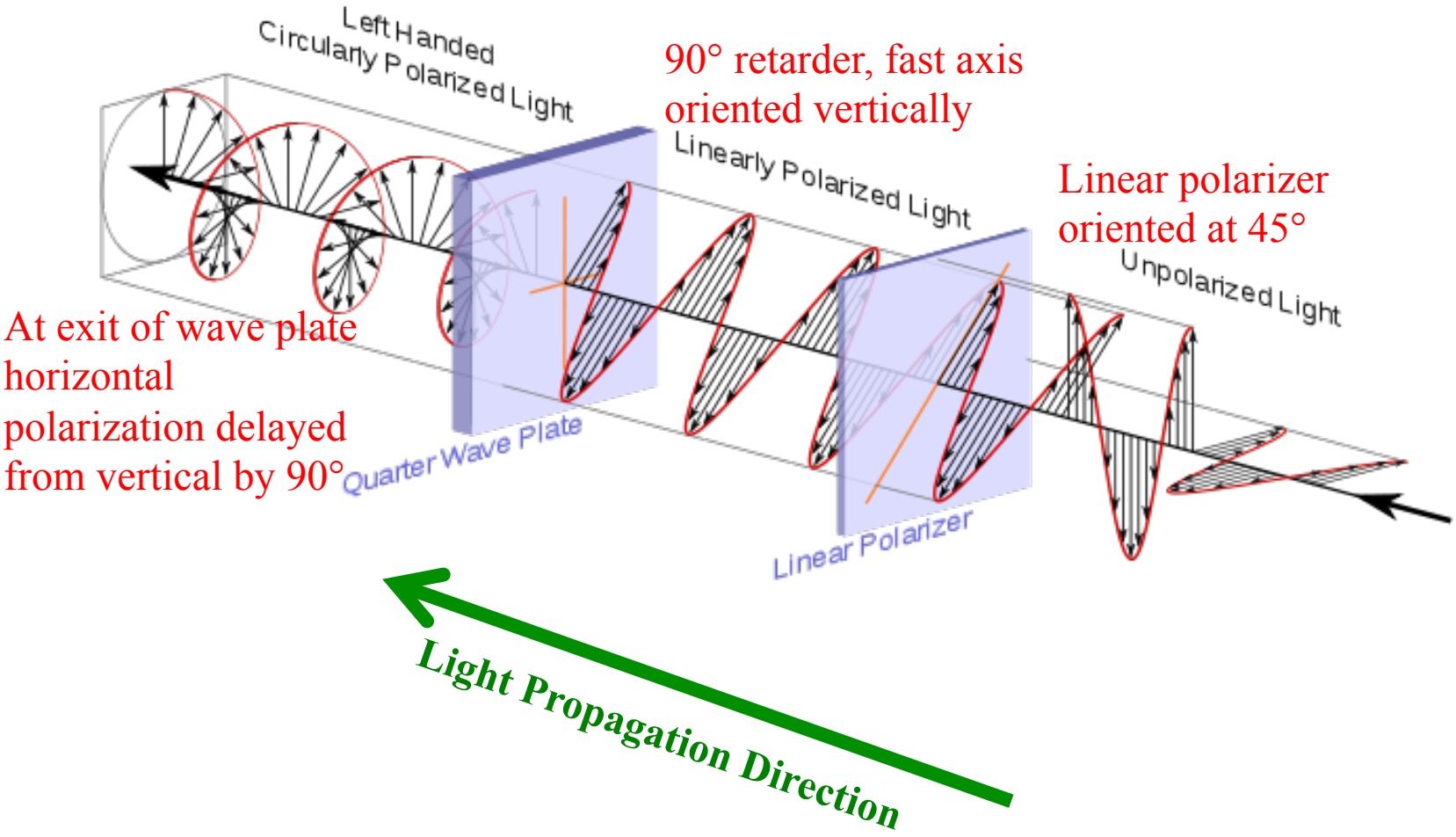

Uses of Retarders – 2: Circular Analyzer

1. **Circular Polarizer:** Generate circularly-polarized light from unpolarized light

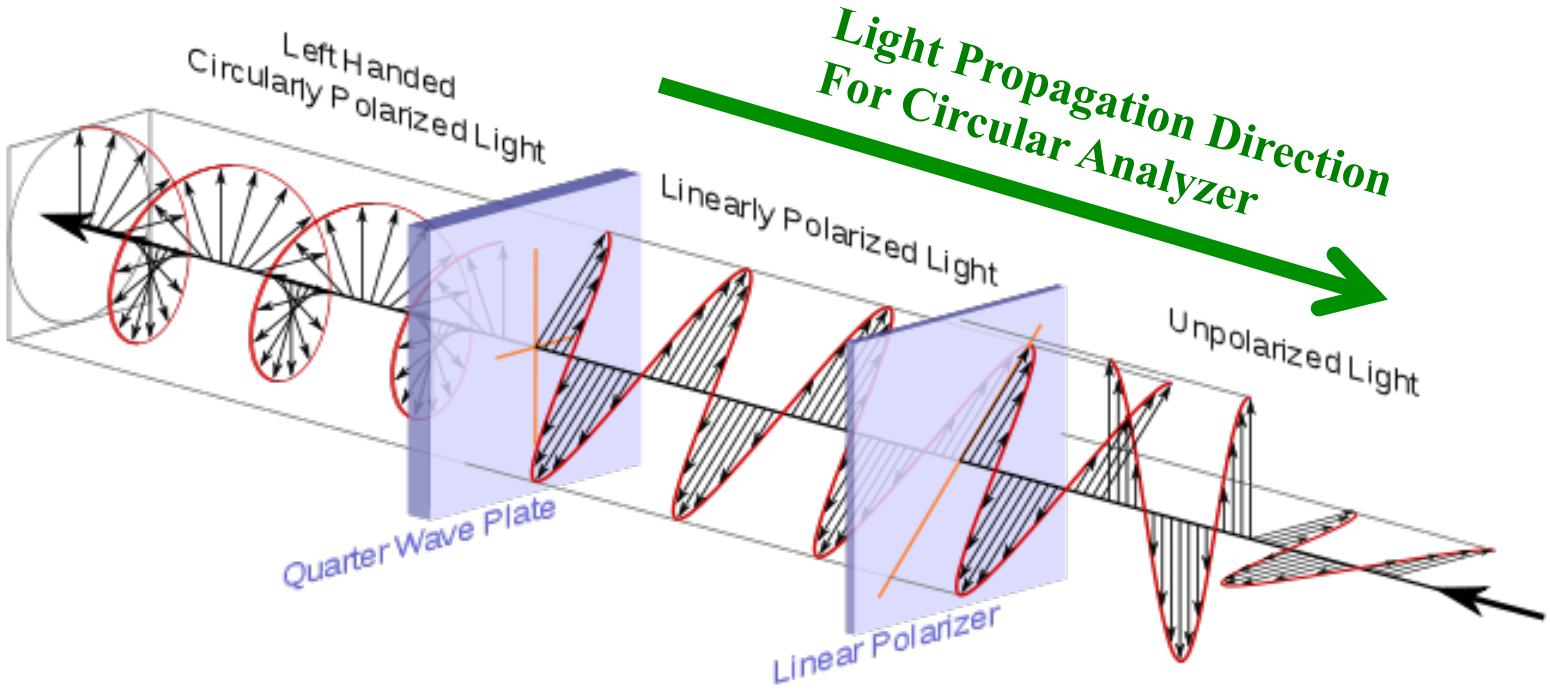

2. **Circular Analyzer:** detect circular polarization

- Run the above device in reverse! Circular polarizer followed by linear polarizer

Uses of Retarders – 2: Circular Analyzer

1. **Circular Polarizer:** Generate circularly-polarized light from unpolarized light

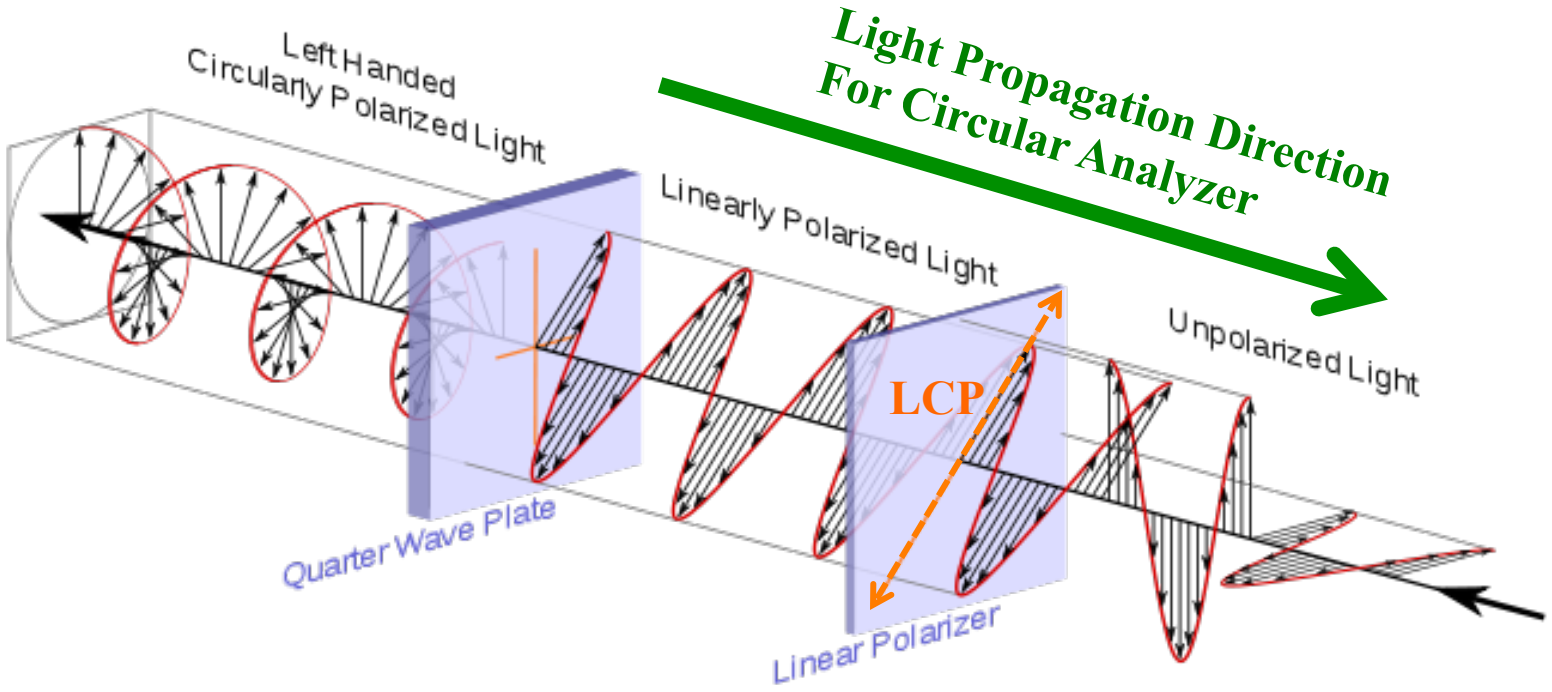

2. **Circular Analyzer:** detect circular polarization

- Run the above device in reverse! Circular polarizer followed by linear polarizer
- **Left-handed circular polarization: linear polarizer oriented at 45° as shown**

Back to 103

Uses of Retarders – 2: Circular Analyzer

1. **Circular Polarizer:** Generate circularly-polarized light from unpolarized light

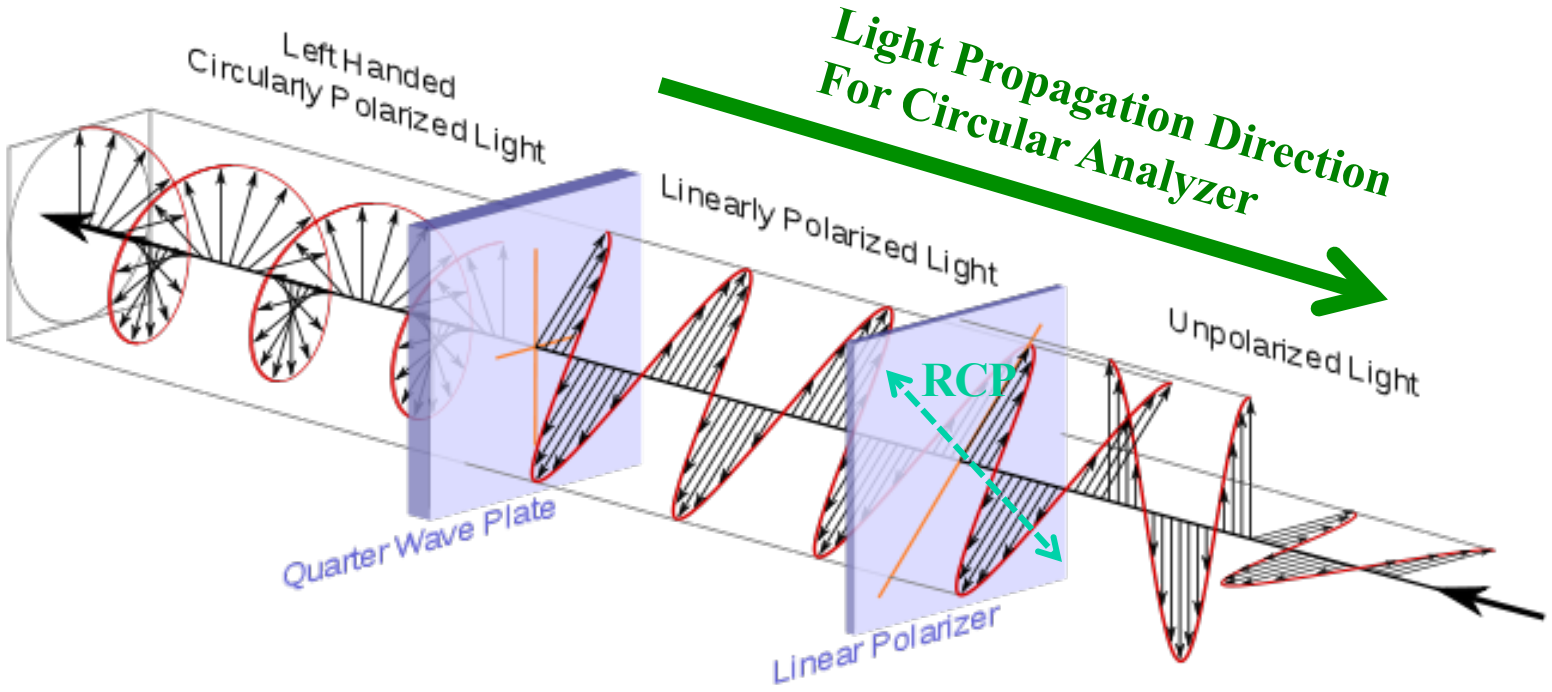

2. **Circular Analyzer:** detect circular polarization

- Run the above device in reverse! Circular polarizer followed by linear polarizer
- **Right-handed circular polarization: linear polarizer oriented at 135° as shown**

Exercises:

III.1. Using Mueller matrices, demonstrate how linear polarization oriented at 45° as shown in the slide "Uses of Retarders – 1: Quarter Wave Retarder" passing through a quarter wave plate oriented with fast axis oriented vertically ($\theta=\pi/2$) the polarizations Q, U, V output of the device. Hint: use the result of Exercise II.3 above.

III.2. Using the above setup with arbitrary orientation of the fast axis θ of the retarder, what value of $0<\theta<\pi/2$ results in unpolarized light on output from the retarder? What orientations produce maximum Q, U, or V?

III.3. Construct the Mueller matrix representation of the circular analyzer shown in the slide "Uses of Retarders – 2: Circular Analyzer". Demonstrate the detection of right- and left-circularly polarized light through the orientation of the linear polarizer.

Uses of Retarders – 4: Half Wave Retarder

- The **half wave plate** retards one of the orthogonal linear polarization states by π radians relative to the other state
- When linear polarization is input at θ to the optical axis, the output linear polarization is **rotated by 2θ** relative to the input
- Consider the Mueller matrix representation of the diagram at left. Use the form for a retarder of retardation Δ rotated by an angle θ:

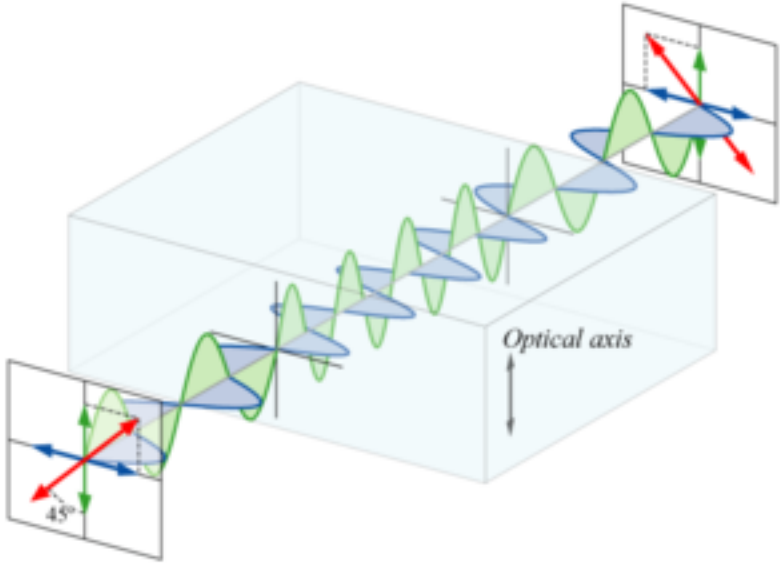

$$\mathbf{M}_{\mathbf{ret}}^{\theta} = \begin{pmatrix} 1 & 0 & 0 & 0 \\ 0 & \cos^2 2\theta + \sin^2 2\theta \cos\Delta & \cos 2\theta \sin 2\theta (1-\cos\Delta) & -\sin 2\theta \sin\Delta \\ 0 & \cos 2\theta \sin 2\theta (1-\cos\Delta) & \sin^2 2\theta + \cos^2 2\theta \cos\Delta & \cos 2\theta \sin\Delta \\ 0 & \sin 2\theta \sin\Delta & -\cos 2\theta \sin\Delta & \cos\Delta \end{pmatrix}$$

- Note in the above representation of $\mathbf{M}_{\mathbf{ret}}$, the vertical axis represents the slow (retarded) axis, as in the diagram above (the green wave proceeds more slowly)
- Note also the diagram is symmetric: it does not matter which end is input or output

Uses of Retarders – 4: Half Wave Retarder

Evaluate $\mathbf{M}_{\mathbf{ret}}$ for $\theta = \pi/4$ and $\Delta=\pi$:

$$\mathbf{M}_{\mathbf{ret}}^{\theta} = \begin{pmatrix} 1 & 0 & 0 & 0 \\ 0 & -1 & 0 & 0 \\ 0 & 0 & 1 & 0 \\ 0 & 0 & 0 & -1 \end{pmatrix}$$

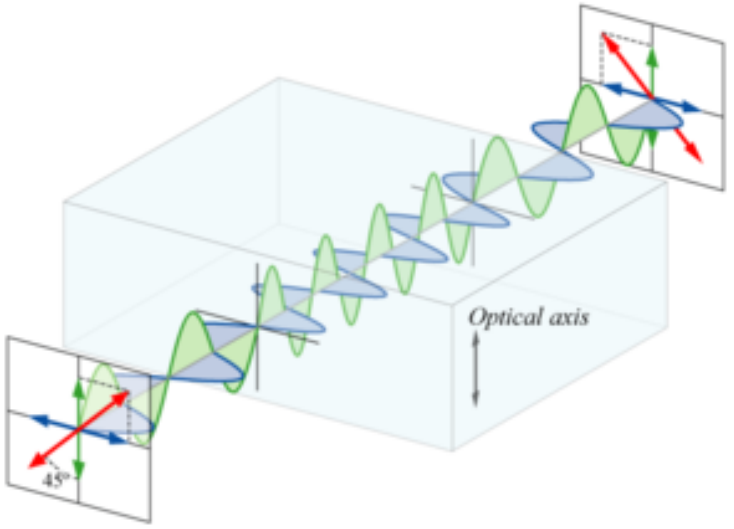

Note that we have rotated the retarder, not the input vector. So the input vector is pure $+Q$: $\mathbf{I} = [Q, Q, 0, 0]^{\mathrm{T}}$. Applying the matrix we see:

$$\mathbf{I}' = \mathbf{M}_{\mathbf{ret}}^{\theta}\mathbf{I} = \left[Q,-Q,0,0\right]^{T}$$ **$+Q$ polarization rotated by 90° to $-Q$**

Note from $\mathbf{M}^{\boldsymbol{\theta}}_{\mathbf{ret}}$ the following properties of this half wave plate:

- $\pm U$ polarization is unaffected because that is oriented along (or perpendicular to) the optic axis
- V is flipped in sign. Therefore, this configuration converts right circular polarization to left circular polarization, and vice versa. **For the half wave plate, output Stokes V is independent of rotation angle θ because $\sin(\Delta=\pi) = 0$.**

Variable Retarders

- Solar polarimetry usually mandates a time-varying "modulation" of the input signal in order to perform analysis of the state of polarization
- There are several classes of retarders that are being used (or have been used):
    a) **Rotating waveplates (i.e. rotating linear retarders)**
    b) **KD*P (potassium diduterium phosphate)**
    c) **Liquid crystals**
    d) **Piezo-elastic modulators**

Variable Retarders – 1: Rotating Wave Plate

- Strictly speaking, not really a variable retarder since the retardation does not change with time
- When a retarder is inserted into the optical beam and rotated, either continuously or in discrete steps, it can serve as a **polarization modulator**, producing time variation of orthogonal linear polarization states

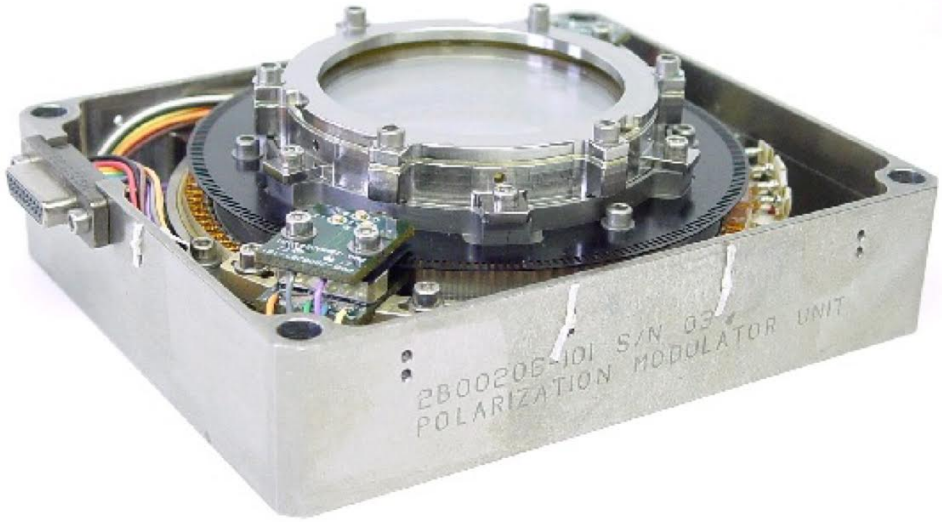

- Following the rotating retarder, a linear polarizer is inserted selecting one of the orthogonal states of polarization
- A quarter wave plate is most efficient at modulating circular polarization, and a half wave plate is most efficient at modulating linear polarization

Variable Retarders – 2: Pockels Cell

- Some crystals have birefringence that is proportional to an applied electric field
- Crystals most commonly used are potassium di-duterium phosphate (KD*P)
- Can vary the retardation at very high speeds, but….
- Pockels cells require high voltage to modulate the retardance (~5kV)
- They are expensive and delicate

Pockels cells were used in the past for solar polarimeters (i.e. Stokes I and II at Sacramento Peak in the 1970's), but are not currently favorites… they have been replaced by other devices such as liquid crystals

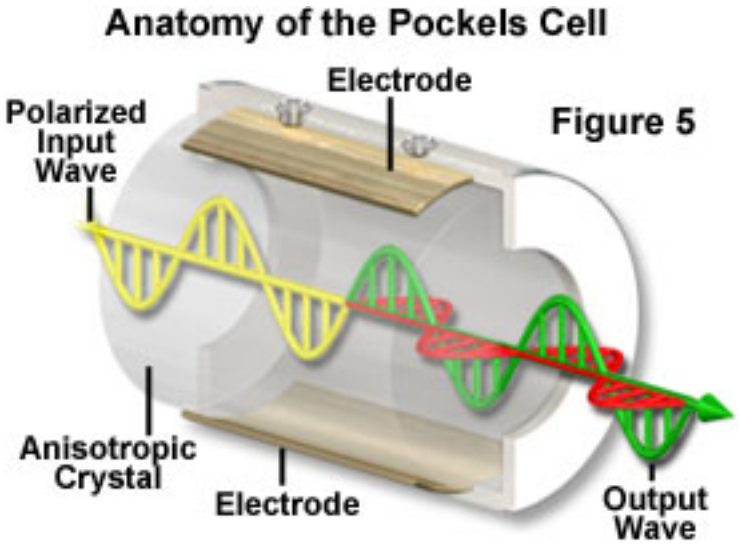

Variable Retarders – 3: Nematic Liquid Crystals

- **Nematic Liquid Crystal Variable Retarders (LCVRs)** are based on liquid crystals used as polarizers in many commercial electronic devices
- Elongated organic molecules produce birefringence when aligned as in their natural state
- When no voltage is applied, maximum retardance
- Applied voltage tilts molecules to along the direction of light propagation, reducing birefringence

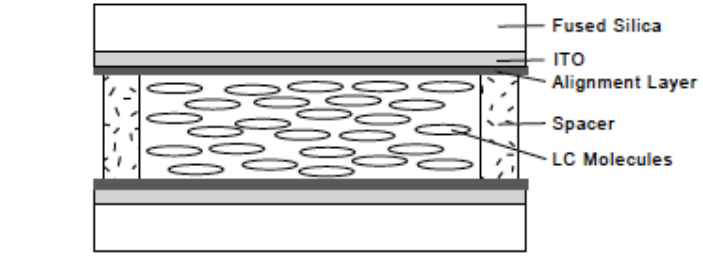

(a) Maximum Retardance (V = 0)

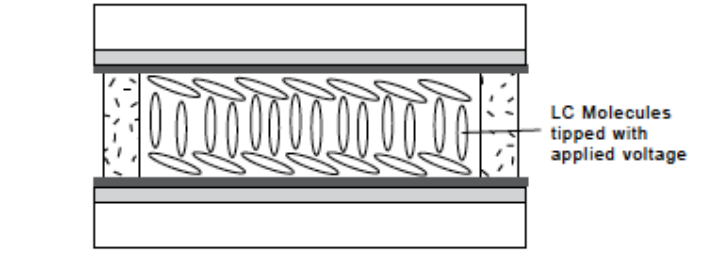

(b) Minimum Retardance (V >> 0)

Advantages:

- Electrically tunable retardance
- Low voltage requirement (<10 V)
- Accepts large incidence angle

Issues:

- Tuning not particularly fast (20 ms)
- Some temperature dependence
- Cannot completely eliminate retardance

Variable Retarders – 4: Ferroelectric Liquid Crystals

Ferroelectric Liquid Crystal (FLC) Variable Retarders:

Organic chiral molecules – retain their handedness (no iron involved!)

- Molecules can be made to switch their orientations in the presence of an electric field
- Bistable device that switches the orientation of the fast axis of the medium

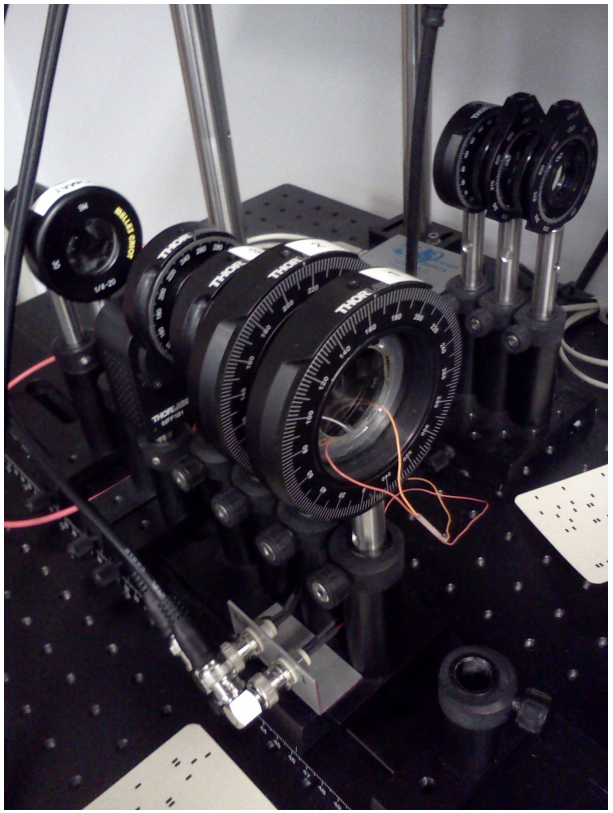

Advantages:

- Fast response time (~150 μs)
- Low voltage requirement (<10 V)

Issues:

- Switching of fast axis orientation only, not variable in the retardance value
- Some temperature dependence of the fast axis orientation (but not the overall retardance)
- Rotation of fast axis limited to about 45°

Variable Retarders – 5: Photo-Elastic Modulators

Photo-Elastic Modulators:

- Stress on isotropic material (glass) causes birefringence
- Alternating stress on the material causes variable retardance
- Easy way to achieve large stress: drive block of glass at its mechanical resonance

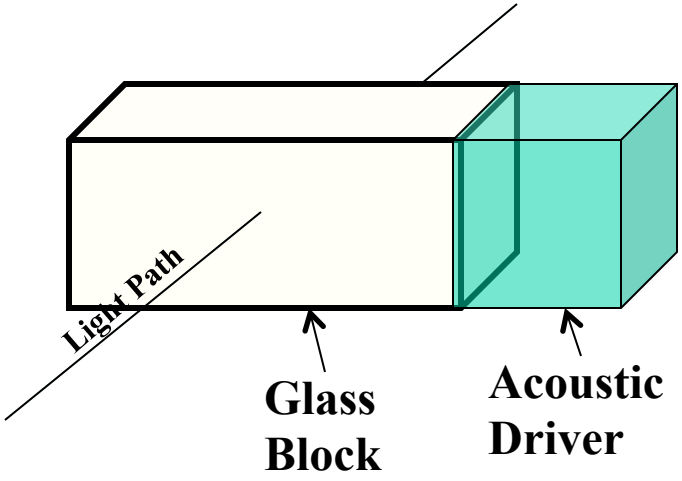

Advantages:

- Typical optical blocks resonate at 20-80 kHz
- Sinusoidal modulation of the retardance
- Large acceptance angle
- Reasonably achromatic
- Amplitude of modulated retardance is adjustable via driver power
- When working, acts as an ultrasonic dog repellant

Issues:

- Typical optical blocks resonate at 20-80 kHz
- Demodulation device must be synchronized to resonant frequency

IV. Requirements for Solar Polarization Measurements

Requirement Categories:

- Polarimetric precision (signal-to-noise ratio)
- Spatial resolution
- Spectral resolution
- Temporal resolution
- Polarimetric accuracy

In solar polarimetric instrumentation, all of these requirements play important roles, and one must balance the tradeoffs among them!

Polarimetric Precision – 1: Photospheric Zeeman Effect

Range of Zeeman polarization signals from photosphere:

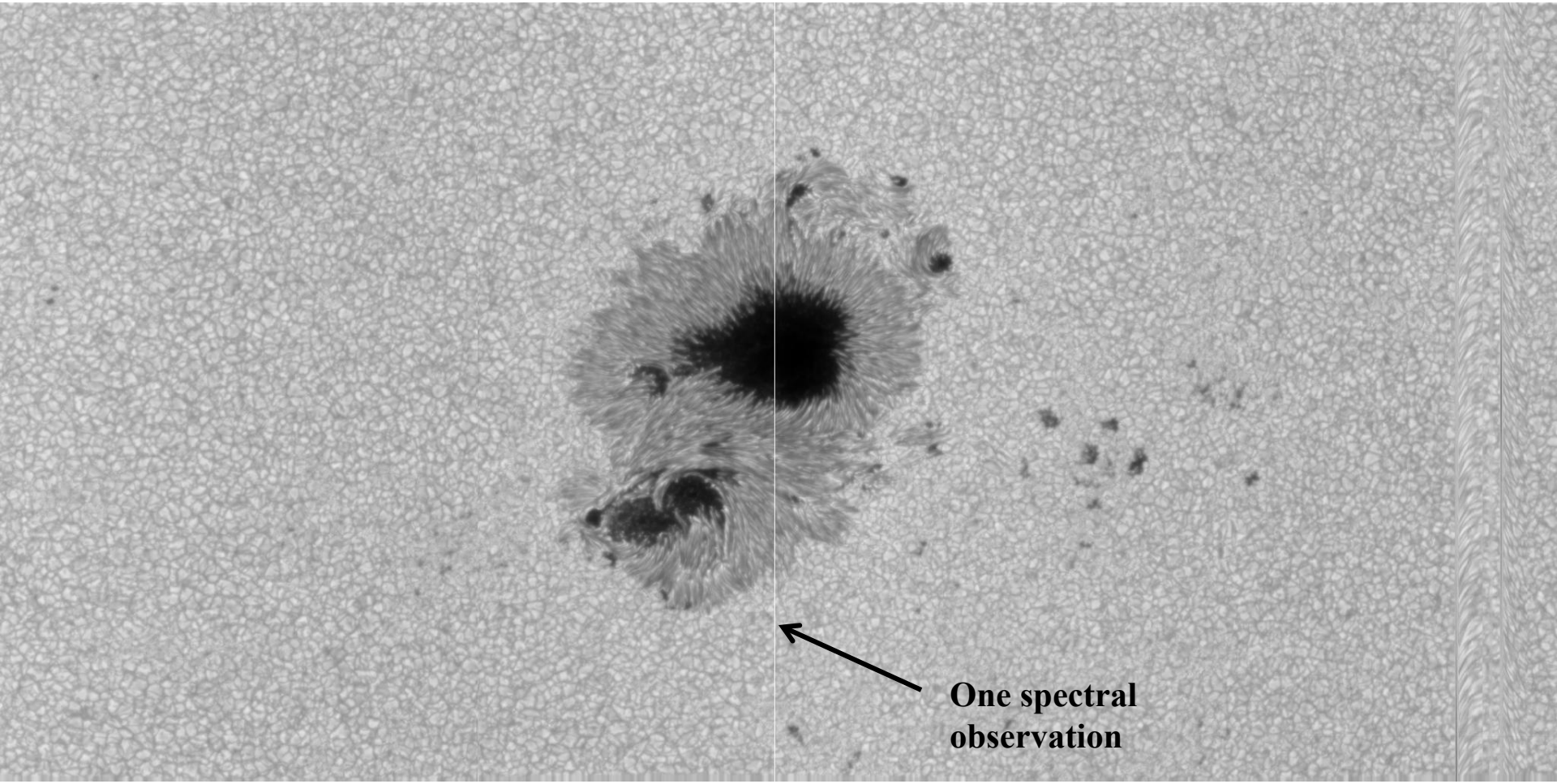

Hinode Spectropolarimeter Continuum Image, 9 December 2006

Polarimetric Precision – 1: Photospheric Zeeman Effect

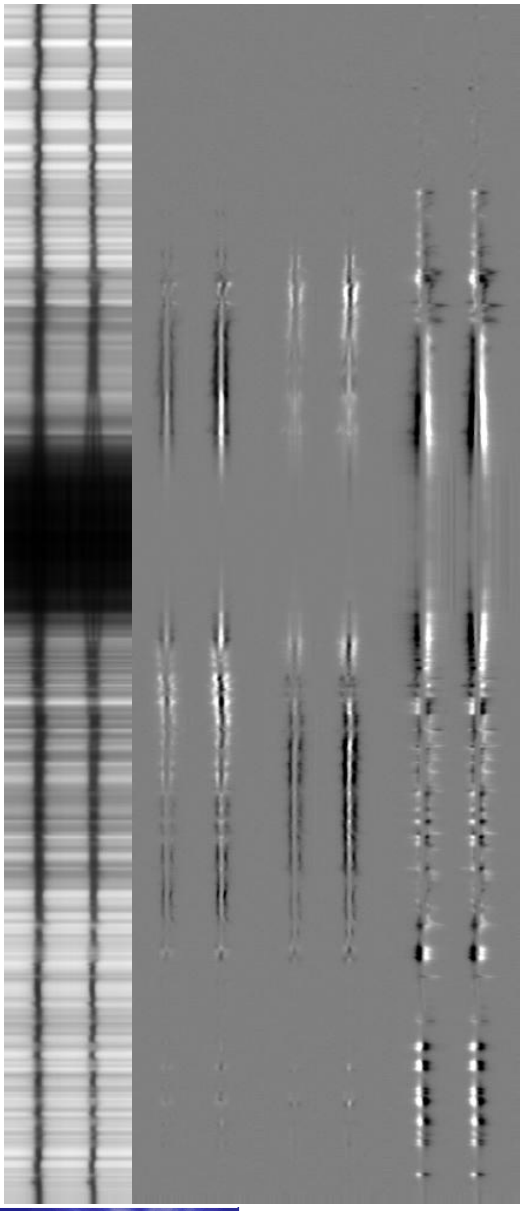

***QUV* Scaling ±0.1I_c**

***QUV* Scaling ±0.005I_c**

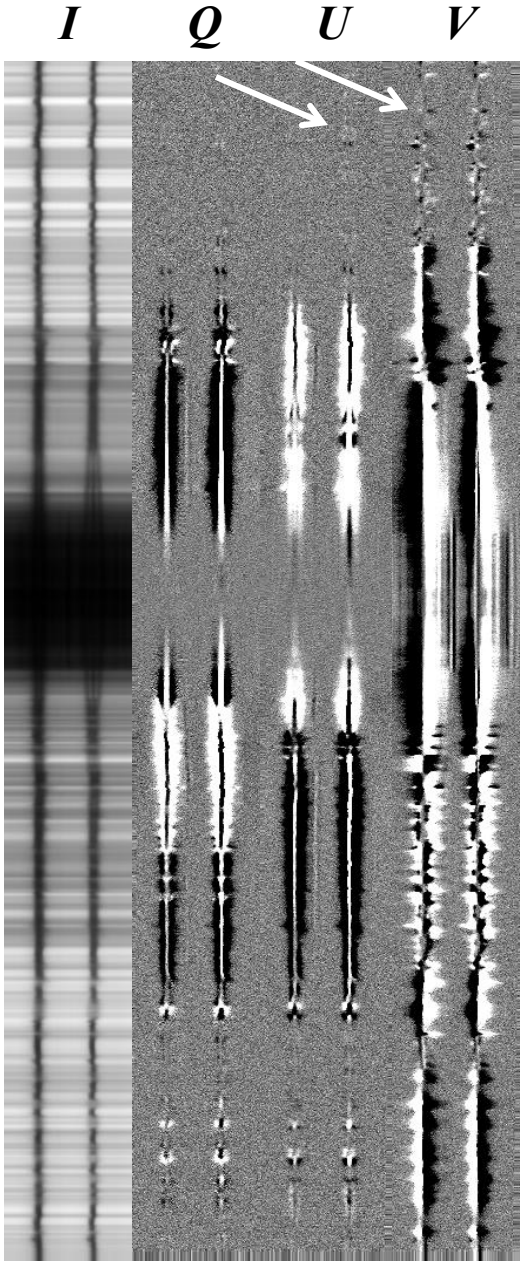

- For Zeeman effect in visible, maximum polarization signal ~0.2I_c (less if lower spectral resolution)
- **Higher polarimetric sensitivity reveals weak polarization features in the quiet Sun**
- Notice that the "salt and pepper" signature of random measurement noise is starting to become visible in the continuum at this scaling
- **Quantitative analysis of magnetic fields is robust when the signal is at least 10x the noise**
- Human eye can pick out very weak signals in the noise

Polarimetric Precision – 1: Photospheric Zeeman Effect

Polarization amplitudes are a few × 10^{-3} or smaller in quiet "internetwork" regions.

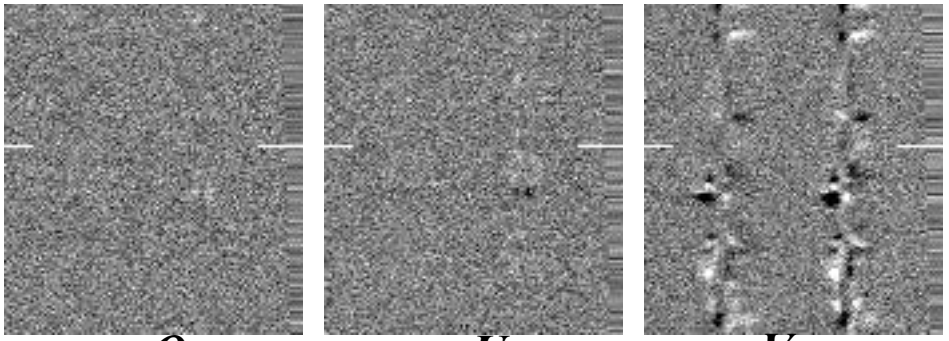

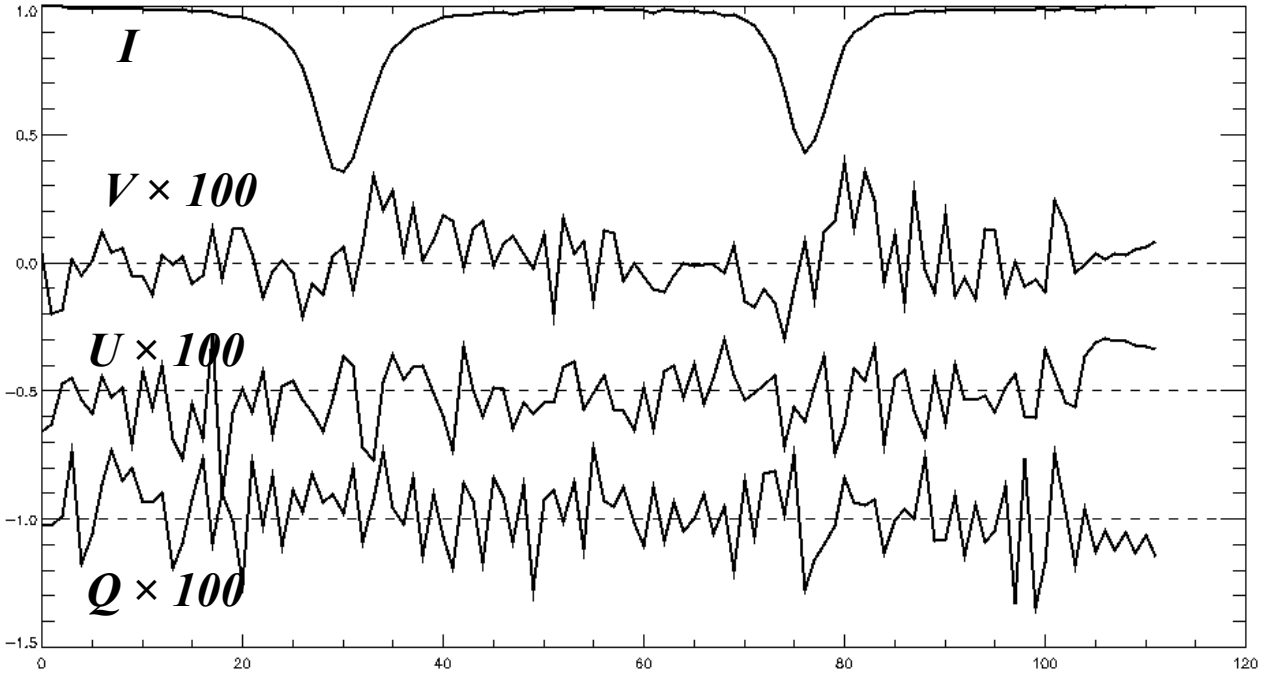

“Normal Map” data:

- **4.8s integration**
- ***rms* Noise = 0.0011 Ic**
- **Scaling = ±0.003**

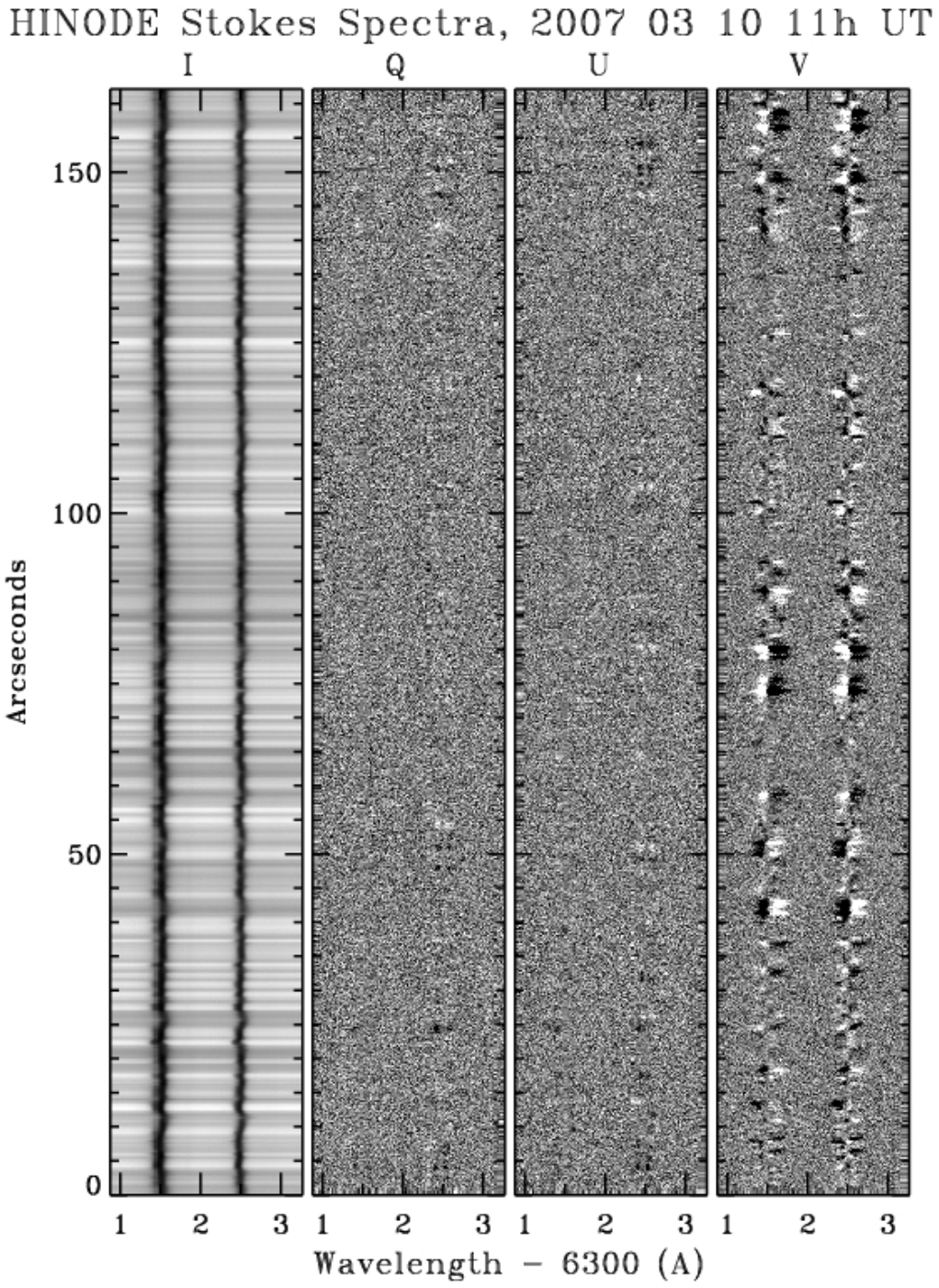

“Deep Magnetogram” Mode Spectrum:

- **9.6 s integration**
- ***Rms* Noise = 0.00078 Ic**
- **Scaling = ±0.003**

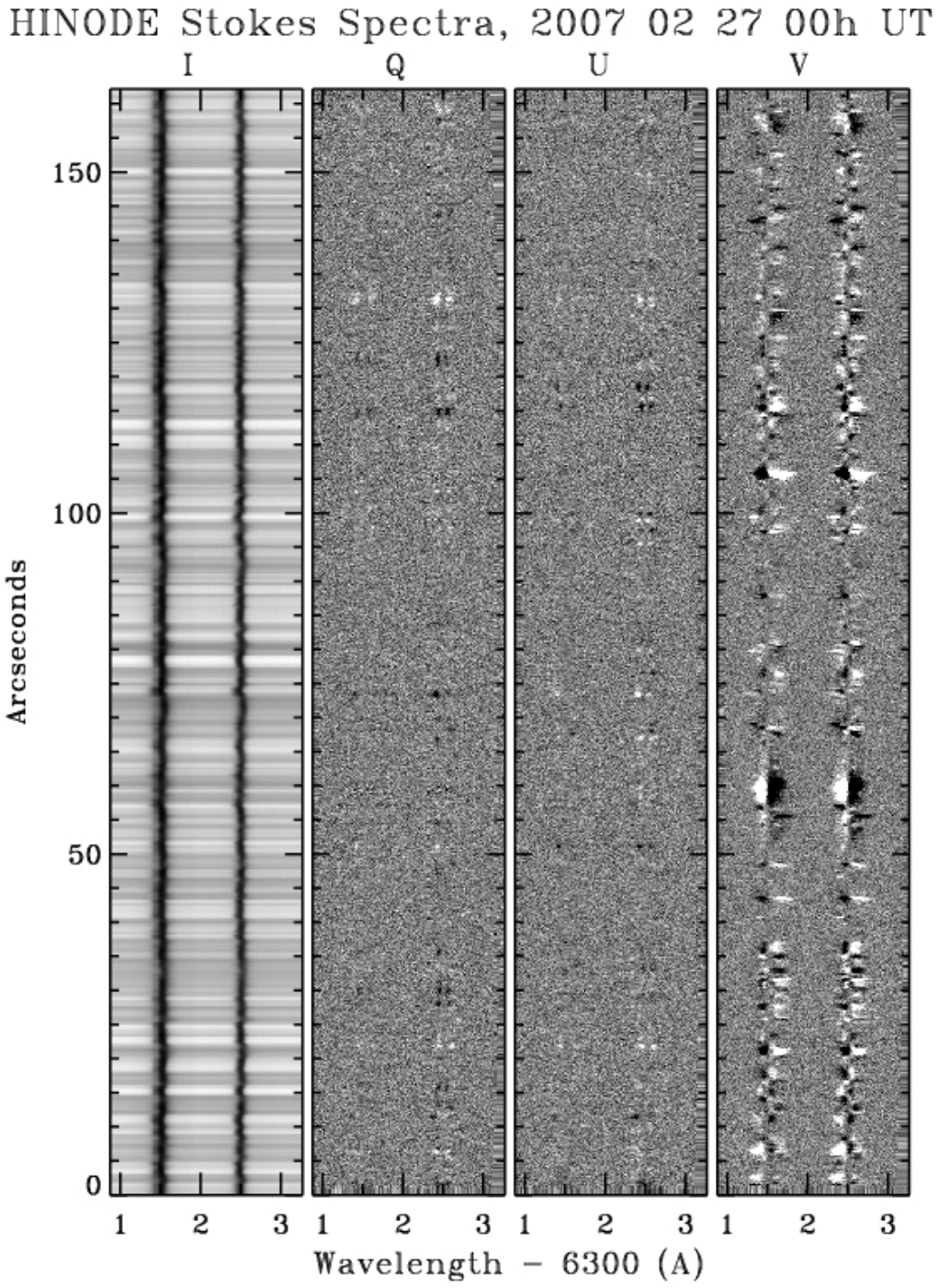

Deep Magnetogram, running time average:

- **67.2 s integration**
- ***Rms* noise = 0.00029**
- **Scaling = ±0.003**

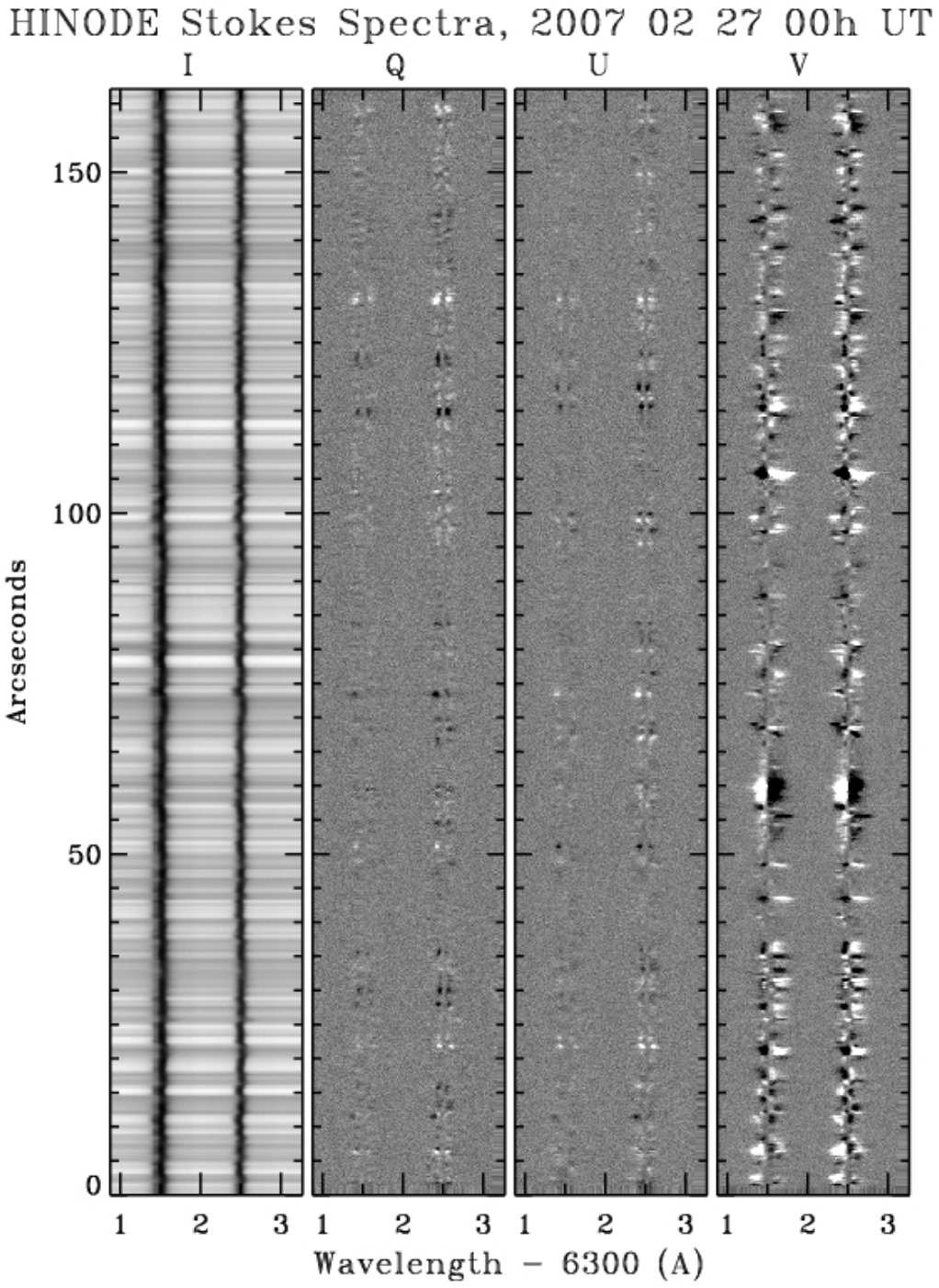

Deep Magnetogram, running time average:

- **67.2 s integration**
- ***Rms* noise = 0.00029**
- **Scaling = ±0.001**
- **Significant Stokes V signals at every position on the slit**
- **Significant Stokes Q,U signals over a large percentage of the slit**
- **Time average degrades *rms* granulation contrast by only .985 (to 7.37%)**

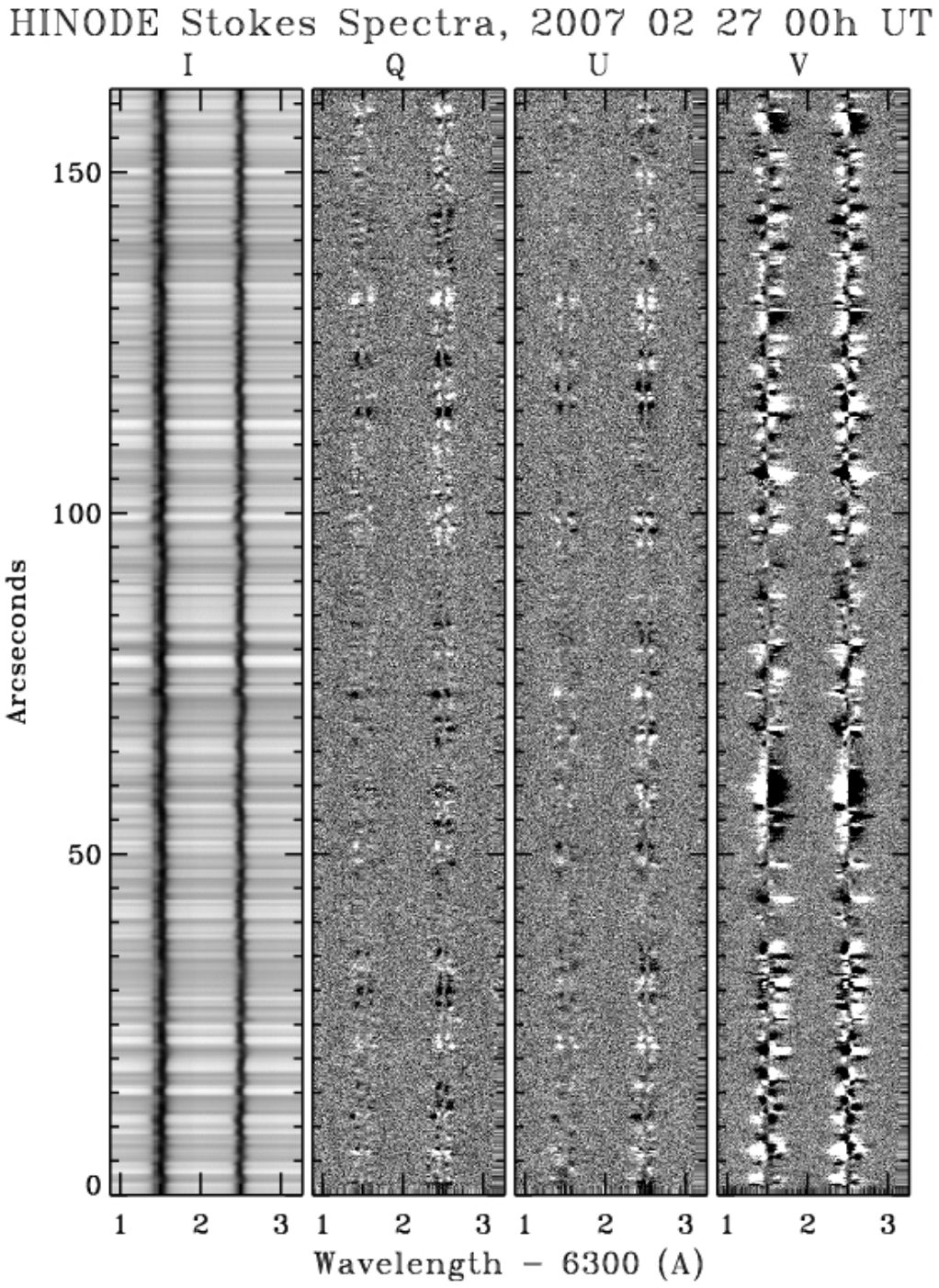

Polarimetric Precision – 2: Chromospheric Zeeman Effect

Simulation of photospheric flux tube expanding through the chromosphere into corona

- Zeeman effect for Ca II 8542 Å
- Circular polarization within reach (10^{-3} to 10^{-2})
- Linear polarization is essentially unobservable (~few × 10^{-6})
- Linear polarization would be in realistic observable range over sunspots
- Scattering polarization will likely dominate Zeeman effect for linear polarization

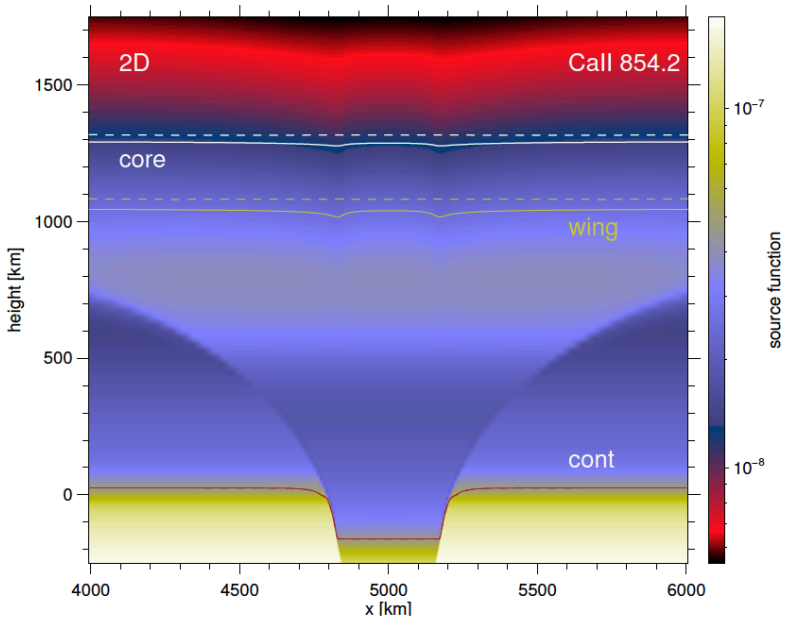

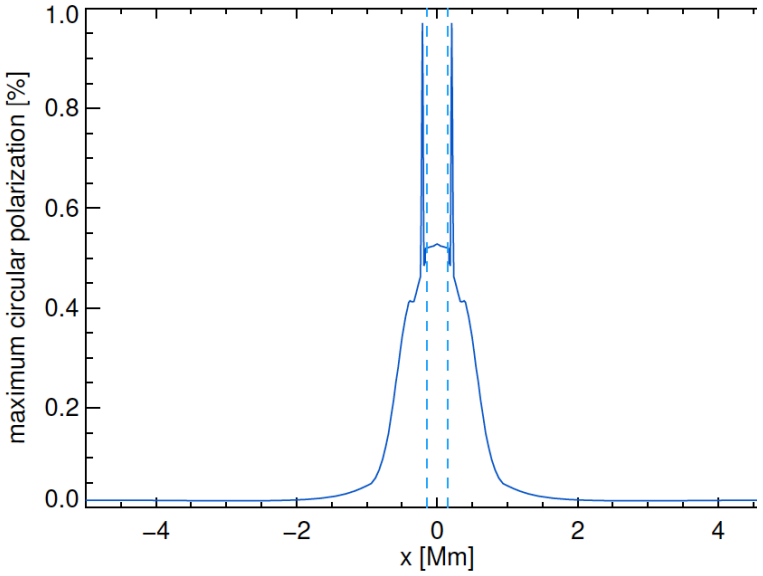

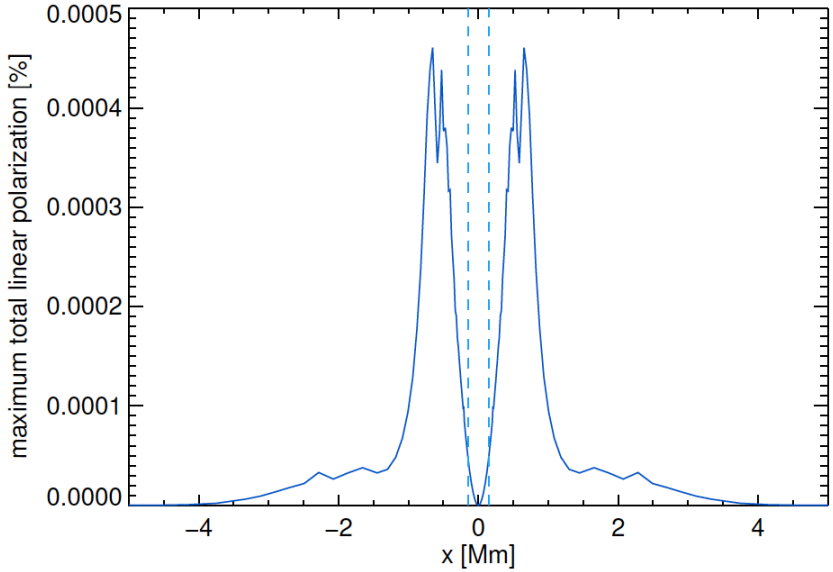

Images from Uitenbroek 2011

Polarimetric Precision – 3: "Second Solar Spectrum"

Scattering gives rise to linear polarization:

- Some portions of the spectrum are rich in linear polarization when observed near the limb
- Maximum polarization is small (typically ~ 10^{-3})
- Visible mainly near solar limb where scattering has favorable geometry for production of polarization

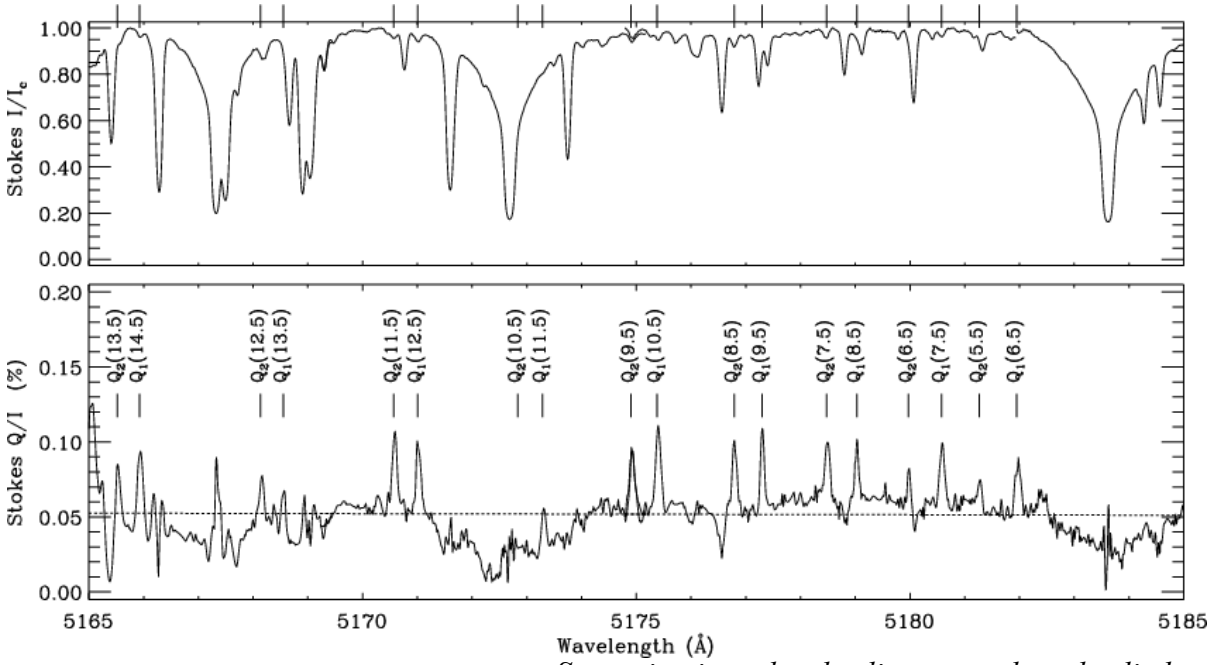

Scattering in molecular lines near the solar limb

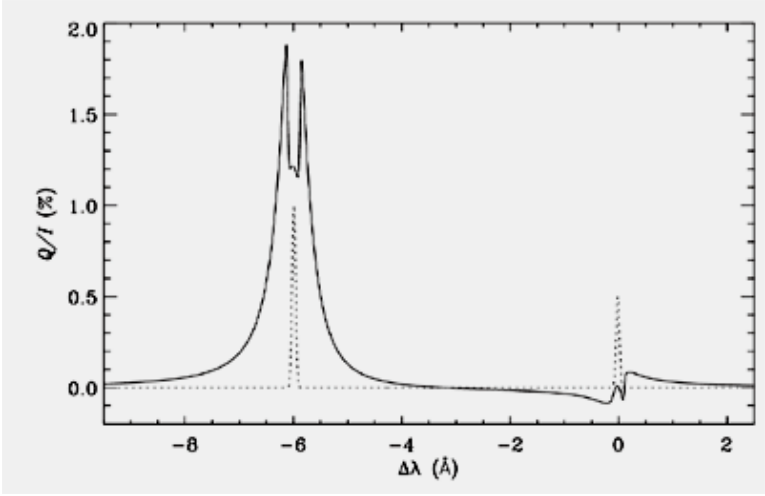

Synthesis of Na D-line scattering polarization just off limb

Polarimetric Precision – 4: Extreme Precision

This record for solar polarimetry still holds?!!!

- Kemp, Henson, Steiner, and Powell 1987
- Sensitivity: *few* × 10^{-7}
- Broad band circular and linear polarization measurements
- Pine Mountain Observatory, Oregon

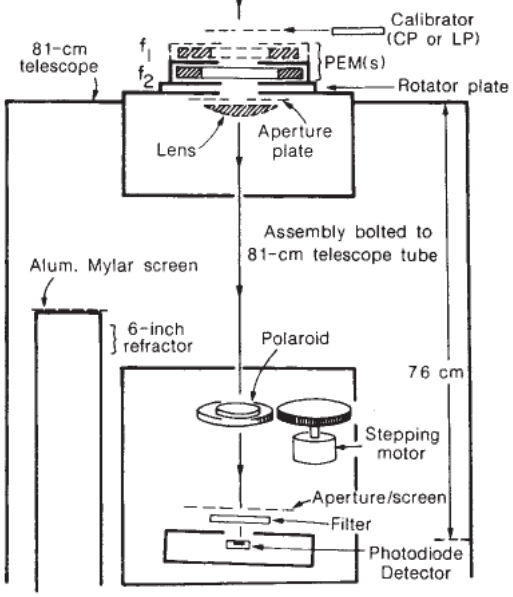

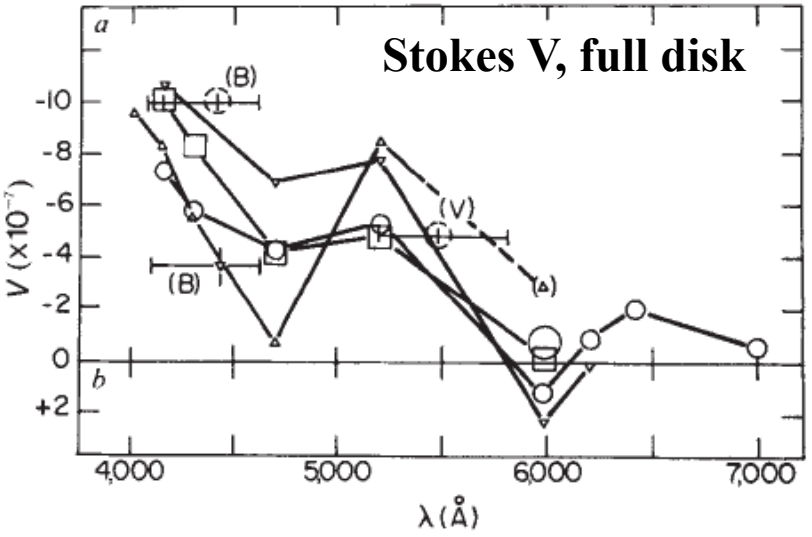

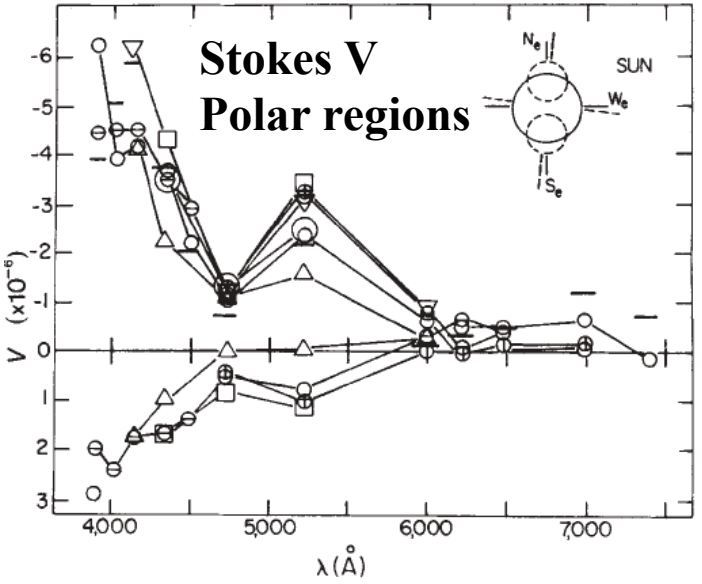

Polarimetric Precision – 5: Photon Gathering

How many photons *N* must be detected to reach a specified signal-to-noise ratio of *R*?

- R is a large number, and photon noise is random, so the signal obeys Gaussian statistics:

For Stokes *I* ----- $N = R^2$

- But typically what is needed is *R* required for the polarization signal. No polarimeter is 100% efficient in modulating the polarization (but schemes sampling only one state of polarization, i.e. *V*, can approach perfection). A polarimeter that modulates *Q, U,* and *V* with equal efficiency has a **maximum theoretical modulation efficiency* of $1/\sqrt{3} = 0.577$.** This means that usually one needs almost $2R^2$ detected photons
- For $R = 10^4$, $N \sim 2 \times 10^8$ detected photons
- Typical CCD detector full-well is 10^5 photoelectrons, therefore would **need 2000 reads of the CCD to achieve S/N = 10^4!**
- *Notes:*
  - *a.* *R* is customarily indicated for the continuum of a spectral observation. It can be significantly smaller in the cores of strong absorption lines
  - b. Typical efficiency of solar optical systems is a few percent at best

*del Toro Iniesta & Collados 2000

Polarimetric Precision – 5: Photon Gathering

Example of influence of various optical elements in a spectro-polarimeter

Moral: make your optical system as simple as possible!!!

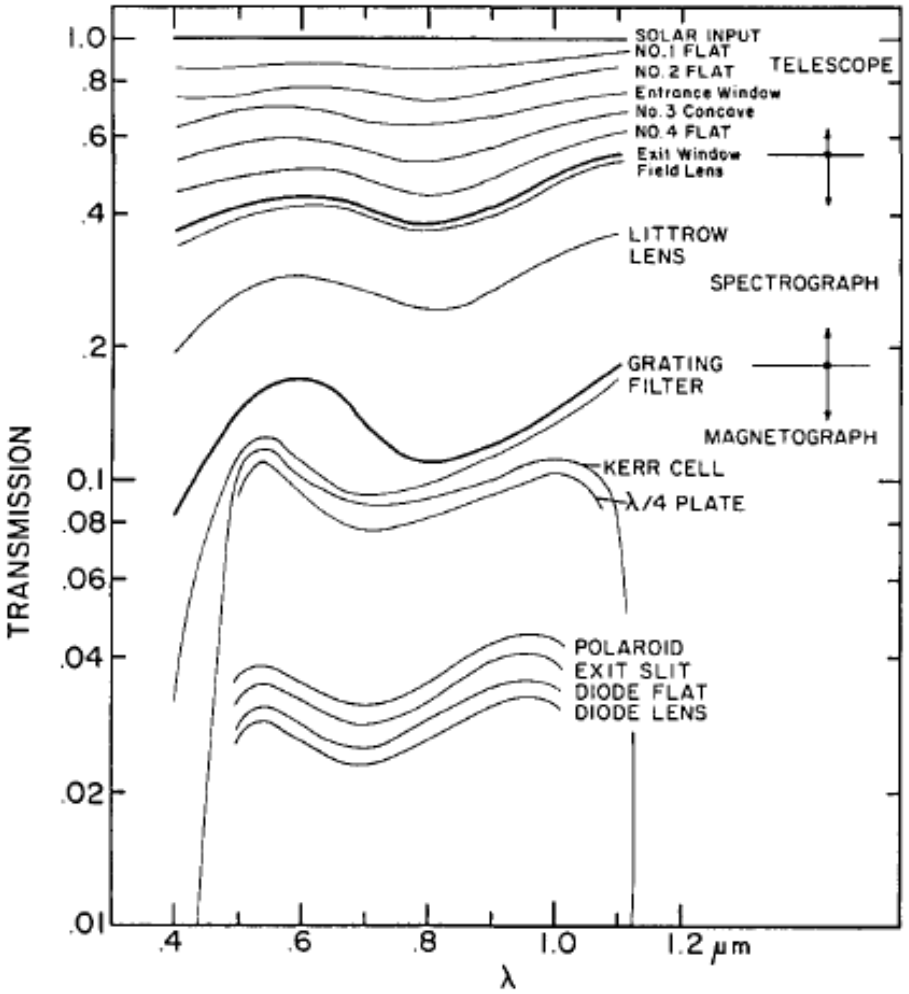

From Pierce et al. 1976

Polarimetric Precision – 5: Photon Gathering

Question: *Does building a bigger telescope provide you with more photons?*
Answer: *Yes and No!*

- *YES!* A larger telescope collects more photons, and these are presented to the focal plane of the telescope.

- *NO!*
  - The Sun is an extended source of light: it fills the image plane of a telescope:
  - The photon flux from the Sun per diffraction resolution limit θ is independent of aperture diameter D:

$$\theta = 1.22\,\lambda/D$$

angular resolution area: $\pi(\theta^2/2) = 0.744\,\pi\lambda^2/D^2$

solar flux at focal plane: $\sim \pi D^2/4$

  - However, smaller features on the Sun move faster across the resolution element, so shorter exposures are necessary at higher resolution!
- **New large telescopes will often operate well away from their diffraction limits in order to gather enough photons for high-precision polarimetry**

Angular Resolution– 1: How Much is Enough?

Solar physicists demand higher and higher angular resolution:

- Photon mean free path in photosphere ~ 50 km (0.07 arc seconds)
- Magnetic structures (current sheets, reconnection zones) could be very much smaller (~meters???)

- How small is 0.07 arc seconds? Granules visible in this movie are about 30 times this size
- Bright structures between granules signal the location of intense magnetic flux
- It would be nice to resolve these structures spatially (and with height) at high polarimetric precision to understand the structure and evolution of these small scale magnetic fields

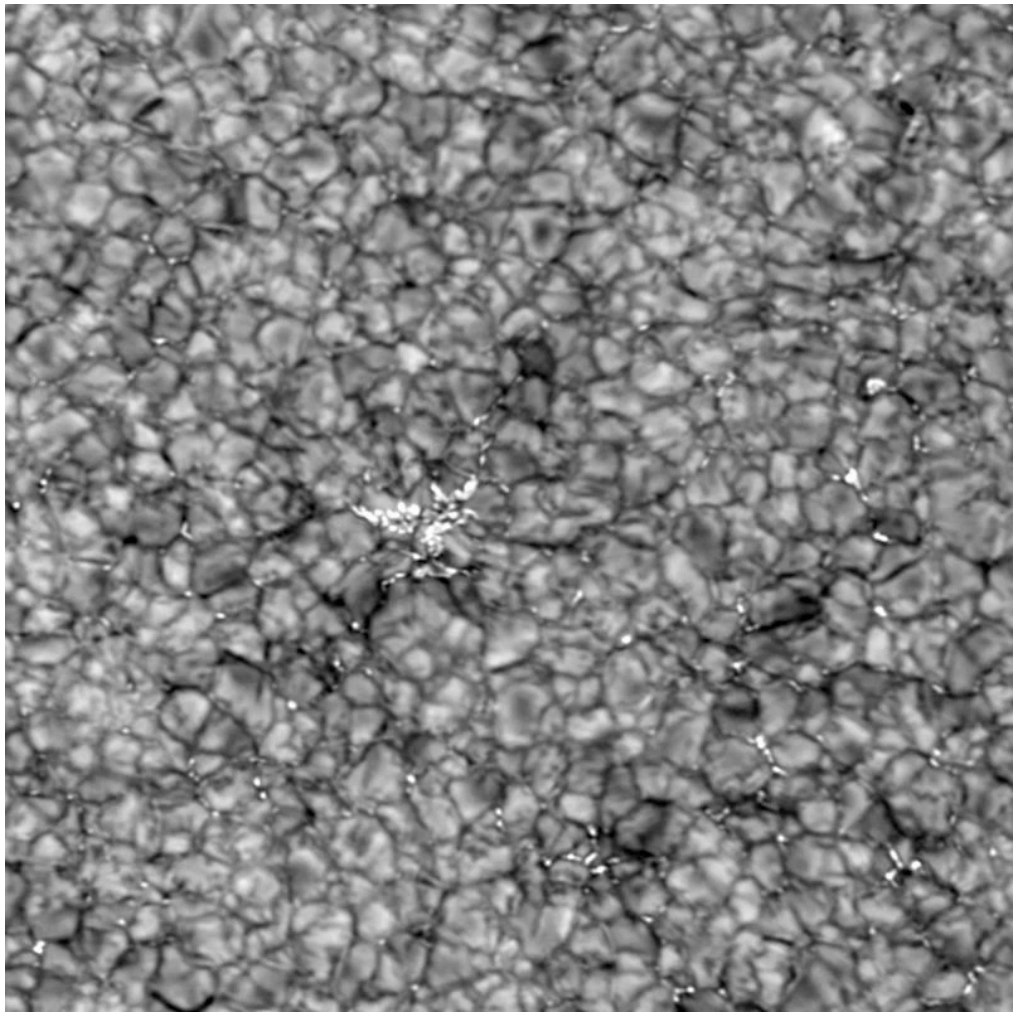

From Institute for Solar Physics website: http://www.isf.astro.su.se/

Angular Resolution– 2: Tradeoff with Speed

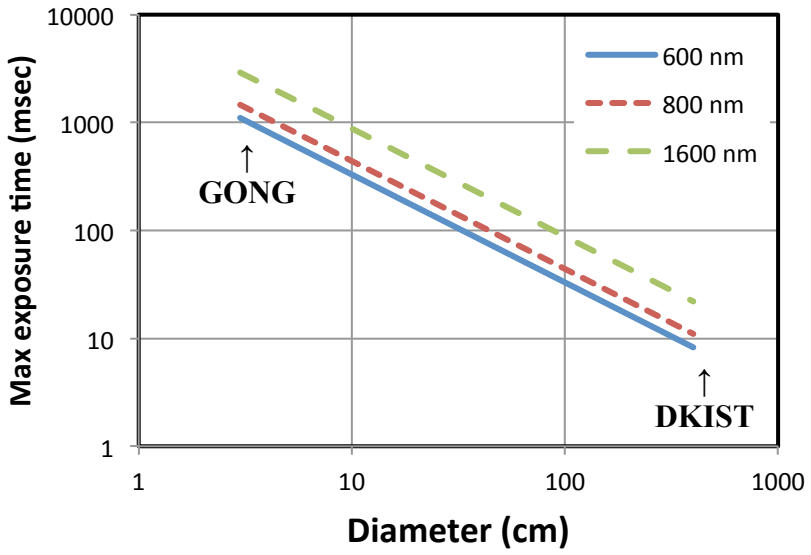

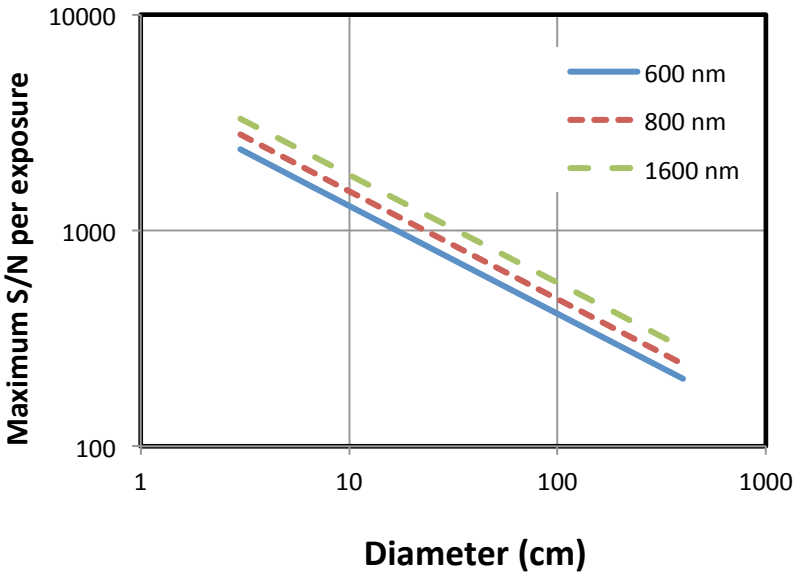

After Keller 2001, via Harvey 2015

Assumptions:

- Diffraction limit at disk center
- 2 pix/resolution limit; **10% overall efficiency!!**
- **0.05 pixel proper motion allowed @ 5km/s**
- S/N is for Stokes *I* continuum; worse for *Q,U,V* and in line core

Angular Resolution– 2: Tradeoff with Speed

- This formulation assumes that feature moves ½ resolution element during the exposure time (very much an upper limit!)
- At optimum tradeoff: $\sigma = [2\,\Delta x^3/v]^{1/2}\,F^{1/2}$

Tradeoff: solar evolution vs. noise:

- Maximum integration time Δt_e allowed by solar evolution:

$$\Delta t_e = \frac{2\,\Delta x}{v}$$

- Minimum integration time to reach a given required rms noise level σ:

$$\Delta t_s = \frac{1}{F\sigma^2\Delta x^2}$$

Δx: spatial sampling,
v: evolution speed,
F: Flux [phot / (s · arcsec^2)]

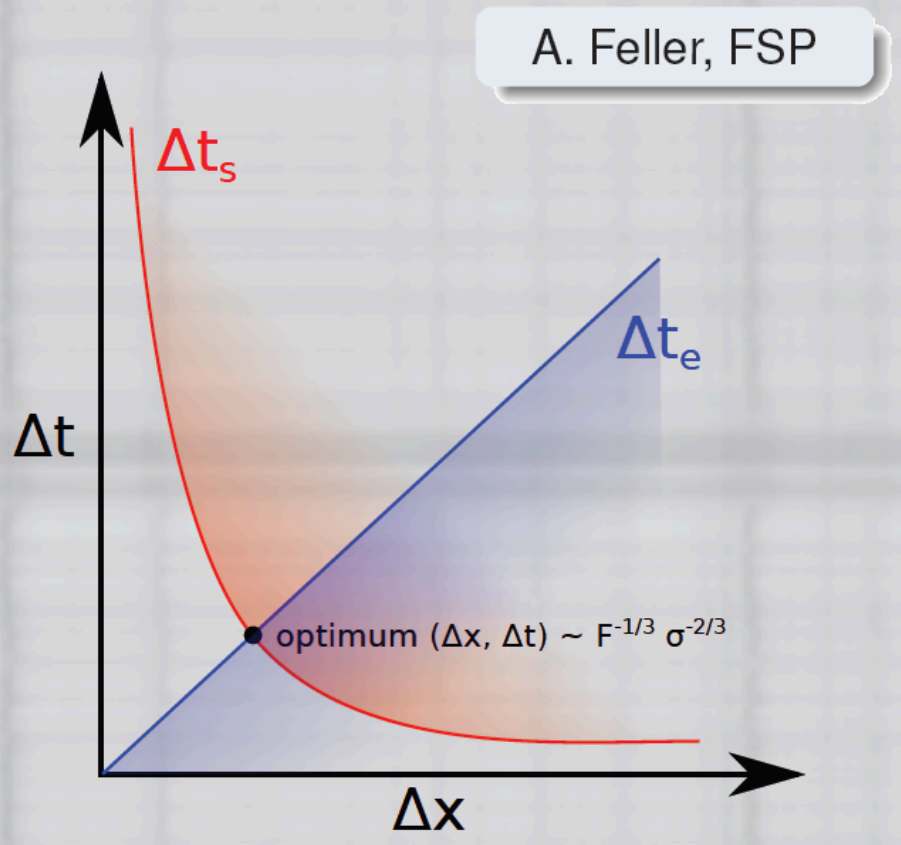

Illustration courtesy of A. Feller (MPS) via A. Lagg (MPS)

Angular Resolution– 3: Chromosphere Fields

- The magnetic field is highly structured in the photosphere
- The photosphere (and also chromosphere) are **highly stratified** in the vertical direction: some 6-7 orders of magnitude of density in 1000-2000 km of height
- Strong, small-scale fields must expand with height, so the chromospheric (and coronal) field should be ***much smoother (and weaker)*** than in the photosphere (**except for current sheets!!**)
- As a result, we can usually relax the spatial resolution requirements for the chromosphere

- Horizontal density changes (on separate field lines) can be highly structured, but that is not the magnetic field!
- One can usually relax the spatial resolution requirements of the photosphere for the chromospheric and coronal fields

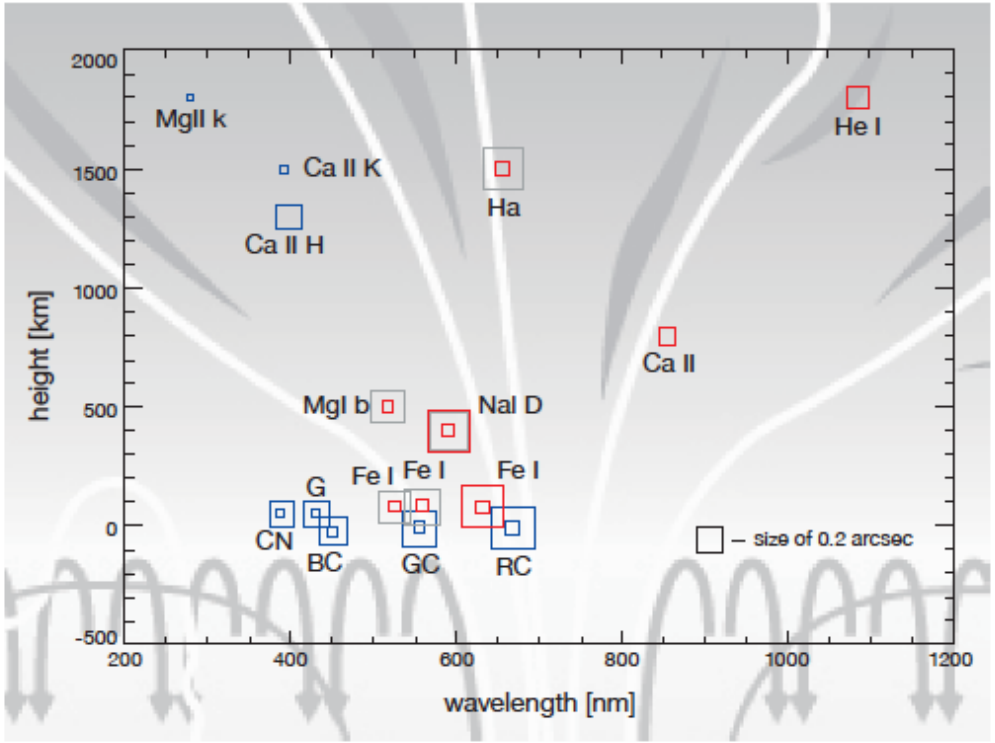

Illustration from Solar-C Mission Proposal, JAXA, NAOJ, NASA, ESA)

Spectral Resolution – 1: Profile Distortions

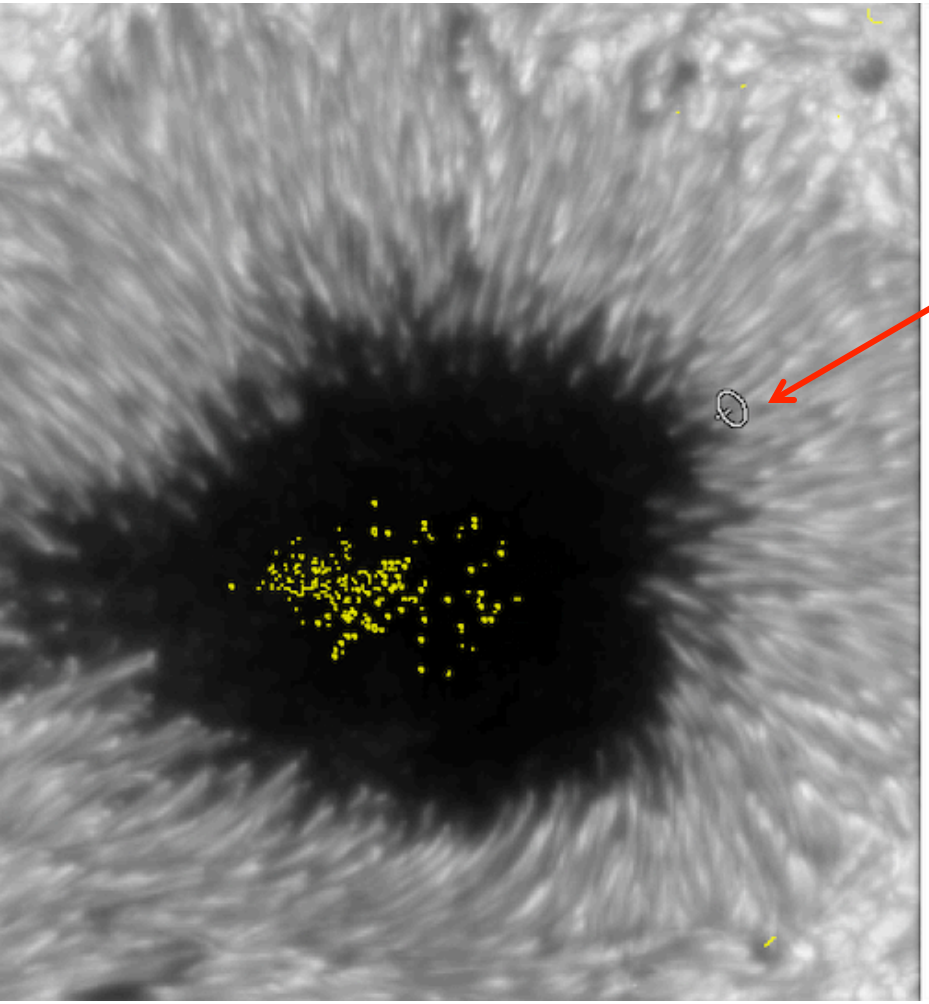

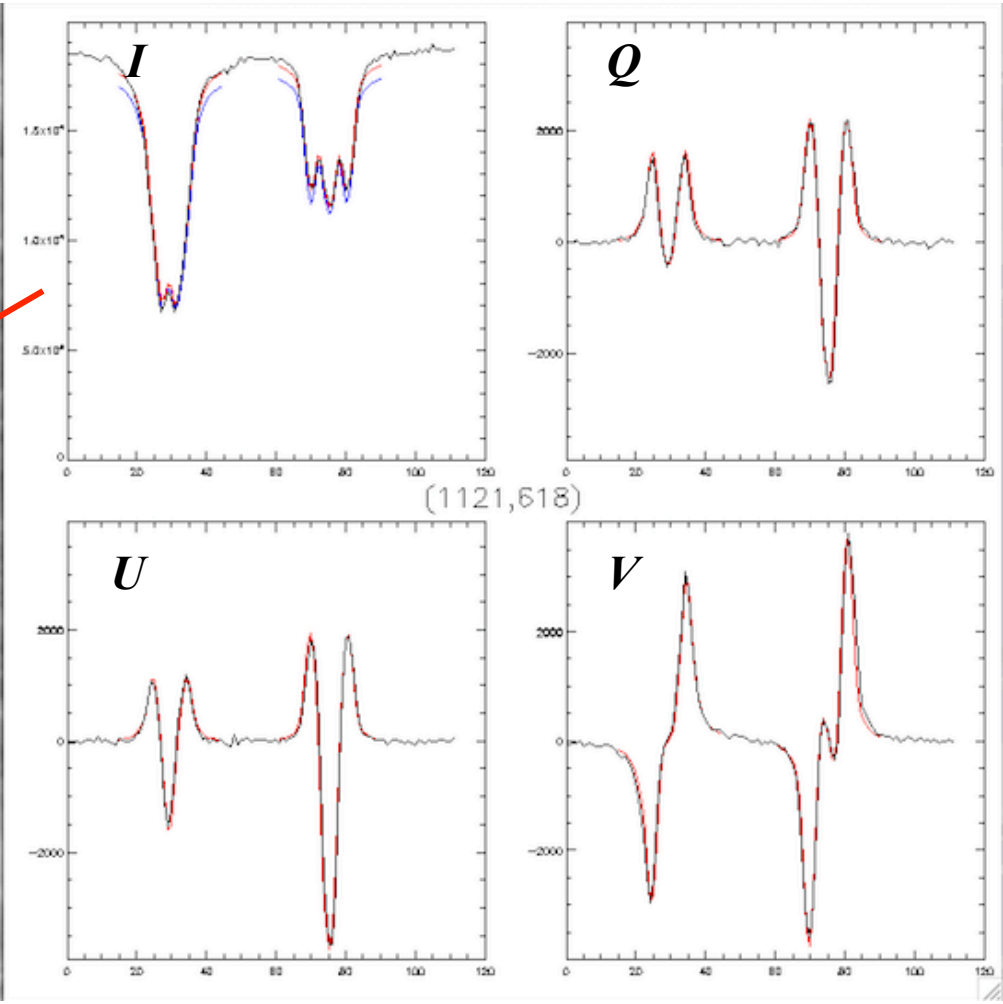

Spectral Resolution – 1: Profile Distortions

- Most filtergraphs operate in the range of 50 < FWHM < 100 mÅ
- Subtle profile features allow one to infer the vector field quantitatively (visible lines)
- Magneto-optical effect is sensitive to inclination of the field and to the line opacity
- Stokes *I* plays a crucial role in determining the magnetic fill fraction

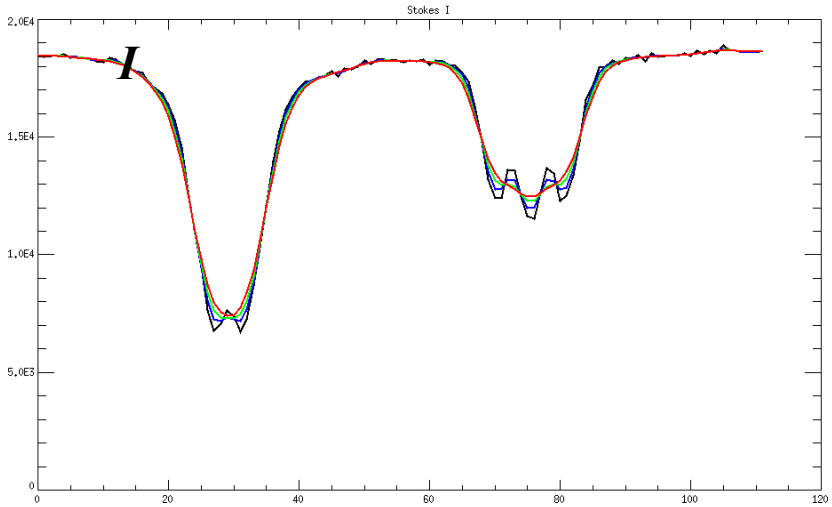

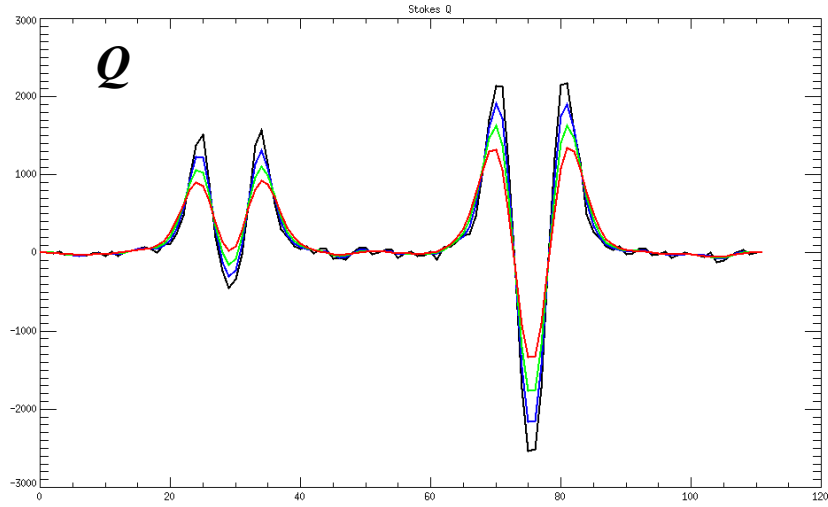

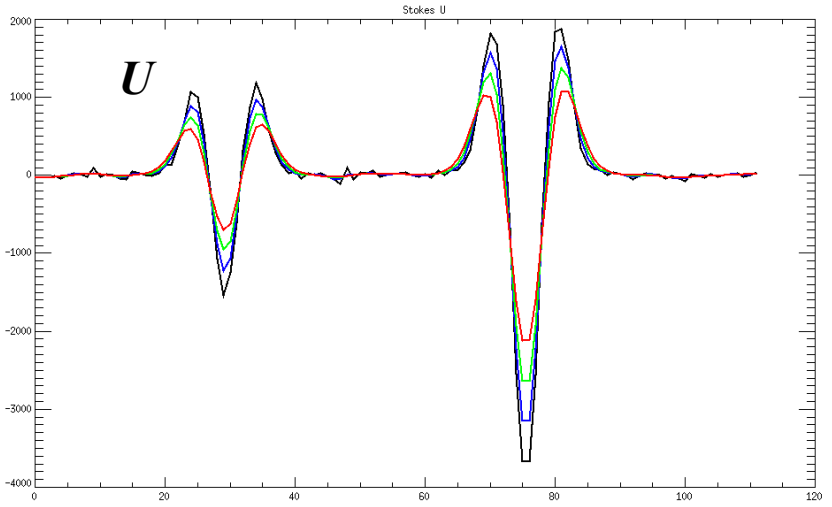

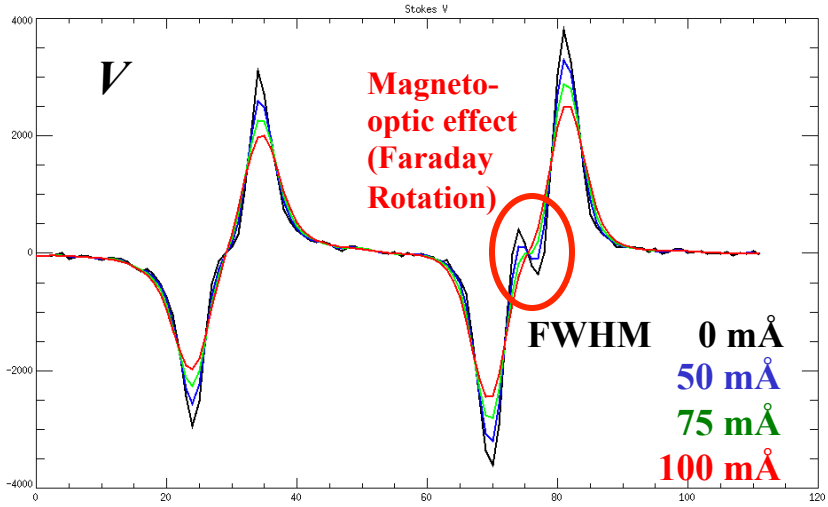

Spectral Resolution – 2: Spectral Coverage

Simultaneous use of two lines having similar formation properties, but differing sensitivity to Zeeman effect improves accuracy of field measurement

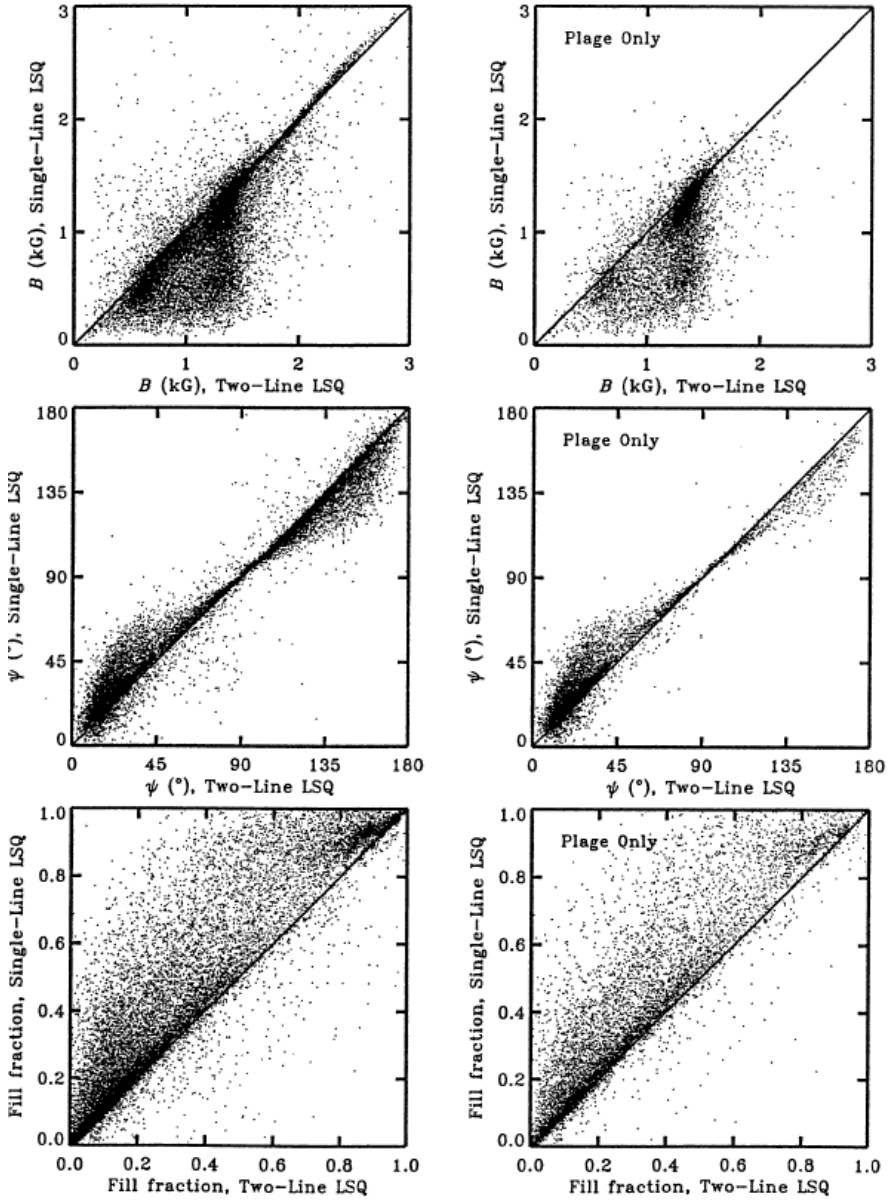

Illustration from Lites et al. 1994

Spectral Resolution – 3: Wavelength Sampling

- At some point one loses information with coarser wavelength sampling
- Nowadays there is an objective way to gauge the sampling interval necessary for a given *S/N*: Principal Components Analysis (PCA)
- Solar information contained in Stokes profiles measured at $S/N = 10^3$ may be represented uniquely by about 10 – 15 orthogonal functions[1]
- In the case of the Fe I 630nm lines: 30-40 mÅ sampling
- Note 1: orthogonal functions likely NOT represented by uniform spectral sampling!
- Note 2: Higher spectral sampling at the same *S/N* improves the overall *S/N* of the observation!

[1] *Casini et al. 2013*

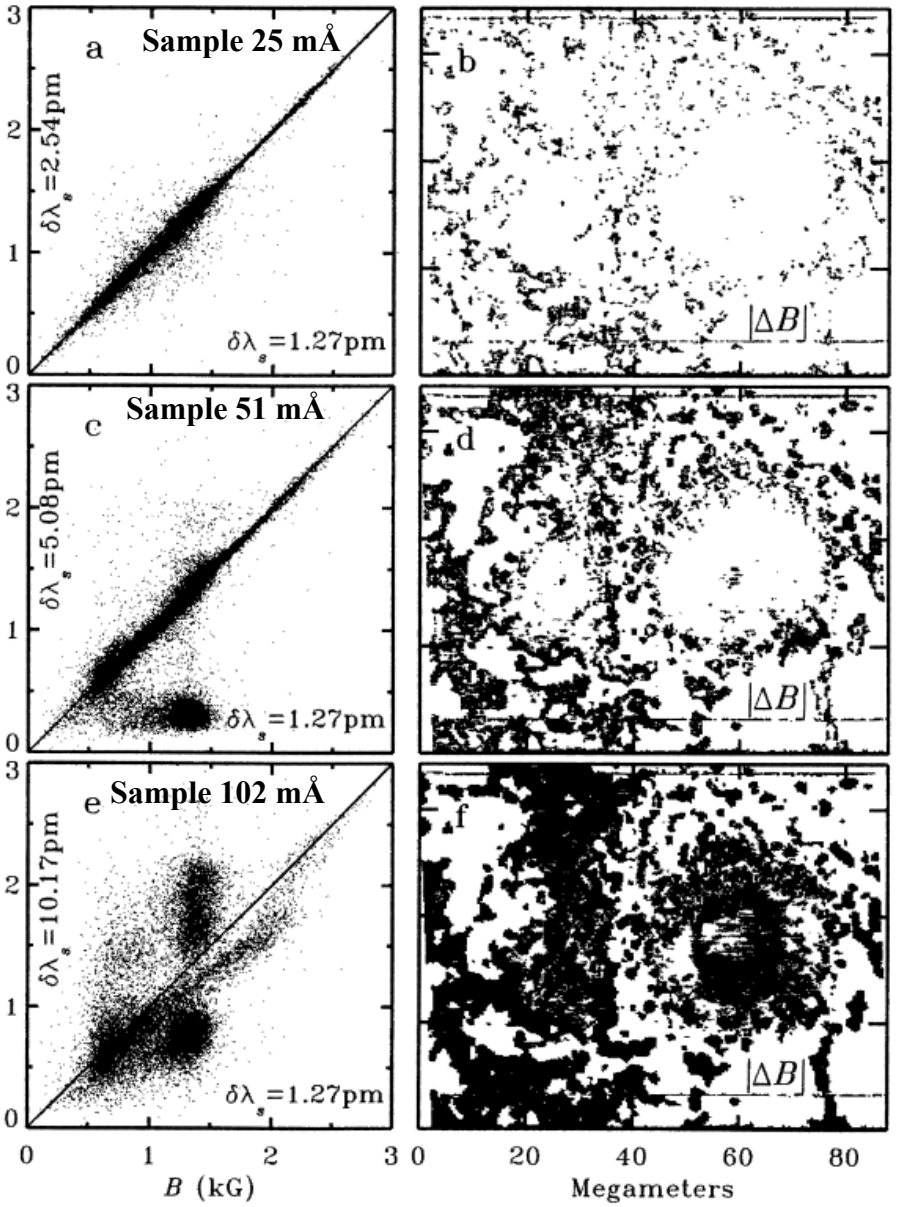

Illustration from Lites et al. 1994

Polarimetric Accuracy

(will be presented in final section on polarization calibration)

V. Approaches to Solar Polarimetry

- **Broad-band Polarimetry**
- **Longitudinal Magnetometry**
  - **Full Stokes Polarimetry**
  - **Zeeman effect**
- **Scattering polarization**
- **Polarization Modulation Schemes**
- **Dual-Beam Polarimetry**
- **Polarization Modulation Efficiency**
- **Seeing, Image Motion, and Modulation Rate**

Broad-Band Polarimetry – 1: Net Circular Polarization

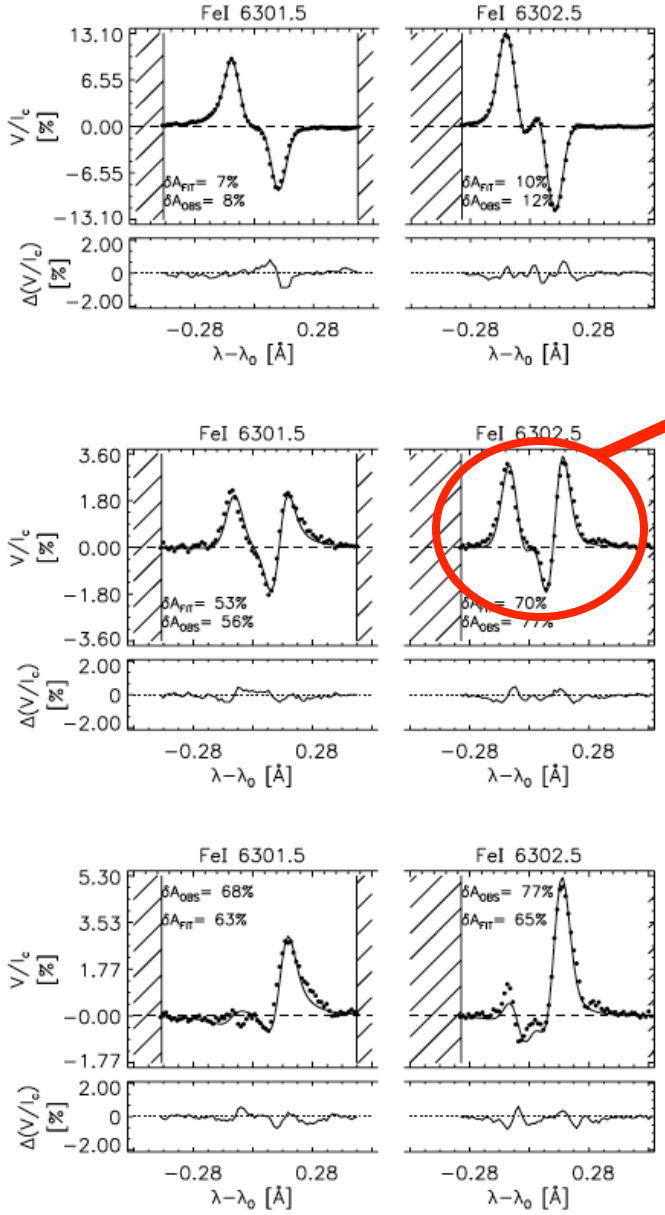

From Borrero et al. 2006

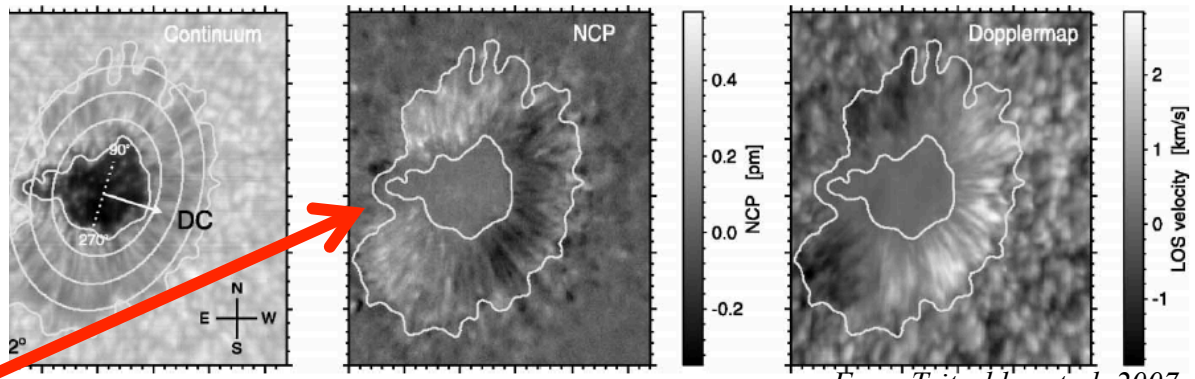

From Tritschler et al. 2007

Net Circular Polarization $NCP = \int V(\lambda) d\lambda$

- Departures from wavelength asymmetry of Stokes *V* give rise to ***NCP***
- Many lines will have similar ***NCP***, so there will be ***broadband circular polarization***
- ***NCP*** arises from gradients of flows along the line-of-sight
- ***NCP*** can be used as a diagnostic of atmospheric structure

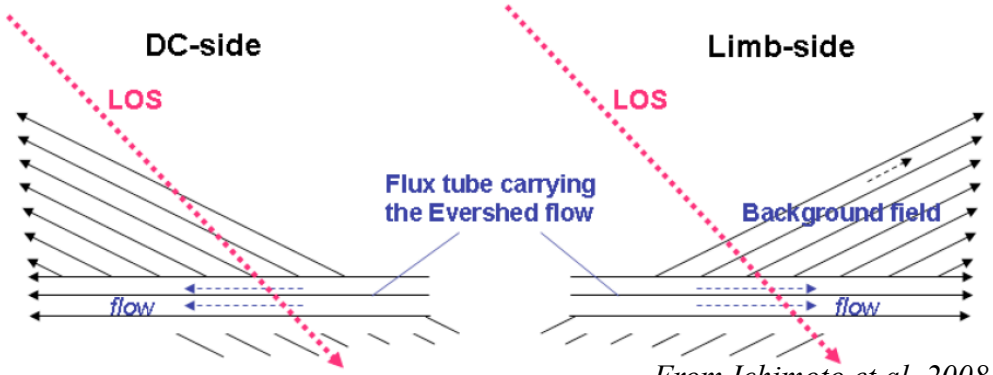

From Ichimoto et al. 2008

Broad-Band Polarimetry – 2: Net Linear Polarization

Net Linear polarization can be used to judge statistical dominance of vertical or horizontal fields in the quiet Sun:

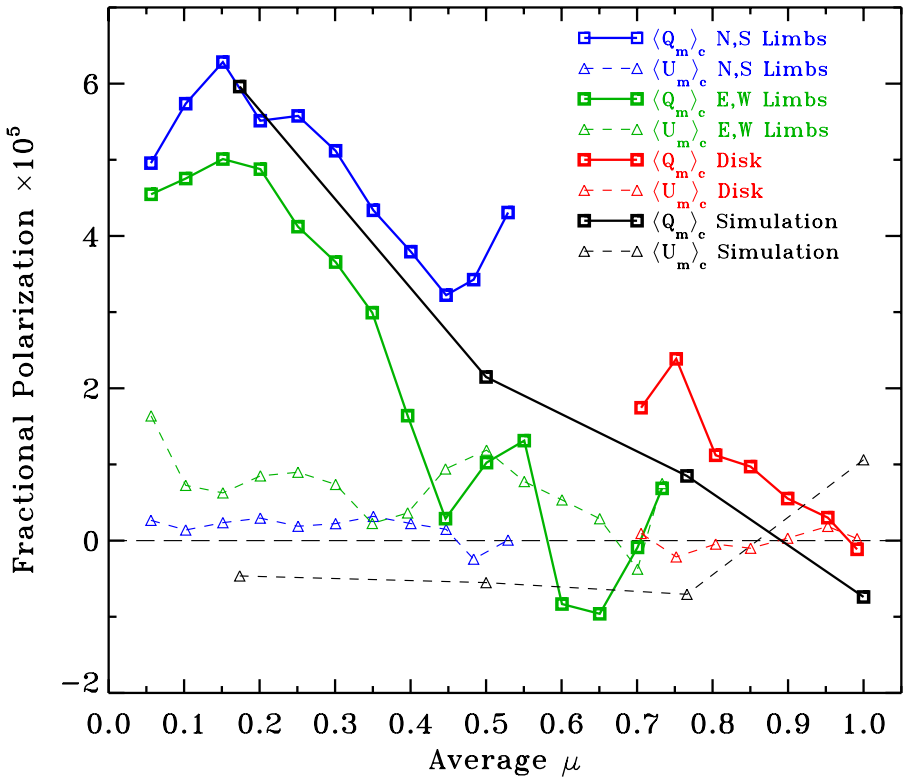

Illustration from Lites et al., 2017

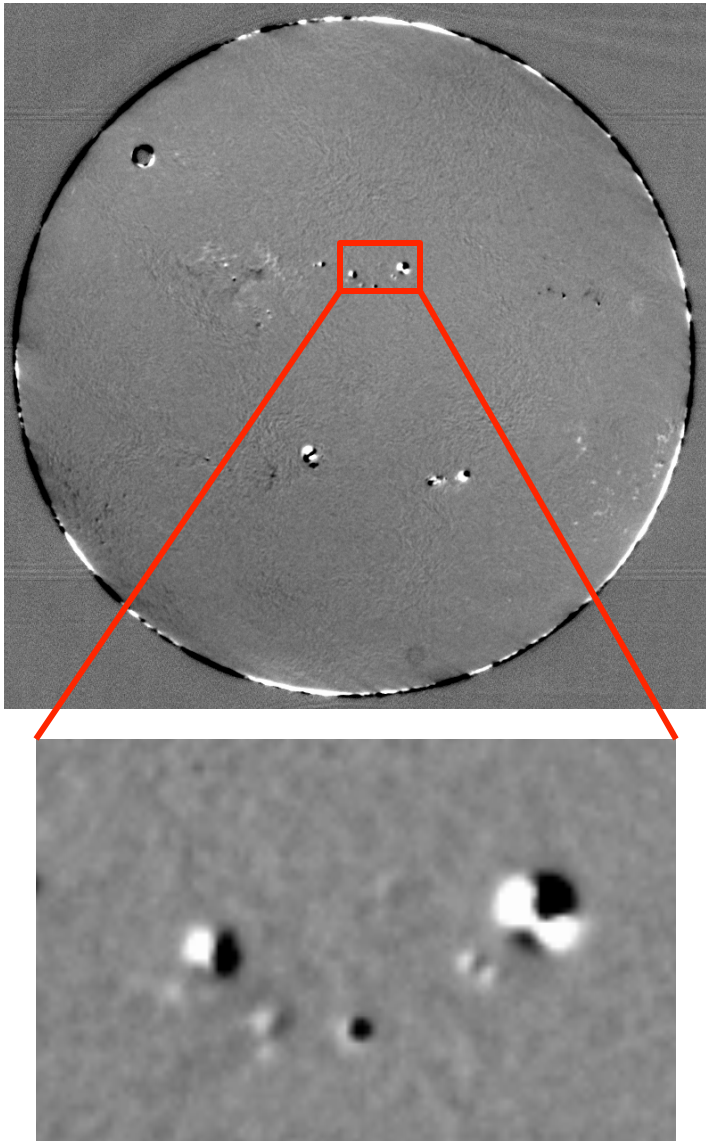

Images from GONG instrument, courtesy J. Harvey, 2015

Longitudinal Magnetometry– 1: Circular Polarization

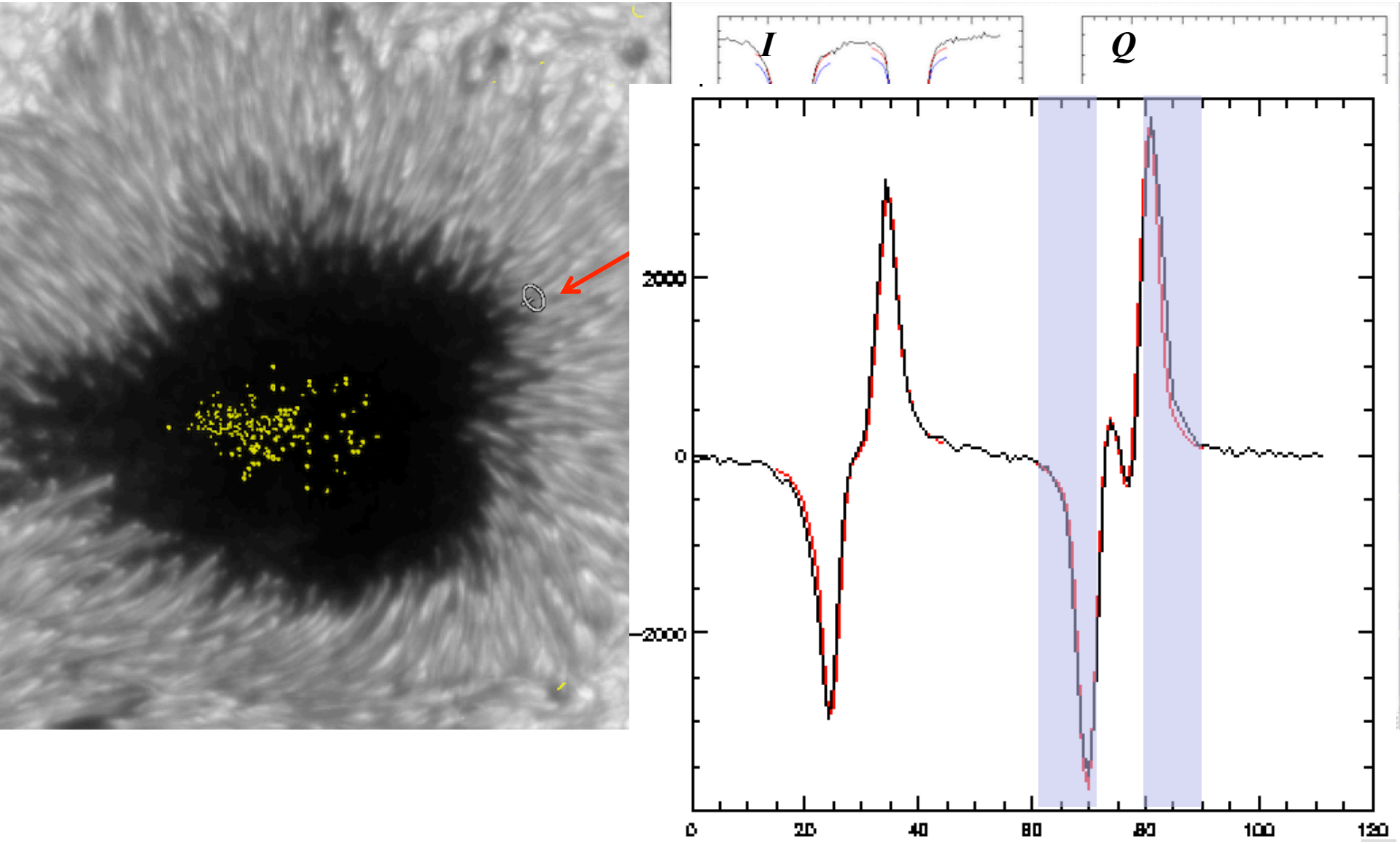

Longitudinal Magnetometry - 2

- Stokes *V* measurement only – Zeeman effect sensitivity to the line-of-sight field component
- Usually at one or two wavelengths only
- Usually filtergraphic measurement (but not always!)
- Many synoptic instruments, past and present
  - Ground-based: Mt. Wilson, Kitt Peak, SOON, SOLIS, Stanford Wilcox …….
  - Space-based: MDI, HMI
- Quantative results limited to the apparent magnetic flux B^L_{app}, not the intrinsic field strength |**B**|

MDI, Solar Maximum, 2002

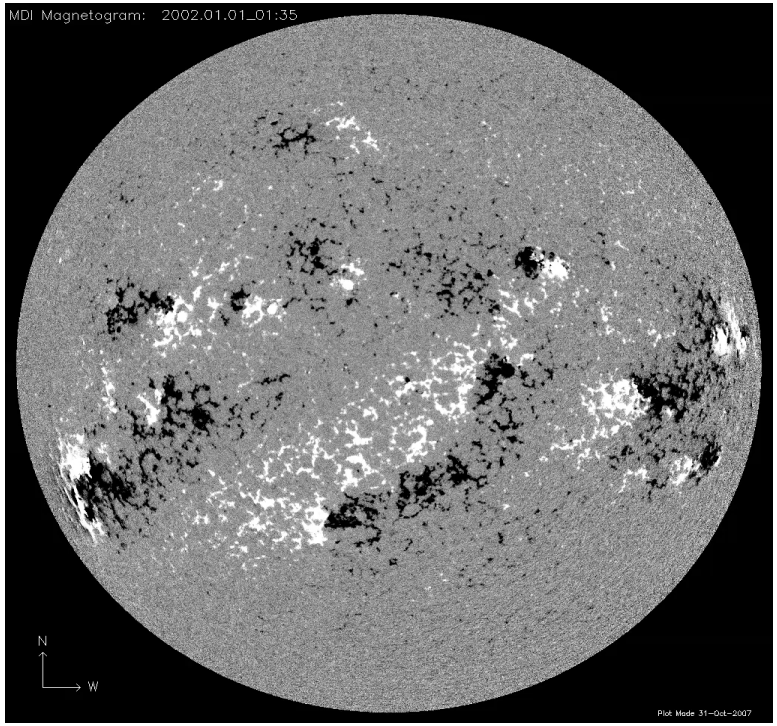

MDI, Solar Minimum, 2009

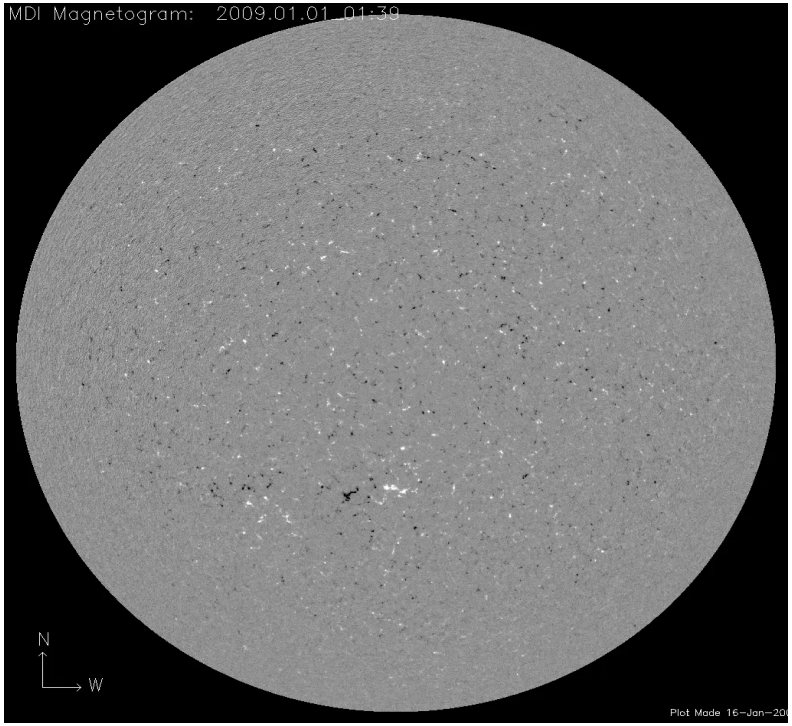

Longitudinal Magnetometry – 3: Can Provide Very Useful Scientific Results

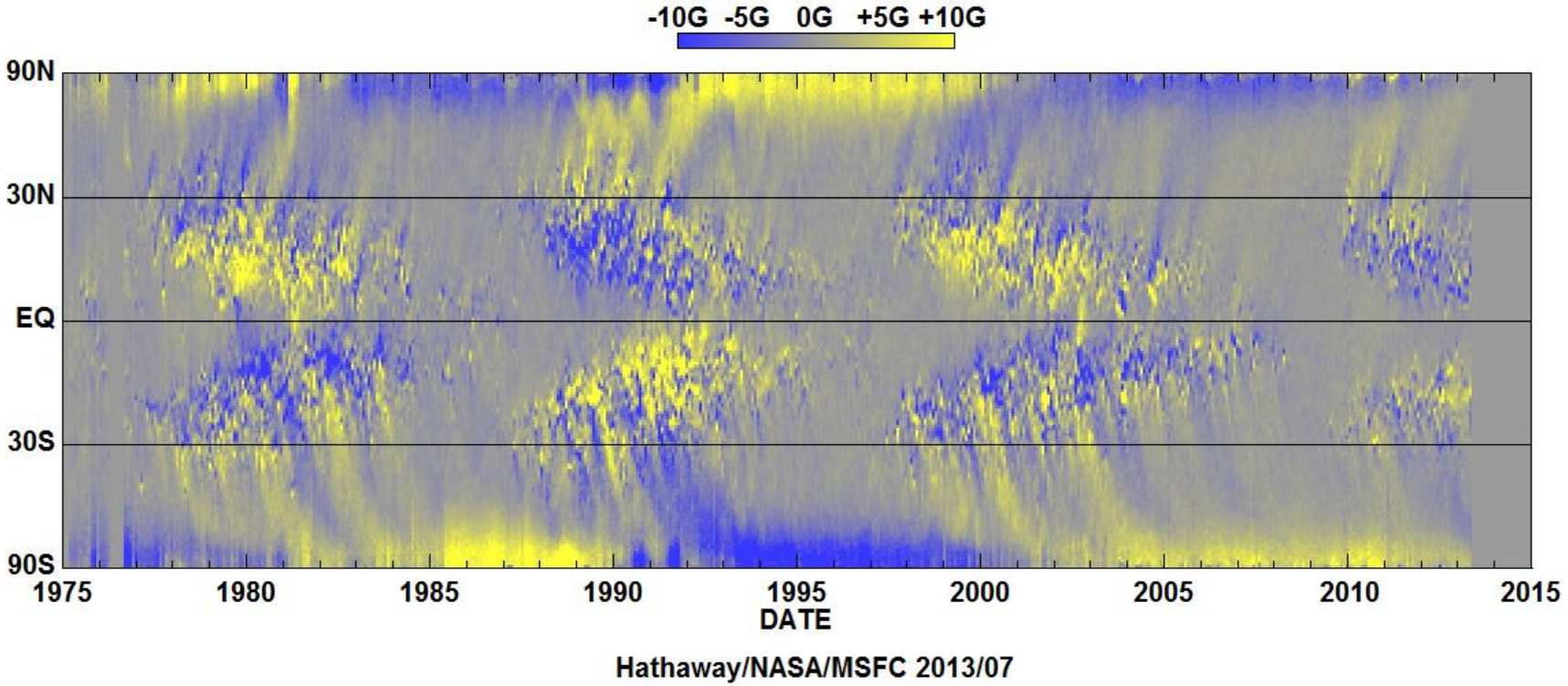

Vector Magnetometry – 1: Qualitative Results

- Early vector magnetographs performed measurements of full state of polarization, but only at one wavelength in a spectral line
- This brand of "vector magnetometry" is usually incapable of delivering quantitative results

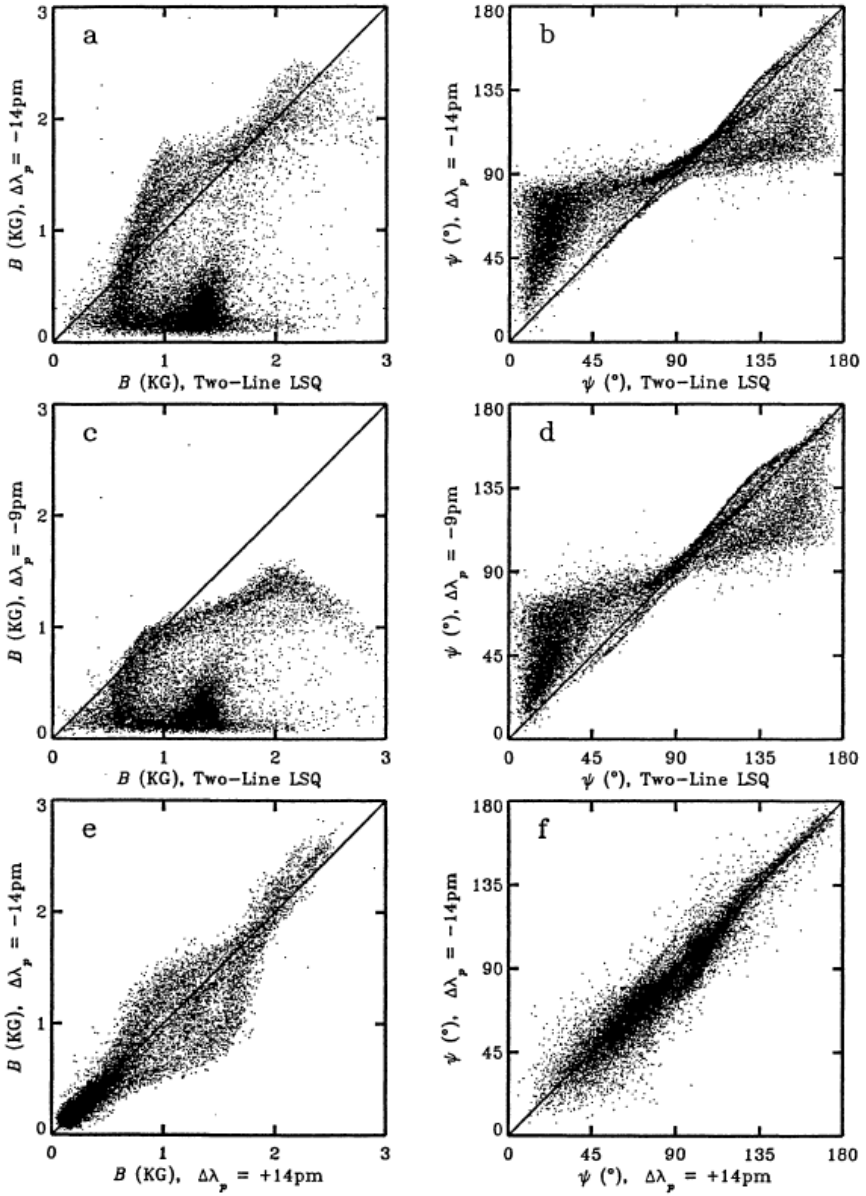

Illustration from Lites et al. 1994

Full Stokes Polarimetry – 2: Ideal Observations

- In the Zeeman effect, Stokes ***Q, U*** arise from the component of the field ***transverse*** to the line-of-sight
- In truth, accurate inference of **B** involves all four Stokes parameters, including ***I***
- Ideal observational information for inference of **B**:

① All four Stokes parameters **simultaneously**
② **Full coverage** of the spectral profile(s)
③ **Fully resolved spectrum**
④ **Two or more spectral lines** with differing sensitivity to the Zeeman effect, observed strictly simultaneously
⑤ **Measurement in time short** compared to the evolution on the Sun (or terrestrial atmospheric conditions; i.e., *seeing*)

- These goals suggest spectroscopic measurements would be ideal, ***but***:
  - Precision of the field measurement is not the only issue driving the science – simultaneous spatial coverage of the solar scene also important
  - For some problems, imaging Stokes polarimetry can proceed fast enough, with high enough spectral resolution, to accomplish the desired science
- ***Always consider the science drivers first when planning astronomical observations!***

Scattering Polarization– 1: Electron Density of the Corona

- Free electrons in the coronal plasma scatter light from the photosphere
- Scattered light is partially linearly polarized due to geometry (c.f. lectures Casini, Jose Carlos del Toro Iniesta)
- Scattering linearly proportional to n_e
- Polarization allows one to separate the light scattered by the instrument and the Earth's atmosphere (both largely unpolarized) from the solar scattering by electrons

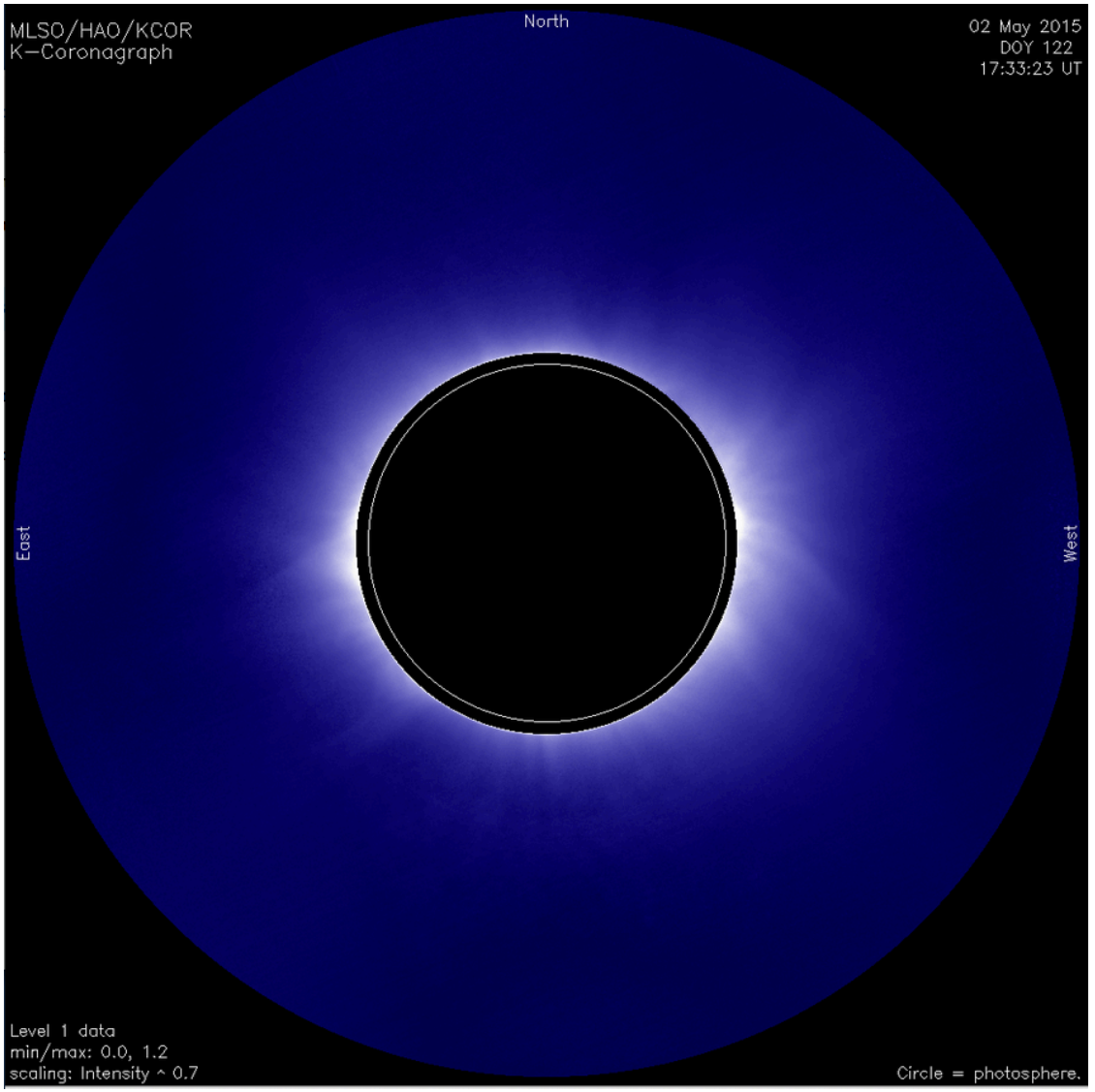

Scattering Polarization– 1: Electron Density of the Corona

- Free electrons in the coronal plasma scatter light from the photosphere
- Scattered light is partially linearly polarized due to geometry (c.f. lectures by Andrés Asensio Ramos, Jose Carlos del Toro Iniesta)
- Scattering linearly proportional to n_e
- Polarization allows one to separate the light scattered by the instrument and the Earth's atmosphere (both largely unpolarized) from the solar scattering by electrons

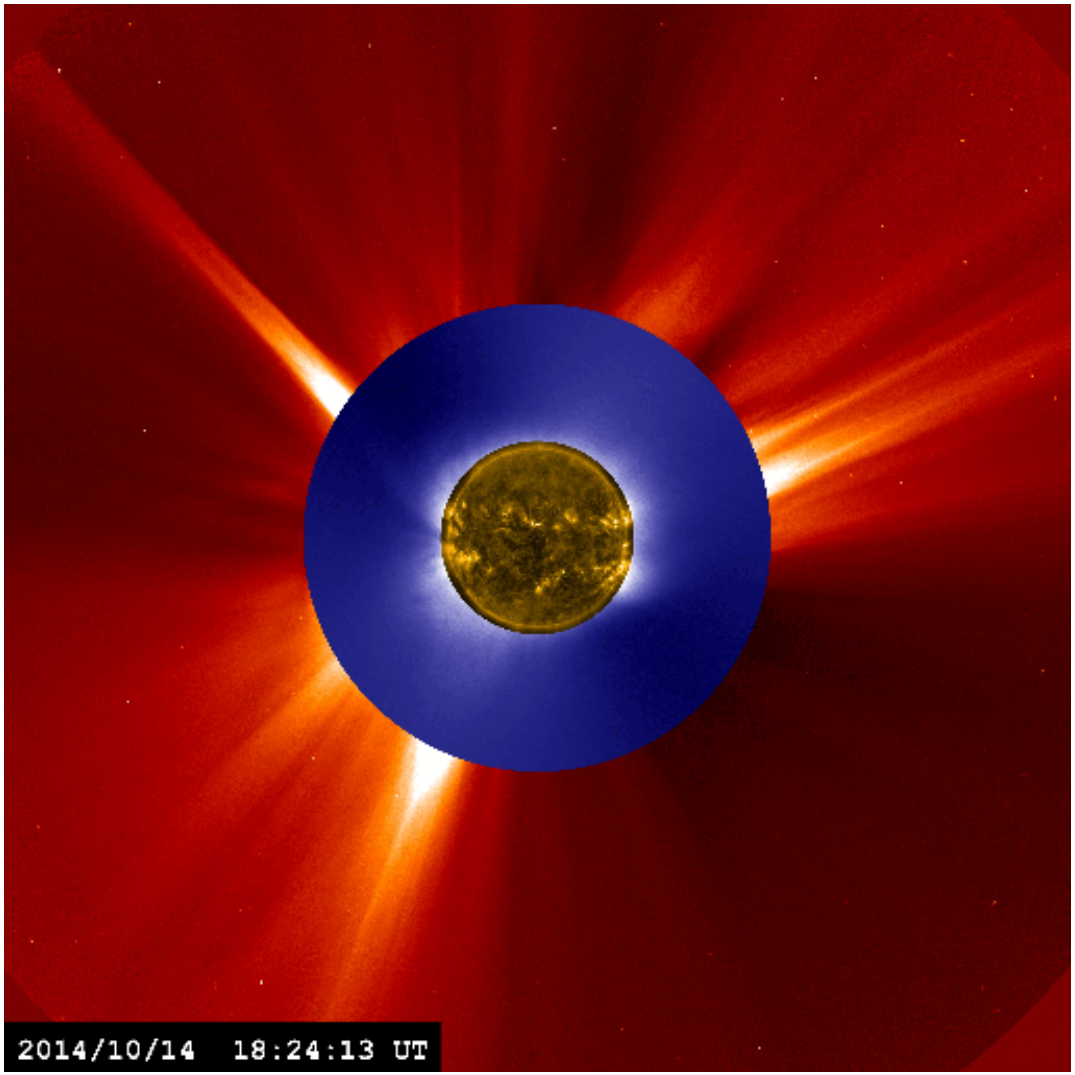

Scattering Polarization– 2: Emission Line Polarization from the Corona

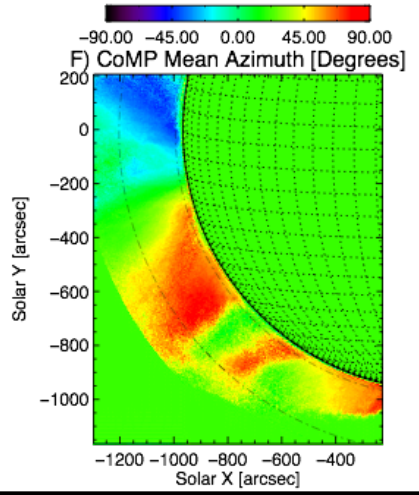

From Tomczyk et al. 2008

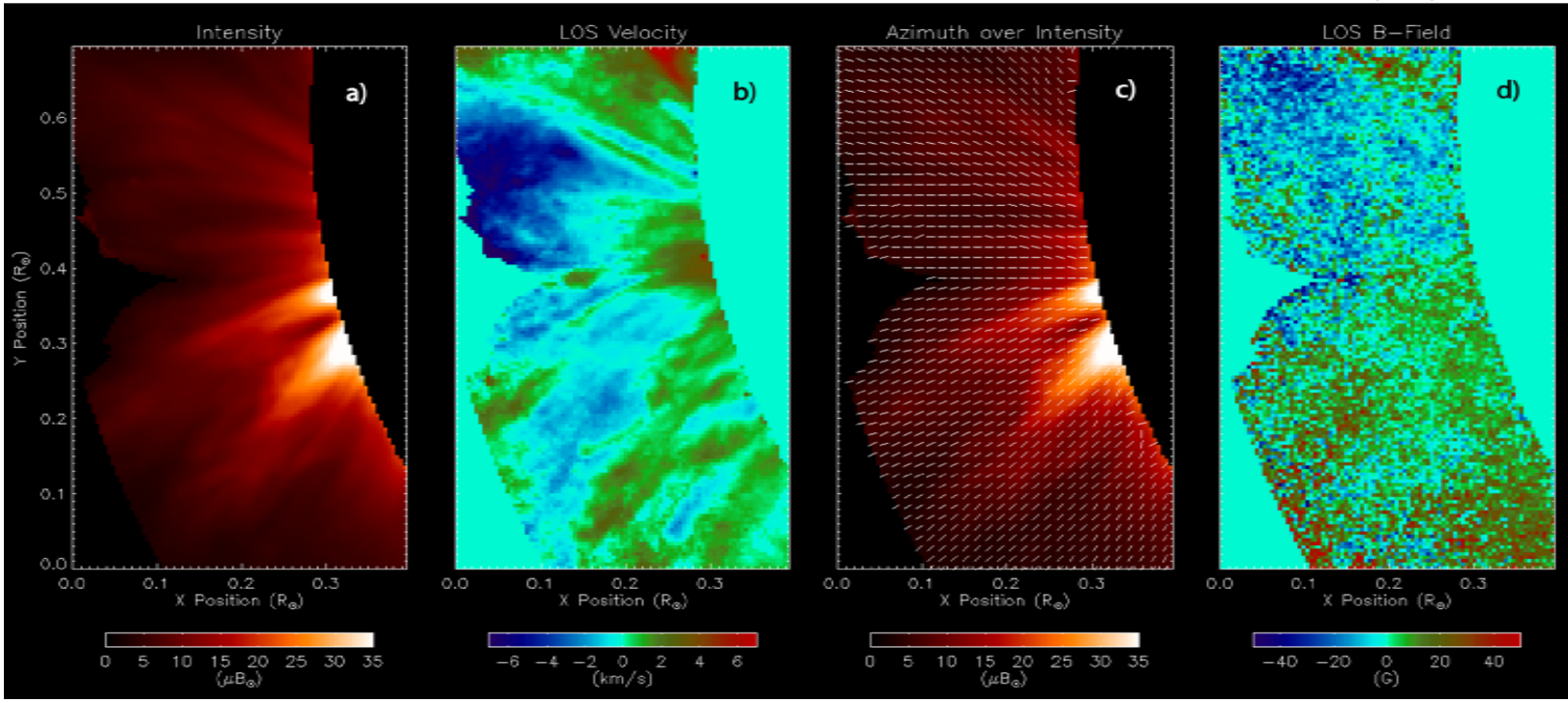

Scattering Polarization– 3: Hanle Effect in Prominences

- TIP observations He I 1083 nm
- HAZEL (Hanle-Zeeman) inversions

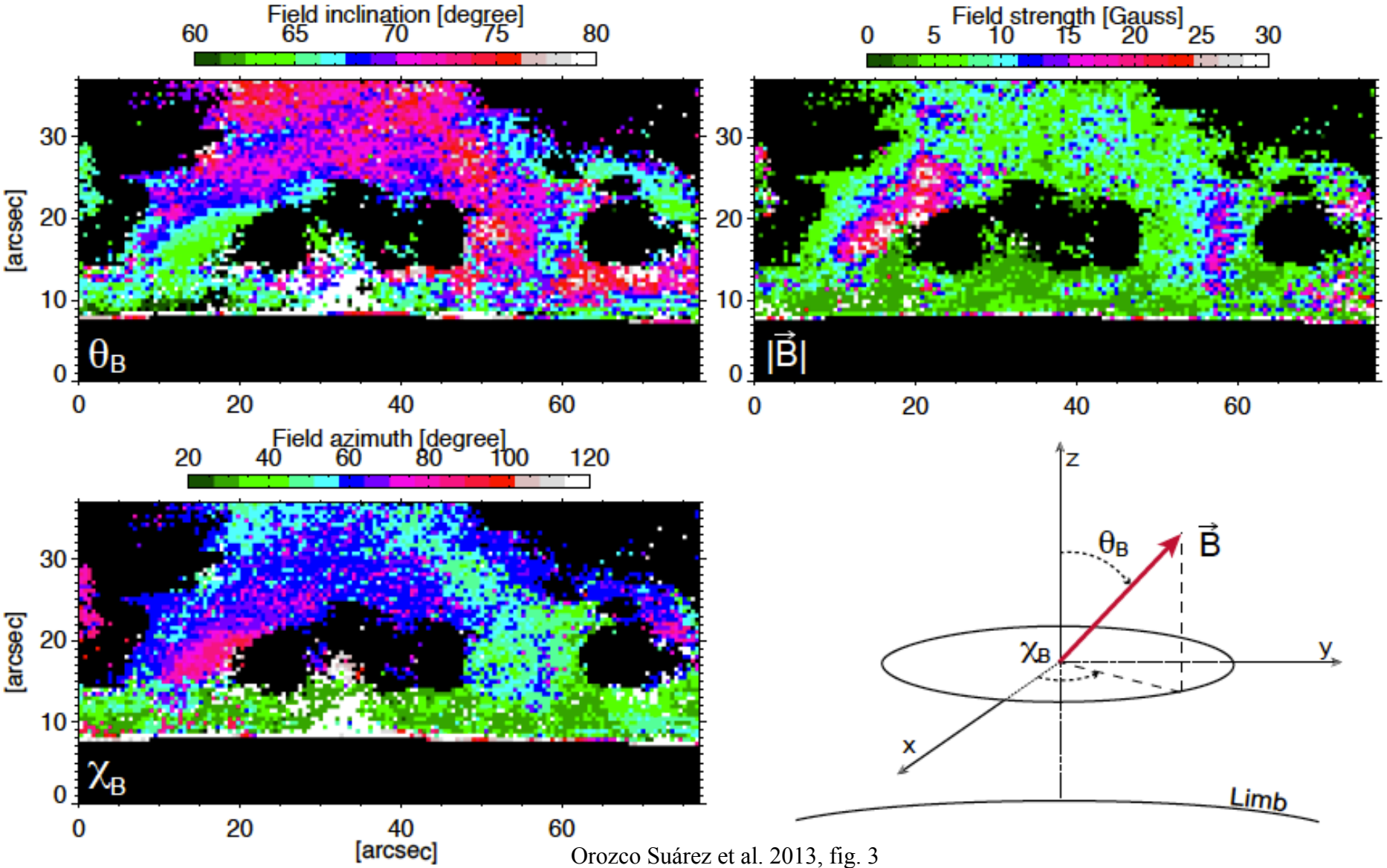

Orozco Suárez et al. 2013, fig. 3

Polarization Modulation Schemes

- For light, we detect photons (energy = intensity), not the electric field
- Polarization measured by inserting (and manipulating) optical elements that affect the polarized component of the light beam
- A basic polarimeter:

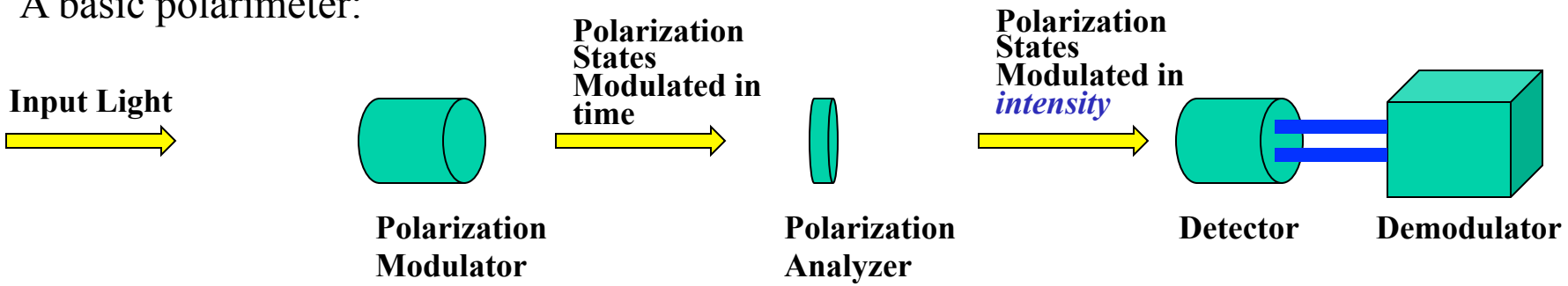

- Altering the polarization state of the detected beam by modifying the transmission (or reflection) of the polarized input light in time is called **modulation.** Typical modulator causes each polarization state (Q,U,V) to have a different frequency or phase. **Example: rotating retarder.**
- The polarization analyzer is a fixed optical device that transmits only a desired state of polarization. Following this element the polarization modulation is converted to a modulation of the intensity. **Example: linear polarizer.**
- The detector converts the time-varying intensity to an electronic signal
- The demodulator selects the signals according to frequency and phase to produce a measure of the input polarization

Polarization Modulation Schemes – 2: Stokes Definition Polarimeter

Recall the "operational" definition of the Stokes parameters **(6 intensity measurements total)**:

$$I = I_{\leftrightarrow} + I_{\updownarrow} = I_{\swarrow} + I_{\searrow} = \langle a_x^2 \rangle + \langle a_y^2 \rangle$$

$$Q = I_{\leftrightarrow} - I_{\updownarrow} = \langle a_x^2 \rangle - \langle a_y^2 \rangle$$

$$U = I_{\swarrow} - I_{\searrow} = 2\langle a_x\, a_y \cos\delta \rangle$$

Circular Analyzer

$$V = I_{\circlearrowright} - I_{\circlearrowleft} = 2\langle a_x\, a_y \sin\delta \rangle$$

A Stokes definition polarimeter is one in which polarizers (linear and circular) are alternately inserted into the beam to directly produce *I+Q, I-Q, I+U, I-U, I+V, I-V*

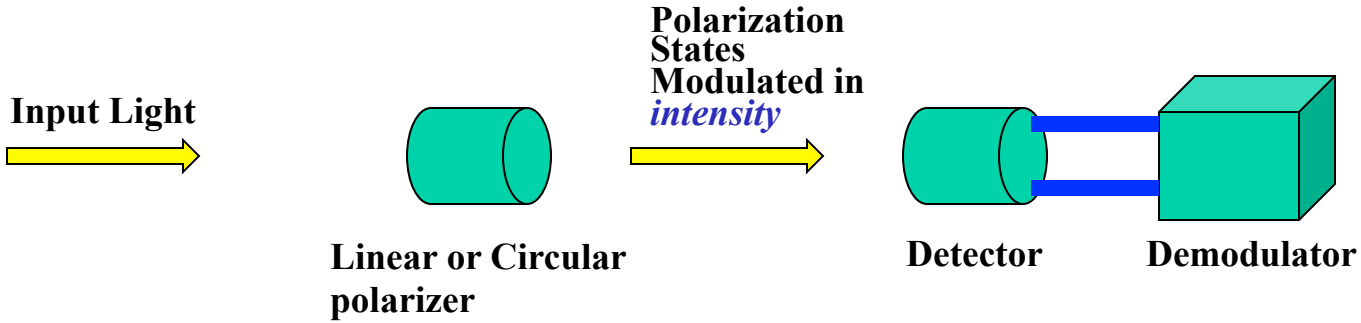

- The efficiency of modulation for this scheme is 100%, but if each Stokes parameter is being measured only for 1/3 of the time, the overall ***modulation efficiency*** of this scheme is 0.33
- It is slow and inefficient to be alternately inserting and removing optical devices from the beam

Polarization Modulation Schemes – 3: Rotating Retarder

- If we use a rotating retarder as a polarization modulator, there are a number of advantages over the Stokes definition scheme

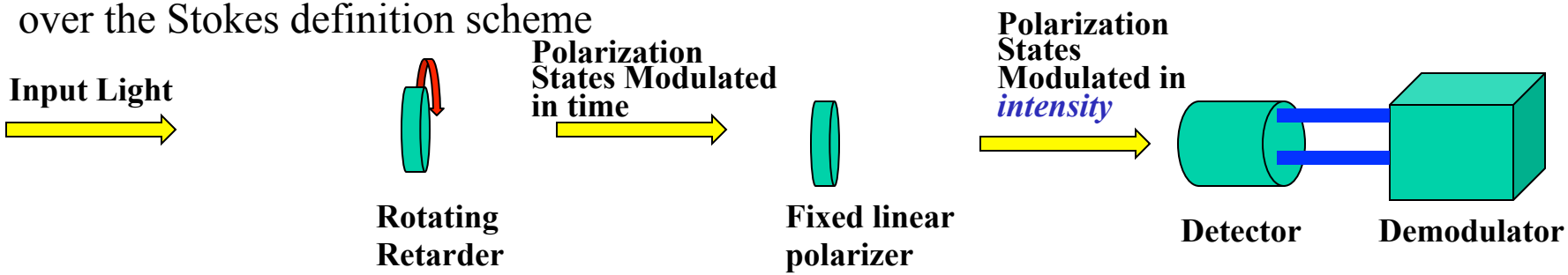

Polarization Modulation Schemes – 3: Rotating Retarder

- If we use a rotating retarder as a polarization modulator, there are a number of advantages over the Stokes definition scheme

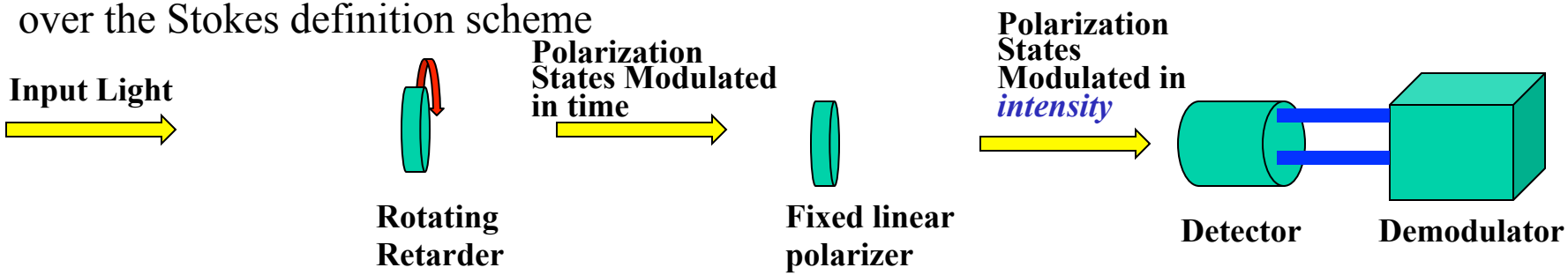

- The Mueller matrix for a rotating retarder of retardance Δ:

$$\mathbf{M}_{\mathrm{ret}}^{\theta} = \begin{pmatrix} 1 & 0 & 0 & 0 \\ 0 & \cos^2 2\theta + \sin^2 2\theta \cos\Delta & \cos 2\theta \sin 2\theta (1-\cos\Delta) & -\sin 2\theta \sin\Delta \\ 0 & \cos 2\theta \sin 2\theta (1-\cos\Delta) & \sin^2 2\theta + \cos^2 2\theta \cos\Delta & \cos 2\theta \sin\Delta \\ 0 & \sin 2\theta \sin\Delta & -\cos 2\theta \sin\Delta & \cos\Delta \end{pmatrix}$$

Polarization Modulation Schemes – 3: Rotating Retarder

- If we use a rotating retarder as a polarization modulator, there are a number of advantages over the Stokes definition scheme

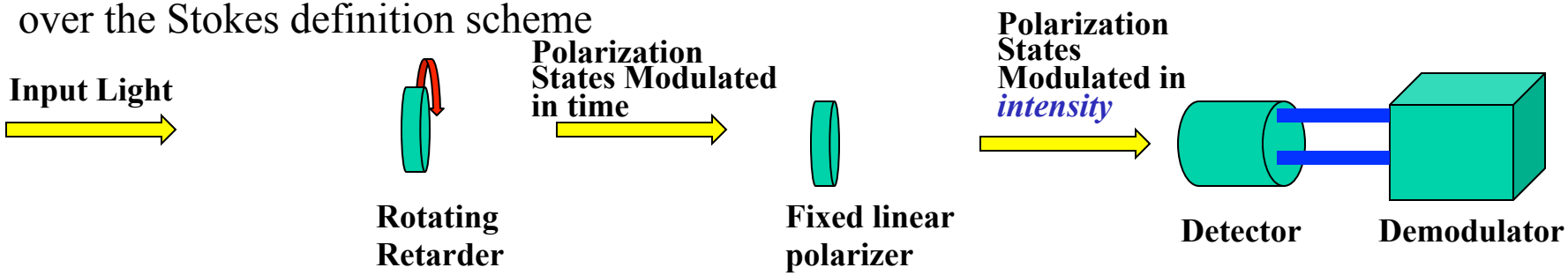

- The Mueller matrix for a rotating retarder **followed by a horizontal polarizer (+*Q*):**

$$\mathbf{M}_{\mathrm{pol}}^{+Q}\mathbf{M}_{\mathrm{ret}}^{\theta} = \begin{pmatrix} 1 & 1 & 0 & 0 \\ 1 & 1 & 0 & 0 \\ 0 & 0 & 0 & 0 \\ 0 & 0 & 0 & 0 \end{pmatrix} \begin{pmatrix} 1 & 0 & 0 & 0 \\ 0 & \cos^2 2\theta + \sin^2 2\theta \cos\Delta & \cos 2\theta \sin 2\theta(1-\cos\Delta) & -\sin 2\theta \sin\Delta \\ 0 & \cos 2\theta \sin 2\theta(1-\cos\Delta) & \sin^2 2\theta + \cos^2 2\theta \cos\Delta & \cos 2\theta \sin\Delta \\ 0 & \sin 2\theta \sin\Delta & -\cos 2\theta \sin\Delta & \cos\Delta \end{pmatrix}$$

Polarization Modulation Schemes – 3: Rotating Retarder

- If we use a rotating retarder as a polarization modulator, there are a number of advantages over the Stokes definition scheme

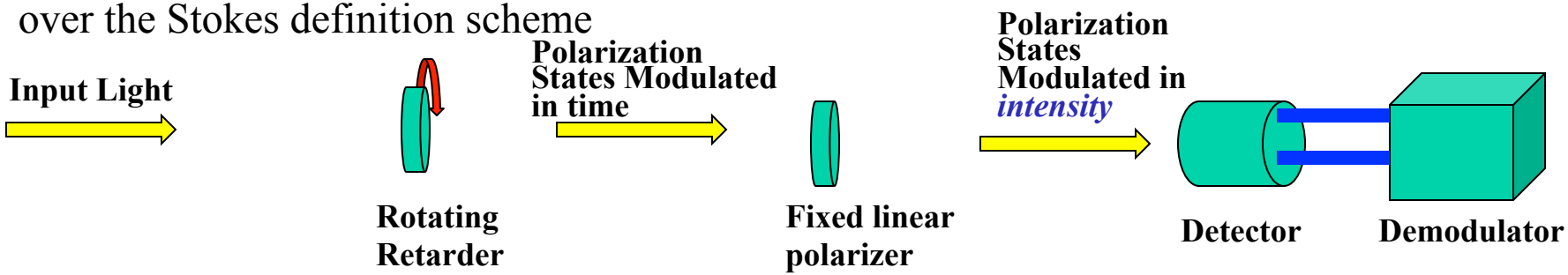

- The Mueller matrix for a rotating retarder of retardance Δ followed by a horizontal polarizer ($+Q$), **acting on a Stokes vector I:**

$$\mathbf{M}_{\mathrm{pol}}^{+Q}\mathbf{M}_{\mathrm{ret}}^{\theta}\mathbf{I} = \begin{pmatrix} 1 & 1 & 0 & 0 \\ 1 & 1 & 0 & 0 \\ 0 & 0 & 0 & 0 \\ 0 & 0 & 0 & 0 \end{pmatrix} \begin{pmatrix} 1 & 0 & 0 & 0 \\ 0 & \cos^2 2\theta + \sin^2 2\theta \cos\Delta & \cos 2\theta \sin 2\theta (1-\cos\Delta) & -\sin 2\theta \sin\Delta \\ 0 & \cos 2\theta \sin 2\theta (1-\cos\Delta) & \sin^2 2\theta + \cos^2 2\theta \cos\Delta & \cos 2\theta \sin\Delta \\ 0 & \sin 2\theta \sin\Delta & -\cos 2\theta \sin\Delta & \cos\Delta \end{pmatrix} \begin{pmatrix} I \\ Q \\ U \\ V \end{pmatrix}$$

Polarization Modulation Schemes – 3: Rotating Retarder

- If we use a rotating retarder as a polarization modulator, there are a number of advantages over the Stokes definition scheme

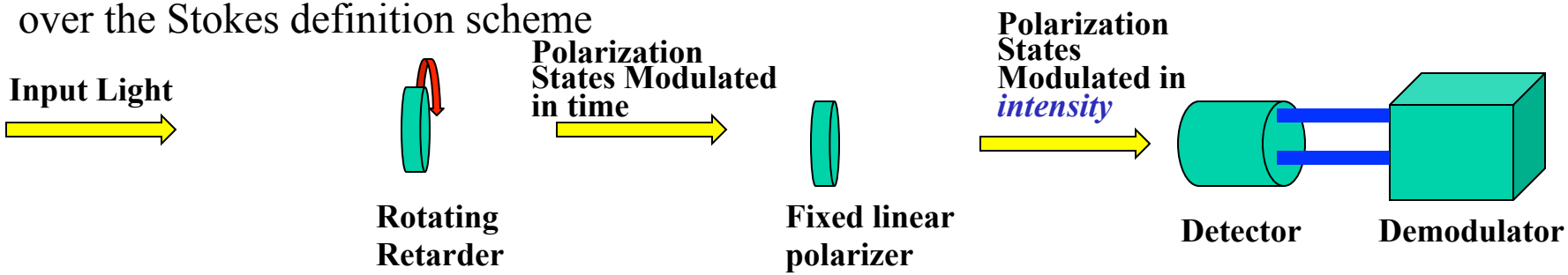

- The Mueller matrix for a rotating retarder of retardance Δ followed by a horizontal polarizer (+*Q*), **acting on a Stokes vector I:**

$$\mathbf{M}_{\mathrm{pol}}^{+Q}\mathbf{M}_{\mathrm{ret}}^{\theta}\mathbf{I} = \begin{pmatrix} 1 & 1 & 0 & 0 \\ 1 & 1 & 0 & 0 \\ 0 & 0 & 0 & 0 \\ 0 & 0 & 0 & 0 \end{pmatrix} \begin{pmatrix} 1 & 0 & 0 & 0 \\ 0 & \cos^2 2\theta + \sin^2 2\theta \cos\Delta & \cos 2\theta \sin 2\theta(1-\cos\Delta) & -\sin 2\theta \sin\Delta \\ 0 & \cos 2\theta \sin 2\theta(1-\cos\Delta) & \sin^2 2\theta + \cos^2 2\theta \cos\Delta & \cos 2\theta \sin\Delta \\ 0 & \sin 2\theta \sin\Delta & -\cos 2\theta \sin\Delta & \cos\Delta \end{pmatrix} \begin{pmatrix} I \\ Q \\ U \\ V \end{pmatrix}$$

- After doing the math, the detected Stokes *I* signal is:

$$Intensity = I + \left[\cos^2 2\theta + \sin^2 2\theta \cos\Delta\right]Q + \left[\cos 2\theta \sin 2\theta(1-\cos\Delta)\right]U - \left[\sin 2\theta \sin\Delta\right]V$$

- If $\theta = \omega t$ then we see that:
  - ***Q* is modulated at 4*ω***
  - ***U* is modulated at 4*ω*, but shifted in phase by +*π*/2**
  - ***V* is modulated at 2*ω***

Polarization Modulation Schemes – 3: Rotating Retarder

Example of half-rotation of a Δ=150° retarder:

After some math, the modulated signals for *Q, U, V* with retarder rotation rate ω are seen to be:

- *Q*: ½[cos4ωt (1 – cosΔ) + (1+ cosΔ)]
- *U*: ½ sin4ωt (1 – cosΔ)
- *V*: - sin2ωt sinΔ

Features of this modulation scheme:

- *Q, U* modulated intensities always equal
- In general, there is a finite offset for *Q* modulated signal
- Selection of retardance determines relative modulation efficiency of *Q,U* vs. *V*
- *Q,U,V* continuously modulated
- *Q* out of phase from *U* by 90°
- Various demodulation schemes are possible: **require at least 8 intensity measurements** per half-rotation of the retarder

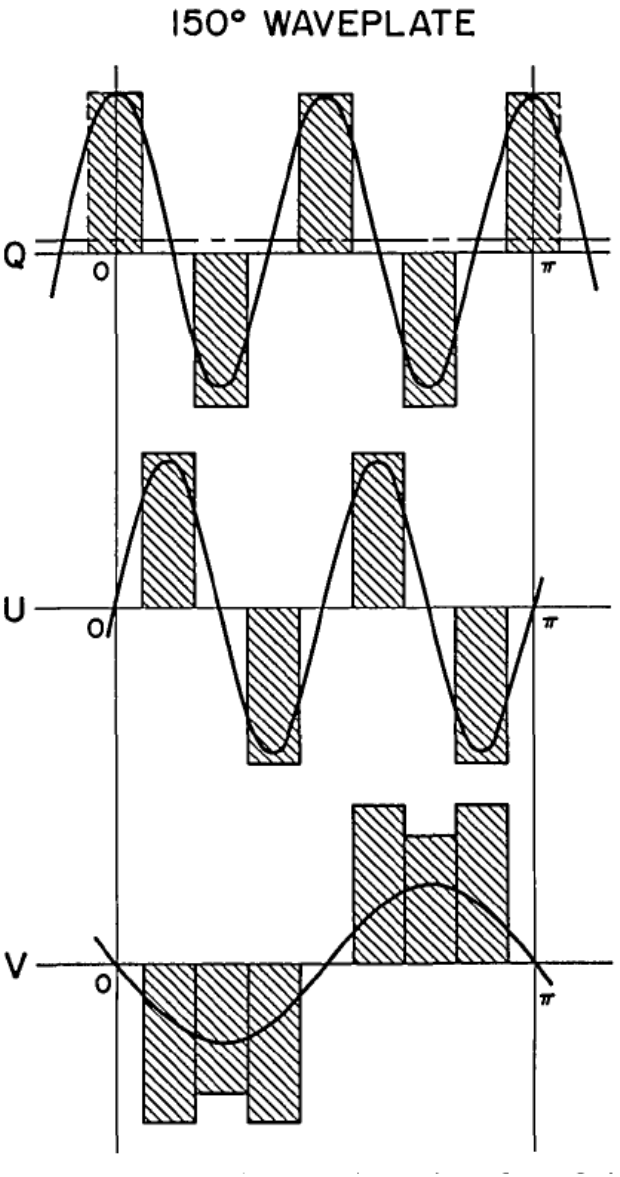

Illustration from Lites 1987

Exercise V.1: For a rotating retarder polarimeter, find the approximate value of retardance Δ when the modulation efficiency of Q and U is equal to that of V.

Polarization Modulation Schemes – 3: Variable Retarder(s)

- Electronically tunable variable retarders, such as liquid crystal variable retarders (LCVRs) are used commonly nowadays:

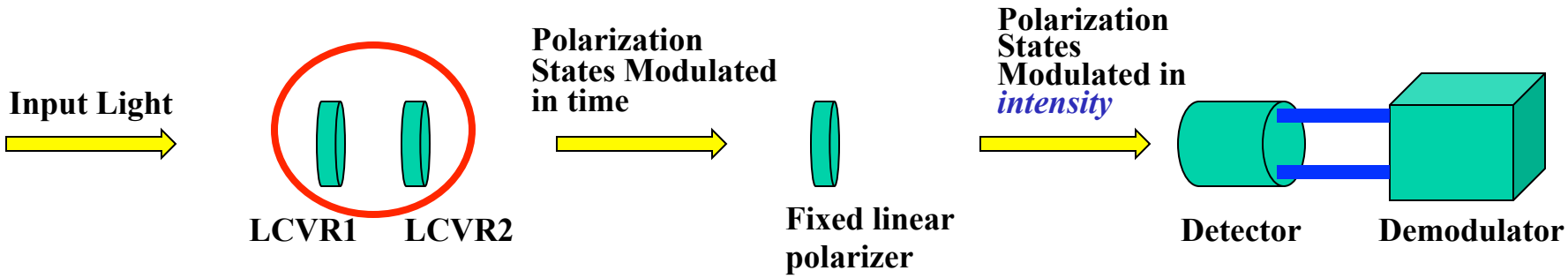

- By adjusting the retardances and orientation of fast axes of the LCVRs, four independent states of the modulated polarization are produced ➔ four Stokes parameters

- In all of the analysis schemes involving a linear polarizer as an analyzer, **at least 50% of the light is lost in the analyzer! Why not use the wasted light?**

Dual-Beam Polarimetry

- Replace the fixed linear polarizer with a device that separates spatially the two orthogonal polarizations (+*Q* and –*Q*):

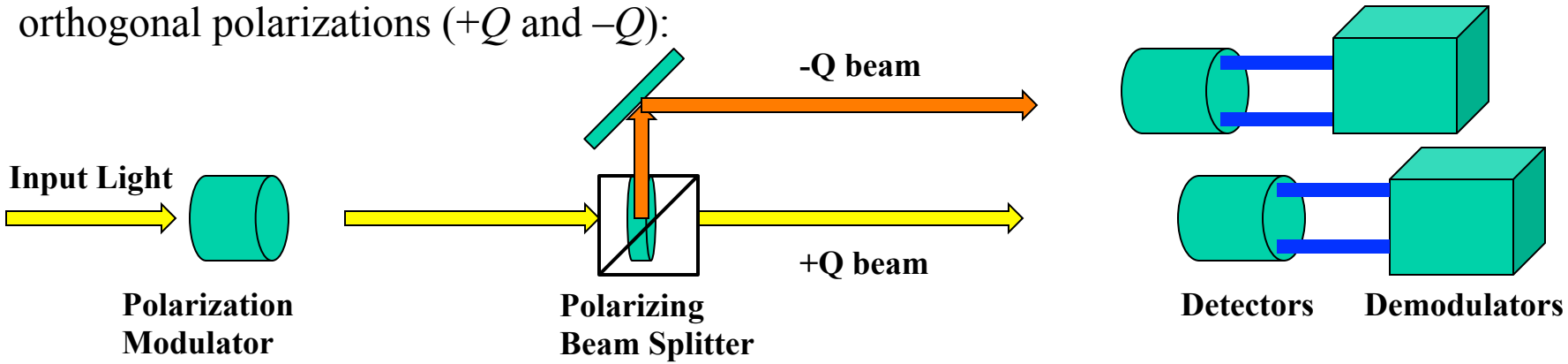

Benefits of a dual-beam polarimeter:

- Use all available light, hence maximize *S/N*
- *Drastically reduce* sensitivity of measurement to polarization crosstalk arising from image motion

$$+Qbeam: Int = I + \left[\cos^2 2\theta + \sin^2 2\theta \cos\Delta\right]Q + \left[\cos 2\theta \sin 2\theta(1-\cos\Delta)\right]U - \left[\sin 2\theta \sin\Delta\right]V$$

$$-Qbeam: Int = I - \left[\cos^2 2\theta + \sin^2 2\theta \cos\Delta\right]Q - \left[\cos 2\theta \sin 2\theta(1-\cos\Delta)\right]U + \left[\sin 2\theta \sin\Delta\right]V$$

- Subtracting the signals from the two beams eliminates temporal fluctuations of Stokes *I*, leaving only temporal fluctuations from the action of the modulator, and from *Q, U, V*
- This system largely eliminates the troublesome *I* ➔ *Q, U, V* crosstalk

Dual-Beam Polarimetry

Illustration from Advanced Stokes Polarimeter showing seeing-induced $I \rightarrow Q,U,V$ crosstalk reduced using dual-beam technique

- Crosstalk among Q,U,V due to image motion is also reduced
- Crosstalk may be represented by an error matrix $\delta\mathbf{X}^{e}$ such that:

$$\mathbf{X}_{\mathbf{instrument}} = \mathbf{X} \pm \delta\mathbf{X}^{e}$$

where $\mathbf{X}$ is the instrument response matrix:

$$X = \begin{pmatrix} X_{11} & X_{12} & X_{13} & X_{14} \\ X_{21} & X_{22} & X_{23} & X_{24} \\ X_{31} & X_{32} & X_{33} & X_{34} \\ X_{41} & X_{42} & X_{43} & X_{44} \end{pmatrix}$$

Diagonal = direct response

$I \rightarrow Q,U,V$ crosstalk

Crosstalk among Q,U,V

$\mathbf{X}$ measures the response of the entire polarimeter (and often, also the telescope) to input polarization. It is not a Mueller matrix, but may be applied as such.

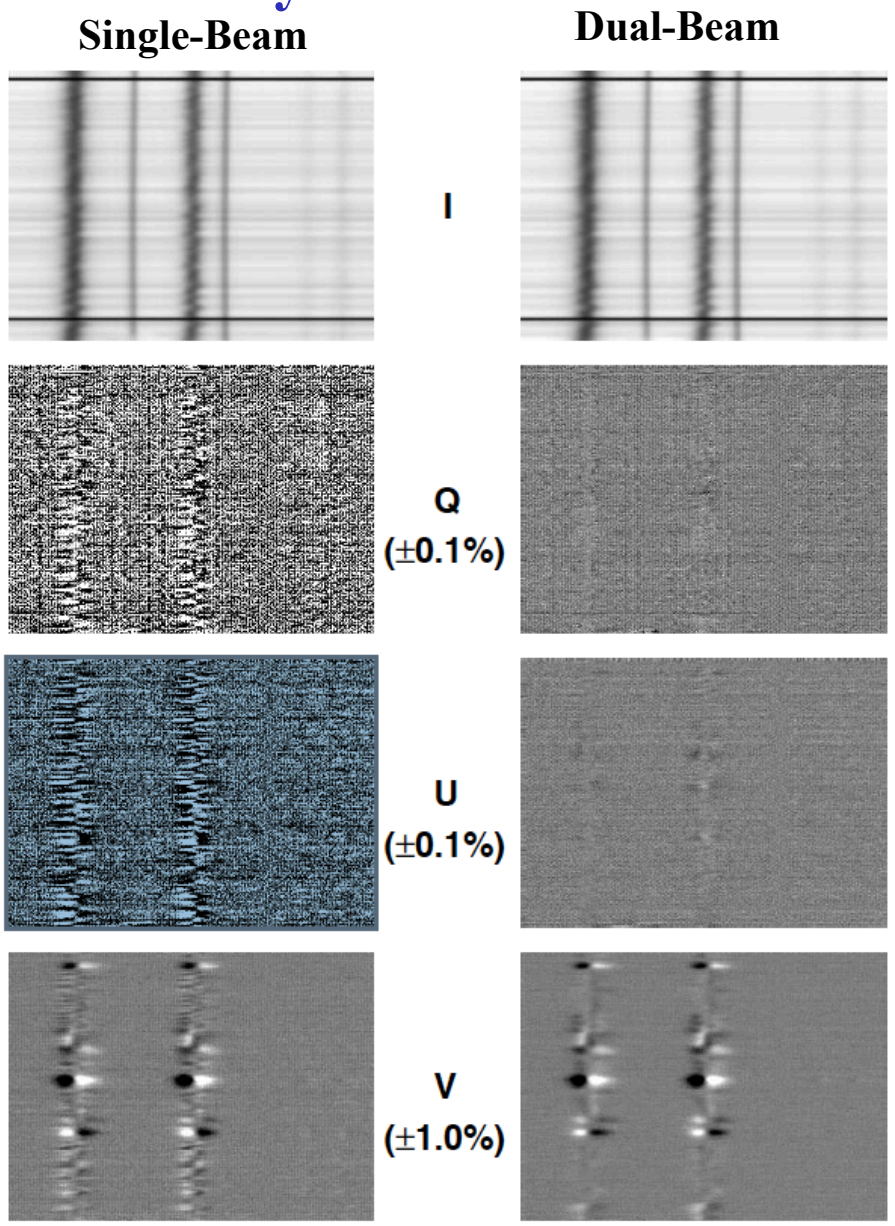

Illustration from Skumanich et al. 1997

Polarization Modulation Efficiency

Modulation efficiency:

- For a given modulation scheme, each Stokes parameter *Q, U, V* may be ascribed a **modulation efficiency** describing the fraction of polarized input is actually detected
- If the efficiency for modulation of *Q, U, V* are equal, then the **maximum efficiency achievable for each is $1/\sqrt{3} = 0.577$** (see del Toro Iniesta 2000)
- Schemes that **modulate and detect all Stokes parameters simultaneously** achieve much higher efficiency than the Stokes definition polarimeter (modulation efficiency of 0.33 for each of *Q, U, V*)

Seeing, Image Motion, and Modulation Rate

Seeing:

- Image motion due to seeing has a monotonically decreasing power with frequency
- Image blurring has analogous behavior
- Both motion and time-variable blurring contribute to crosstalk during polarization measurement
- Adaptive optics helps, but does not eliminate seeing crosstalk (Judge et al. 2004, Casini et al. 2012)

Solar Motions:

- Evolution of the solar scene is present even in the absence of any seeing

Instrumental pointing jitter:

- Even in space, residual jitter of pointing will cause image motion

Typical Power Spectrum of Seeing Motion

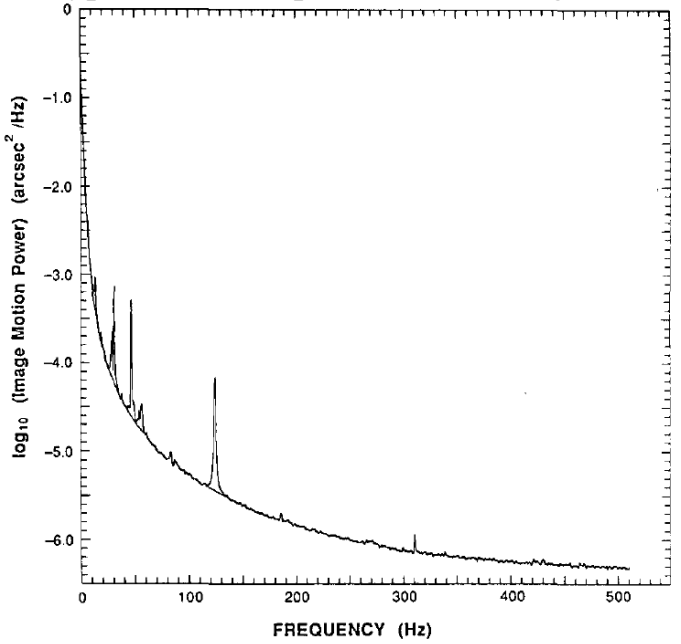

Illustration from Lites 1987

To completely avoid issues with seeing crosstalk or instrument jitter at the 10^{-3} level, **the modulation/demodulation of a single-beam polarimeter should proceed at hundreds of Hz, and even faster at higher polarimetric precision**

Overcoming Seeing, Image Motion

Even in observations from space, residual jitter of pointing will cause crosstalk

How to overcome polarimetric errors from seeing and image motion:

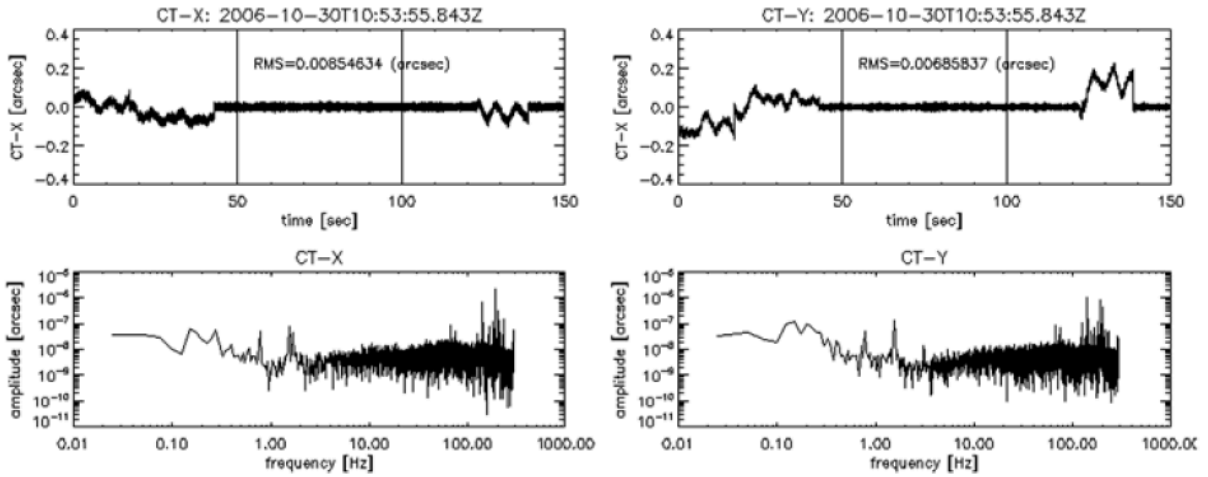

Illustration from Shimizu et al. 2008

- **Dual-beam polarimetry**
- **Reduce image motion:**
  - Tip-tilt correction
  - Adaptive optics
- **Beat the image motion:**
  - Modulate, demodulate, and detect the polarization at a rate high relative to residual level of seeing

- **Amount of tolerable residual crosstalk depends on the science goal**
- **Estimates of residual crosstalk in presence of seeing:**
  - Lites 1987
  - Judge et al. 2004
  - Casini et al. 2012

VI. Spectral Discriminators

- **Classical Slit Spectrograph**
- **Fabry-Pérot Interferometer**
- **Lyot Filter**
- **Michelson Interferometer**
- **Hybrid Discriminators**
- **Dual-Beam Polarimetry**
- **Polarization Modulation Efficiency**
- **Seeing, Image Motion, and Modulation Rate**

5-Dimensional Data Hyper Cube [*x, y, λ, Polarization, time*]

- Polarization usually multiplexed in time: reduces the cube to 3 dimensions [*x,y,λ*]
- Limited by detectors that are 2-dimensional

- Spectrographic observations: simultaneous imaging of [*y, λ*]
- Spectrograph slit steps temporally across the solar image in the *x*-direction

- Filtergraph observations: simultaneous imaging of [x, *y*]
- Filter tunes in λ at separate times to build up cube

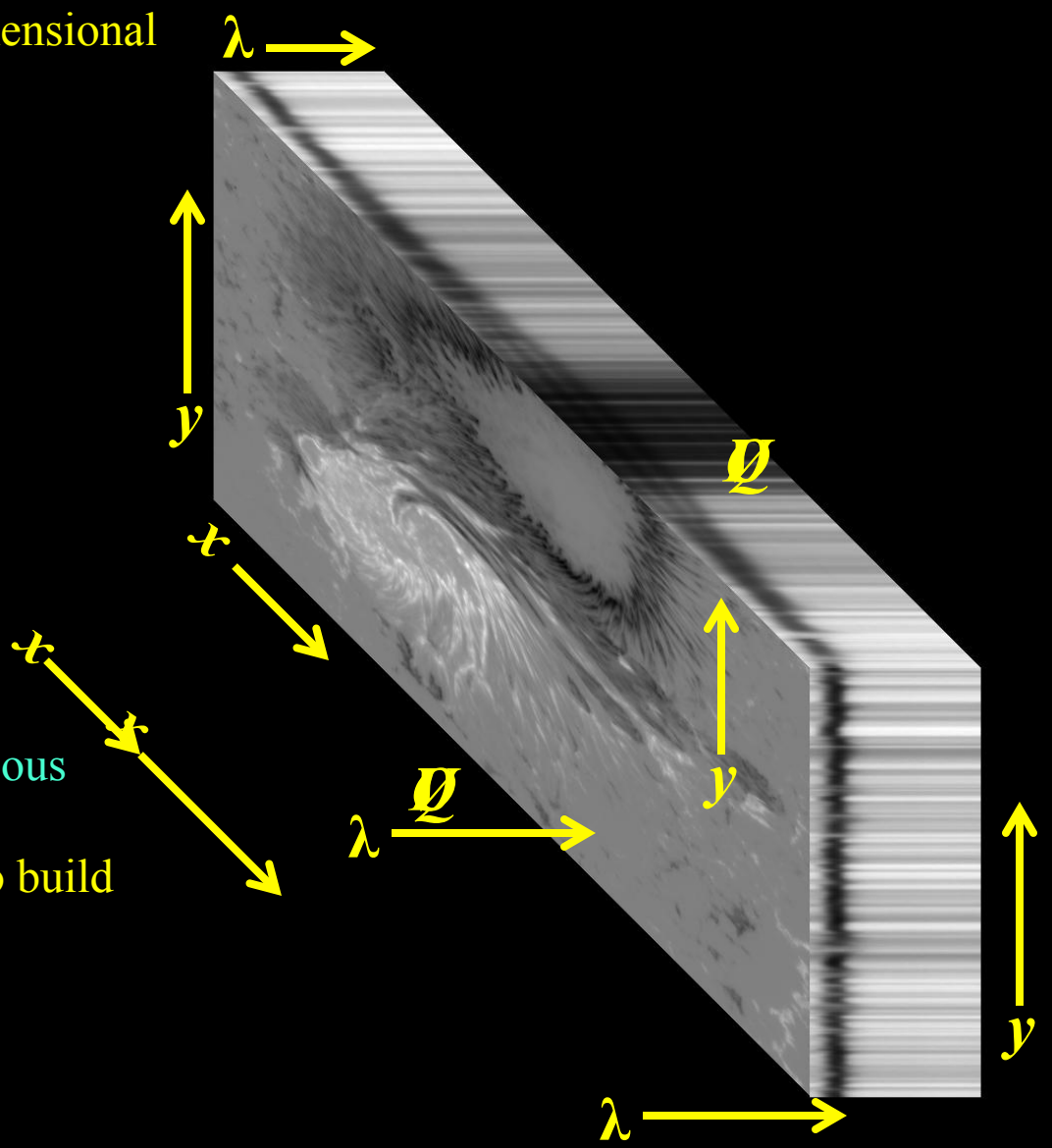

Classes of Spectral Discriminators

Nearly all spectral discriminators in use for solar polarimetry rely on **interference** to separate wavelengths:

- Grating spectrographs
- Lyot filters
- Fabry-Pérot interferometers
- Michelson interferometers

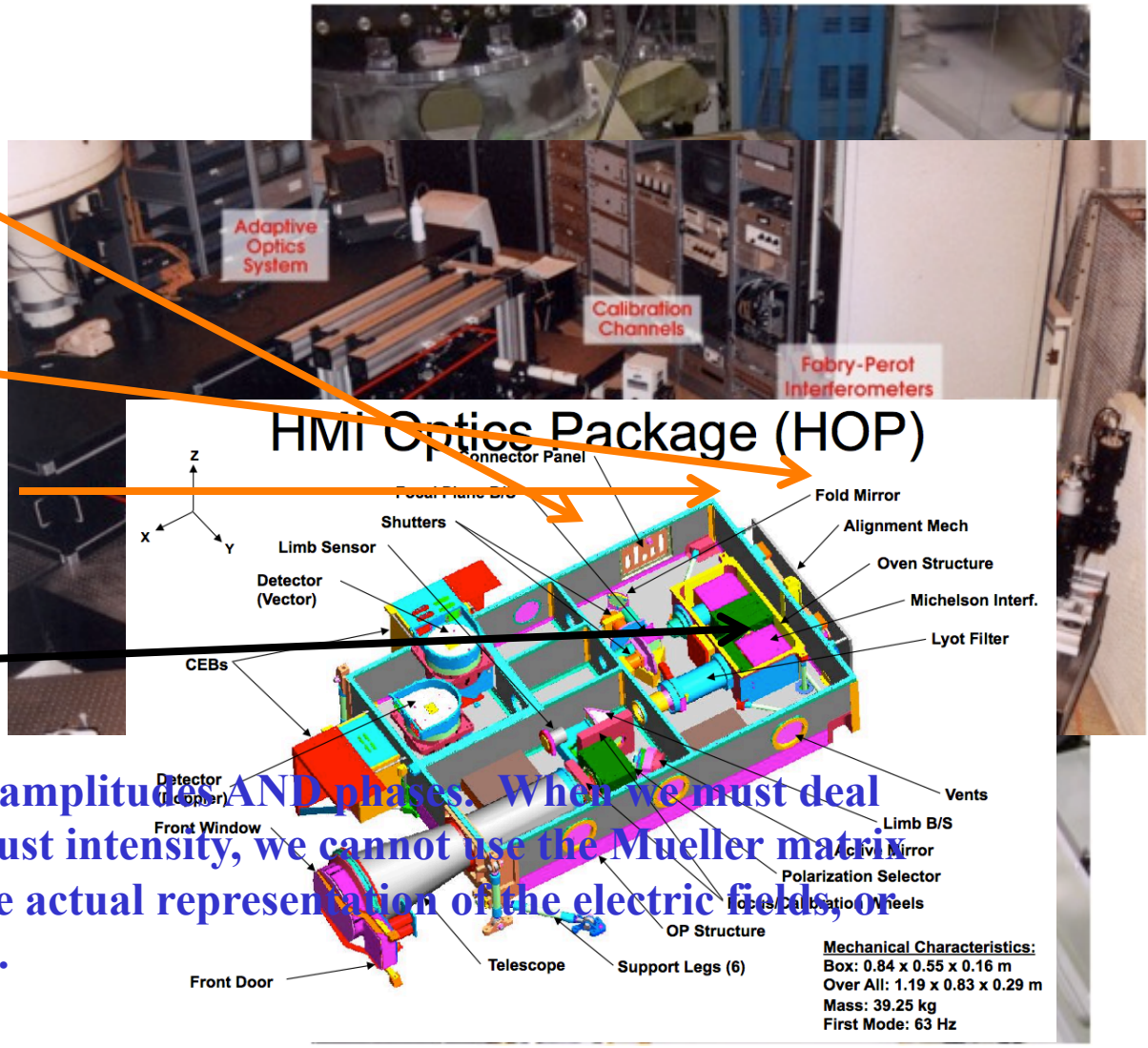

Interference deals with wave amplitudes AND phases. When we must deal with phase information, not just intensity, we cannot use the Mueller matrix formulation. We must use the actual representation of the electric fields, or the Jones matrix formulation.

Classical Slit Spectrograph

Advantages for Solar Polarimetry:

- Reasonably simple optical system
- High spectral resolution
- Simple to achieve integrity of the simultaneous wavelength variation
- Good throughput

Issues:

- Simultaneous sample of solar surface is one-dimensional
- Usually not as compact as filter-based systems
- Often more spectral (continuum) information than necessary, but……**can capture highly-shifted Doppler velocity events**

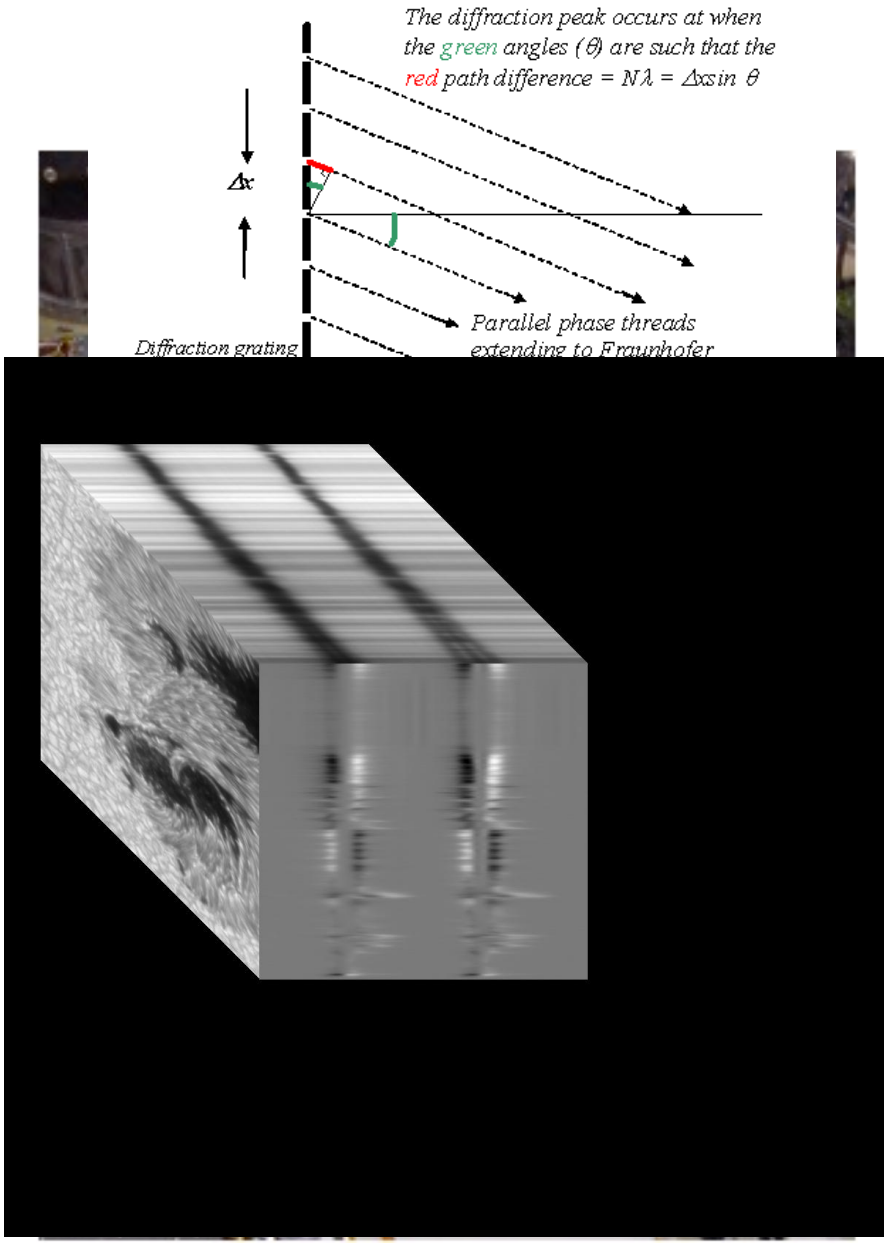

Fabry-Pérot Interferometer

Interference of multiply-reflected rays inside the cavity

- Reasonably simple optical system

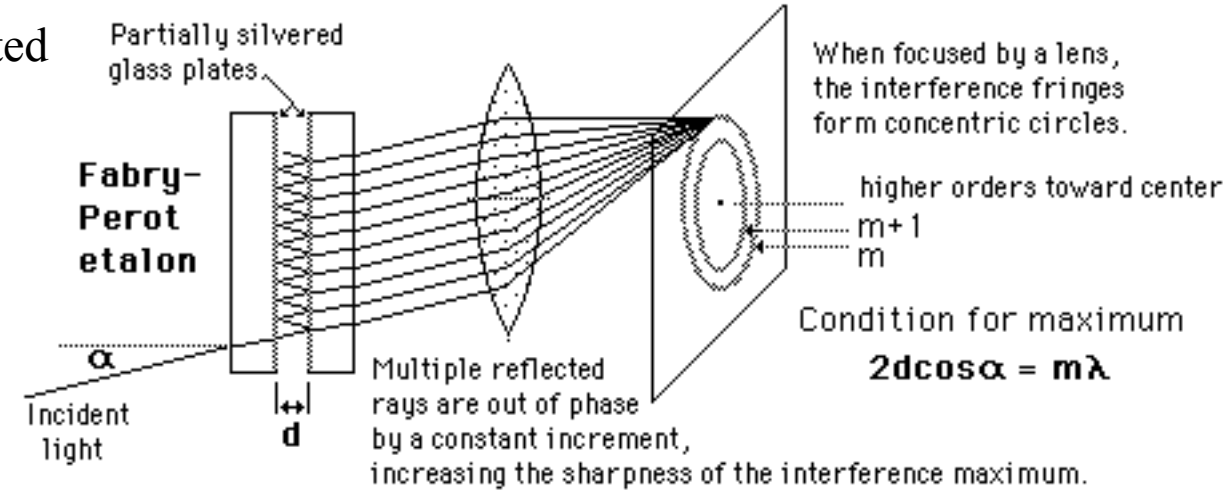

Advantages for Solar Polarimetry:

- With two sequential interferometers one can achieve spectral resolutions comparable to those of spectrographs
- Simultaneous spatial coverage for a single sample wavelength
- Tune in frequency by varying cavity thickness, or by tilting the interferometer
- High throughput
- Compact

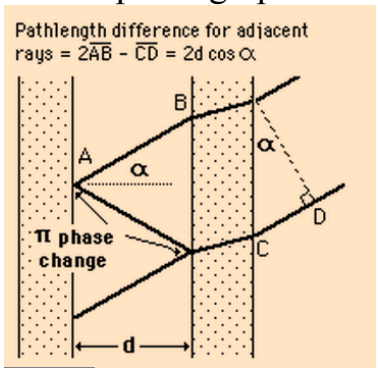

Issues:

- Spectral resolution profile typically Lorentzian (extended "wings")
- Spectral coverage scales with number of wavelength samples
- Necessary to operate at large f-ratios: tradeoff between:
  - **F-P near pupil**: image collimated, **degradation of image quality** (large wavefront errors due to many reflections)
  - **F-P telecentric** (pupil image collimated, near focal plane): **variation of point-spread function** across the image
- F-P systems require **extreme optical quality** because of multiple reflections (wavefront errors ≈ λ/500 rms)

Fabry-Pérot Interferometer

Telecentric vs Collimated:

1. Classic (collimated) mount

- The FPs are near a re-imaged pupil
- All rays from one point in image plane pass through FP parallel to each other (collimated)
- Path length in FP shifts to blue radially away from optical axis
- Maximum sensitivity to image quality degradation, but spectral resolution uniform and high over image

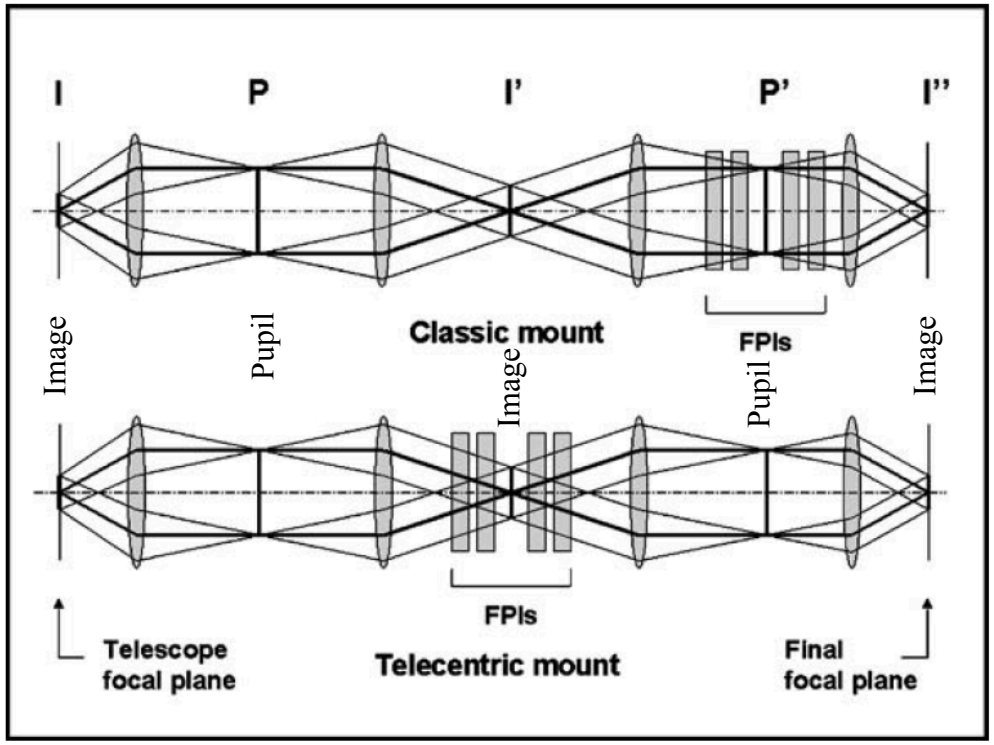

From Cavallini 2006

2. Telecentric mount

- FP near an image plane
- All points within the image pass through FP in equivalent conical bundles of rays
- Spectral resolution is broadened by the conical path of the rays passing through the FP – but wavelength position is the same for all points in the image plane
- Wavelength shift across pupil leads to wavelength-dependent image quality

Fabry-Pérot Interferometer

- Etalon: refractive index ***n***, spacing ***d***
- **Free spectral range** $\Delta\lambda \approx \lambda^2/(2\, n\, d\, cos\theta)$
- Full width half maximum = $\delta\lambda$
- **Finesse** $F = \Delta\lambda/\delta\lambda$

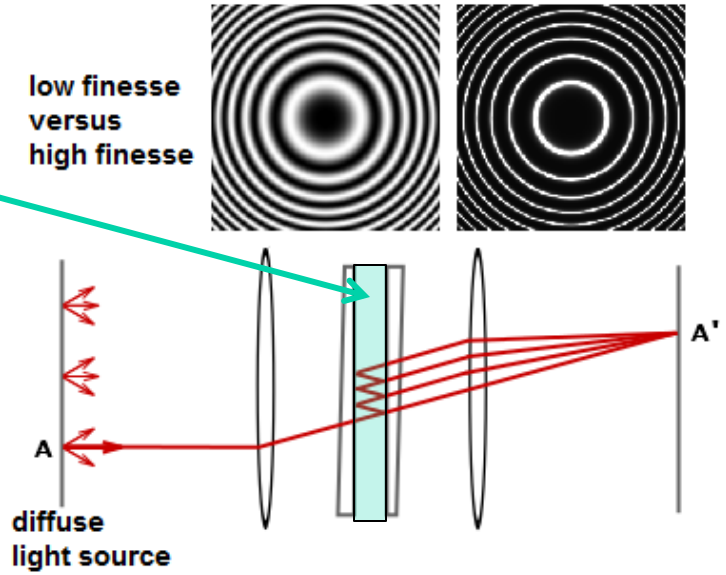

Notes on Fabry-Pérot Interferometer:

- Free spectral range $\Delta\lambda$ adjusted by width of cavity ***d***
- $\delta\lambda$ adjusted by the reflectivity of the cavity surfaces
- Interferometers have extended wings because interference of multiply-reflected beams is never complete
- Etalons can be air-spaced and separation mechanically adjusted, or solid crystals, i.e. $LiNbO_3$, that may be tuned electro-optically
- Polarization varies with incidence angle
- Typically need two or more interferometers in series

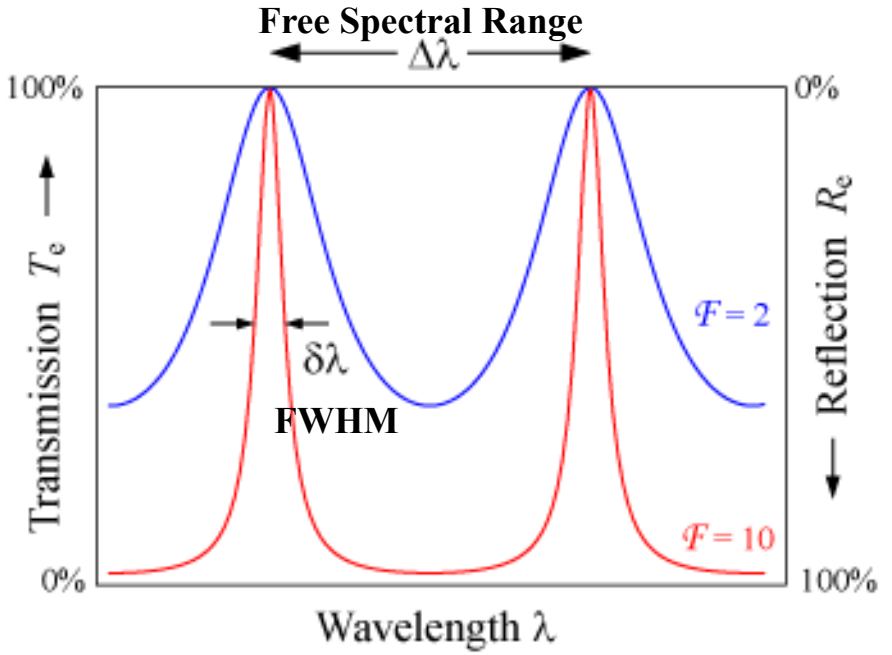

Lyot (Birefringent) Filter

Lyot filter: Interference of beams of phase introduced by birefringence in a crystal, not by spatial separation as in a spectrograph or Fabry-Pérot interferometer

- Consider unpolarized light entering linear polarizer followed by a birefringent crystal. Assume the amplitude is A after passing the polarizer. Consider a uniaxial crystal with positive optical sign (quartz) with **optical Axis (OA) oriented at 45° to the polarizer.** On exit of the crystal:

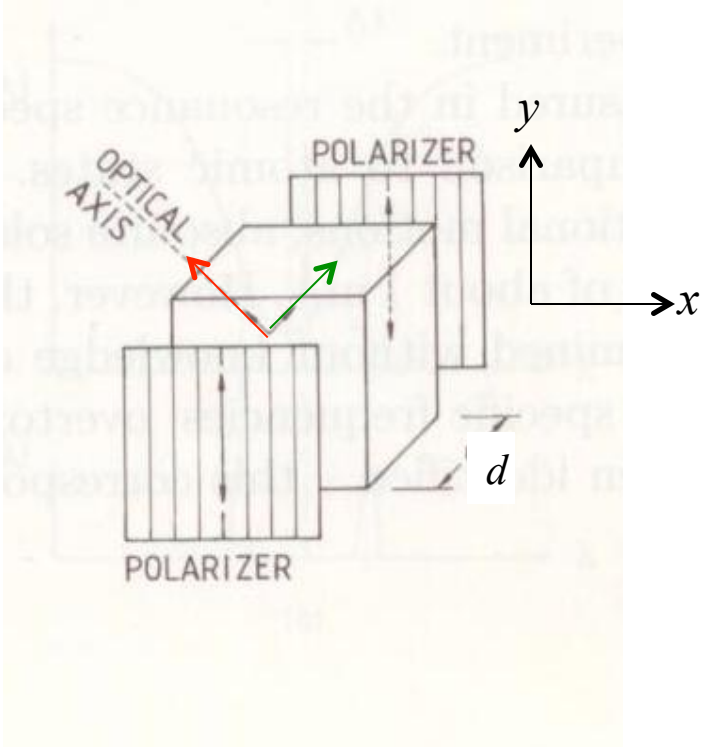

- o-ray: elec. field perpendicular to OA: $[A/\sqrt{2}]e^{i\omega t}$
- e-ray: elec. field along OA: $[A/\sqrt{2}]e^{i(\omega t-\delta)}$ – retarded by δ radians where $\boldsymbol{\delta = 2\pi(n_o-n_e)d/\lambda}$

- 2nd polarizer oriented same direction as first

  Amplitude after passing 2nd polarizer:

- Wave amplitude along ***y:*** $E_y = [A/\sqrt{2}][\cos(\omega t-\delta) + \cos(\omega t)] = \sqrt{2}A\cos(\delta/2)\cos(\omega t - \delta/2)$
- Intensity of the output $I = 2A^2\cos^2[\pi(n_o-n_e)d/\lambda]$, **is modulated sinusoidally in wavelength**

Lyot Filter – 2: Multiple Stacked Elements

- Each element has a retarder of the same material, but twice as long as the previous
- With twice the retardance of previous elements, successive elements generate periodic transmission with half the wavelength spacing of the peaks
- Can generate a very narrow filter using multiple elements

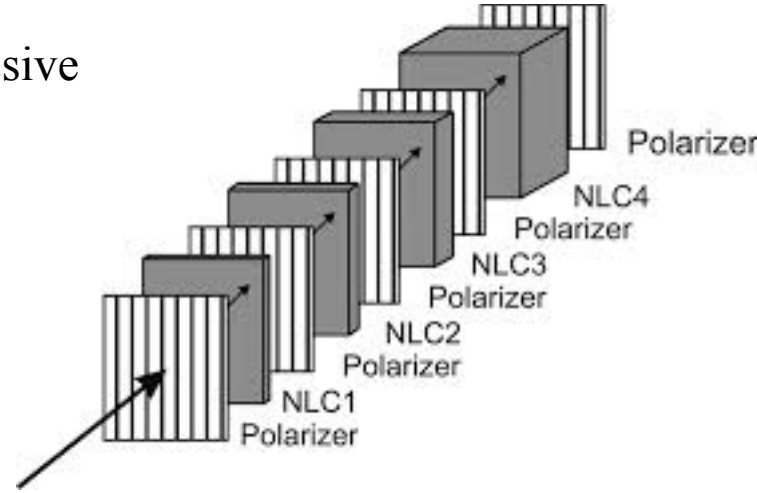

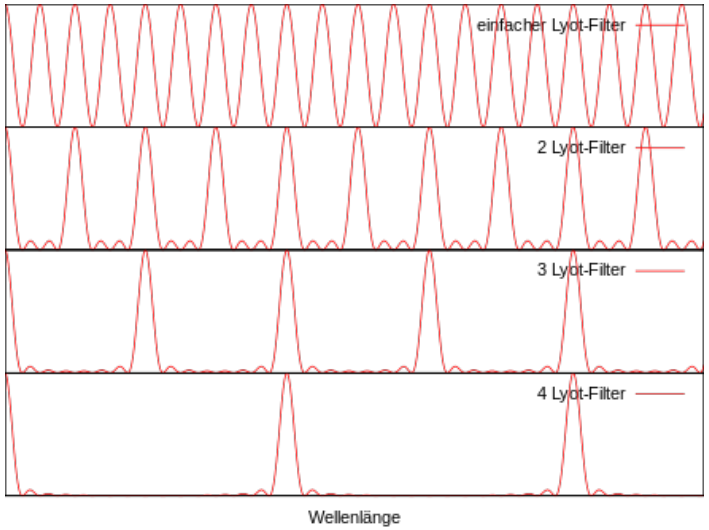

Lyot Filter – 3: Tuning in Wavelength

- Start with the single element birefringent filter:
- Insert a ¼-wave plate with optic axis oriented at 45° to that of the crystal optic axis (OA oriented vertically):
- Then rotate the final linear polarizer by an angle θ:

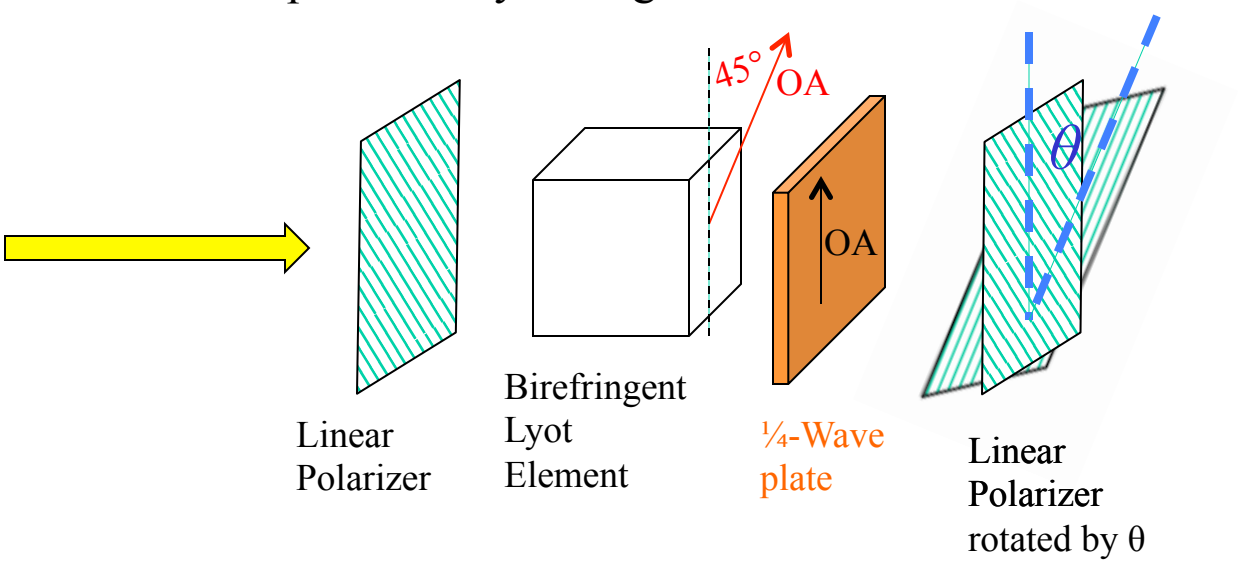

- For the direction of rotation of the exit polarizer shown (clockwise looking at the light source), the intensity of light observed goes as $\cos^2(\delta/2 + \theta)$
- Rotation of the exit polarizer by $[0 - \pi]$ then shifts the periodic filter transmission through one full cycle in wavelength!

Exercise VI.1: Using definition of the components of electric field entering the birefringent crystal, derive the expression above for the light intensity emerging from the system.

Lyot Filter – 4: Multiple Tuned Elements

- By adding a ¼-wave plate and a rotatable polarizer to each of the successive elements of the stack, **one can have a filter that is completely tunable over its entire wavelength range: Universal Birefringent Filter (UBF)**

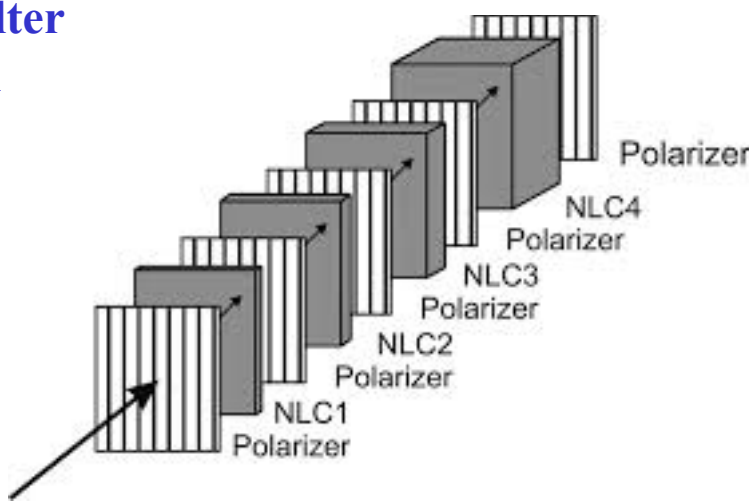

Advantages:

- Fully tunable in λ
- Accepts a large field-of-view

Drawbacks:

- Many optical elements that must be precisely cut and aligned
- Lots of internal reflections – ghost images
- Large optical path, many polarizers lead to low throughput
- Difficult and expensive to acquire the thicker crystal elements

Universal Birefringent Filter, NSO, Sac Peak USA

Demonstration retarders: halfwave = 280nm
Quarterwave = 138 nm
Colored curves for multipliers of half-wave plate (i.e. 2 = full wave retardance)

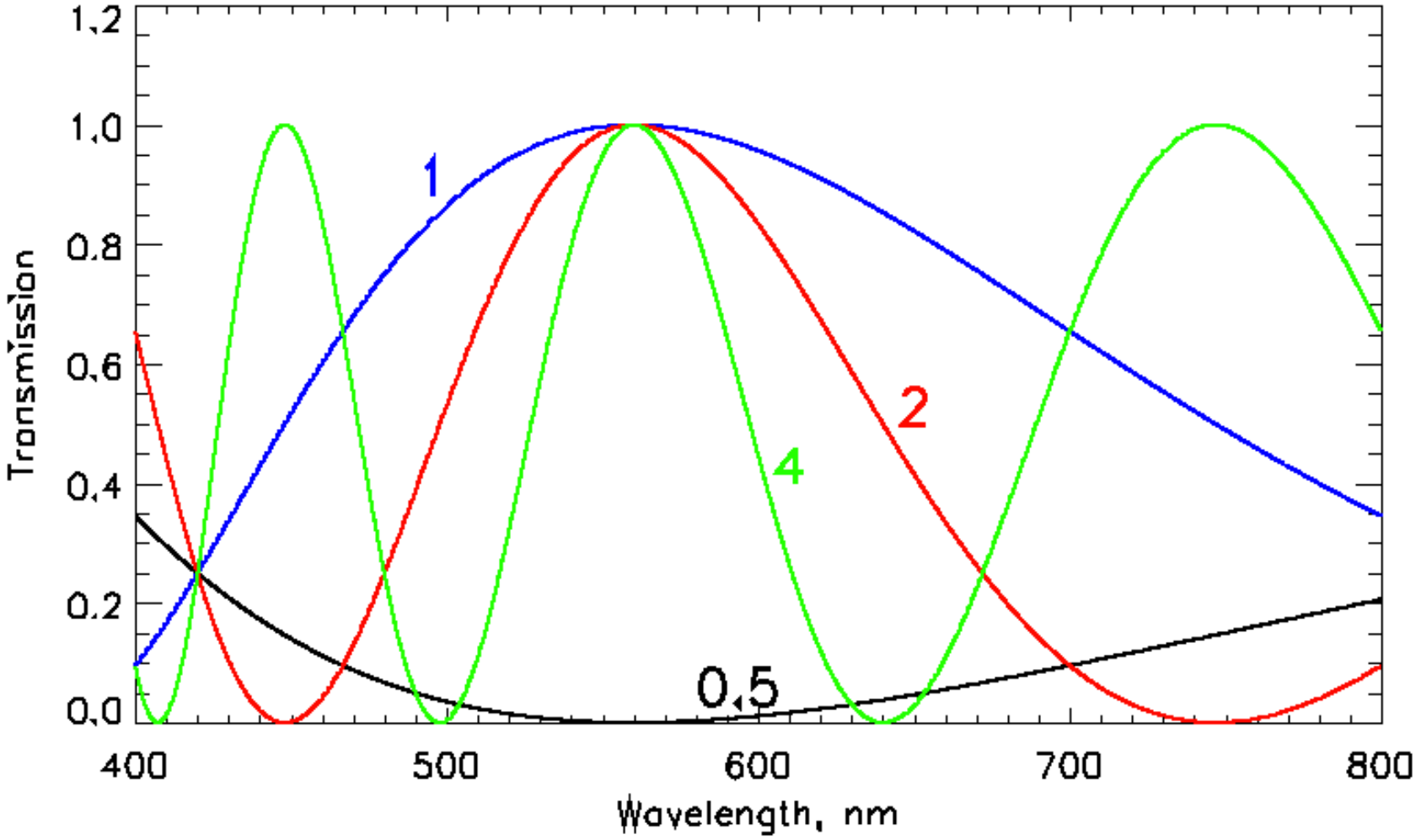

ChroMag Instrument Overview

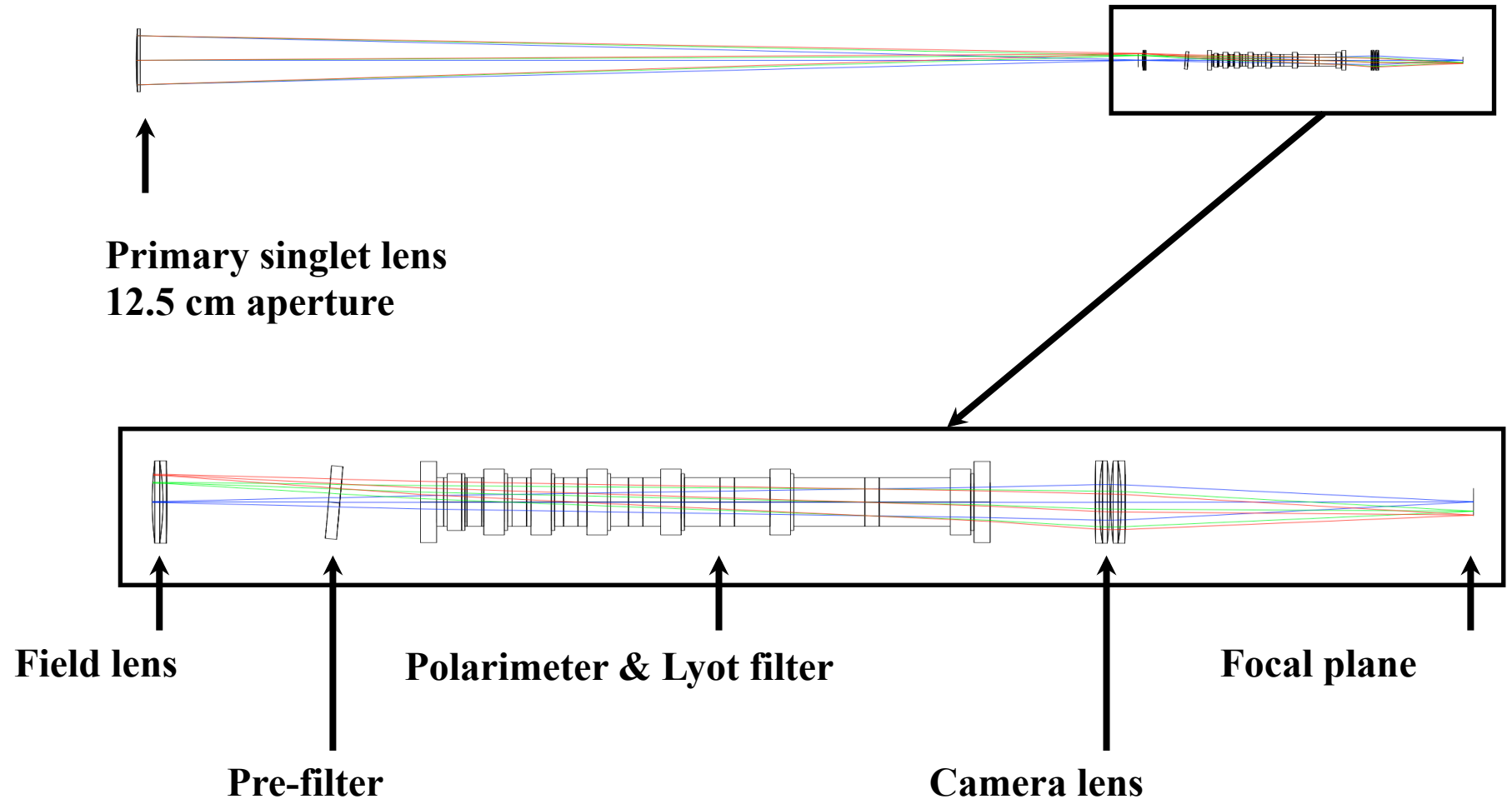

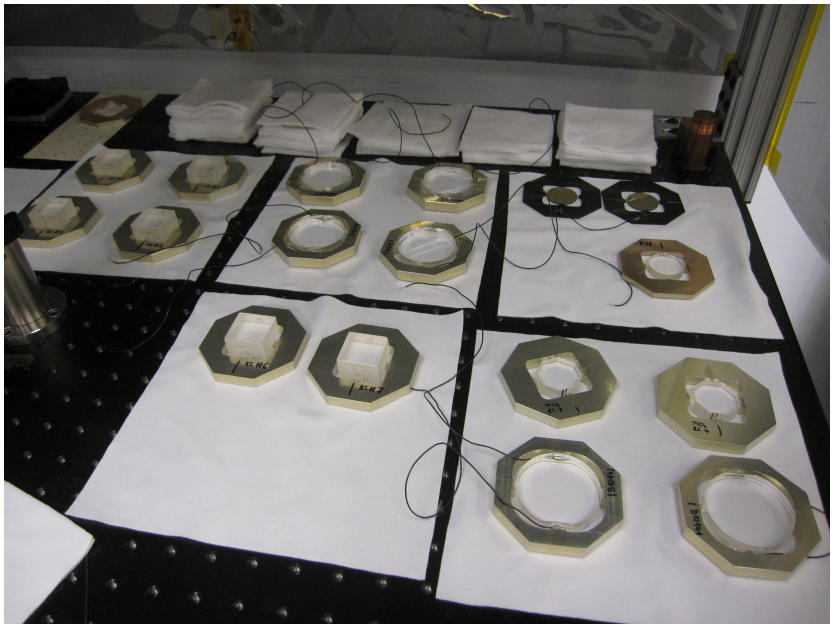

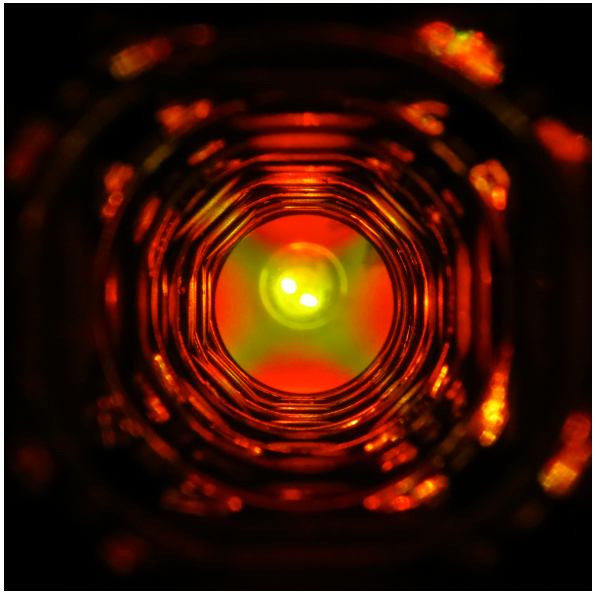

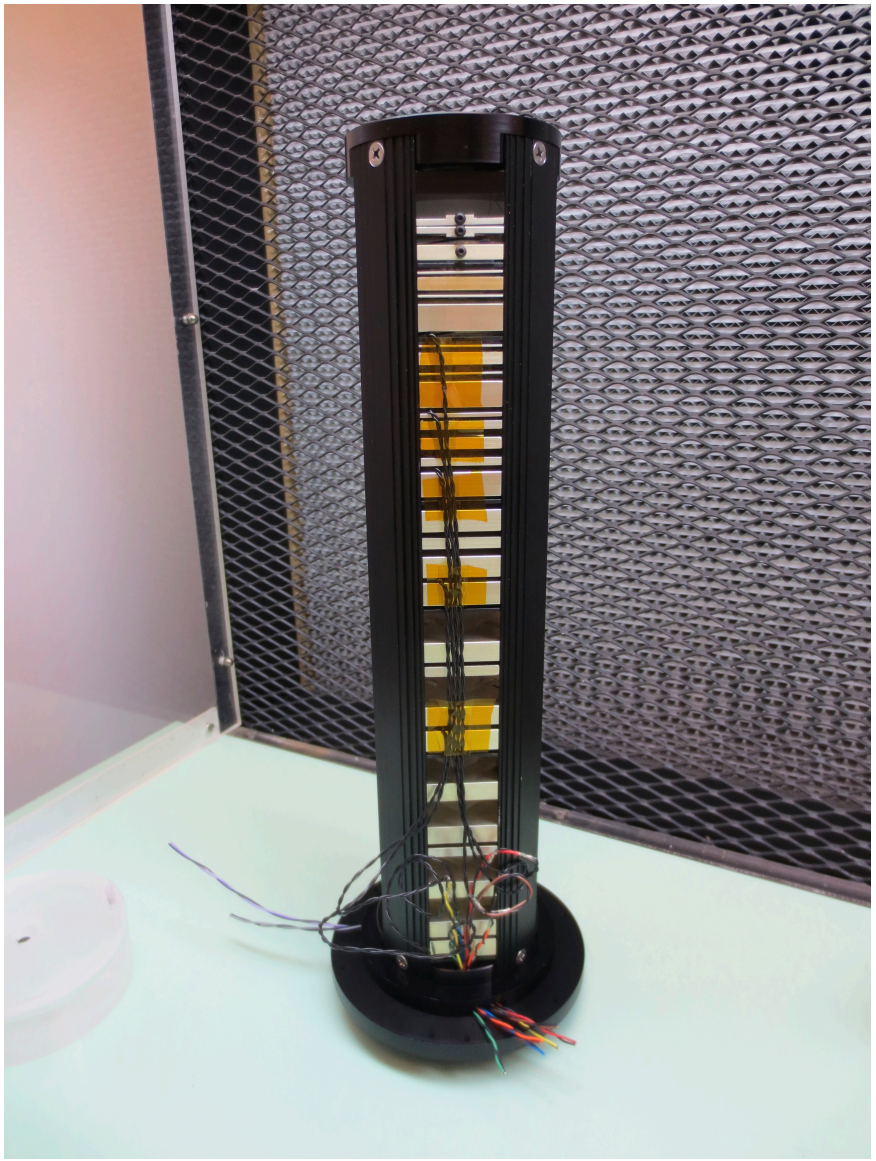

Michelson Interferometer Filter

- The two "arms" of the interferometer differ in optical path length
- The interfering beam on output will have the $\sin^2$ intensity variation with wavelength common to other interference-based monochromators
- Polarization can be used to optimize the design and to allow wavelength tuning
- Path difference of interfering beams on output:

$$\Delta = 2(n_1 d_1 - n_2 d_2)$$

- Phase difference:

$$\delta = 2\pi\Delta/\lambda$$

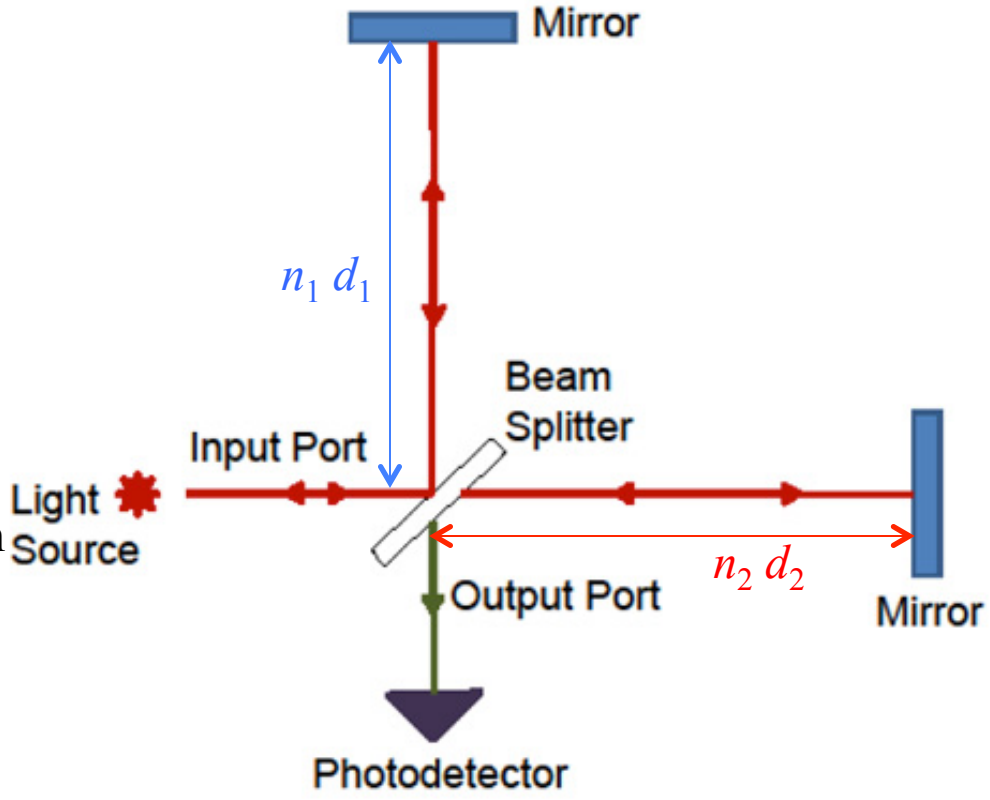

One aspect of all interferometric imagers is sensitivity to field-of-view effects: different oblique rays will experience interference at different wavelengths

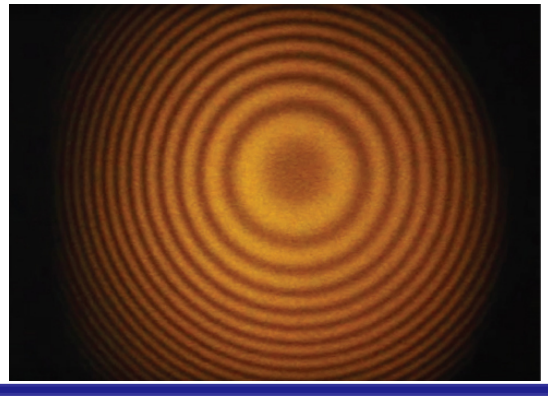

Michelson Interferometer Filter – 2: Wide Field Version

- The Michelson interferometer may be modified with a glass block on one arm (or one on each arm, each block having a different index of refraction and thickness).
- The glass blocks on the horizontal and vertical arms have thicknesses and indices of refraction such that the oblique beams follow the same paths within the symmetrical beam splitter block

- Snell's law of refraction: $n_1 \sin\theta_1 = n_3 \sin\theta_3$

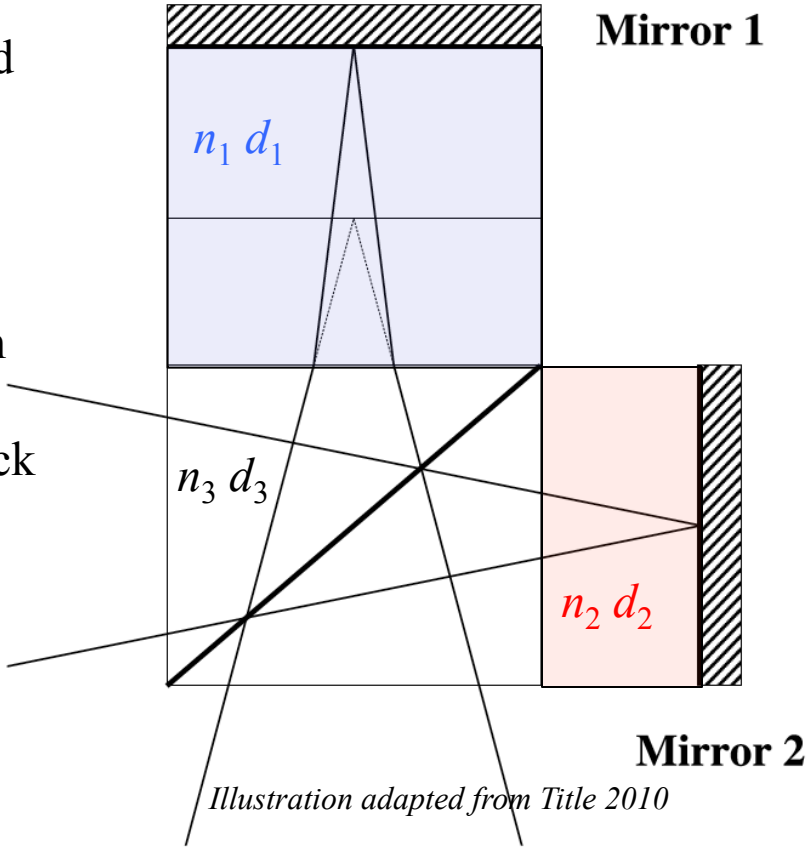

Illustration adapted from Title 2010

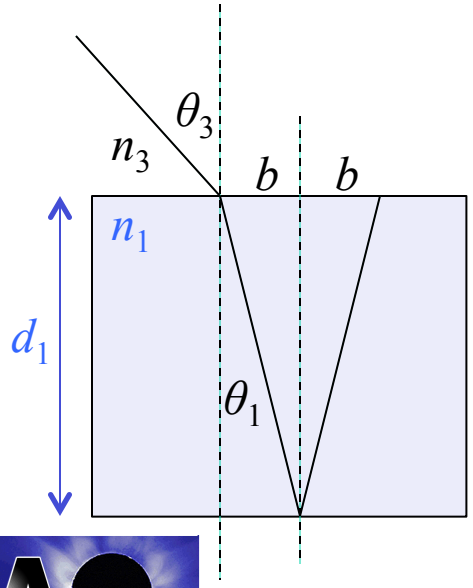

- For beams to take same path through the beam splitter, the distance $b = d_1 \sin\theta_1$ should be equal for both arms. Thus we require:

$$b = (n_3 \sin\theta_3)\ d_1/n_1 = (n_3 \sin\theta_3)\ d_2/n_2$$

or

$$d_1/n_1 = \quad d_2/n_2$$

Michelson Interferometer Filter – 3: Wide Field Version

- Under these conditions, the path difference of the two arms may then be written:

$$\Delta = 2(n_1 d_1 - n_2 d_2) = 2\, d_1 (n_1^2 - n_2^2)/n_1$$

and the phase difference becomes:

$$\delta = 2\pi\Delta/\lambda = 4\pi\, d_1 (n_1^2 - n_2^2)/(n_1 \lambda)$$

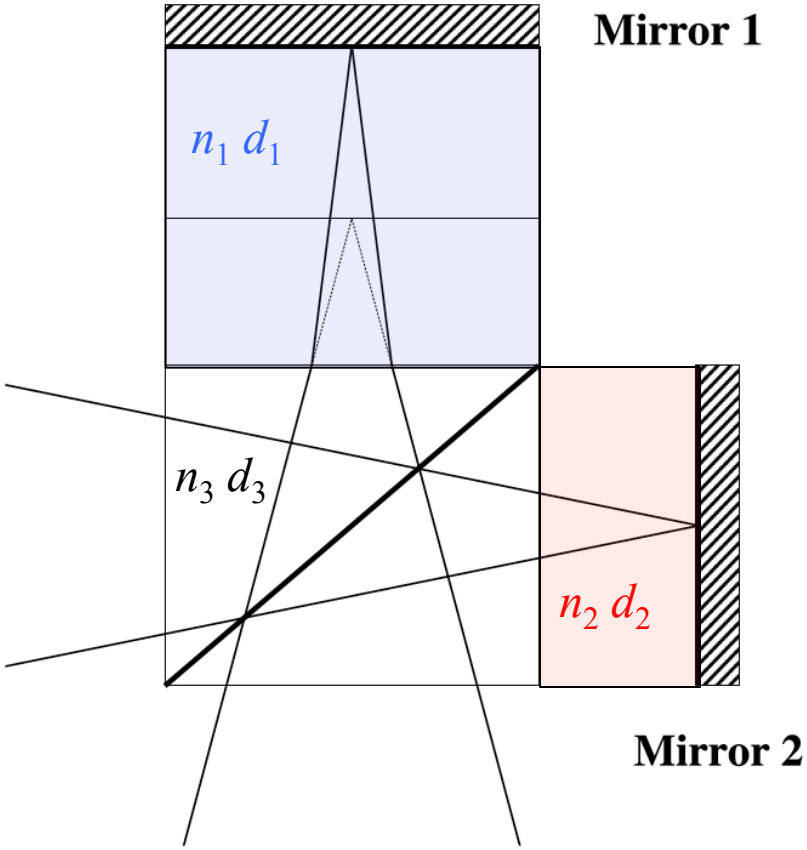

Illustration adapted from Title 2010

Michelson Interferometer Filter – 4: Tuning and Optimizing with Polarization

- Illuminate Michelson with light polarized at 45°
- Beam Splitter is **polarizing**, reflecting the S-wave (polarized perpendicular to the plane of reflection) and transmitting the p-wave (polarized in the plane of incidence)
- **Quarterwave plates** in front of the mirrors on each arm are traversed twice, becoming half wave retarders and rotating the plane of polarization by 90°
- The roles of reflection/transmission of the beams at the beam splitter are then reversed, so that the two beams exiting from the interferometer have opposite polarizations
- The **quarterwave plate at the exit** of the device, followed by a rotatable linear polarizer, allows tuning of the interference in wavelength in the **same fashion as illustrated for the Lyot filter**

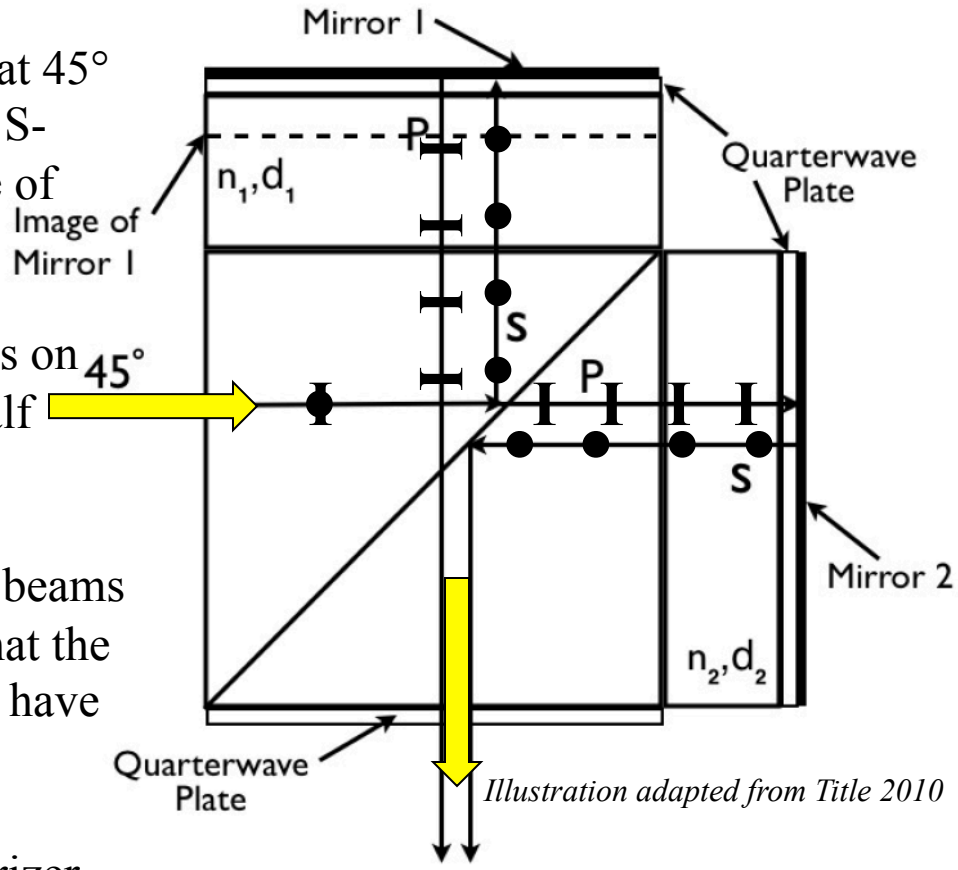

Illustration adapted from Title 2010

Notes on Interferometric Devices

- All imaging devices described (Fabry-Pérot, Lyot, Michelson) must be maintained at nearly constant temperature to maintain optical properties of retarders, etc.
- Each device has its merits and drawbacks relative to the others
  - Behavior relative to overall properties of feed optical system
  - Sensitivity to field-of-view effects
  - Availability and ease of manufacture of relative optical components
  - Shape and roughness of optical surfaces
  - Required pre-filters
  - Physical size of device
- The spectrograph is a simple device that is largely immune to these ills of imaging devices, but it has separate merits and drawbacks

Hybrid Discriminators – Simultaneous Spatial/Spectral Information

The quest is for *simultaneous* 2-d spatial + spectral information continues……

Some hybrid spectrographic/imaging techniques have been proposed

Illustrated by a few examples:

1. Image Slicers/Fiber Optics
2. Subtractive Double Pass Spectrographs: MSDP
3. Hadamard Spectroscopy
4. Stereoscopic Spectroscopy

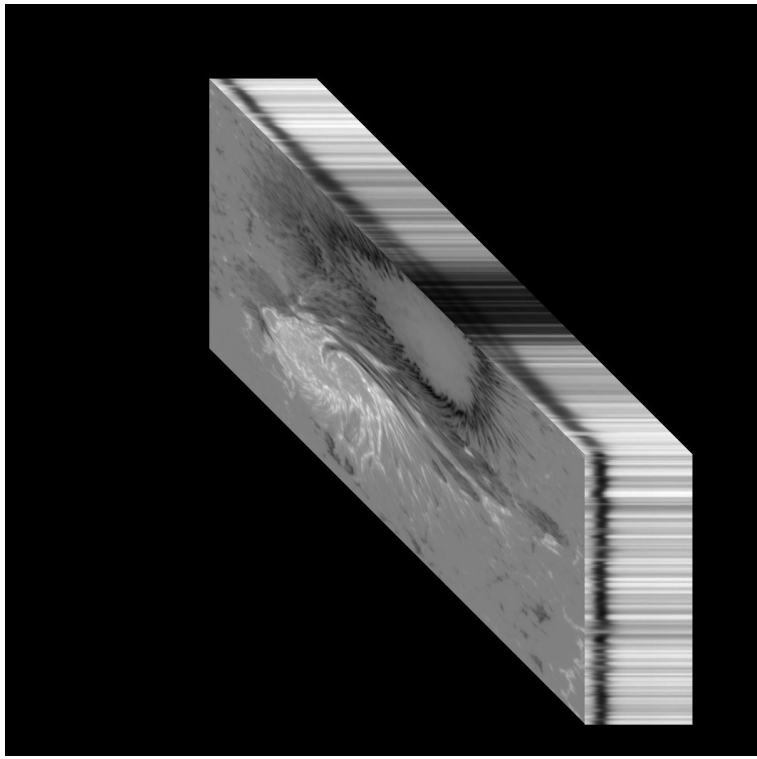

Hybrid Discriminators – 1: Image Slicers and Fiber Optics

Achieve 2-D simultaneously using a spectrograph

1. Image slicer

- complicated prism array, transfer portions of 2-D image to spectrograph slit
- Restore image in post-observation processing

2. Fiber optics

- Performs same function as image slicer, but with bundles of fiber optic cables

3. Multiple Slits

- Multiple slits instead of one, each separated by a small distance (**FIRS**)
- Narrow-band filter assures no overlap in focal plane of spectrograph
- Slit scanning a small distance equal to the separation of the slits
- Allows spectral/spatial imaging of a narrow, tall patch of Sun

Input Image Mask

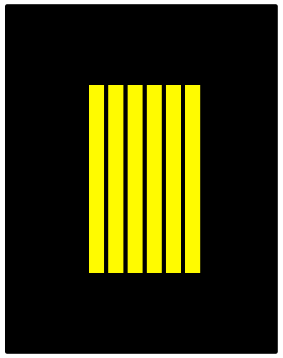

Spectrograph Slit

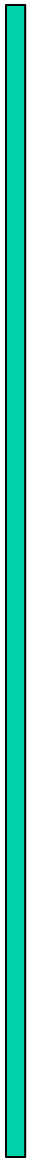

Hybrid Discriminators – 2: Subtractive Double-Pass Spectrographs

- Spectrograph has no slit
- Lens L1 collimates the light from Grating 1
- Slit selects spatial/spectral information
- Grating 2 operates opposite of Grating 1, thus is "subtractive"
- Lens L3 restores the image at the camera

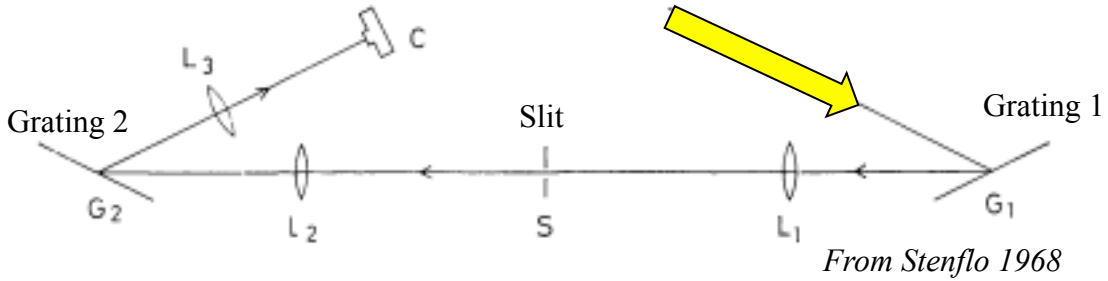

From Stenflo 1968

- Final image is monochromatic at each position, but wavelength varies across the image
- Possible to carry out this scheme with a single spectrograph:

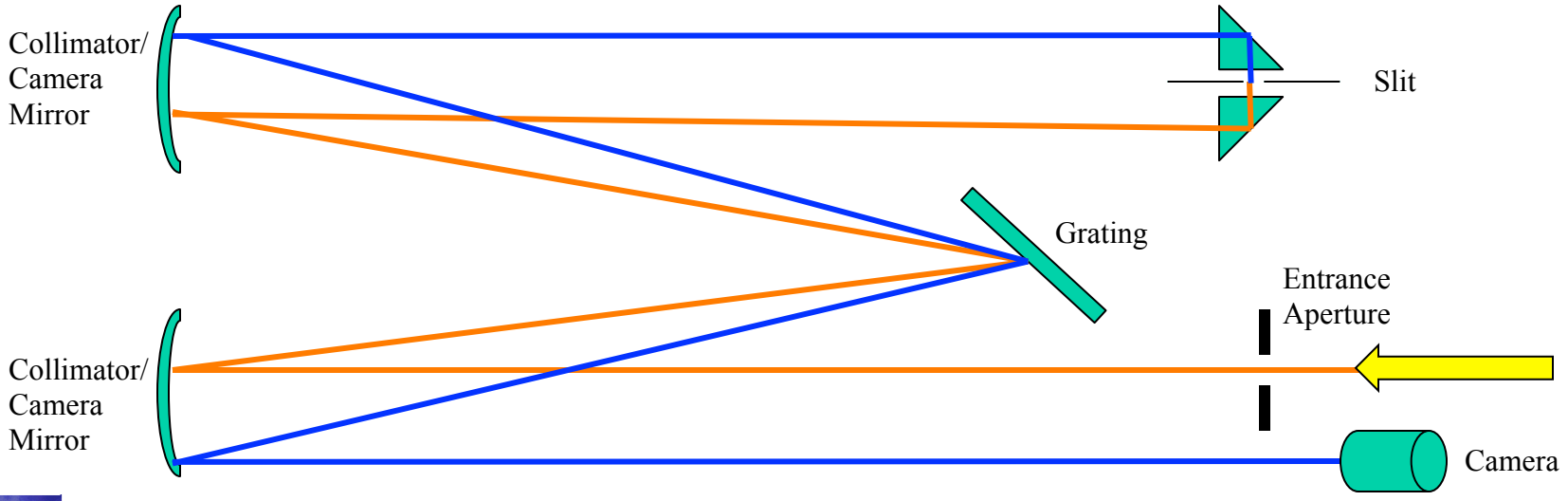

Hybrid Discriminators – 2: Subtractive Double-Pass Spectrographs -- MSDP

- **MSDP: Multichannel Subtractive Double Pass**

- Replace slit with complicated image slicer/slit device
- 16 pseudo-monochromatic rays pass back through the system, forming narrow-band images at the camera

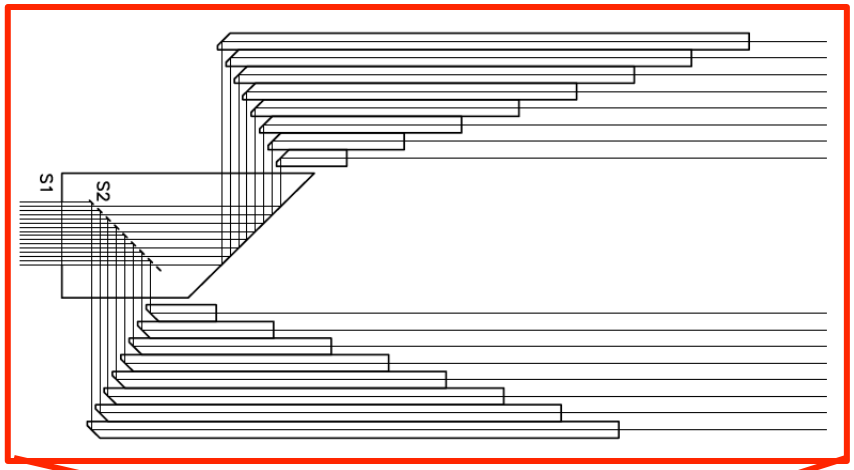

Illustration from Mein 2002

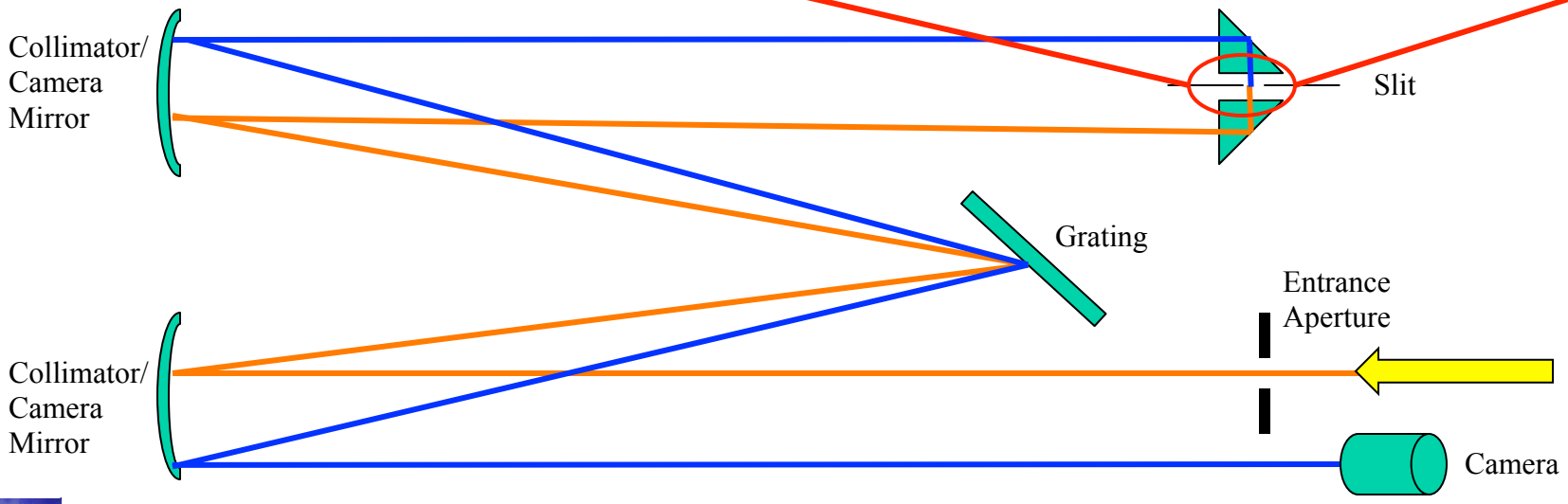

Hybrid Discriminators – 2: Subtractive Double-Pass Spectrographs -- MSDP

Hα

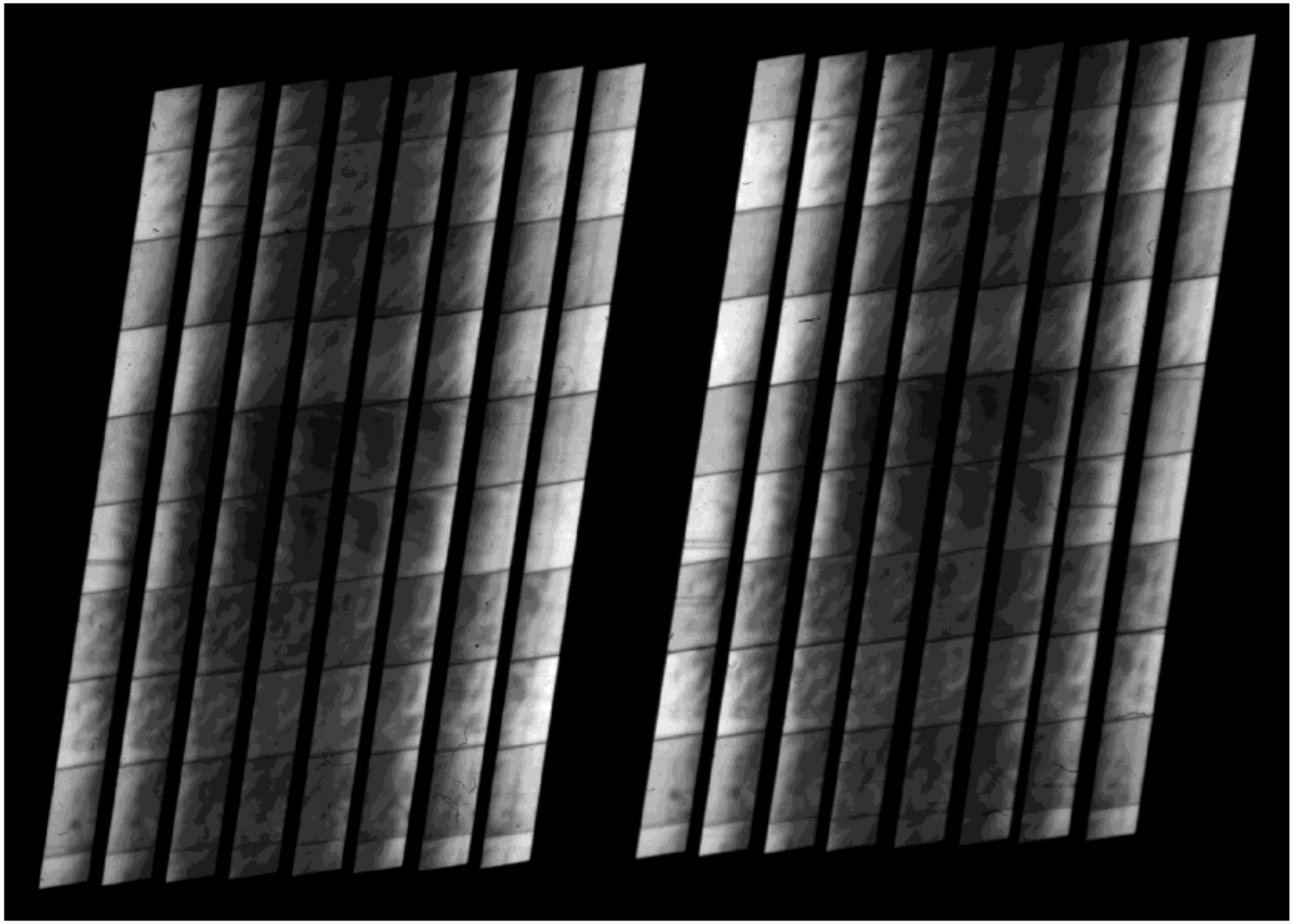

$\lambda \longrightarrow$

Illustration from Mein 2002

Hybrid Discriminators – 3: Hadamard Mask Multiplexing – Tunis

- **TUNIS: Tunable Universal Narrowband Imaging Spectrograph**

- Replace slit with a specific slit-like mask that may be scanned back and forth along the dispersion
- Apertures of mask have a particular spacing and width: multiplex the spatial and spectral information
- Mask scanned horizontally making exposure at each of 17 positions
- Linear combinations of these 17 positions allow one to recover (demultiplex) monochromatic images at 17 wavelengths

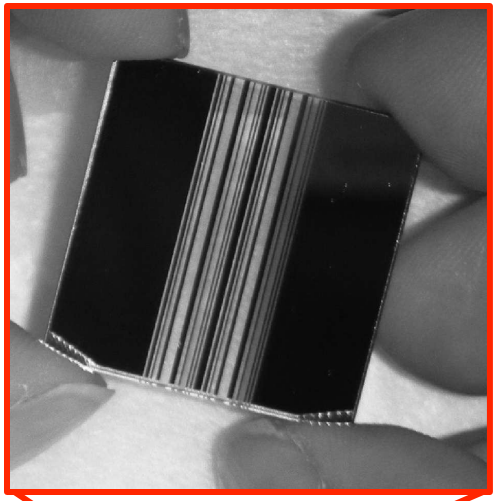

Image from López Ariste 2011

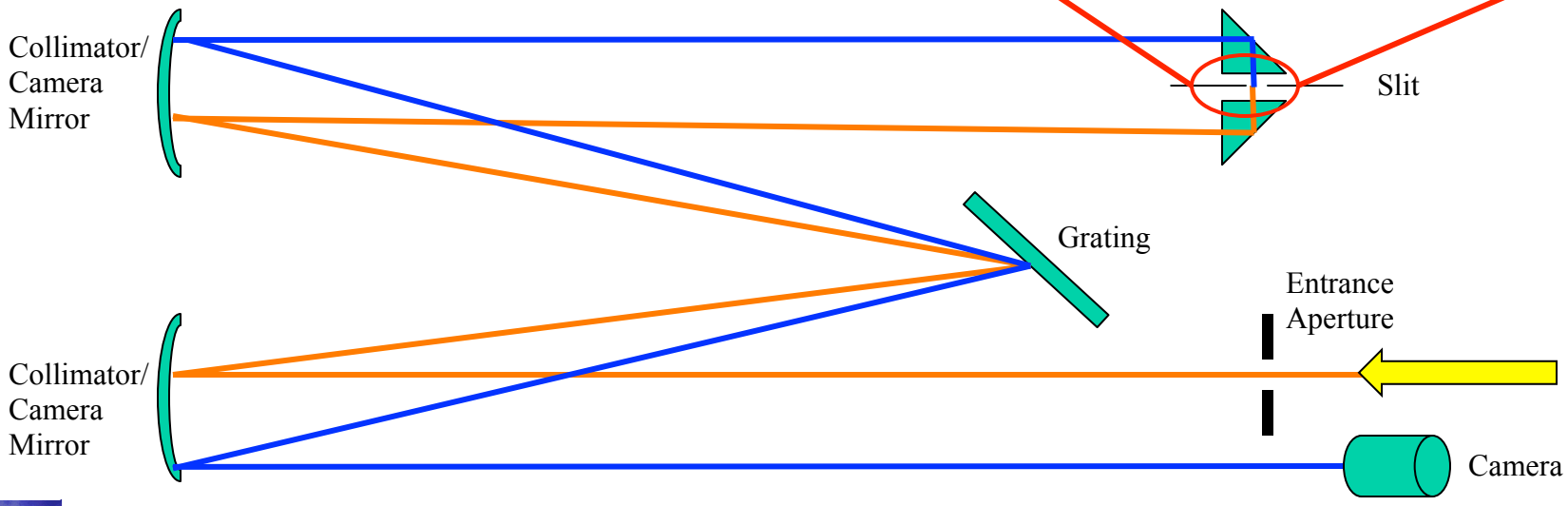

Hybrid Discriminators – 3: Hadamard Mask Multiplexing – Tunis

Multiplexed raw images

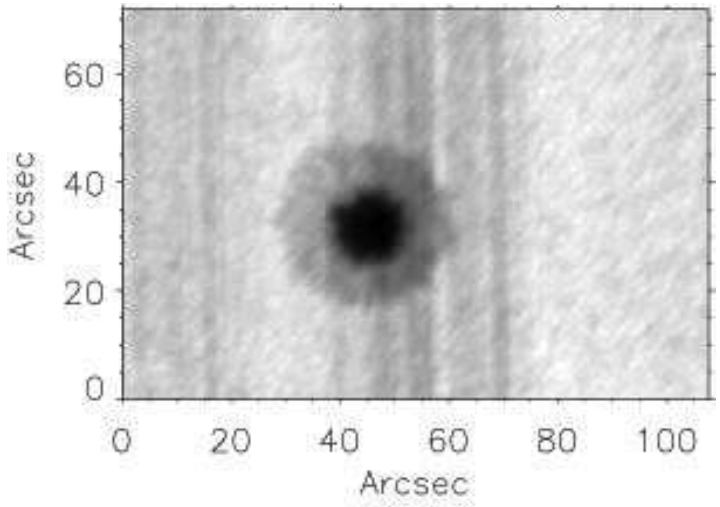

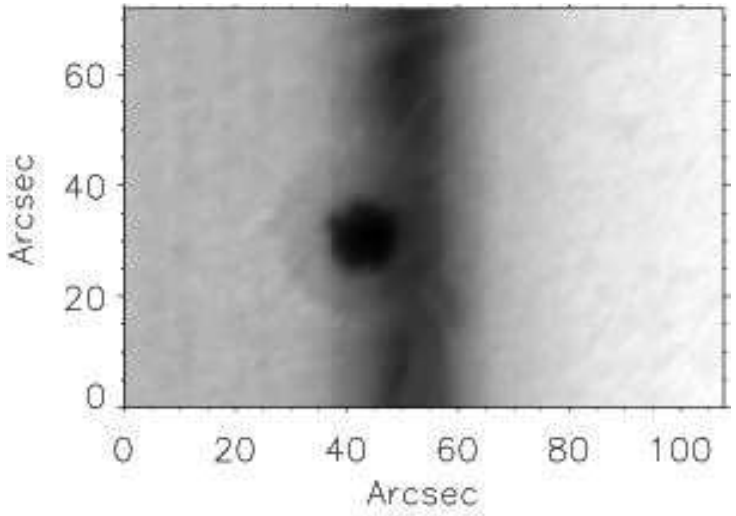

Demultiplexed images – one of 17 for different spectral positions

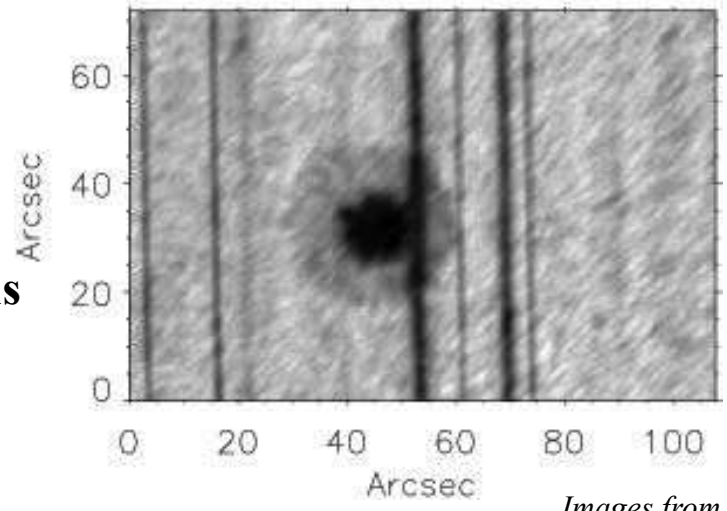

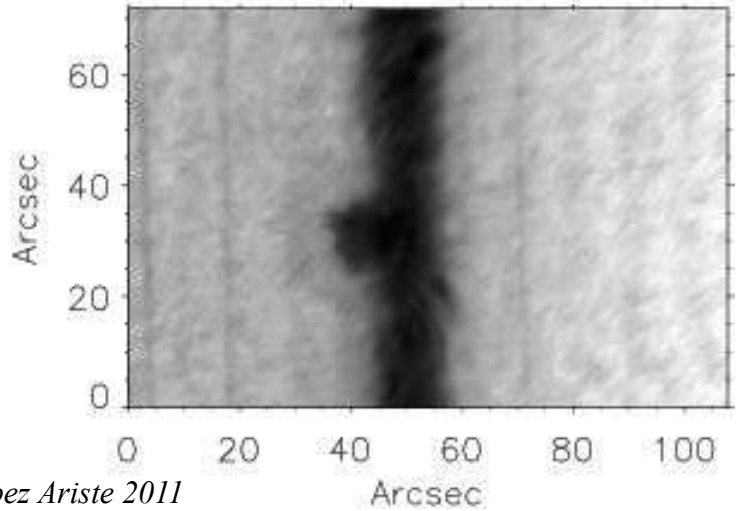

Images from López Ariste 2011

Hybrid Discriminators – 4: Stereoscopic Spectroscopy

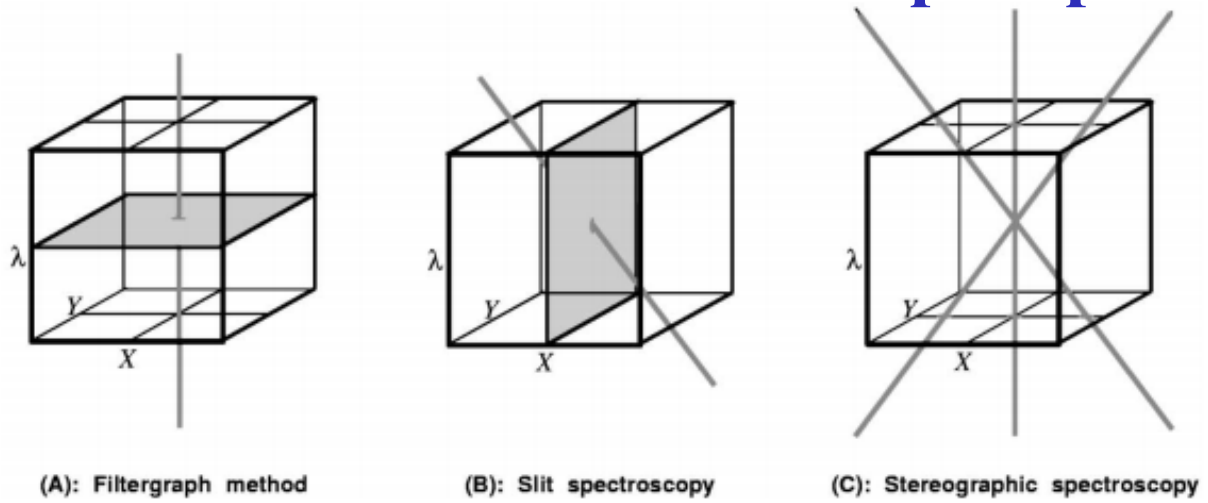

SHAZAM: Solar High-speed Zeeman Magnetograph

Illustrations from DeForest et al. 2004

- Spectrograph has no slit
- Focal plane images are convolution of spatial/ spectral information
- Extraction

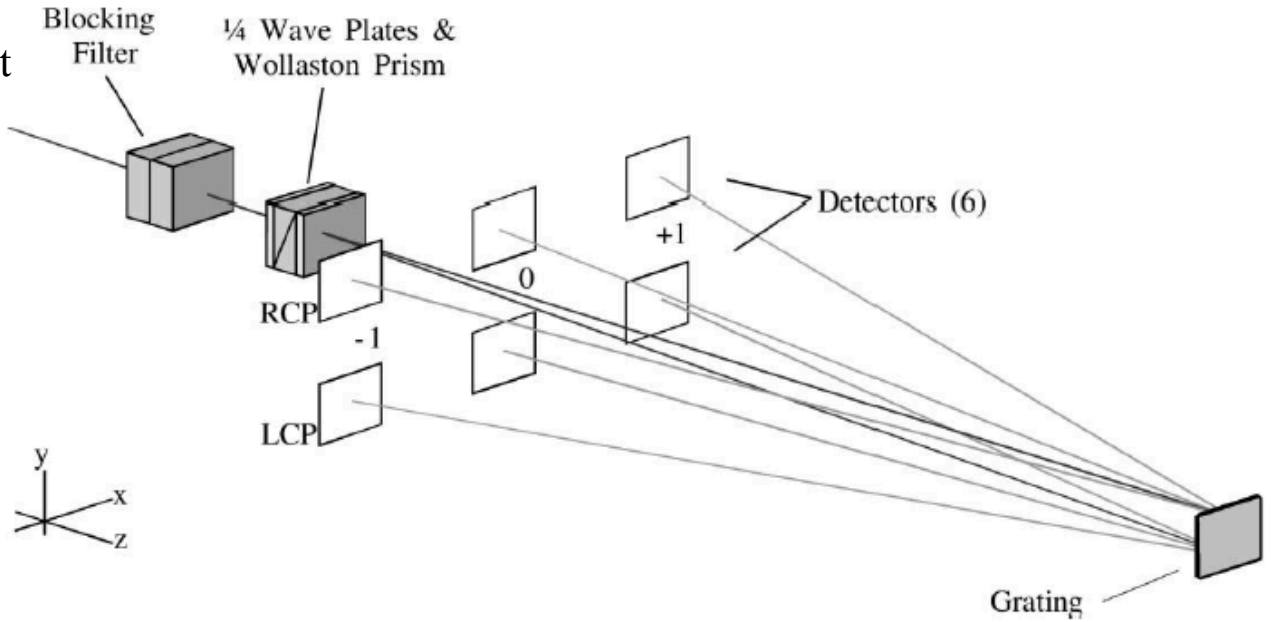

Hybrid Discriminators – Simultaneous Spatial/Spectral Information

Some issues with hybrid schemes:

- Instrumental limitations on wavelength range and spectral purity
- The untangling of mixed spectral/spatial information may be compromised in the presence of noise and other observational error sources
- CCD exposure may be dominated by a large contribution from the continuum: reduces S/N in spectral lines
- For TUNIS: spatial/spectral information is multiplexed together so that all wavelength/spatial information is effectively averaged over the duration of the Hadamard mask scan. Does this really buy more efficiency? And what is the cost in spatial resolution?

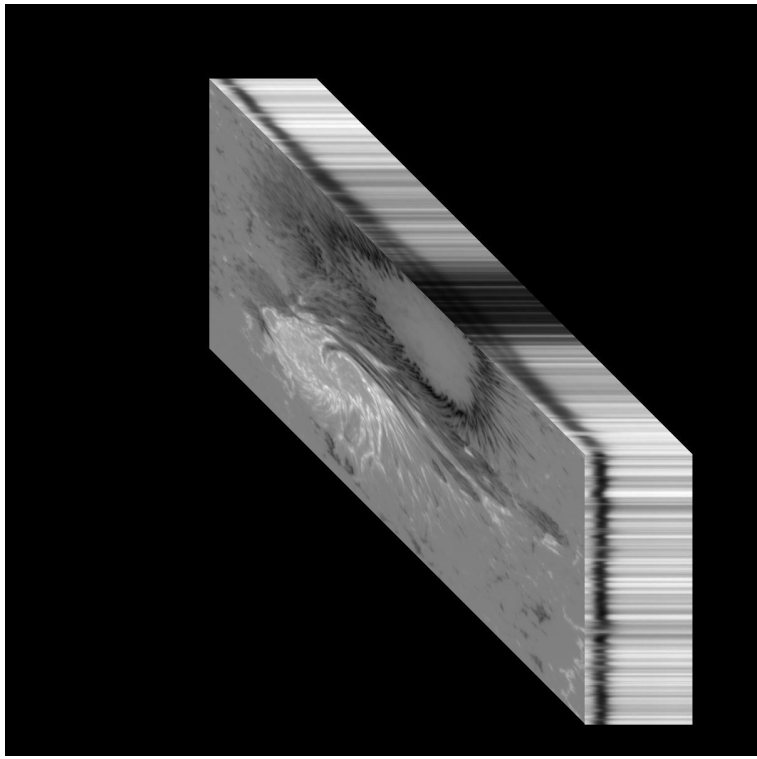

VII. Detectors for Solar Polarimetry

Desirable Qualities of Detectors for Solar Polarimetry

1. **High quantum efficiency** (the efficiency with which photons are converted to photoelectrons)
2. **Rapid read-out** (to beat seeing motions, or evolution of the solar scene)
3. **Spectral sensitivity** (many observations are desirable to carry out in the infrared)
4. **Large dynamic range** (large full-well capacity)
5. **Linear response** to photon signals
6. **High charge transfer efficiency** (if architecture is like a CCD where charge is transferred laterally upon read-out)
7. **Large number of pixels** (allows sampling images at high resolution, or detection of multiple spectral lines in spectroscopic observations)

Photon Noise, Dark Current, "Read-out" Noise

- **Photon noise N_p** is the inescapable error associated with sensing (counting) *n* photoelectrons
  - If one makes a large number of equal measurements of a constant signal originating from a randomly-timed source, the uncertainty in detection of the signal obeys Poisson statistics
  - For significantly large *n*, the distribution of the errors is Gaussian
  - The rms error of the sampling process is $N_p = \sqrt{n}$

- **Dark Current N_d** is a random charge that builds up on a detector when no light is present
  - Increases linearly with exposure time
  - Usually negligible for typical fast read-out rates of solar polarimetry

- **Read-out noise N_{read}** is a random noise associated with the process of reading the electronic signal of the detector
  - Usually is a function of temperature of the electronics (cold = low noise)

- **Highly desirable to have $N_{read} << N_p$**

Photon Noise, Dark Current, "Read-out" Noise

- The noise levels are usually expressed in terms of number of photoelectrons
- These noise sources are random in nature
- Signal-to-Noise ratio *S/N*:

$$S/N = \frac{n}{N_p + N_d + N_{read}}$$

- Assume N_d is negligible
- When $N_p >> N_{read}$, $S/N \approx n^{1/2}$
- When $N_p << N_{read}$, $S/N \approx \left(1 + \frac{N_{read}}{N_p}\right)^{-1} n^{1/2}$
- In order to achieve the same S/N in the absence of read noise, one **must integrate a factor of $(1 + N_{read}/N_p)^2$ longer**

Some Promising New Trends in Detectors

- **CCD (Charge-Coupled Device) Detectors:**
  - Mainstay detector for solar polarimetry for many years
  - large arrays with many parallel read-out channels
  - Read-out noise scales with read-out speed
  - Power consumption scales with read-out speed (implications for space applications)
  - Many-channel read-out enables lower read noise along with rapid readout
  - Ideal for ZIMPOL-type polarimetry

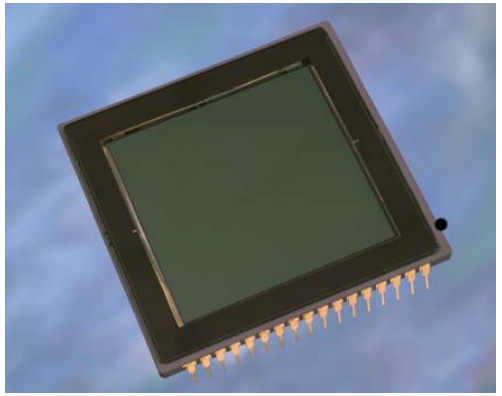

4096 x 4096 Kodak 16803 CCD

- **Active-Pixel Sensor Imagers:**
  - Each pixel has its own amplifier
  - Frequently use CMOS (Complementary Metal Oxide Semiconductor) technology
  - Very low read noise and low power consumption
  - Fast frame rates becoming standard
  - Possibilities for advanced architecture at the pixel level
  - Earlier models had “rolling shutter” because successive rows read out sequentially – now cameras exist with full frame simultaneous exposure

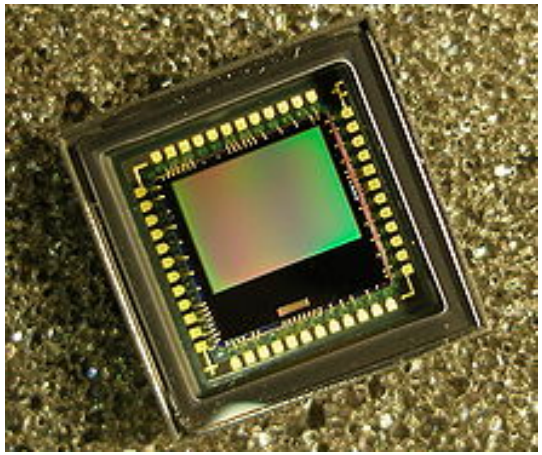

Some Promising New Trends in Detectors

Impressive specifications for some new cameras. One example……..

On-Chip Charge Caching ➔ On-Chip Demodulation

- Upper surface active in photon collection
- ≥ 3 subsurface arrays – allows storage of all four Stokes parameters
- Vertical shifting, accumulation of charge
- Relatively slow readout

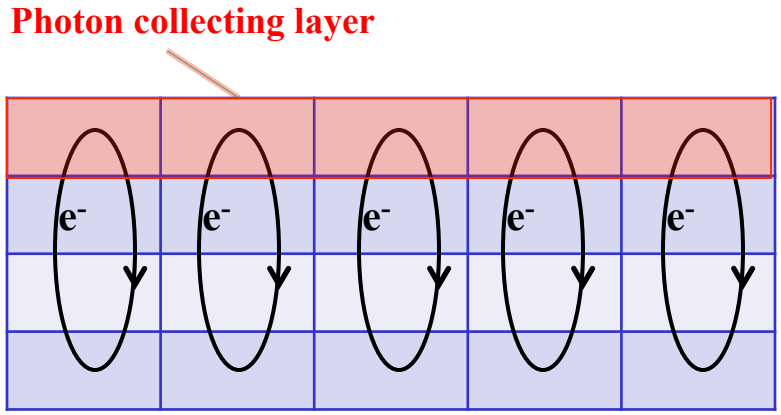

VIII. Methods for Polarization Calibration

Polarization: Accuracy vs. Precision

Polarimetric precision: the level of the smallest signals that may be detected

- Usually governed by the random noise in the measurement
- Can assign an *rms* precision for each Stokes parameter $\boldsymbol{\sigma} = [\sigma_I\ \sigma_Q\ \sigma_U\ \sigma_V]^{\mathrm{T}}$. (In general the values of $\sigma_I\ \sigma_Q\ \sigma_U\ \sigma_V$ may differ slightly from one another depending on the modulation/demodulation scheme.)
- As indicated previously, apparently the record for polarimetric precision for Solar polarimetry is still held by Kemp et al. 1988

Polarimetric Accuracy: the accuracy with which the measurement represents the observed light source

- Systematic errors in the calibration of the polarimeter (and other artifacts of the measurement process) usually lead to polarimetric accuracy worse than polarimetric precision
- Polarization accuracy is related to the accuracy of the instrument response matrix **X**

What is Polarization Calibration?

- The telescope and polarimeter together make a series of measurements that constitute the polarization data
- Usually the product of the observation is a 4-vector, $\mathbf{I}_{obs}$, like a Stokes vector, containing the full information of the polarized intensity
- But this vector results not only from the telescope and polarimeter optics, but also from the camera and demodulation electronics
- Because the camera and demodulator electronics are not optical devices, we cannot construct a Mueller matrix for the entire system
- Instead, we determine an instrument response matrix, **X**, that is similar in most ways to a Mueller matrix, but may not obey all the properties of the optical Mueller matrix

$$\mathbf{I}_{obs} = \begin{pmatrix} I_{obs} \\ Q_{obs} \\ U_{obs} \\ V_{obs} \end{pmatrix} = \begin{pmatrix} X_{11} & X_{12} & X_{13} & X_{14} \\ X_{21} & X_{22} & X_{23} & X_{24} \\ X_{31} & X_{32} & X_{33} & X_{34} \\ X_{41} & X_{42} & X_{43} & X_{44} \end{pmatrix} \begin{pmatrix} I_{sun} \\ Q_{sun} \\ U_{sun} \\ V_{sun} \end{pmatrix} = \mathbf{X}\mathbf{I}_{sun}$$

- If we can determine **X**, then we can recover the Stokes vector input to the telescope:

$$\mathbf{I}_{sun} = \mathbf{X}^{-1}\mathbf{I}_{obs}$$

- Thus, **polarization calibration is the process of determination of X, and hence $\mathbf{X}^{-1}$**

Relating Polarimetric Accuracy to the Polarimetric Precision

If $\mathbf{X}$ is the actual response matrix and $\mathbf{X}_{meas}$ is the measured response matrix, then the error in the inference of the Stokes vector entering the telescope is:

$$\Delta\mathbf{I} = \mathbf{I}_{meas} - \mathbf{I}_{sun} = (\mathbf{X}_{meas}^{-1}\mathbf{X} - \mathbf{1})\mathbf{I}_{sun}$$

Here 1 is the identity matrix:

$$\mathbf{1} = \begin{pmatrix} 1 & 0 & 0 & 0 \\ 0 & 1 & 0 & 0 \\ 0 & 0 & 1 & 0 \\ 0 & 0 & 0 & 1 \end{pmatrix}$$

We desire relationship between $\Delta\mathbf{I}$ on one hand, and the precision of measurement of the Stokes vector $\Sigma_{meas} = \mathbf{X}_{meas}^{-1}\sigma$ on the other hand.

In order that errors from calibration are less than the random noise, we require

$$\Delta\mathbf{I} < \Sigma_{meas}$$

Thus for the error in the response matrix $\Delta\mathbf{X} = \mathbf{X} - \mathbf{X}_{meas}$:

$$\Delta\mathbf{X}\mathbf{I}_{sun} < \Sigma_{meas}$$

$|\Delta\mathbf{X}|$ is known as the tolerance matrix.

Relating Polarimetric Accuracy to the Polarimetric Precision

One may immediately fill in the first column of the tolerance matrix $|\Delta\mathbf{X}|$ understanding that the intensity-to-polarization tolerance is equal to the targeted random noise level:

$$|\Delta\mathbf{X}| < \begin{pmatrix} - & - & - & - \\ \sigma_Q & - & - & - \\ \sigma_U & - & - & - \\ \sigma_V & - & - & - \end{pmatrix}$$

The **diagonal elements of $|\Delta X|$** are a special case.

- $|\Delta\mathbf{X}|_{11}$ = error in the absolute intensity calibration, not considered here
- Diagonal elements $|\Delta\mathbf{X}|_{22}$ $|\Delta\mathbf{X}|_{33}$ $|\Delta\mathbf{X}|_{44}$ indicate the scale errors of the polarization signals. Limits set by requirements of scientific analysis of the spectral profiles, i.e. a_I, a_Q, a_U, a_V.
- Because this tolerance is nearly always much greater than the random noise, we have:

$$|\Delta\mathbf{X}| < \begin{pmatrix} a_I & - & - & - \\ \sigma_Q & a_Q & - & - \\ \sigma_U & - & a_U & - \\ \sigma_V & - & - & a_V \end{pmatrix}$$

Relating Polarimetric Accuracy to the Polarimetric Precision

The polarization crosstalk terms:

For a given scientific objective one expects a maximum polarization $\mathbf{P}_{max} = [1\ p_Q\ p_U\ p_V]^{\mathrm{T}}$. Suppose that we input the maximum for Stokes Q: $\mathrm{P}_{maxQ} = [1\ p_Q\ \ 0\ 0]^{\mathrm{T}}$.

As p_Q is nearly always considerably less than unity, we may relax the tolerance on crosstalk terms among the polarization states Q, U, V by the corresponding amount:

$$|\Delta\mathbf{X}| < \begin{pmatrix} - & - & - & - \\ \sigma_Q & a_Q & \sigma_Q / p_U & \sigma_Q / p_V \\ \sigma_U & \sigma_U / p_Q & a_U & \sigma_U / p_V \\ \sigma_V & \sigma_V / p_Q & \sigma_V / p_U & a_V \end{pmatrix}$$

Finally, **the crosstalk from polarization *Q*, *U*, *V* into intensity:**

Errors in relative intensity are governed by data analysis, so adopt the scaling tolerance

$$|\Delta\mathbf{X}| < \begin{pmatrix} a_I & a_I / p_Q & a_I / p_U & a_I / p_V \\ \sigma_Q & a_Q & \sigma_Q / p_U & \sigma_Q / p_V \\ \sigma_U & \sigma_U / p_Q & a_U & \sigma_U / p_V \\ \sigma_V & \sigma_V / p_Q & \sigma_V / p_U & a_V \end{pmatrix}$$

Relating Polarimetric Accuracy to the Polarimetric Precision

In practice one makes estimations of parameters $a_{I,Q,U,V}$ and $p_{Q,U,V}$ based on the science requirements:

- The relative accuracy (i.e., fractional accuracy) of the Stokes profiles demanded by the analysis is typically:

  $a_I, a_Q, a_U, a_V \sim$ few percent

- The typical maximum Stokes signals for various applications:
- Photospheric Zeeman effect: $p_Q = p_U = 0.15, p_V = 0.2$
- Chromospheric Hanle/Zeeman effect: $p_Q = p_U = 0.005, p_V = 0.02$
- Photospheric scattering polarization: $p_Q = p_U = 0.002$

Complications of Polarization Calibration

- Only need to introduce 15 known (and different) polarization states into the telescope to determine **X** (X_{ij} are customarily normalized by X_{11}), however……
- In many telescopes, the polarization changes in time due to moving optical components
- Optical devices change and degrade with time
- Properties of variable retarder modulators (LCVRs, FLCs) drift with temperature
- It is problematic to introduce known polarization into large telescopes
- Instrumental polarization varies within the field-of-view

Because of these complications, a number of calibration strategies have been deployed, each adapted to the unique situation of the polarization measurement

But first illustrate with a case where many (but not all) of these problems were absent

Example: Calibration of the *Hinode* Spectro-Polarimeter

Method: Illuminate entrance of telescope with natural sunlight, passing through large polarizers

Telescope 50-cm Aperture

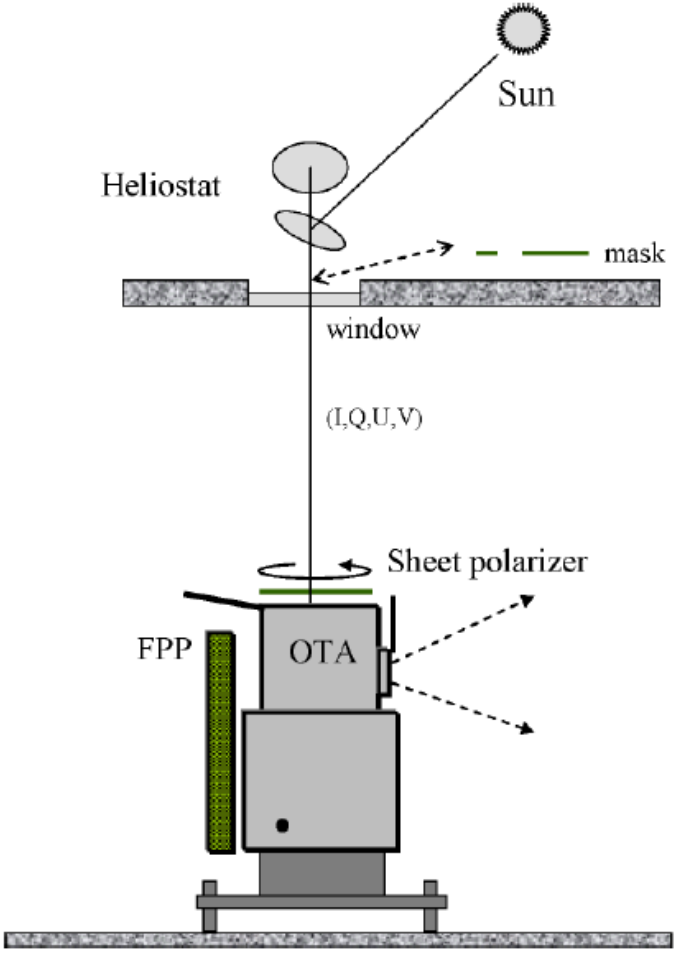

Figure from Ichimoto et al. 2008

Example: Calibration of the *Hinode* Spectro-Polarimeter

Method: Illuminate entrance of telescope with natural sunlight, passing through large polarizers

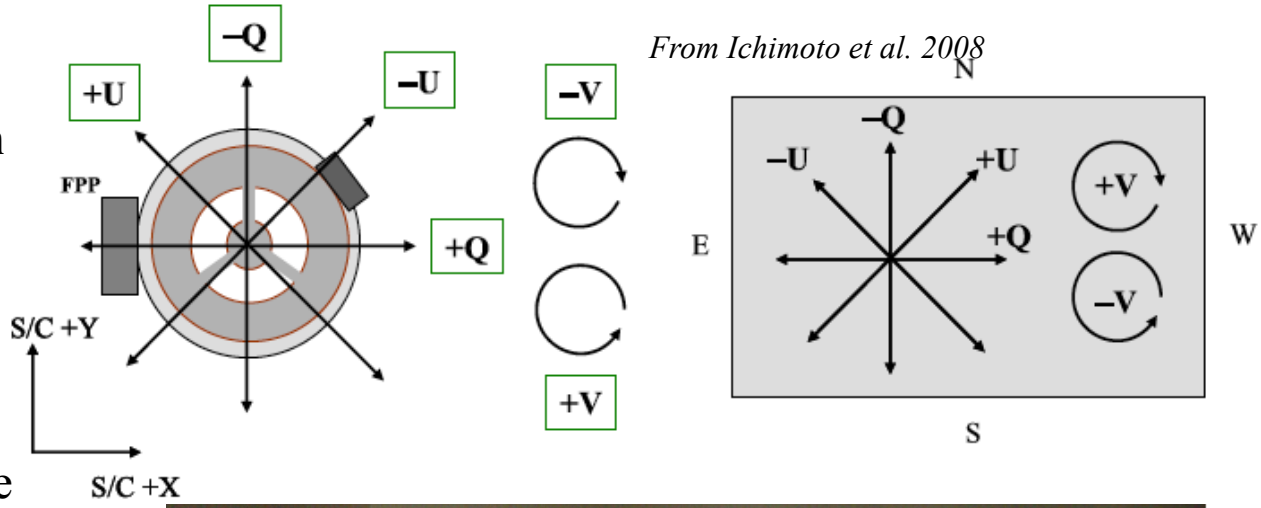

From Ichimoto et al. 2008

3 polarizers, 4 positions each

- Linear polarizer
- Right circular polarizer
- Left circular polarizer

- The Mueller matrices of the sheet polarizers are known except for the two angles θ_R, θ_L of the fast axis of the circular polarizers relative to the orientation angles
- Except for these two angles, the input polarizations are therefore known

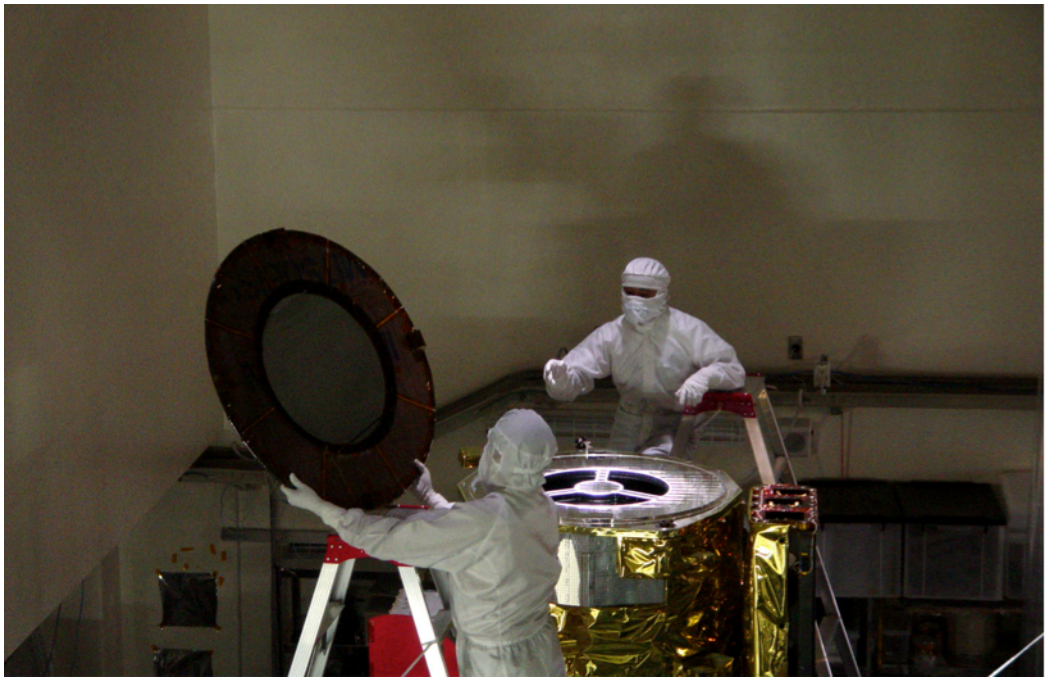

Polarizer being placed at entrance of Hinode/Solar Optical Telescope

Example: Calibration of the *Hinode* Spectro-Polarimeter

For each **normalized** input calibration Stokes vector $\mathbf{i}_k = [1\ q_k\ u_k\ v_k]$ we have a set of 4 equations relating the output $\mathbf{I}_k$ to the input $\mathbf{i}_k$:

$$\begin{pmatrix} I^k_{obs} \\ Q^k_{obs} \\ U^k_{obs} \\ V^k_{obs} \end{pmatrix} = I_k \begin{pmatrix} 1 & x_{12} & x_{13} & x_{14} \\ x_{21} & x_{22} & x_{23} & x_{24} \\ x_{31} & x_{32} & x_{33} & x_{34} \\ x_{41} & x_{42} & x_{43} & x_{44} \end{pmatrix} \begin{pmatrix} 1 \\ q_k \\ u_k \\ v_k \end{pmatrix}$$

I_k is the input intensity to the telescope for each measurement k.

The first equation of this system indicates the conversion of polarization to intensity. Normalizing the equations by I^k_{obs} then reduces the system to three equations for the intensity-normalized Stokes parameters:

$$\begin{pmatrix} Q^k_{obs} / I^k_{obs} \\ U^k_{obs} / I^k_{obs} \\ V^k_{obs} / I^k_{obs} \end{pmatrix} = \frac{1}{I^k_{obs}} \begin{pmatrix} x_{21} & x_{22} & x_{23} & x_{24} \\ x_{31} & x_{32} & x_{33} & x_{34} \\ x_{41} & x_{42} & x_{43} & x_{44} \end{pmatrix} \begin{pmatrix} q_k \\ u_k \\ v_k \end{pmatrix}$$

The system is **nonlinear in the 15 unknowns of X** owing to the normalization by I^k_{obs}.

Example: Calibration of the *Hinode* Spectro-Polarimeter

Number of equations = 12 polarization states × 3 relative Stokes parameters = 36
Number of unknowns = 15 X matrix elements + 2 angles (θ_R, θ_L) = 17

Solve by nonlinear least-squares fitting procedure.

***Hinode* SOT/SP Calibration Data Set and Fits**

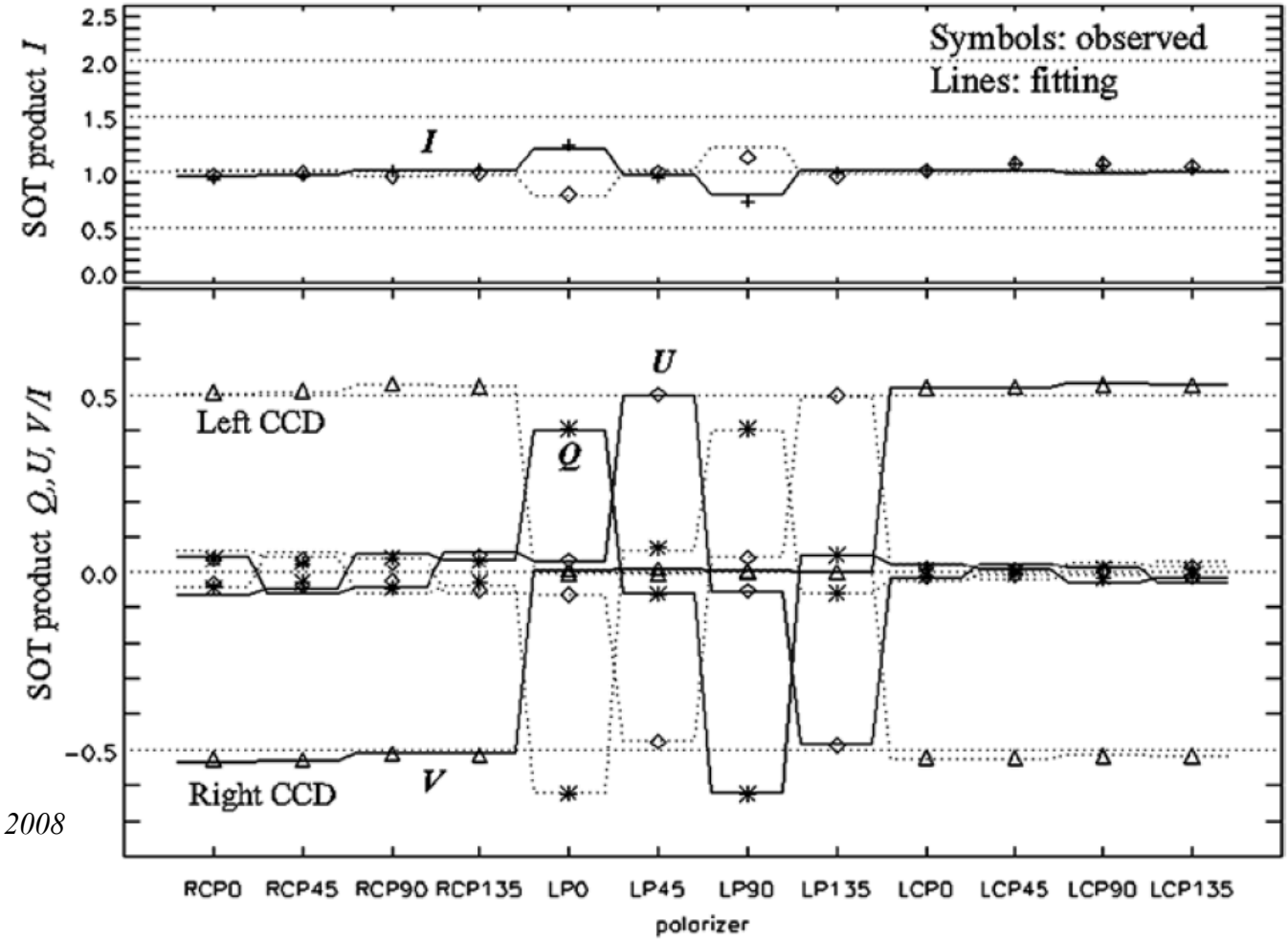

Figure from Ichimoto et al. 2008

Example: Calibration of the *Hinode* Spectro-Polarimeter

***Hinode* SOT/SP X-matrix spectra and median values**

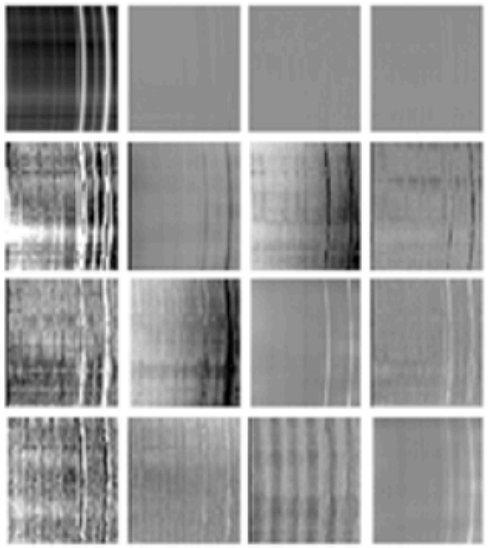

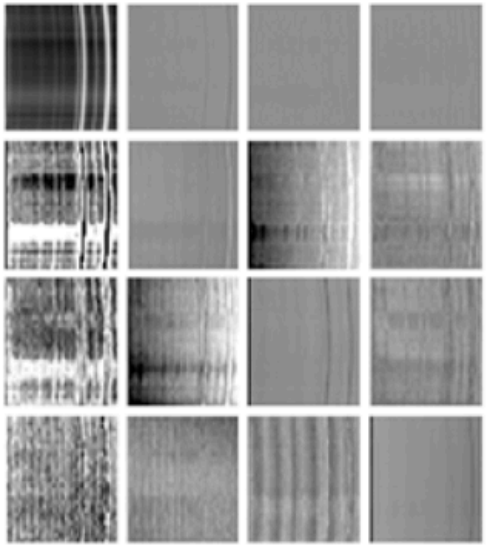

- Shown for both beams of the dual-beam system
- Note that the **matrices are nearly diagonal**
- **Q to I crosstalk term** is a feature of any rotating retarder
- ***I* ➔*Q,U,V* terms poorly determined** because no input of unpolarized light (easily determined on-orbit from spectral continuum)

Median Mueller matrix

Left

1.0000	−0.2232	−0.0142	−0.0063
0.0028	−0.4819	−0.0642	0.0007
0.0022	−0.0529	0.4814	−0.0030
−0.0034	−0.0026	0.0043	0.5249

Right

1.0000	0.2077	0.0199	−0.0079
−0.0039	0.4886	0.0551	0.0005
−0.0021	0.0427	−0.4918	0.0034
0.0035	0.0013	−0.0044	−0.5304

$$|\Delta X| < \begin{pmatrix} - & 0.333 & 0.333 & 0.250 \\ 0.001 & 0.050 & 0.007 & 0.005 \\ 0.001 & 0.007 & 0.050 & 0.005 \\ 0.001 & 0.007 & 0.007 & 0.050 \end{pmatrix}$$

Most of the off-diagonal crosstalk terms are even less than the error tolerance matrix, so **there was almost no need to calibrate the polarization for this instrument at all!**

However: A Time Dependence of the SP Calibration!

- Assessment of the residual SP instrumental polarization is carried out each year using the annual SP flat field data
- The SP continuum has shown a progressively increasing polarization, primarily in Stokes Q, that is not compensated by the original pre-launch polarization calibration
- This polarization continues to be well-corrected by the residual I -> Q,U,V polarization correction of SP_PREP
- The current level of residual polarization (as of mid-2017) in the Stokes Q continuum is 5×10^{-3} of the continuum intensity, with polarization levels in U, V about one order of magnitude smaller

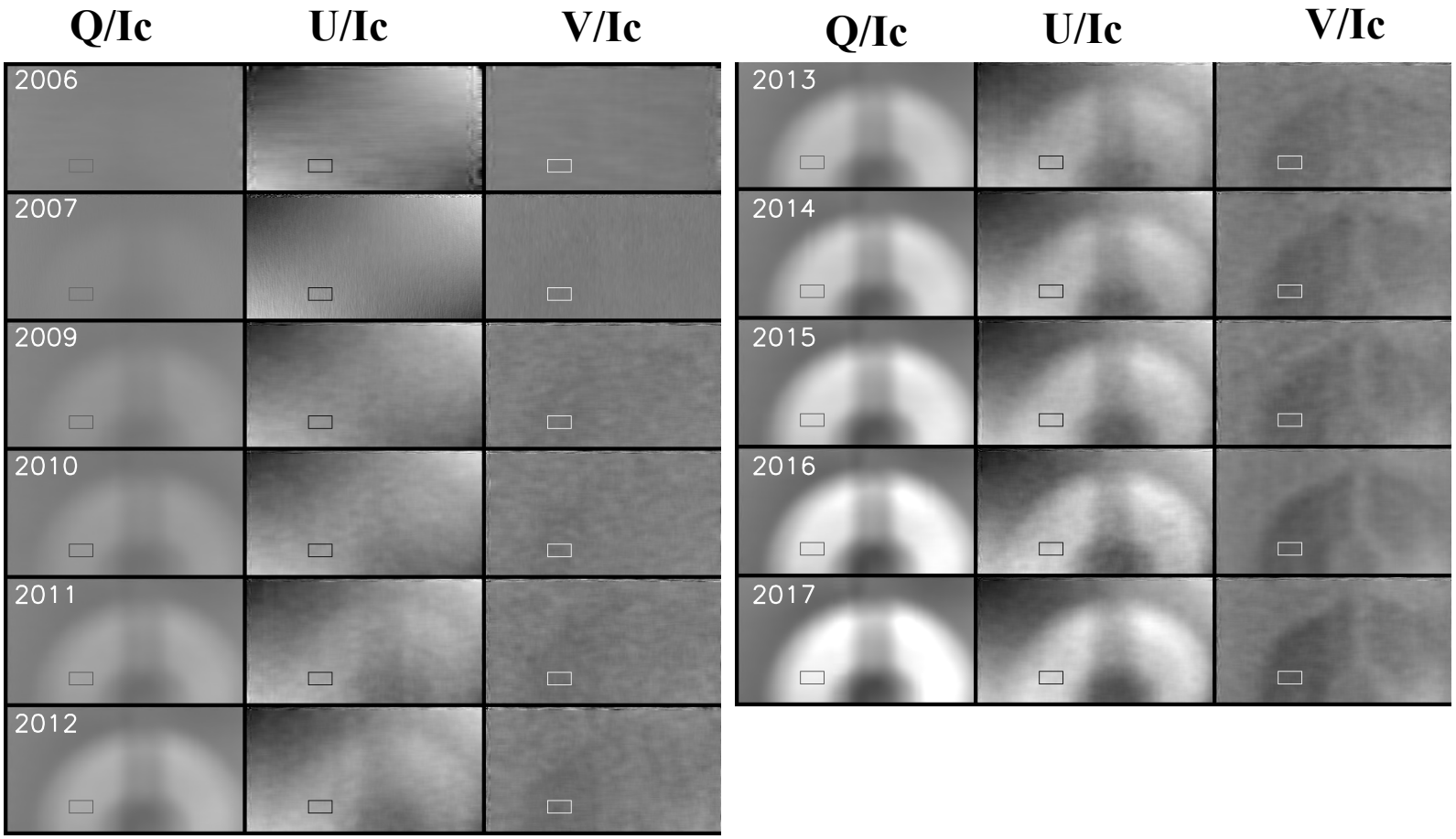

- Images of residual polarization over the full SP field-of-view (314 x 162”) as a function of year
- Outlined area is region of averaging to arrive at the curves presented in the next slide
- Images are scaled $\pm 6\times10^{-3}$ for Q/Ic and $\pm 6\times10^{-4}$ for U/Ic and V/Ic
- No full scan data available for 2008

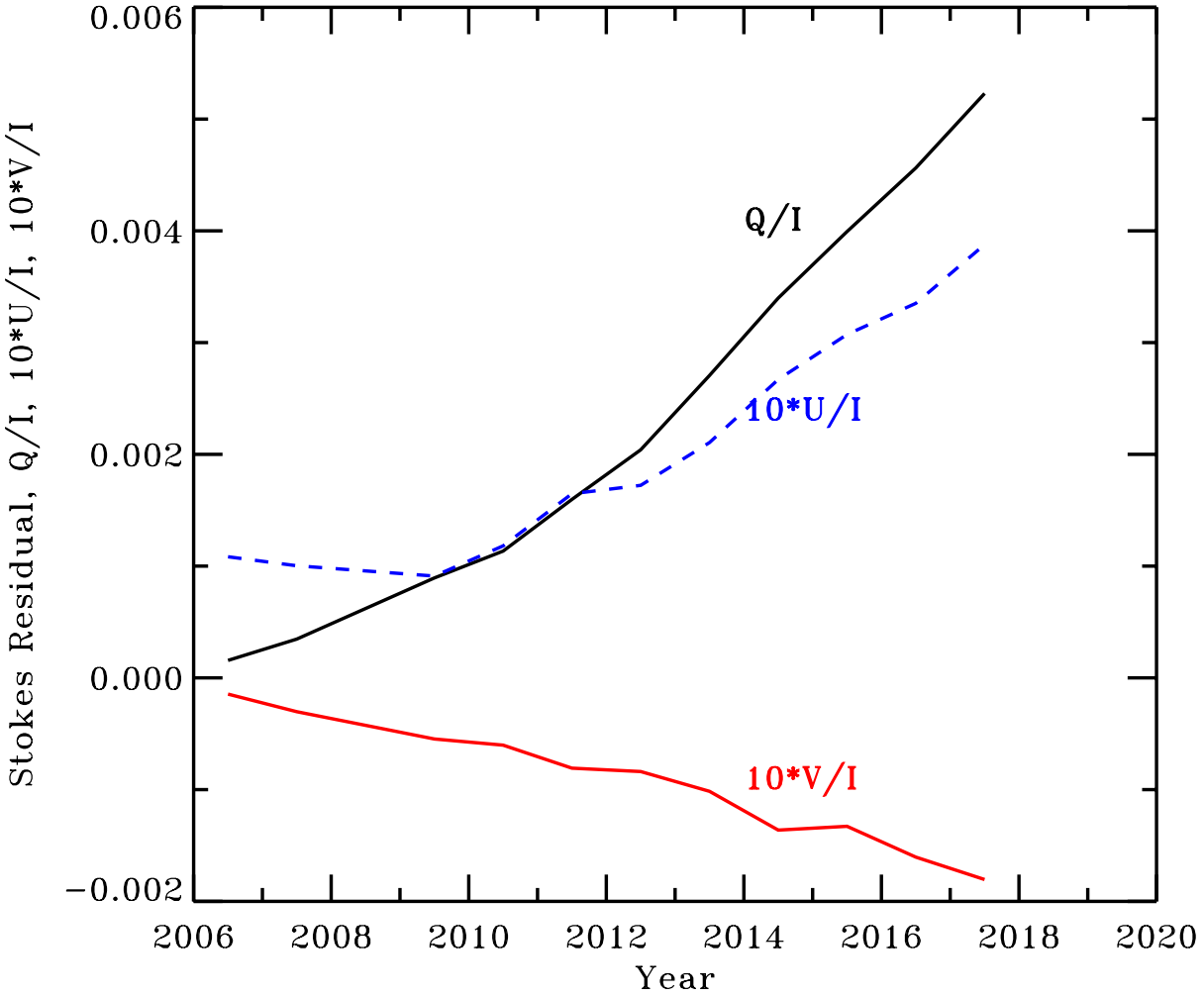

- Time dependence of residual polarization in Q, U, V
- Curves represent averages of signal in region outlined in previous slide
- U/Ic and V/Ic curves are multiplied by a factor of 10

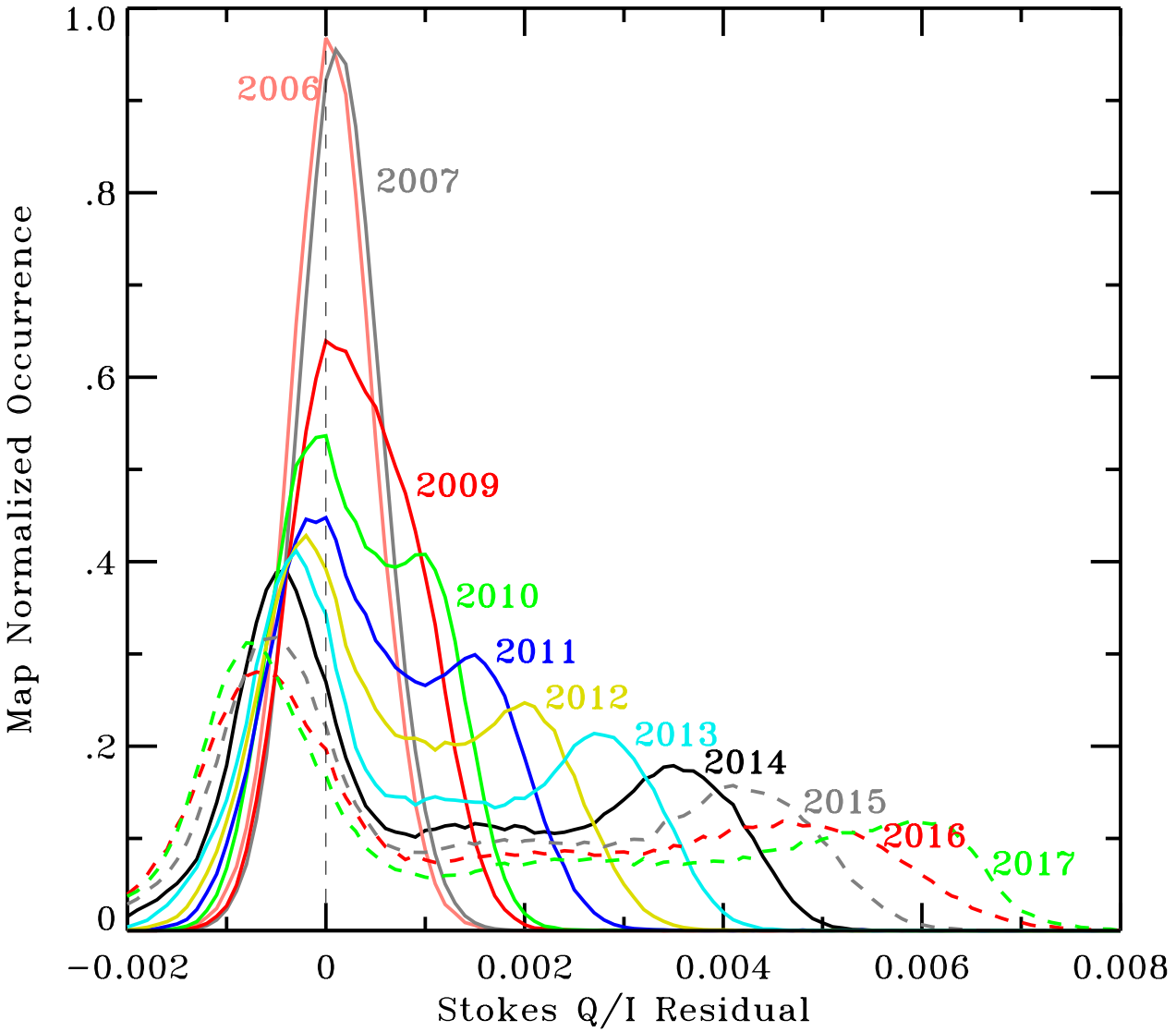

- Histograms of the distribution of residual Q/Ic polarization signals are presented for each of the years considered
- Progressive strengthening of both positive and negative signals is seen

ASP – A More Complicated Calibration Problem

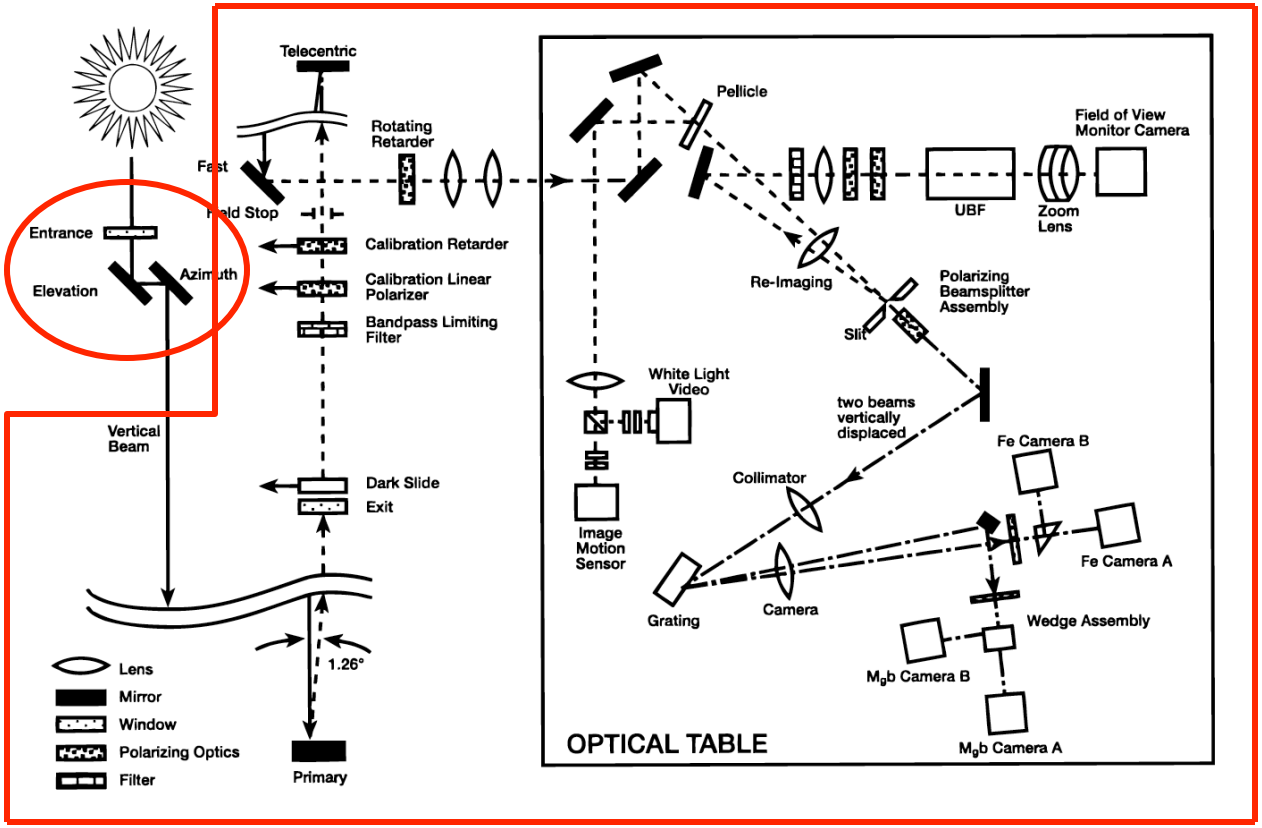

- To track the Sun: turret rotates about vertical for azimuth, and elevation mirror rotates about a horizontal axis
- Entire rest of telescope and table rotates about a vertical axis to compensate for image rotation
- **Polarization properties of mirrors depend on reflection angles – changing throughout the day**

ASP – A More Complicated Calibration Problem

Approach to ASP polarization calibration:

- Separate the problem into a **telescope response Matrix T** and the **polarimeter response X:**

$$\mathbf{I}_{obs} = \mathbf{X}\mathbf{T}(t)\mathbf{I}_{sun}$$

- **T** is time-dependent

ASP – A More Complicated Calibration Problem

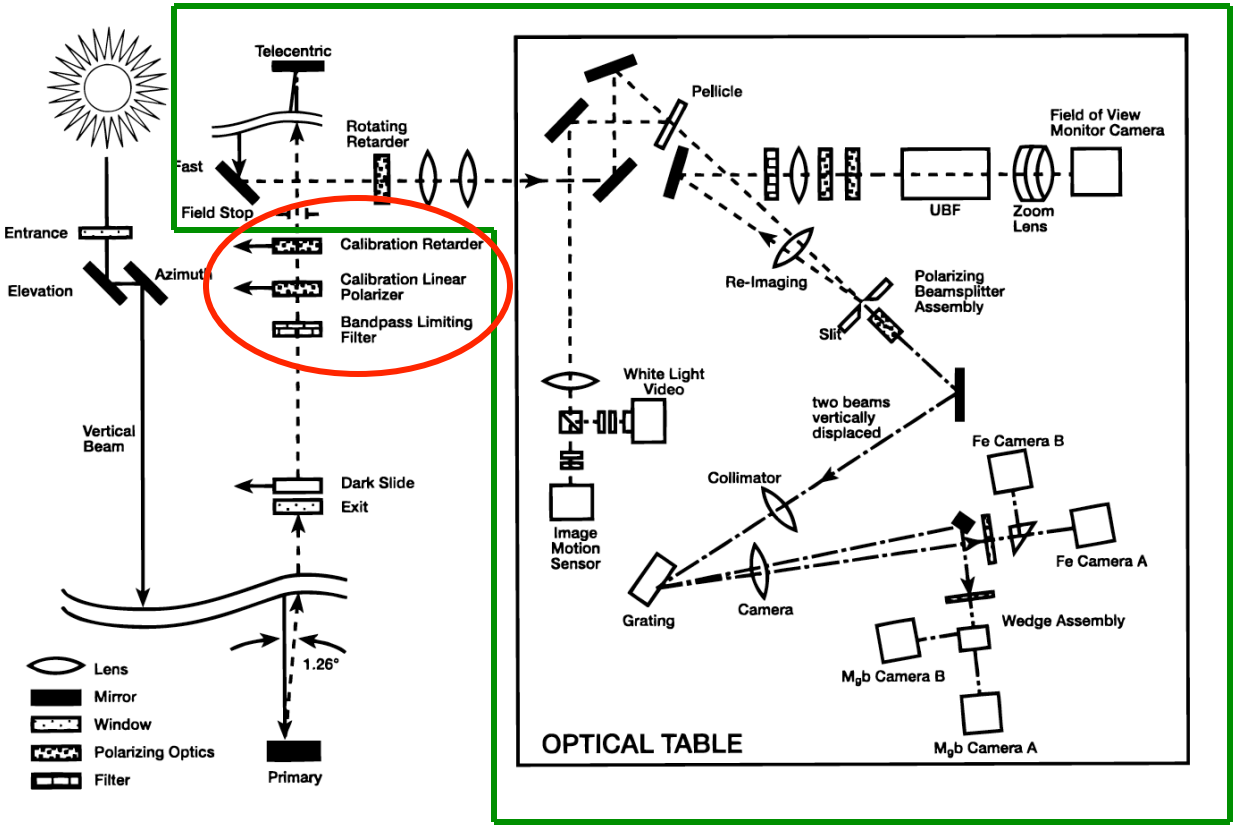

- The **polarimeter X** is everything following the **calibration optics**
- **The X-matrix does not vary with the pointing**

ASP – A More Complicated Calibration Problem

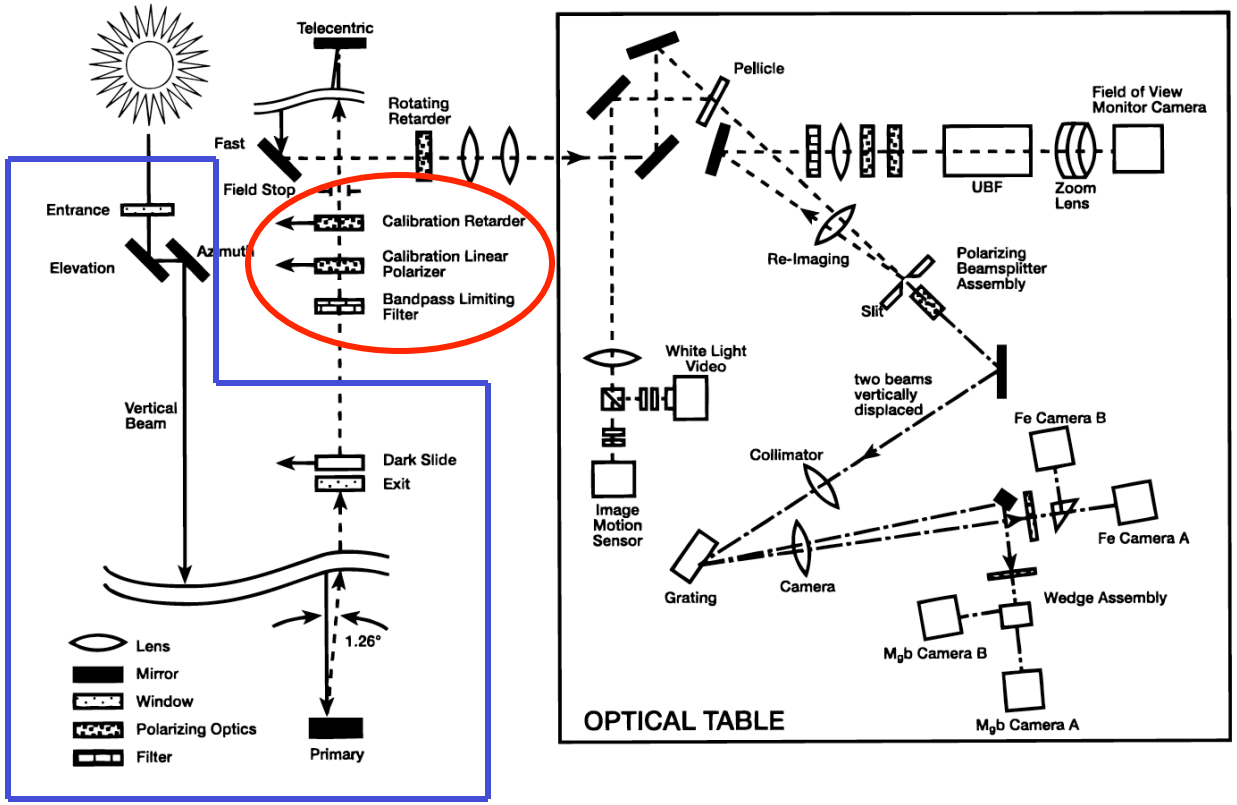

- The **Telescope T** is everything preceding the **calibration optics**
- The **X-matrix** does not vary with the pointing
- The **X-matrix** is determined by inserting combinations of linear polarizer and calibration retarder into the beam, and rotating them, just as was done for *Hinode*/SOT

ASP – A More Complicated Calibration Problem

Approach to ASP polarization calibration:

T-Matrix:

- Establish a numerical model of the telescope polarization
- Use the known orientation of the telescope mirrors from data logging
- Use the rest of the polarimeter to observe throughout an entire day the polarization with large sheet linear polarizers in front of the telescope
- Sheet polarizer is rotated through 360° in increments of 45°
- Mueller matrix of a mirror reflection (x is in plane of incidence and directed toward mirror surface, y is normal to plane of incidence, z is in direction of propagation, and $[x,y,z]$ form a right-handed coordinate system, r_x r_y ($r_x<r_y$) are intensity reflection coefficients, δ is the phase difference between x and y amplitudes after reflection):

$$\mathbf{M}_{mirror} = \begin{pmatrix} \frac{r_x + r_y}{2} & \frac{r_x - r_y}{2} & 0 & 0 \\ \frac{r_x - r_y}{2} & \frac{r_x + r_y}{2} & 0 & 0 \\ 0 & 0 & \sqrt{r_x r_y}\cos\delta & \sqrt{r_x r_y}\sin\delta \\ 0 & 0 & -\sqrt{r_x r_y}\sin\delta & \sqrt{r_x r_y}\cos\delta \end{pmatrix}$$

- **Upper-right** quadrant introduces **linear polarization**, **lower-left quadrant retardance**

ASP – A More Complicated Calibration Problem

T-Matrix (continued):

$$\mathbf{M}_{mirror} = \begin{pmatrix} \frac{r_x + r_y}{2} & \frac{r_x - r_y}{2} & 0 & 0 \\ \frac{r_x - r_y}{2} & \frac{r_x + r_y}{2} & 0 & 0 \\ 0 & 0 & \sqrt{r_x r_y}\cos\delta & \sqrt{r_x r_y}\sin\delta \\ 0 & 0 & -\sqrt{r_x r_y}\sin\delta & \sqrt{r_x r_y}\cos\delta \end{pmatrix}$$

- Analytic expressions for r_x r_y in terms of the angle of incidence θ, the indices of refraction (n_λ) and absorption (κ_λ) (recall $n_{complex} = n + i\kappa$) of the metallic film, the thickness d of the film, and the index of refraction of the mirror blank v (see Skumanich et al. 1997).
- Indices of refraction and absorption for aluminum:

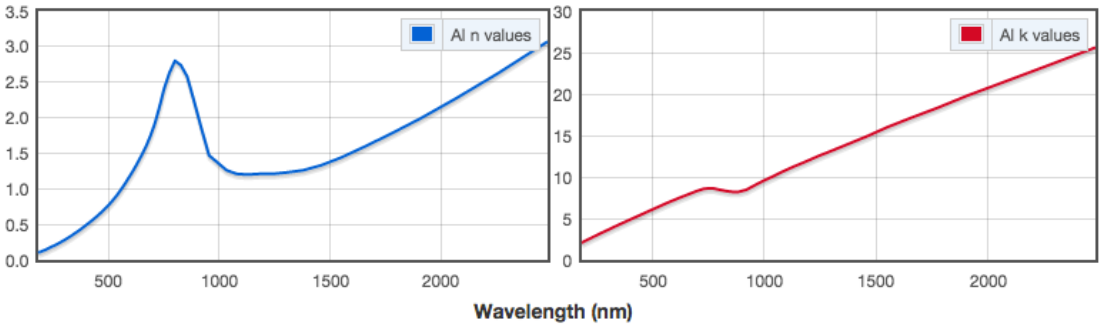

ASP – A More Complicated Calibration Problem

ASP T-Matrix (continued):

- The T-matrix is determined from observations of the entrance linear polarizer:
  - **Angles of incidence θ known** from telescope pointing information
  - For the telescope mirrors, **n_λ, κ_λ, d, v are parameters** of the least-squares fit
  - The **entrance and exit windows** of the telescope are modeled as pure retarders with retardance value and orientation angle for each yielding 4 more variables of the fit
  - **Cycle entrance polarizer** through many rotations through day – sample the range of angles of the telescope mirrors
- **Turret mirrors create eliptical polarization:** at oblique angles polarize and retard the polarization: no need for circular polarizers
- **Self-calibrate** properties of the telescope optics

What if there is No Source of Polarized Light?

- Sometimes it is not possible to fill the entire aperture of the telescope with known or nearly-known polarization
- May use **"radiant point" of a sunspot umbra** where field is apparently directed along the line-of-sight
  - On average, no linear polarization from normal Zeeman triplets: pure *V*
  - Stokes *V*-like anti-symmetric signals in *Q,U* indicate crosstalk from *V* ➔ *Q,U*
  - Minimize Stokes *Q,U* to determine parameters of **T**

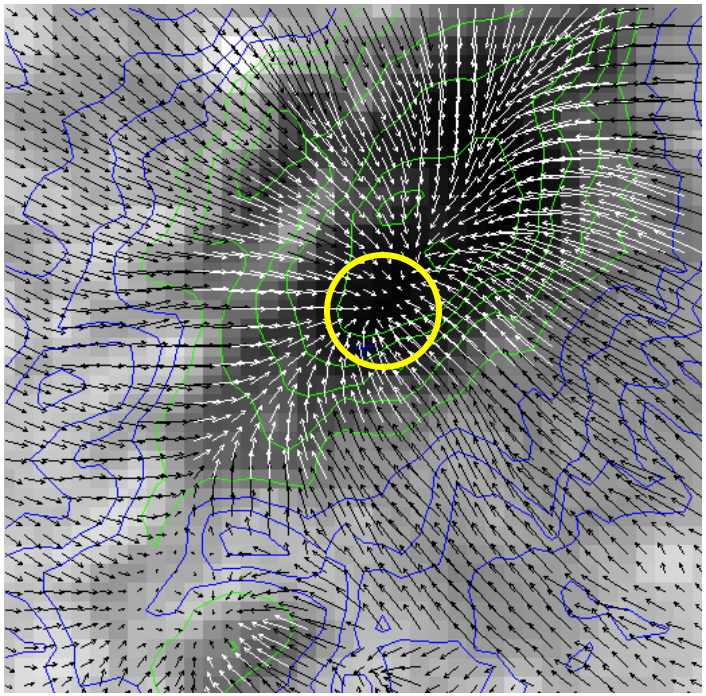

- Some spectral lines **produce no linear polarization** as a result of the Zeeman effect. One such line is Fe II 614.9 nm. Those lines may be used to determine **T** in a fashion similar to that of the sunspot radiant point, but only at these wavelengths (see Sanchez Almeida & Vela Villahoz 1993 for a list of appropriate lines)
- These methods have been demonstrated to work for the ASP

IX. Modern Solar Polarimeters – Ground-Based

Ground-Based Solar Polarimetry

- Much pioneering work in solar polarimetry in 20th Century:

- First solar longitudinal magnetograms (Babcock 1953);
- First solar vector magnetograms (Stepanov & Severny 1962[1],

- Routine longitu... several observatories since the1970's
- Here consider t... full-Stokes polarimetry
- Illustration wit... cannot cover all existing and in-developmen...

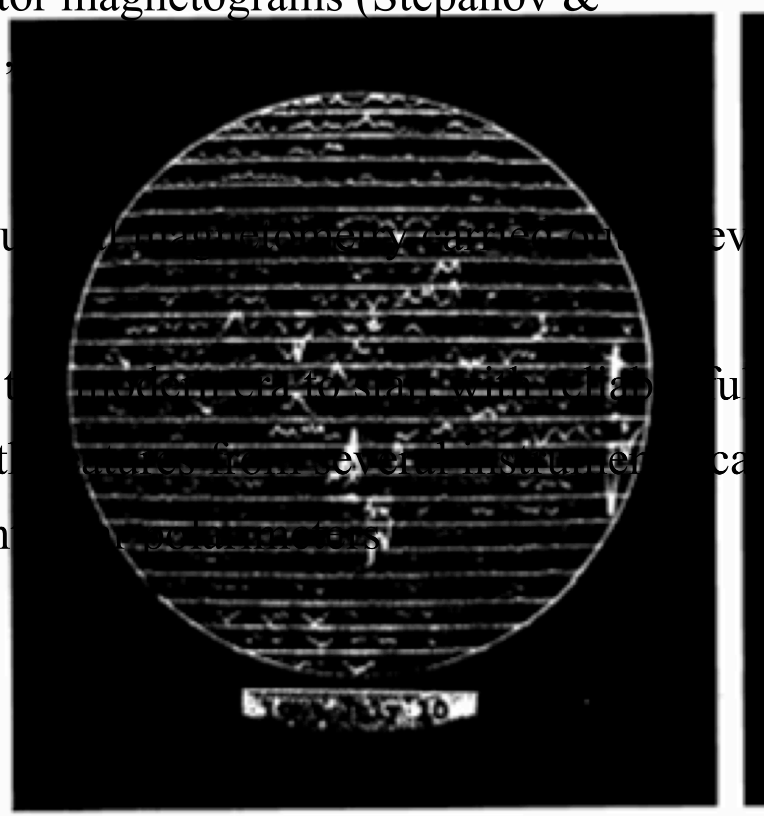

FIG. 5.—Magnetograms of the sun. The axis is vertical, with north ... fiducial line. A deflection equal to the interval between traces indicat... is toward the o... the opposite deflections on the traces nearest the north and south pole... The length of the slit (0.04 of the sun's diameter) is approximately ...

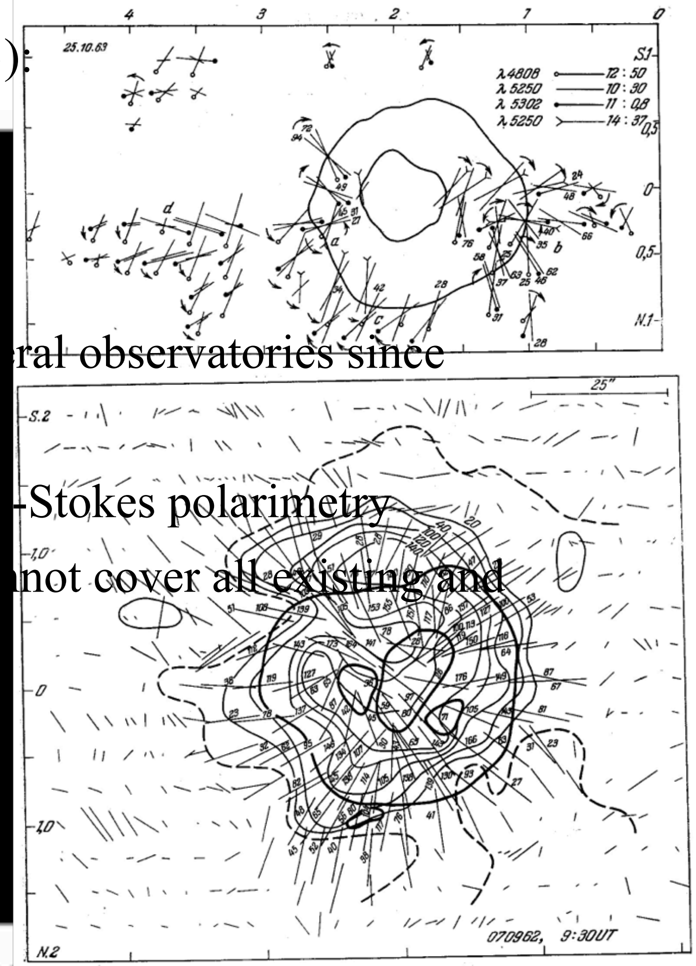

Рис. 19. Сверху положение вектора $H_\perp$ для линий, возникающих на разных глубинах: λ 4808 — внизу, λ 5250 — средний уровень, λ 5302 — верхний уровень фотосферы.

Запись в λ 5250 сделана дважды для исключения возможных поворотов вектора со временем (время записи указано рядом с обозначением вектора $H_\perp$). Особенно сильные вращения с глубиной—в участках *a*, *b* и *c*. Круглые стрелки показывают направление поворота с глубиной. Сплошные замкнутые контуры — контуры тени и полутени пятна. Внизу — пример комбинированной карты изогаусс продольного поля $H_\parallel$ и направлений и длин вектора $H_\perp$ (в случае больших длин она указана цифрой). Видны сильные повороты вектора $H_\perp$ в пределах пятна (оконтурено более толстой линией) [27].

[1]*Stepanov & Severny (1962): Izv. Krymsk. Astrofiz. Obs., 28, 166-193.*
[2]*Severny (1966): Uspechi fiz. nauk, 88, 3-50.*

Ground-Based Spectro-Polarimeters – 1: The Advanced Stokes Polarimeter (ASP)

- Heritage from prior instruments that recorded full-Stokes Spectra: **Stokes I and Stokes II**
- First instrument that combined the following attributes:
  - Simultaneous, spectrally-resolved *I, Q, U, V* profiles
  - Spectral imaging with 2-D detectors
  - High frame rate (at least for that era: late 1980's): 60 Hz
  - Dual-beam polarimetry
  - Image-frame demodulation
  - High resolution capability at a large solar telescope (DST at Sac Peak, NSO)
  - Rapid image motion compensation ("tip-tilt mirror")

Dunn Solar Telescope (DST), National Solar Observatory, Sunspot, NM USA

Ground-Based Spectro-Polarimeters – The Advanced Stokes Polarimeter

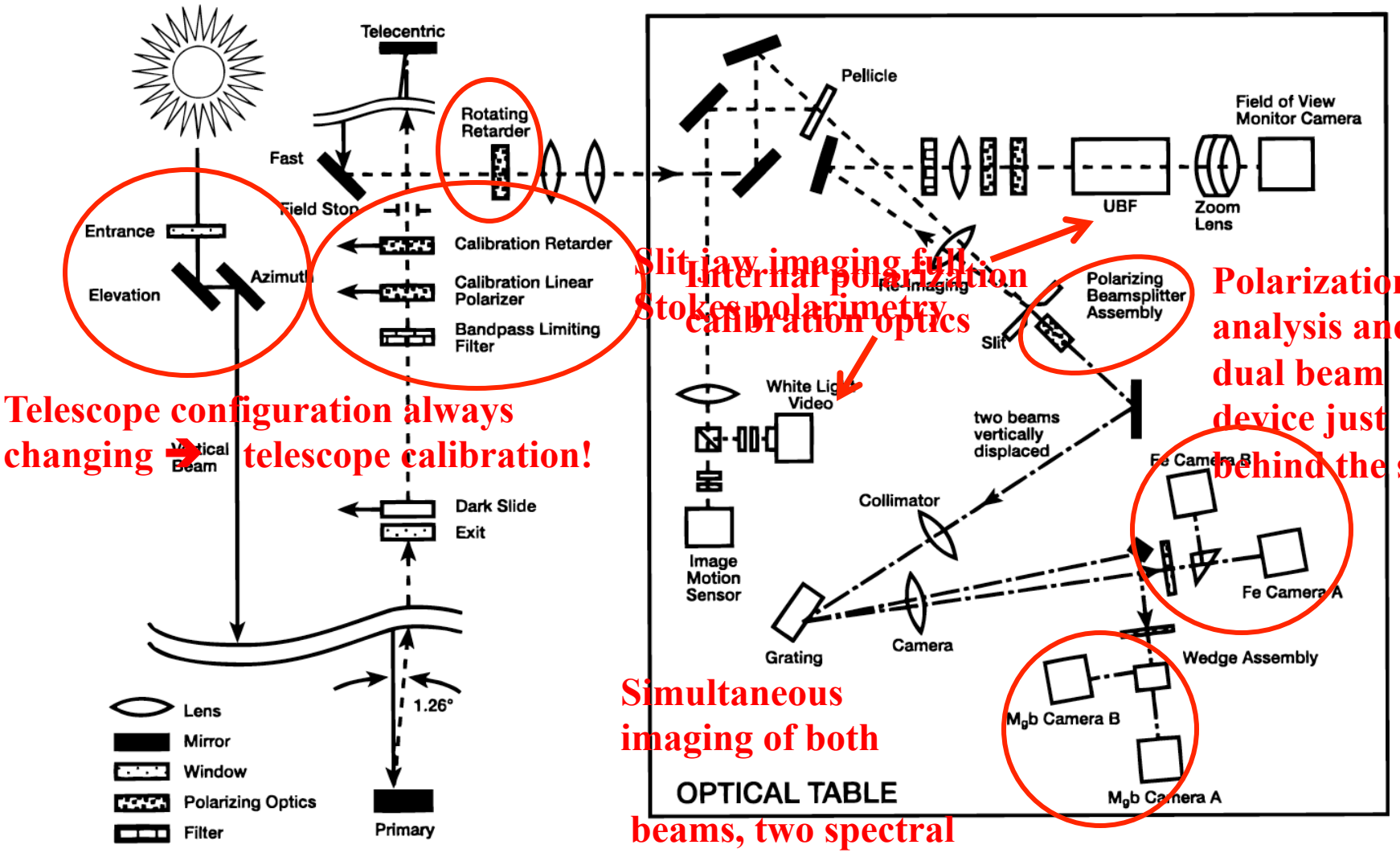

Slit jaw imaging full Stokes polarimetry

Internal polarization calibration optics

Polarization analysis and dual beam device just behind the slit

Telescope configuration always changing → telescope calibration!

Simultaneous imaging of both beams, two spectral regions

Polarization Measurements

Zeeman Effect

Inferred Vector Magnetic Field

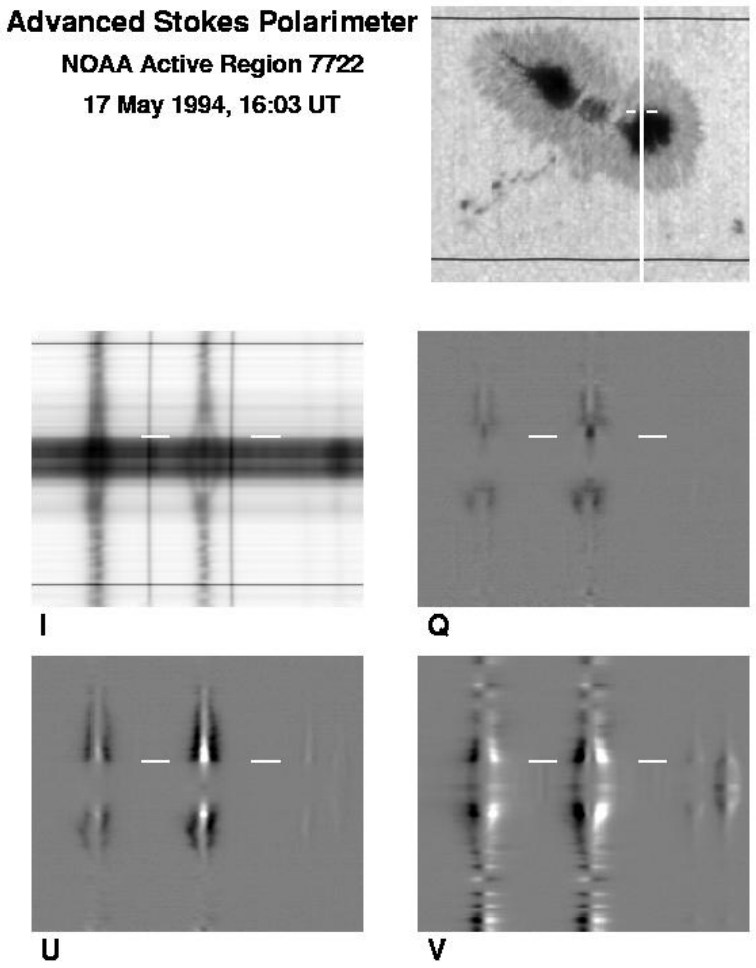

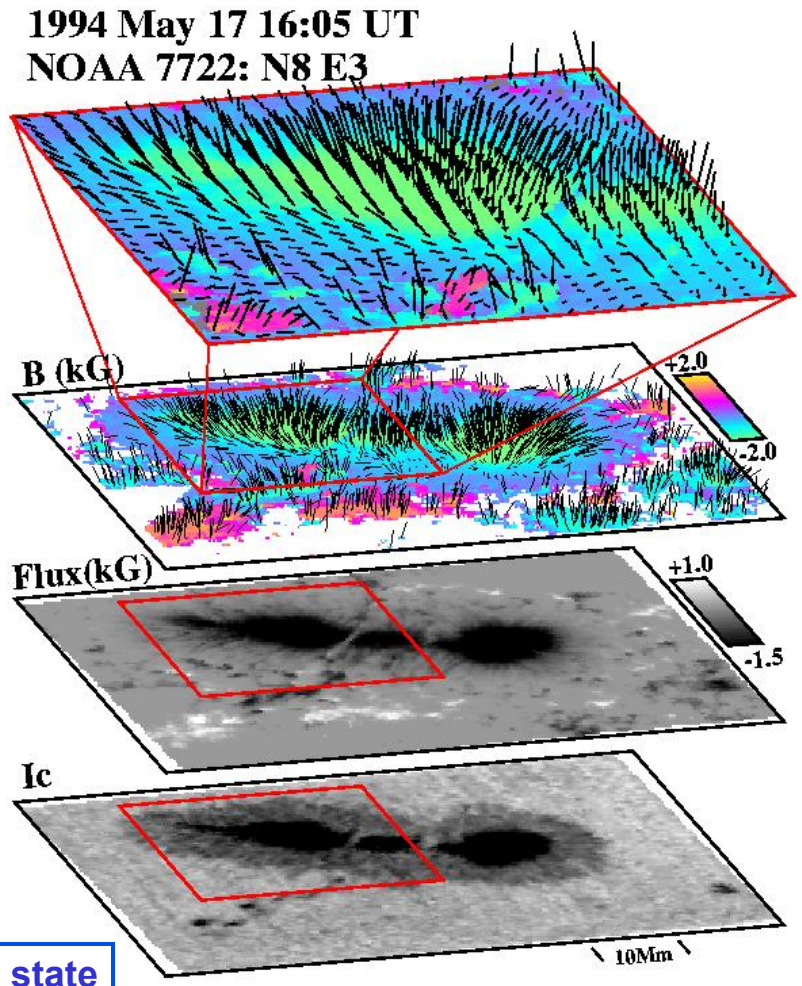

The Stokes 4-vector $\{I, Q, U, V\}^T$ describes the complete state of polarization of light

Ground-Based Spectro-Polarimeters – 2: Spectro-Polarimeters with Infrared Capability

- Observing chromospheric fields in the IR
- Three instruments described: SPINOR and FIRS at the DST of NSO, and TIP at the Vacuum Tower Telescope on Tenerife
- And now GRIS: GREGOR Infrared Spectrograph at the GREGOR telescope on Tenerife

Ground-Based Spectro-Polarimeters – 3: Spectro-Polarimeters with Infrared Capability -- SPINOR

- **SPINOR: Spectro-Polarimeter for Infrared and Optical Regions**
- A modification of the Advanced Stokes Polarimeter configuration
- Like ASP, uses a rotating retarder, but achromatic
- Infrared to 1.6μ possible using CCD cameras sensitive to the infrared
- Achromatic optics replace some ASP optics, particularly the calibration optics

- **New frontier for observational solar physics is the measurement of the magnetic field vector in the chromosphere and corona**

Polarimetry in near-IR: Ca II IR Triplet

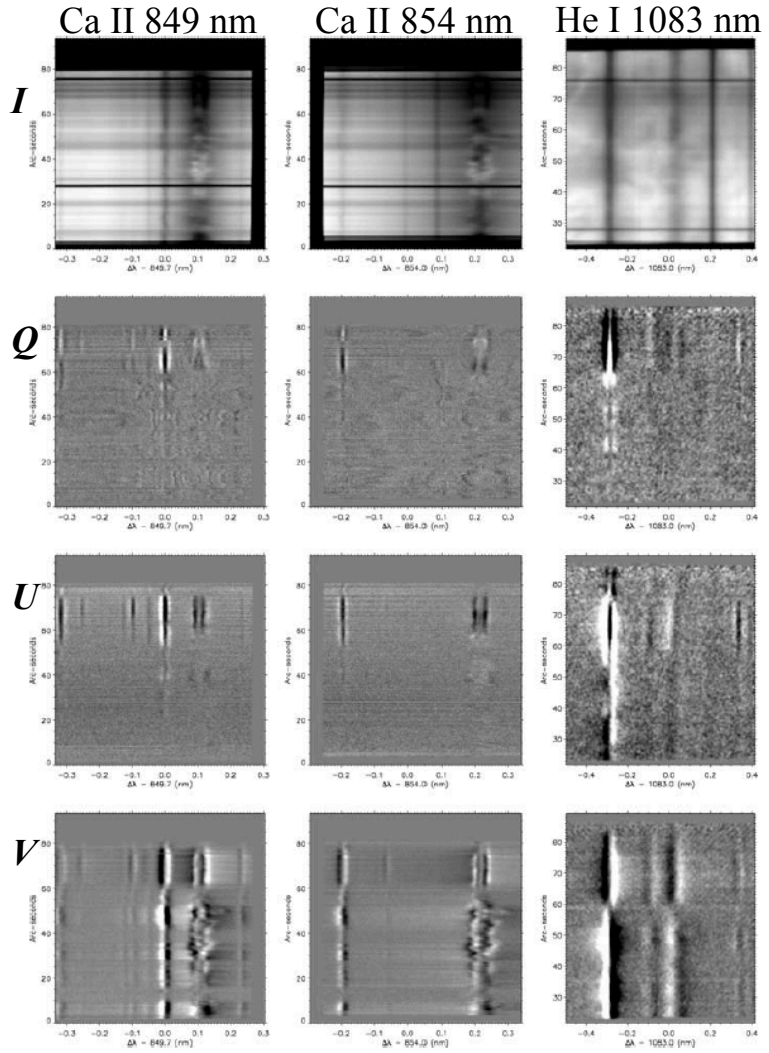

From Socas-Navarro et al. 2006

Ground-Based Spectro-Polarimeters – 3: Spectro-Polarimeters with Infrared Capability -- SPINOR

- **SPINOR: Spectro-Polarimeter for Infrared and Optical Regions**
- A modification of the Advanced Stokes Polarimeter configuration
- Like ASP, uses a rotating retarder, but achromatic
- Infrared to 1.6μ possible using CCD cameras sensitive to the infrared
- Achromatic optics replace some ASP optics, particularly the calibration optics

Polarimetry in near-IR: Ca II IR Triplet

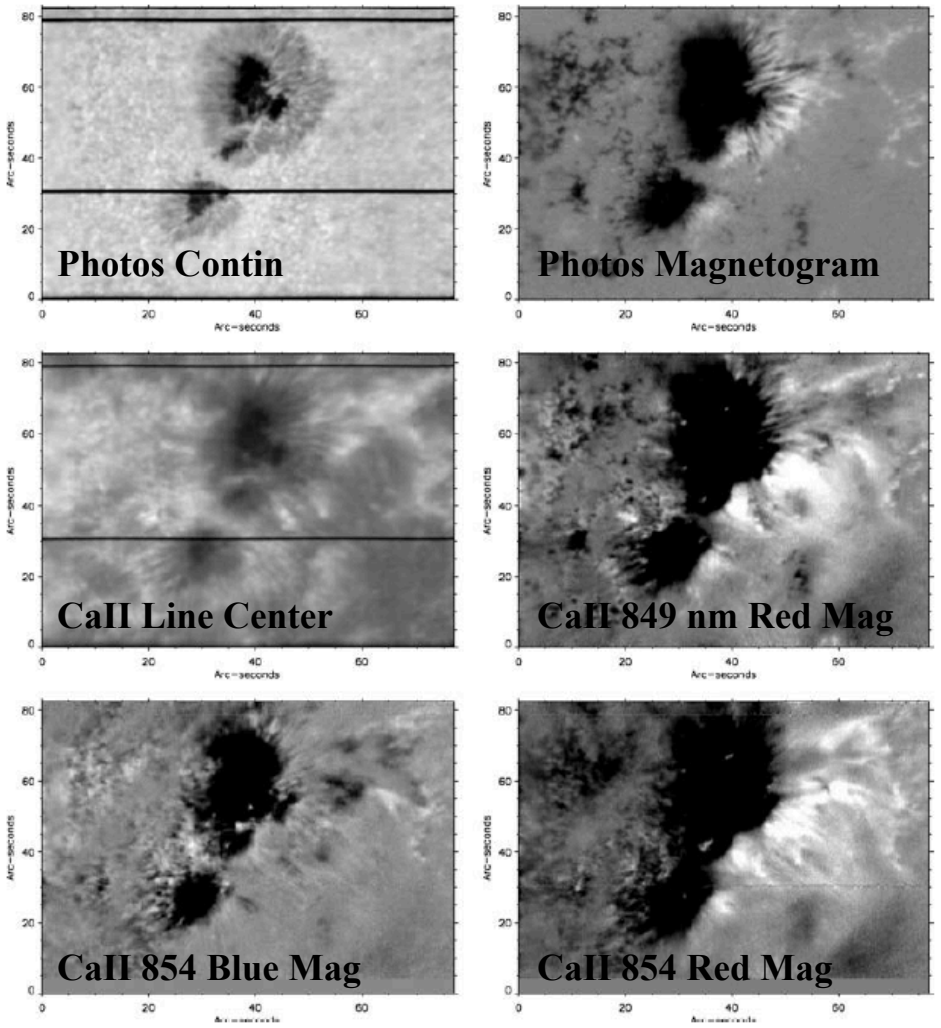

Adapted from Socas-Navarro et al. 2006

Ground-Based Spectro-Polarimeters – 4: Spectro-Polarimeters with Infrared Capability -- FIRS

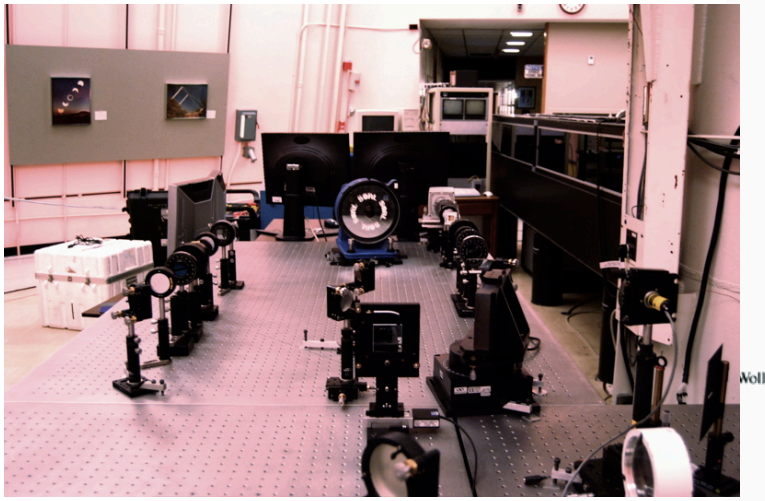

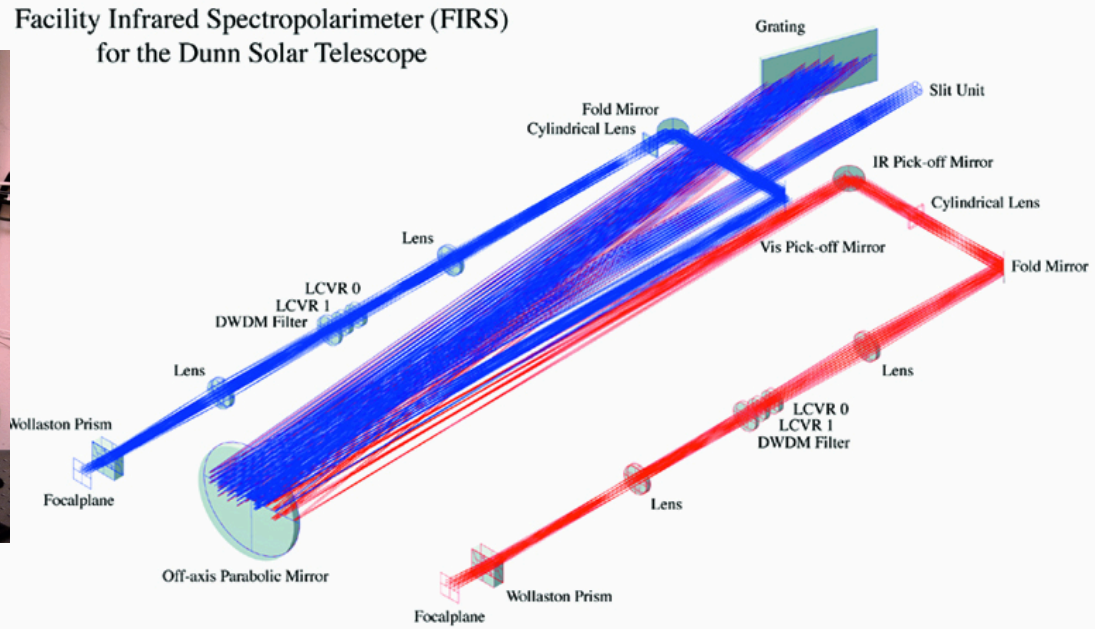

- **FIRS: Facility Infrared Spectro-polarimeter**
- Optimized for visible 630 nm and IR 1565 nm (both photospheric)
- Modulators for each wavelength: liquid crystal variable retarders (nematic LCVRs)
- Four parallel slits imaged at focal plane, narrow band filter
- Wollaston prisms for dual-beam spectro-polarimetry

Ground-Based Spectro-Polarimeters – 5: Spectro-Polarimeters with Infrared Capability – TIP II

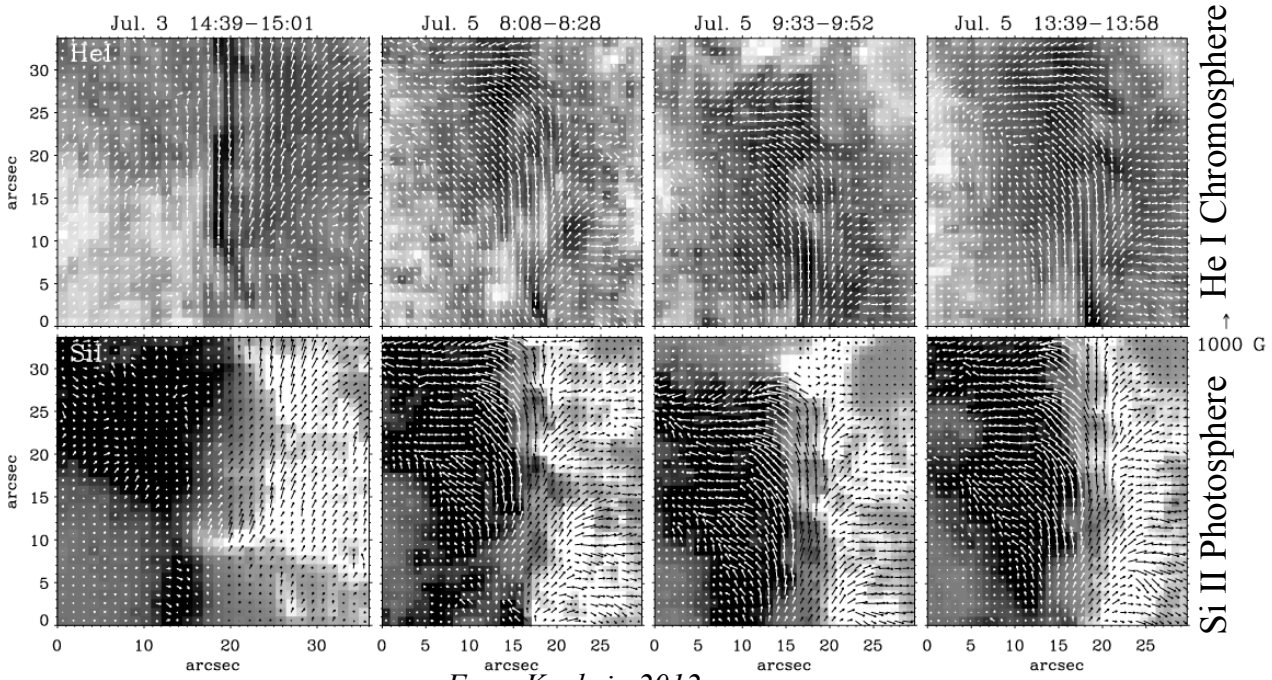

From Kuckein 2012

- **TIP II: Tenerife Infrared Polarimeter II − Now at GREGOR**
- Spectroscopic instrument
- Principal lines: He I 1083 nm (chromosphere), Fe I 1565 nm (photosphere)
- Modulator: pair of Ferroelectric Liquid Crystals (FLCs)
- HgCdTe CCD detector (1024 x 1020) and bandpass filters contained in cryostat at 77° K
- Polarizing beam splitter for dual-beam spectropolarimetry
- Typical 10-s exposure gives S/N = 10^3 at 1083 nm

Ground-Based Imaging Polarimeters

- Restrict sample to instruments with:
  - Good spectral resolution
  - May scan the solar spectrum
  - Full Stokes polarimetry (*I, Q, U,V*)

- Three instruments are described (NOW OUTDATED LIST)
  - TESOS/VIP at the German VTT on Tenerife
  - CRISP at the Swedish Solar Observatory on La Palma
  - IBIS at the National Solar Observatory/Sunspot NM USA

Ground-Based Imaging Polarimeters – 1: TESOS/VIP

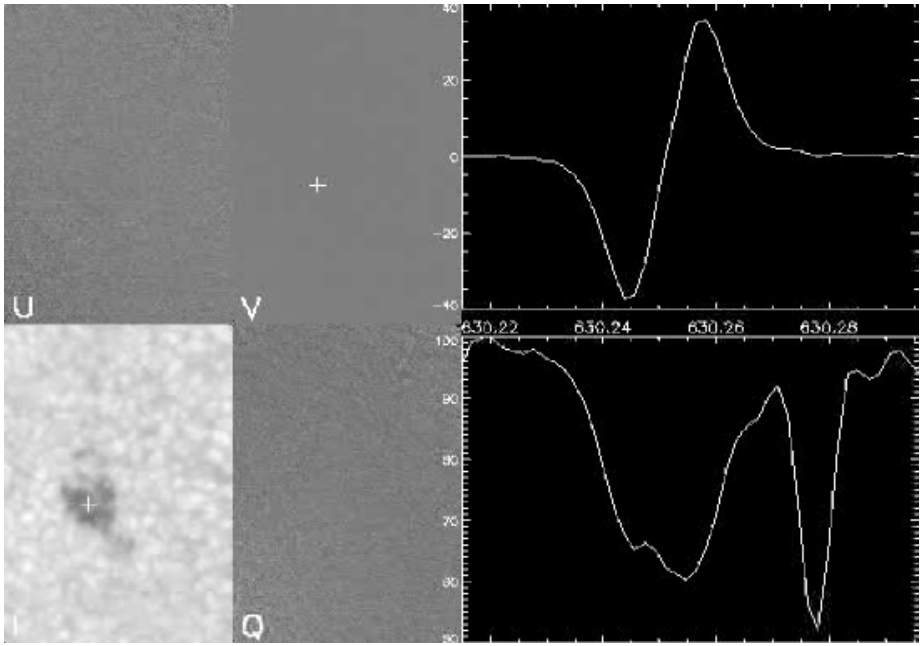

TESOS/VIP: Triple Etalon Solar Spectrometer/Visible Imaging Polarimeter

- Wavelength isolation: three Fabry-Pérot interferometers in series
- Spectral resolution of about 20 mÅ
- Modulator: pair of nematic LCVRs
- Dual-beam polarization analysis: Wollaston prism
- Wavelength range: from 420 – 700 nm
- Up to four spectral regions observed in rapid sequence

Ground-Based Imaging Polarimeters – 1: TESOS/VIP

Wollaston Prism for Dual Beam Polarimetry

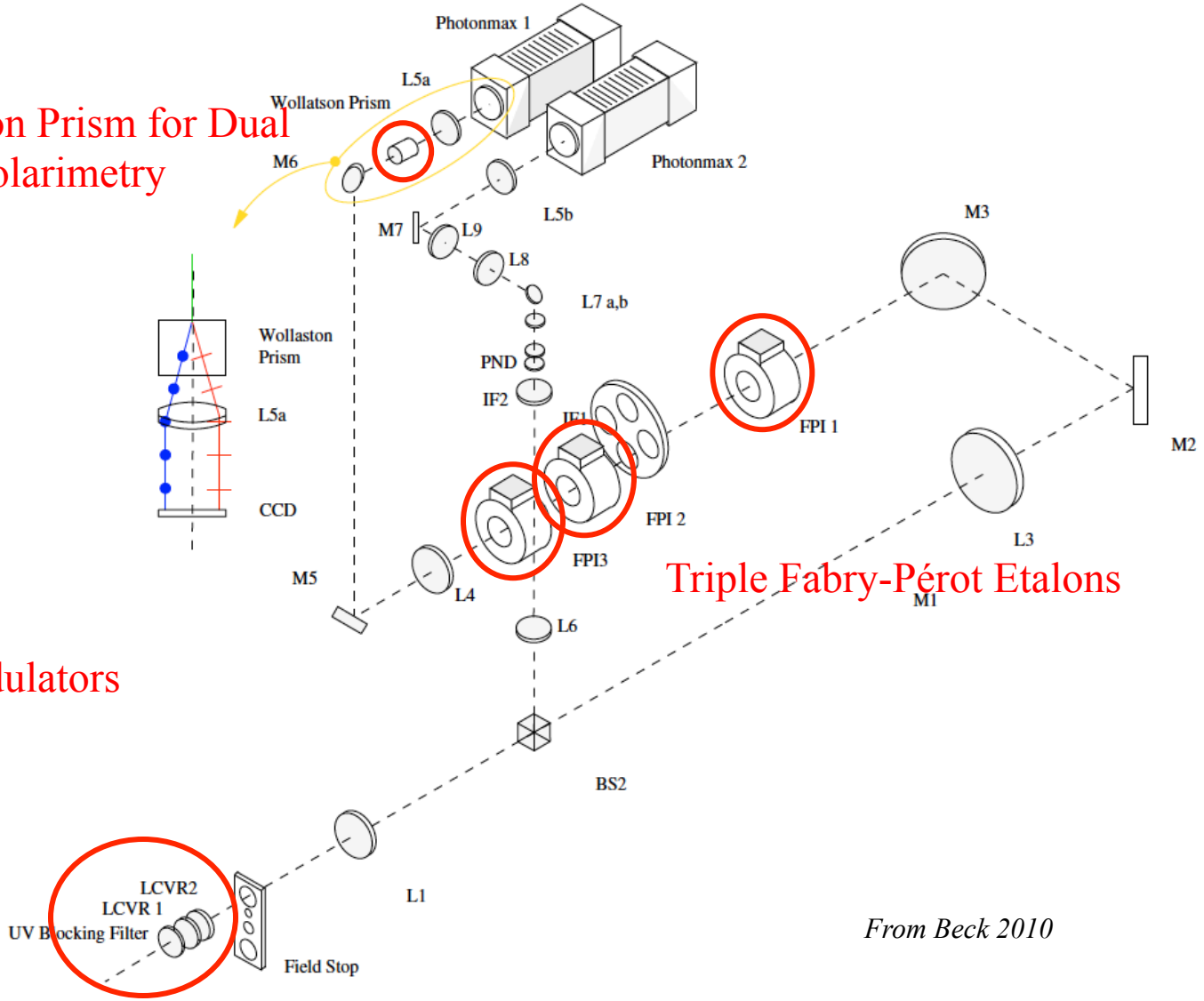

Triple Fabry-Pérot Etalons

Two LCVRs as modulators

From Beck 2010

Ground-Based Imaging Polarimeters – 2: CRISP

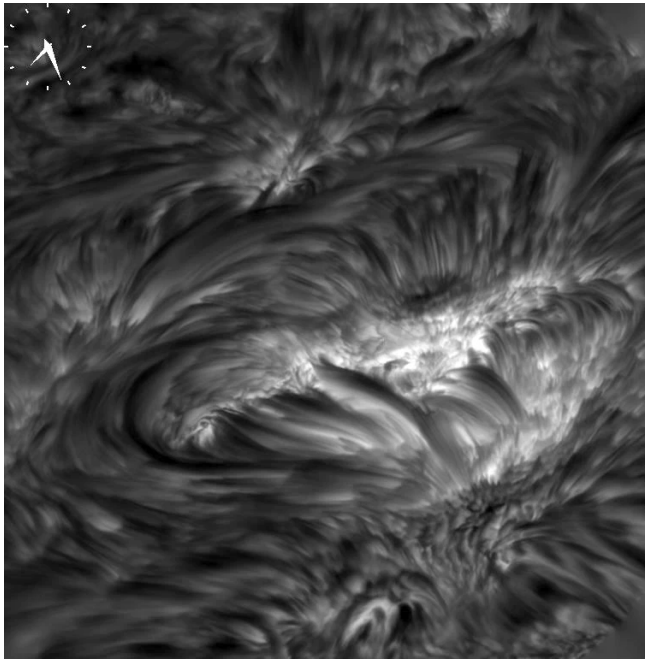

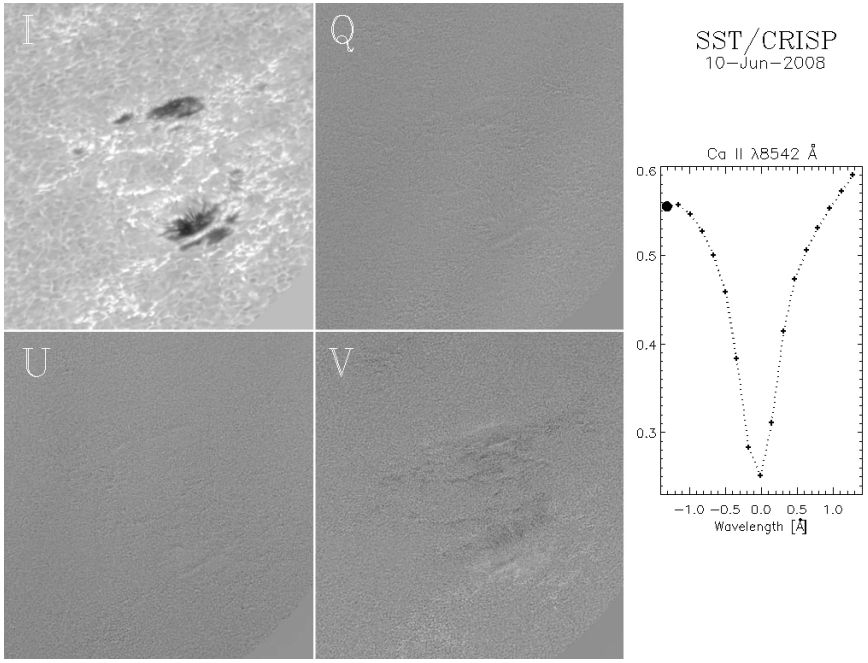

CRISP: Crisp Imaging Spectro-Polarimeter

- Over-riding advantage of Swedish Solar Telescope is **extremely high angular resolution**
  - Unobstructed 1-m aperture
  - Simple optical systems
  - Sophisticated post-observation image restoration
  - **Extreme attention to details of optical quality**

Ground-Based Imaging Polarimeters – 2: CRISP

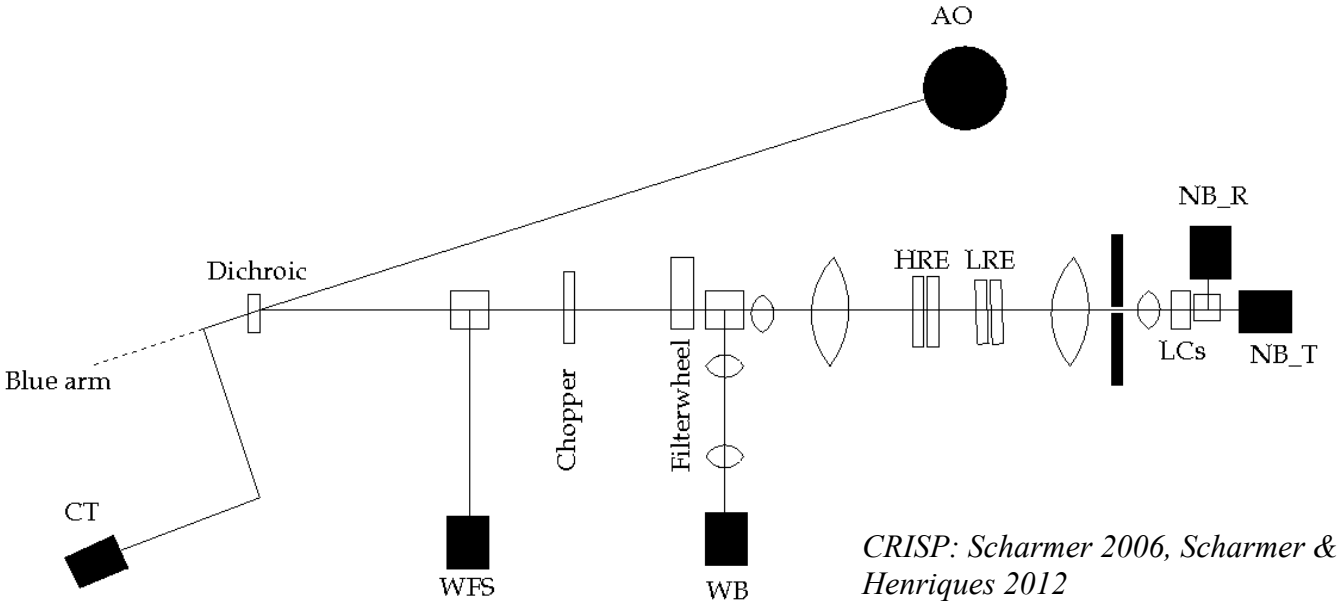

CRISP: Scharmer 2006, Scharmer & Henriques 2012

CRISP: Crisp Imaging Spectro-Polarimeter

- Wavelength isolation via two Fabry-Pérot etalons
- Spectral resolution about 60 mÅ
- Two nematic LCVRs for polarization modulation
- Dual-beam polarimetry via polarizing beam splitter analyzer
- Adaptive optics PLUS detailed image restoration (MFMOBD)
- Telecentric optical system for Fabry-Pérot path (pupil image at infinity)

Ground-Based Imaging Polarimeters – 2: CRISP

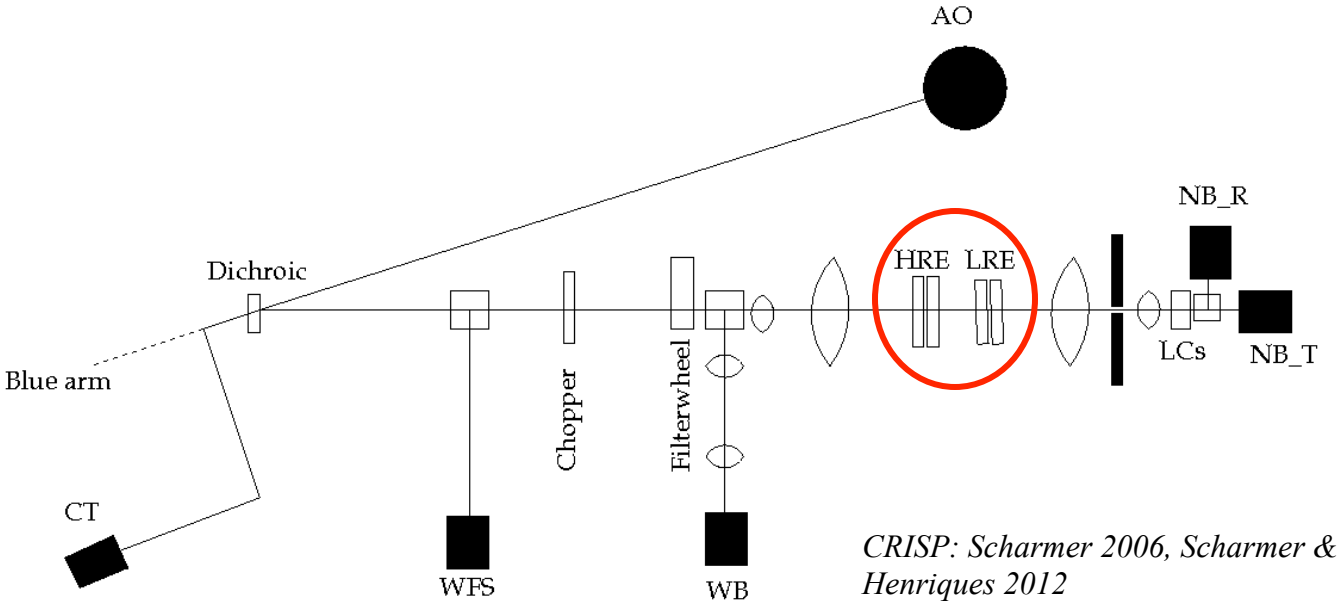

CRISP: Scharmer 2006, Scharmer & Henriques 2012

CRISP: Crisp Imaging Spectro-Polarimeter

- Wavelength isolation via two Fabry-Pérot etalons
- Spectral resolution about 60 mÅ
- Two nematic LCVRs for polarization modulation
- Dual-beam polarimetry via polarizing beam splitter analyzer
- Adaptive optics PLUS detailed image restoration (MFMOBD)
- Telecentric optical system for Fabry-Pérot path (pupil image at infinity)

Ground-Based Imaging Polarimeters – 2: CRISP

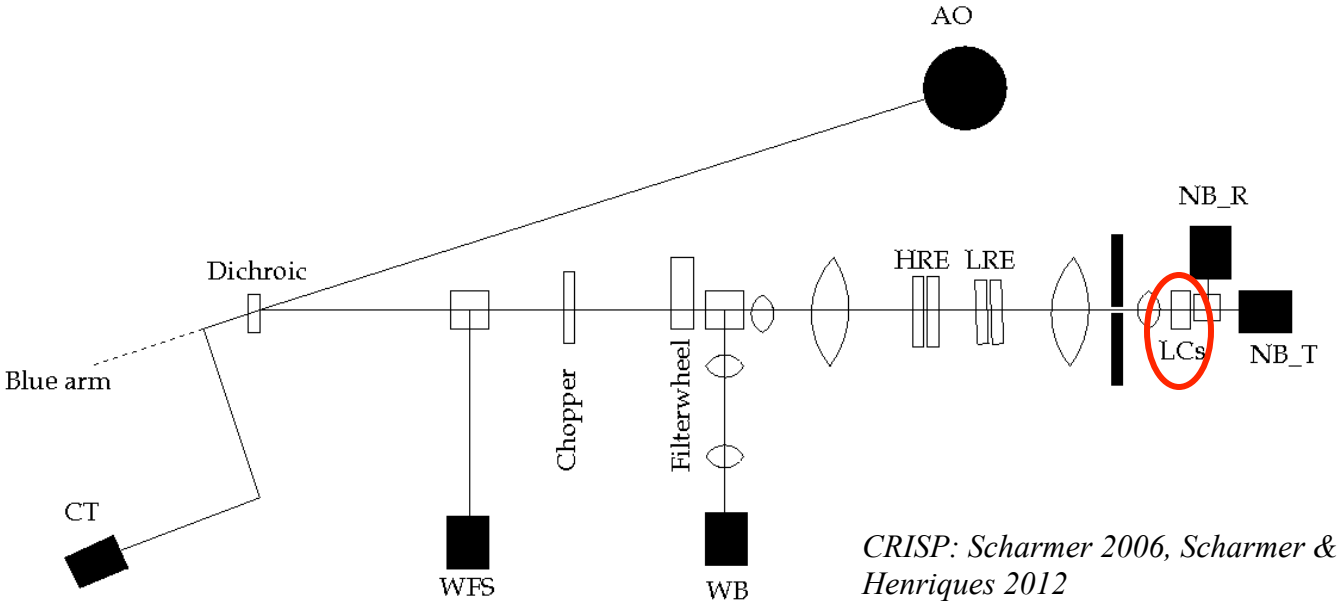

CRISP: Scharmer 2006, Scharmer & Henriques 2012

CRISP: Crisp Imaging Spectro-Polarimeter

- Wavelength isolation via two Fabry-Pérot etalons
- Spectral resolution about 60 mÅ
- Two nematic LCVRs for polarization modulation
- Dual-beam polarimetry via polarizing beam splitter analyzer
- Adaptive optics PLUS detailed image restoration (MFMOBD)
- Telecentric optical system for Fabry-Pérot path (pupil image at infinity)

Ground-Based Imaging Polarimeters – 2: CRISP

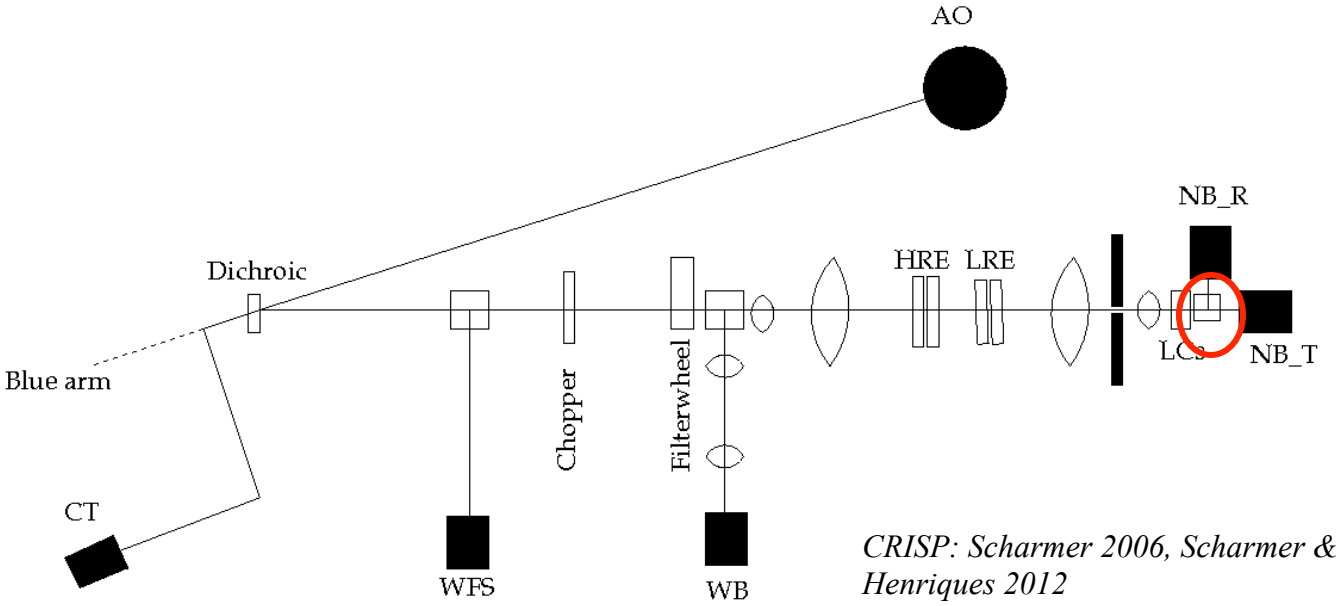

CRISP: Scharmer 2006, Scharmer & Henriques 2012

CRISP: Crisp Imaging Spectro-Polarimeter

- Wavelength isolation via two Fabry-Pérot etalons
- Spectral resolution about 60 mÅ
- Two nematic LCVRs for polarization modulation
- Dual-beam polarimetry via polarizing beam splitter analyzer
- Adaptive optics PLUS detailed image restoration (MFMOBD)
- Telecentric optical system for Fabry-Pérot path (pupil image at infinity) – **spectral resolution varies in image plane, but highest quality image**

Ground-Based Imaging Polarimeters – 3: IBIS

IBIS: Interferometric Bidimensional Spectrometer

- Universal filter (580 – 860 nm)
- Wavelength isolation via two Fabry-Pérot etalons
- Spectral resolution 20 - 30 mÅ
- Two nematic LCVRs for polarization analysis
- Dual-beam polarimetry via a polarizing beam splitter near the focal plane
- Operates in collimated mode

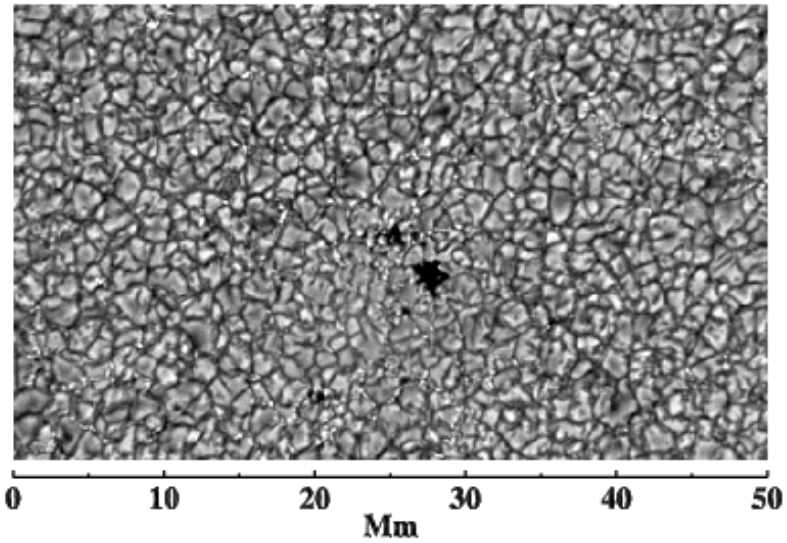

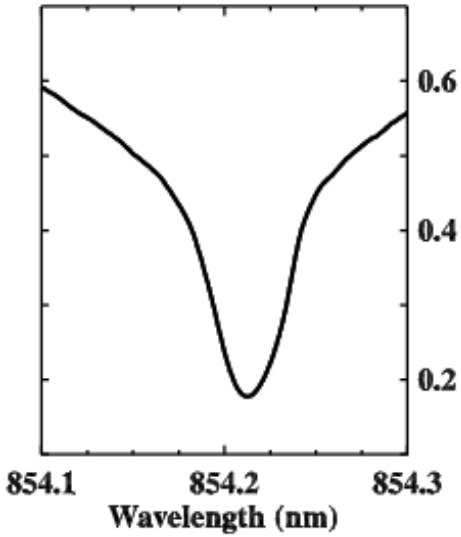

Images from IBIS website: http://www.arcetri.astro.it/science/solare/IBIS/IBIS_main.html

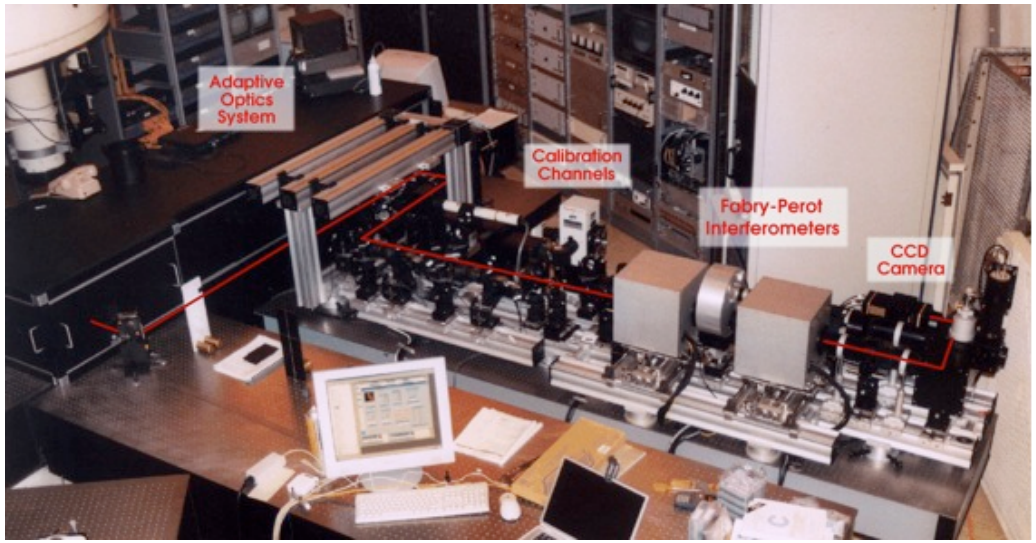

Ground-Based Multi-Use Polarimeter: ZIMPOL

ZIMPOL: Zürich Imaging POLarimeter

- More a system of modulation/demodulation-detecting rather than a specific solar polarimeter
- Now being used in both nighttime and solar astronomy
- Uses photo-elastic modulators to modulate the polarization at kHz rates
- Demodulation is done on the detector itself by shuffling charge among adjacent pixels

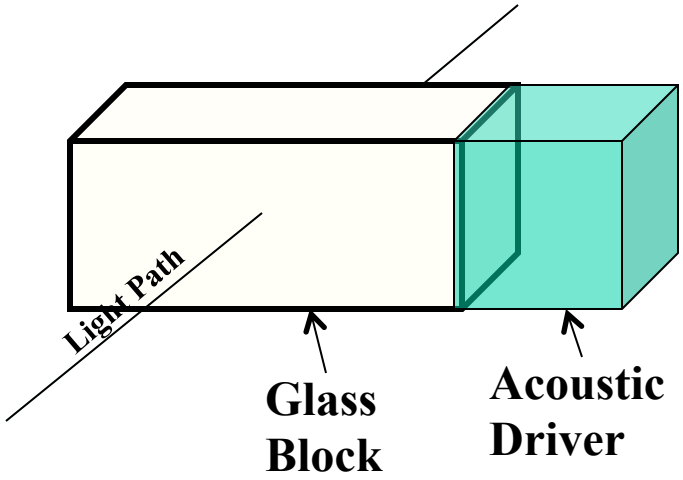

Charge shuffling on the detector

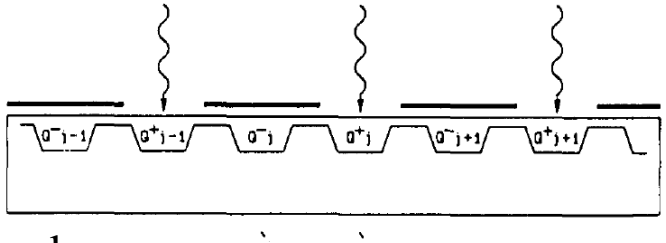

- CCD detector is altered with opaque mask on alternate columns
- Charge is shuffled back and forth by one pixel at the rate of modulation of the photo-elastic modulator
- CCDs have very large transfer efficiency, so this process may proceed many 1000s of times without loss
- When charge wells are full, the detector is read out
- Alternate rows are added for intensity, subtracted for polarization

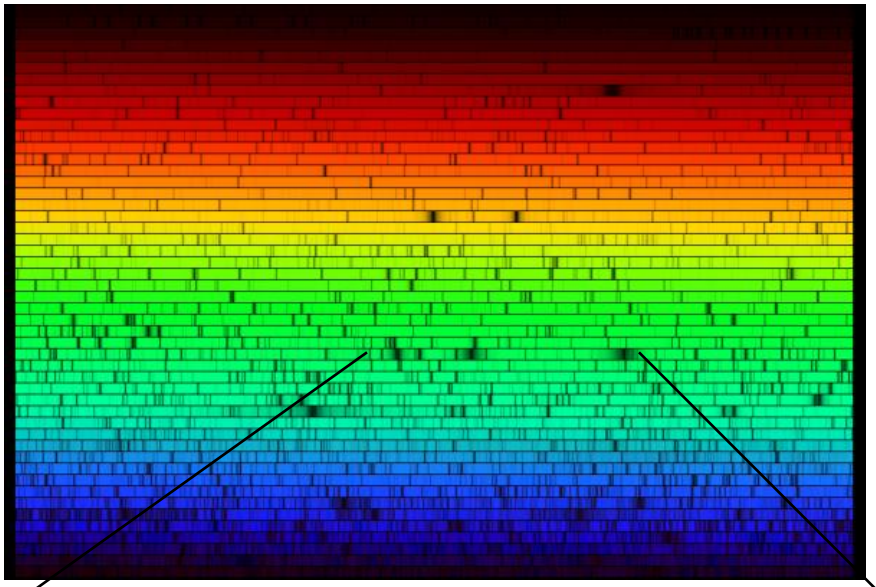

ZIMPOL
allows vector polarimetry with a polarimetric precision of 10^{-5} because **modulation is rapid compared to all sources of image motion**

This opened the door to the "Second Solar Spectrum"

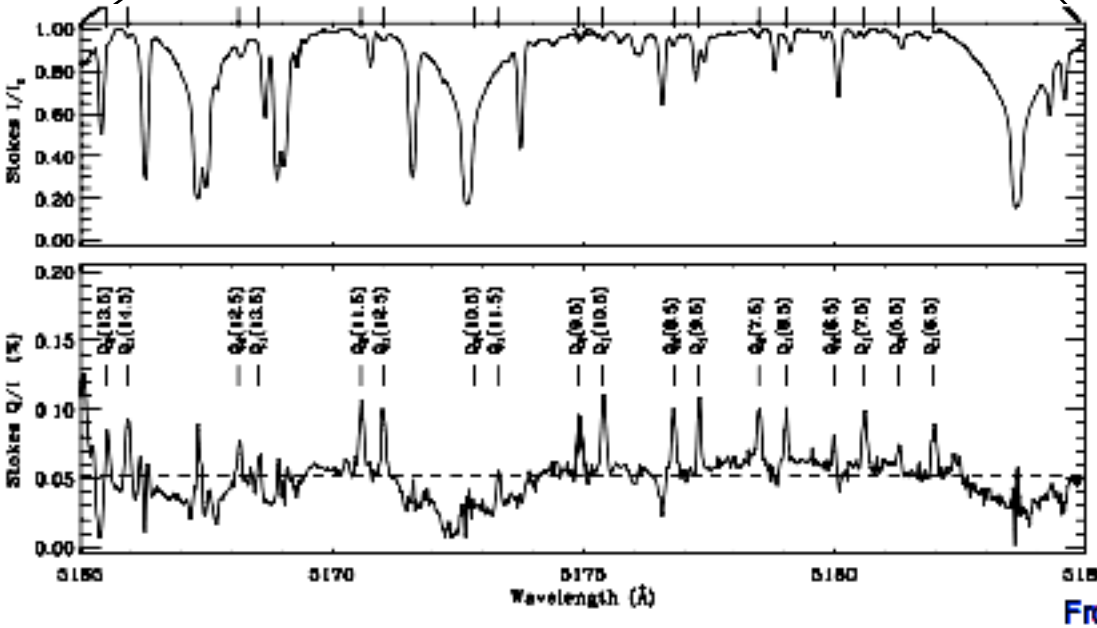

First solar spectrum

Second solar spectrum

From Gandorfer's Atlas

Slide modified from presentation of Stenflo 2015

Ground-Based Multi-Use Polarimeter: ZIMPOL

- Early versions of the device allowed only for measurement of *I* and one polarization state (*Q*, *U*, *V*) at a time
- Loss of signal from masked pixel columns
- Addition of second photo-elastic modulator with different retardation, but same frequency, would allow measurement of all Stokes parameters, but…..**it was not possible to synchronize the frequencies of two glass blocks vibrating at their resonant frequency!**
- Although less elegant, the device detector may be used with pairs of ferroelectric liquid crystals that modulate polarization at rates of up to a few kHz

Ground-Based Multi-Use Polarimeter: ZIMPOL

Evolved Zimpol (II and -3):

- Rapid (kHz) modulation via piezo-electric polarization modulator
- Phased rapid shifting of charge horizontally on the chip
- **3-pixel mask**, one exposed pixel
- **Microlens array**
- Preserve efficiency with microlens array, but unequal spatial sampling for square pixels

ZIMPOL-3 Camera

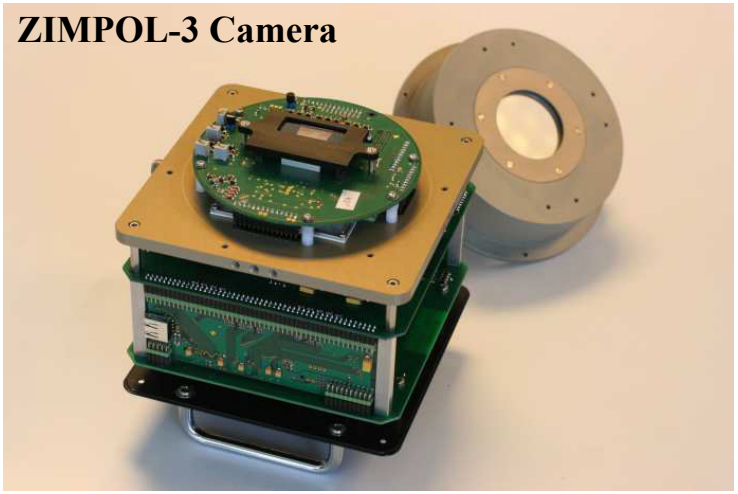

Image from Ramelli et al. 2010

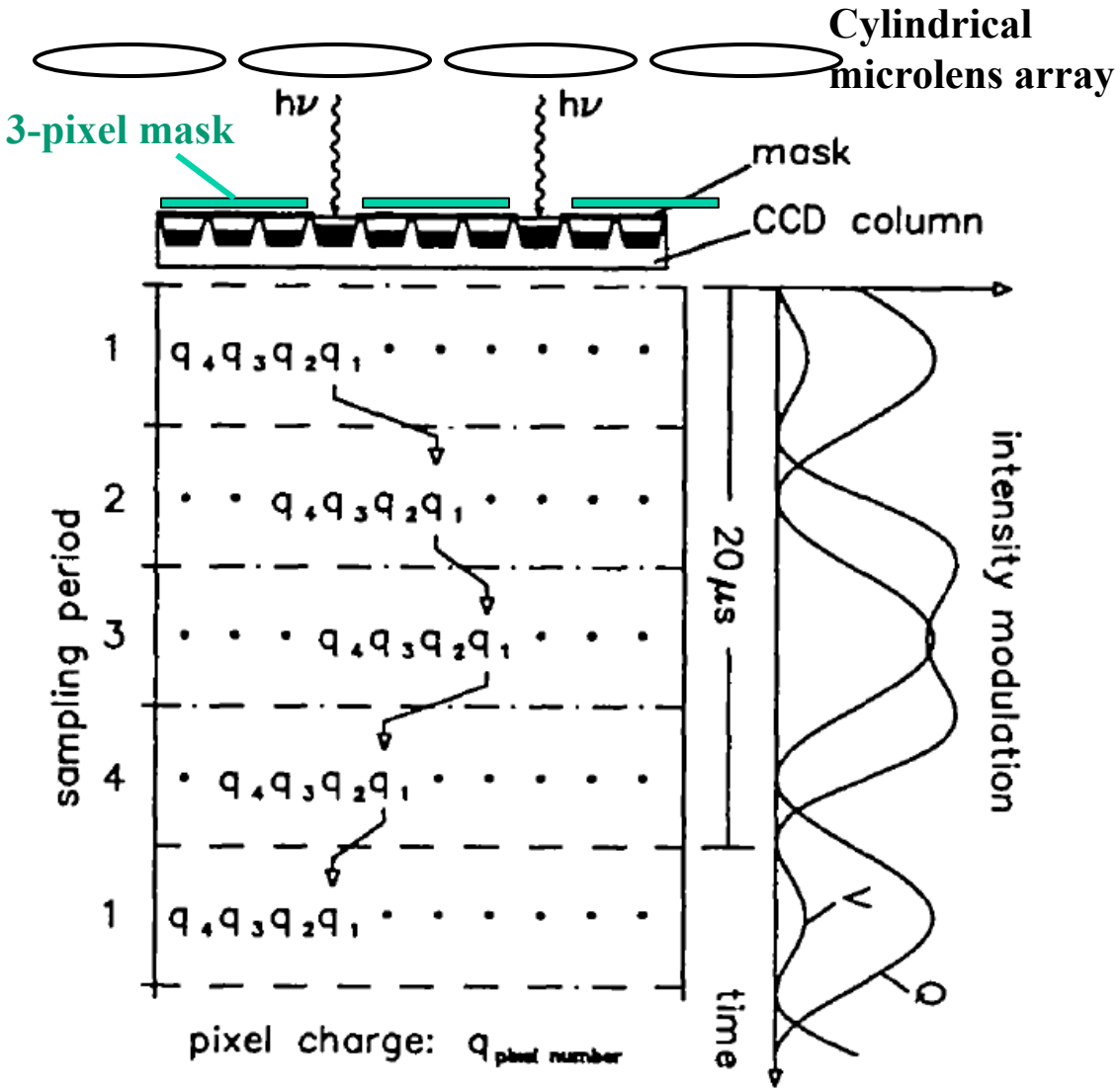

Adapted from Povel 2001

X. Space-Based Solar Polarimeters

The Solar Magnetic Field – Why Go To Space?

- **Continuity of time coverage**
  - **No interruptions due to weather, seeing**
  - **Minimization of interruptions due to night**
- **Uniform image quality**
- **Possibility of high angular resolution**
- **Enhance polarimetric precision by reducing polarization crosstalk (no "seeing")**
- **Access to the ultraviolet**

Challenges for Space Measurements of Magnetic Fields

- **Weight, power, size need to be minimized simultaneously:**
  - **Limit flexibility of instrument**
- **Instrument must be ultra-reliable:**
  - **Simplicity**
  - **Minimize number mechanisms**
  - **On-board redundancy where possible**
- **Environmental constraints:**
  - **Possibility of large temperature fluctuations, especially if instrument is powered off for any reason**
  - **High radiation exposure**
  - **Possibility of ultraviolet contamination**
- **Data constraints:**
  - **Full Stokes measurements require 4x the data of intensity alone**
  - **High data rates restricted by limits on telemetry**
  - **Onboard processing and compression usually necessary**

To the present time, very few space instruments capable of measurement of magnetic fields:

- ***Spacelab 2*/Solar Optical Universal Polarimeter (Spacelab 2/SOUP) – launched 29 July 1985** ***(failure of universal filter, no magnetic field data)***
- ***Solar and Heliospheric Observatory*/Michelson Doppler Imager (*SoHO*/MDI) – launched 2 December 1995**
- ***Hinode* – Solar Optical Telescope/Narrowband Filter Instrument and Spectro-Polarimeter (SOT/NFI, SOT/SP) – launch 22 September 2006**
- ***Sunrise*/Imaging Magnetograph eXperiment (*Sunrise*/IMaX) – launched 6 June 2009, 12 June 2013**
- ***Solar Dynamics Observatory*/Helioseismic and Magnetic Imager (*SDO*/HMI) – launched 11 February 2010**
- **Solar Ultraviolet Magnetograph Investigation (SUMI) – launched 31 July 2010, 5 July 2012** ***(no substantive results reported yet)***

To the present, very few space instruments capable of measurement of magnetic fields:

- ~~*Spacelab 2*/Solar Optical Universal Polarimeter (Spacelab 2/SOUP) – launched 29 July 1985 *(failure of universal filter, no magnetic field data)*~~
- *Solar and Heliospheric Observatory*/Michelson Doppler Imager (*SoHO*/MDI) – launched 2 December 1995
- *Hinode* – Solar Optical Telescope/Narrowband Filter Instrument and Spectro-Polarimeter (SOT/NFI, SOT/SP) – launch 22 September 2006
- *Sunrise*/Imaging Magnetograph eXperiment (*Sunrise*/IMaX) – launched 6 June 2009, 12 June 2013
- *Solar Dynamics Observatory*/Helioseismic and Magnetic Imager (*SDO*/HMI) – launched 11 February 2010
- Solar Ultraviolet Magnetograph Investigation (SUMI) – launched 31 July 2010, 5 July 2012 *(no substantive results reported yet)*

To the present, very few space instruments capable of measurement of magnetic fields:

- ~~*Spacelab 2*/Solar Optical Universal Polarimeter (Spacelab 2/SOUP) – launched 29 July 1985 *(failure of universal filter, no magnetic field data)*~~
- *Solar and Heliospheric Observatory*/Michelson Doppler Imager (*SoHO*/MDI) – launched 2 December 1995, observed until 12 April 2011
- *Hinode* – Solar Optical Telescope/Narrowband Filter Instrument and Spectro-Polarimeter (SOT/NFI, SOT/SP) – launch 22 September 2006
- *Sunrise*/Imaging Magnetograph eXperiment (*Sunrise*/IMaX) – launched 6 June 2009, 12 June 2013
- *Solar Dynamics Observatory*/Helioseismic and Magnetic Imager (*SDO*/HMI) – launched 11 February 2010
- ~~Solar Ultraviolet Magnetograph Investigation (SUMI) – launched 31 July 2010, 5 July 2012 *(no substantive results reported yet)*~~

To the present, very few space instruments capable of measurement of magnetic fields:

- ~~*Spacelab 2*/Solar Optical Universal Polarimeter (Spacelab 2/SOUP) – launched 29 July 1985 *(failure of universal filter, no magnetic field data)*~~
- *Solar and Heliospheric Observatory*/Michelson Doppler Imager (*SoHO*/MDI) – launched 2 December 1995
- *Hinode* – Solar Optical Telescope/Narrowband Filter Instrument and Spectro-Polarimeter (SOT/NFI, SOT/SP) – launch 22 September 2006
- *Sunrise*/Imaging Magnetograph eXperiment (*Sunrise*/IMaX) – launched 6 June 2009, 12 June 2013
- *Solar Dynamics Observatory*/Helioseismic and Magnetic Imager (*SDO*/HMI) – launched 11 February 2010
- ~~Solar Ultraviolet Magnetograph Investigation (SUMI) – launched 31 July 2010, 5 July 2012 *(no substantive results reported yet)*~~

➔*All of these experiments utilize the Zeeman effect to infer magnetic fields*

Brief Survey of Successful Photospheric Magnetic Field Measurements from Space

1. The *SoHO*/MDI instrument (December 1995 – April 2011)

- **Primary mission objective: Doppler velocities for helioseismology, *not* magnetic field measurements**
- **2” per pixel full disk, hi-res mode of 0.6” per pixel near disk center**
- **High resolution mode: 11x11 arcmin**
- **Two Michelson interferometers plus a Lyot filter yield spectral resolution of about 100 mÅ**
- **Michelson central wavelength tunable by rotating retarders**
- **Polarization analyzer selecting RCP, LCP allows sequential circular polarization measurements – longitudinal field measurements only**
- **Five wavelengths separated by 75 mÅ around line center**

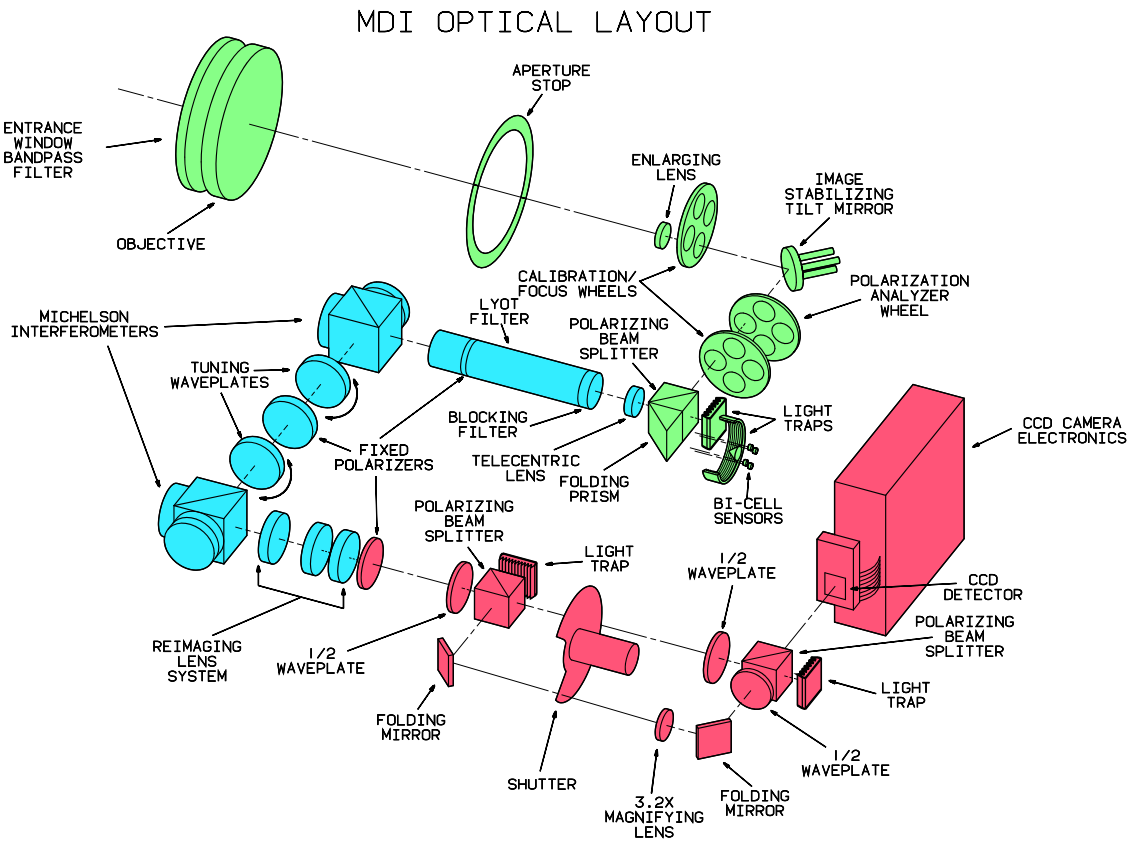

Operation at Ni I 6768 Å

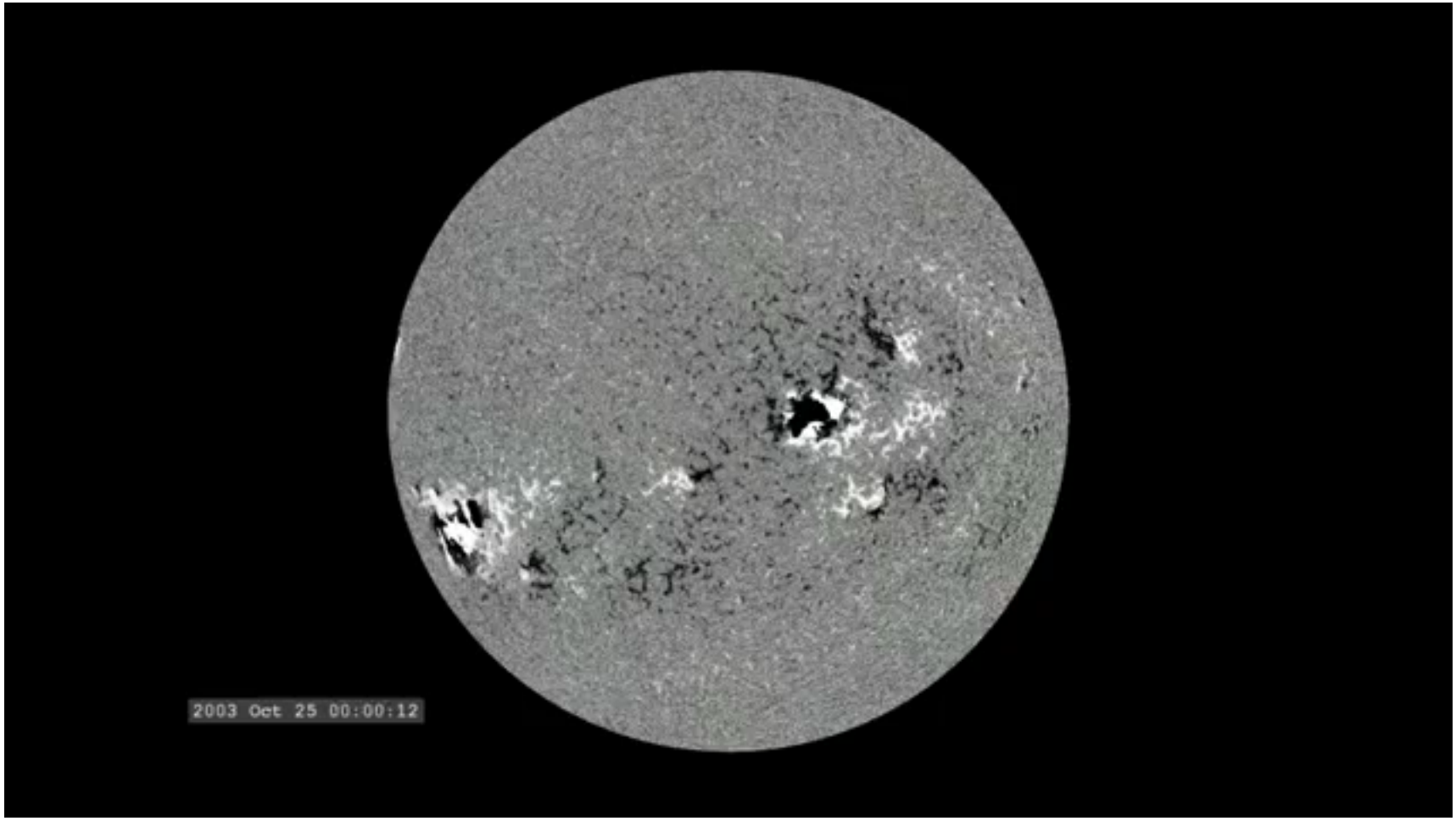
2003 Oct 25 00:00:12

Limitations of MDI instrument:

- **Measurements of Longitudinal field only**
- **Limited S/N**
- **High-resolution mode still not very high angular resolution**

Important Uses of MDI Magnetograms:

- **Evolution of photospheric field accompanying solar activity (CMEs, flares, prominences, …..)**
- **Nearly continuous record of large-scale field evolution with uniform image quality *spanning more than one solar cycle***
- **Boundary conditions for magnetic field extrapolations**

Sainz Dalda and Martínez Pillet 2008

Flux Decay of Active Regions with MDI – Sainz Dalda and Martínez Pillet 2008

- **Studied the rate of decay of net flux in three active regions**
- **During observed periods, 50-70% of flux vanishes**
- **Only about a quarter of this vanished flux may be identified as cancellation at the neutral line**
- **Simultaneous *TRACE* observations show outward-moving events in chromosphere and corona at cancellation sites**
- **Most flux loss appears to be "in-situ", at least when observed at the spatial resolution of MDI**
- **Recent study with *Hinode* SOT/SP suggests flux removal proceeds at as-yet unresolved scales**

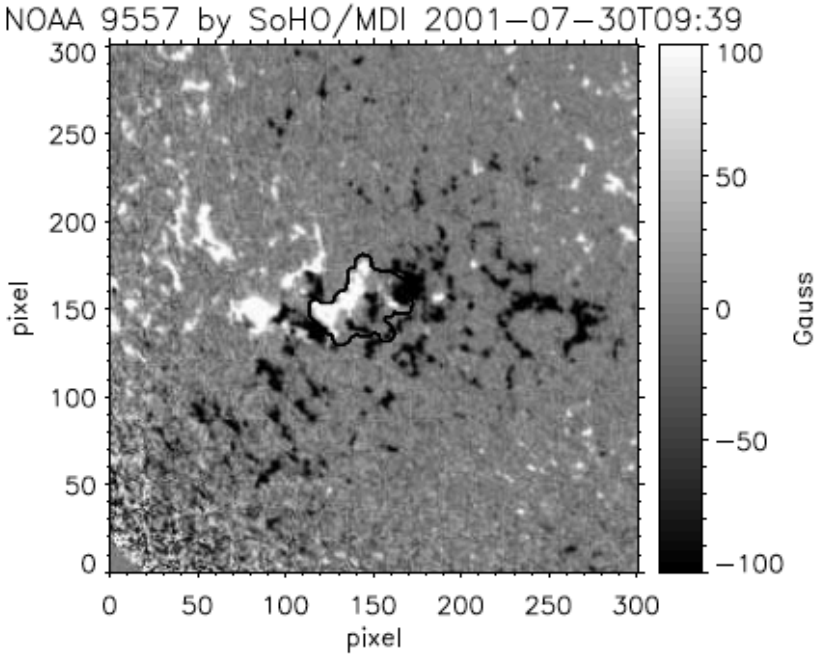

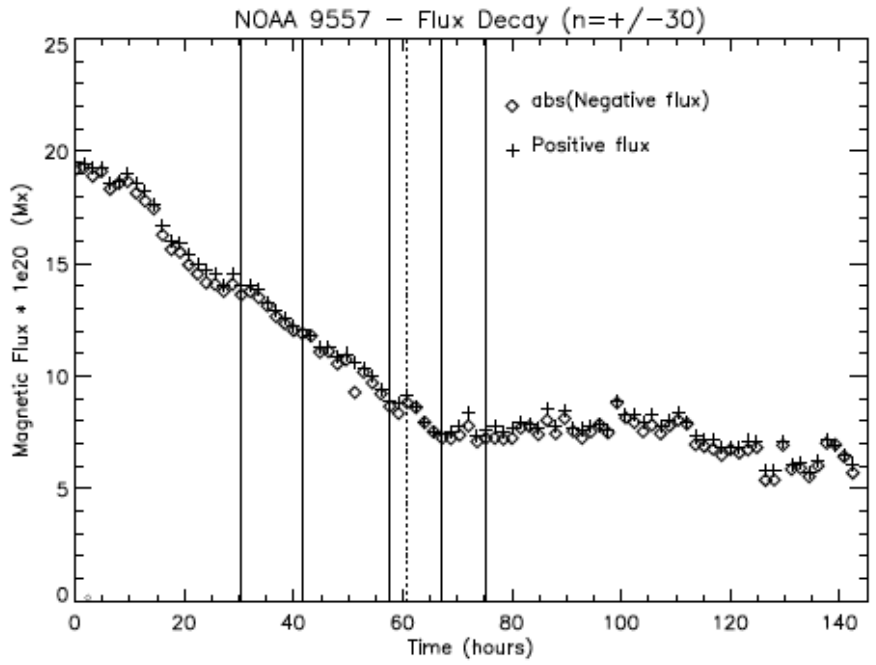

Cancelling Flux at Polarity Inversion Line with SOT/SP – Kubo et al. 2014

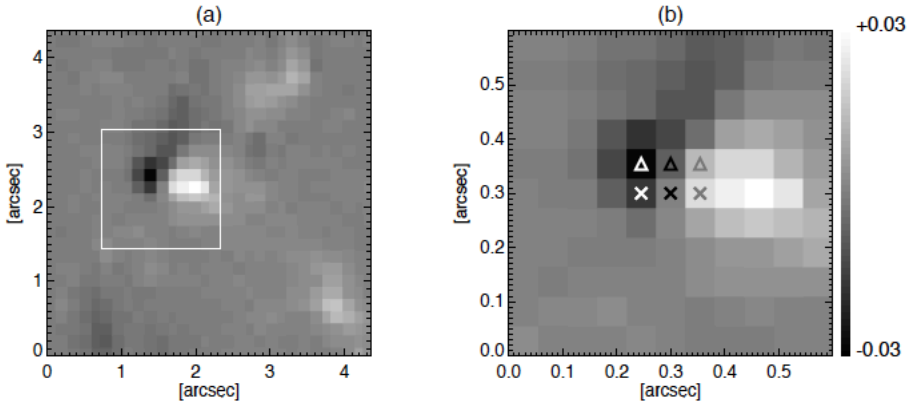

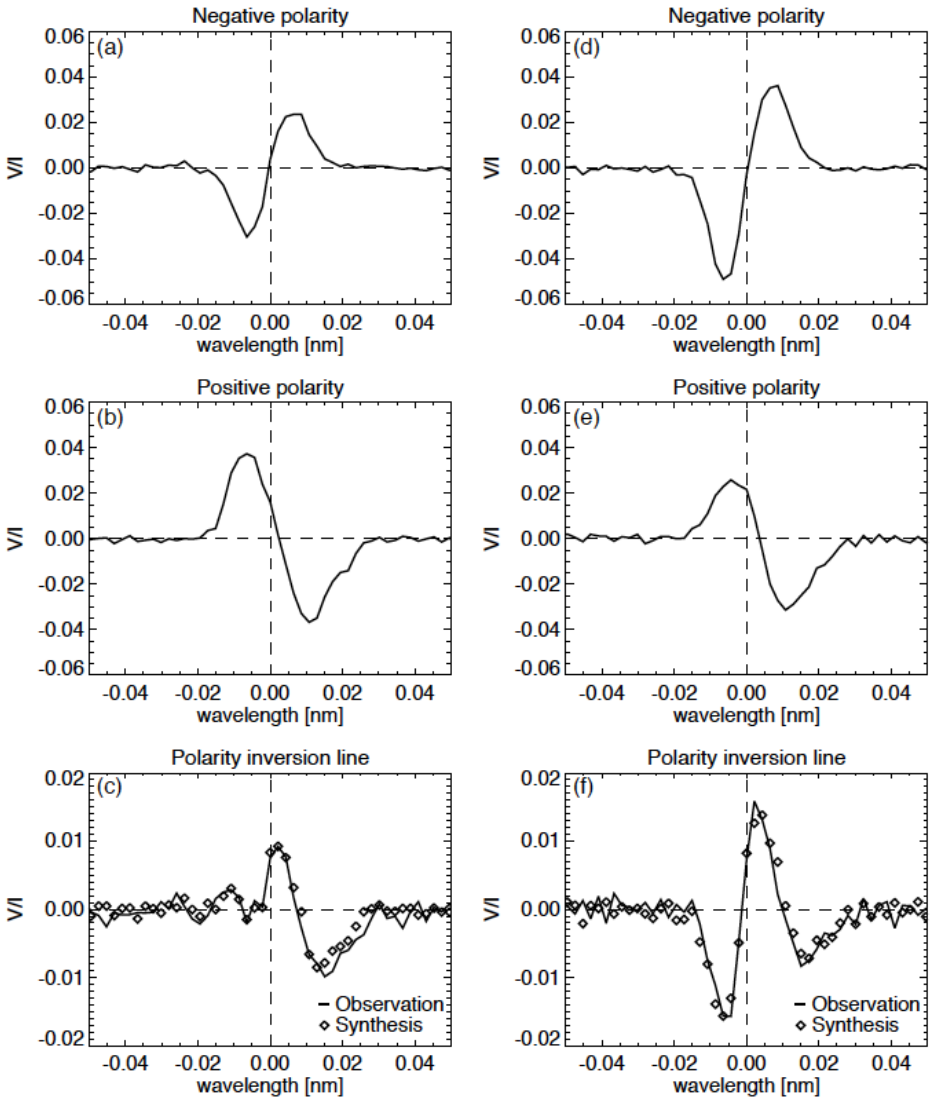

Newer high-resolution results shed light on the cancelation process at very small scales:

Flux cancellation proceeds at scales below the resolution limit of *Hinode*/ SOT

2. The *Hinode*/SOT instruments (October 2006 – Present)

- First space mission with emphasis on precision measurements of magnetic fields
- First high resolution magnetic field measurements from space: ≤0.3 arcsec
- Two instruments
  - SOT/Narrowband Filtergraph Instrument (NFI)
  - SOT/Spectro-Polarimeter (SP)

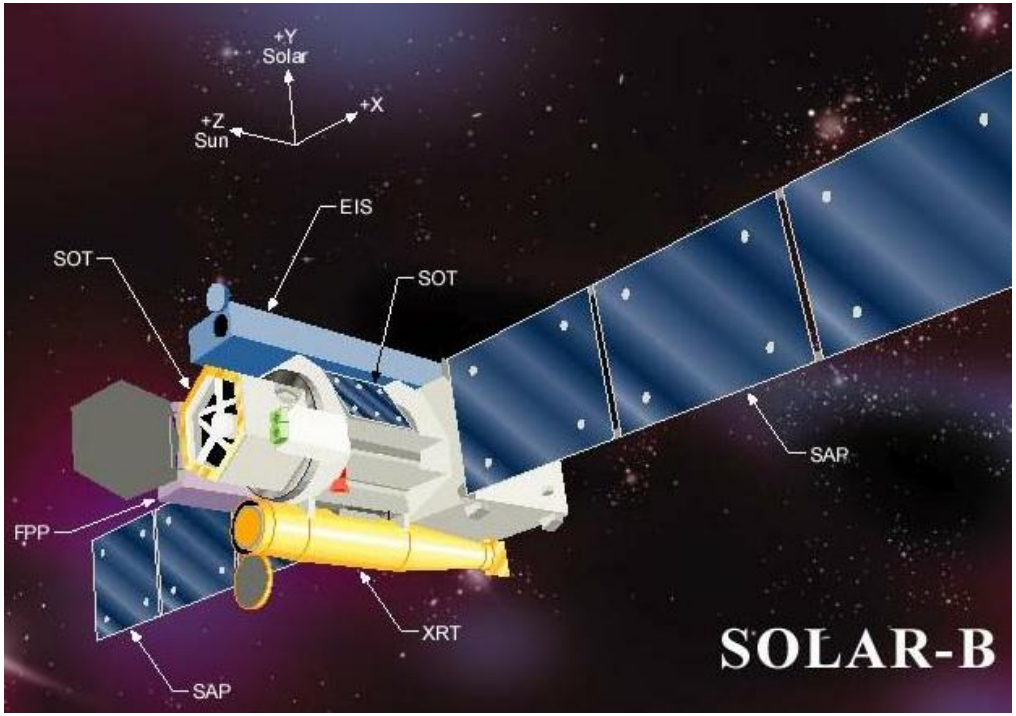

Status 8+ years after launch:

- SOT/SP operating nominally with slight throughput degradation
- SOT/NFI had failure of detector in 2016, no longer operational

Optical layout of SOT

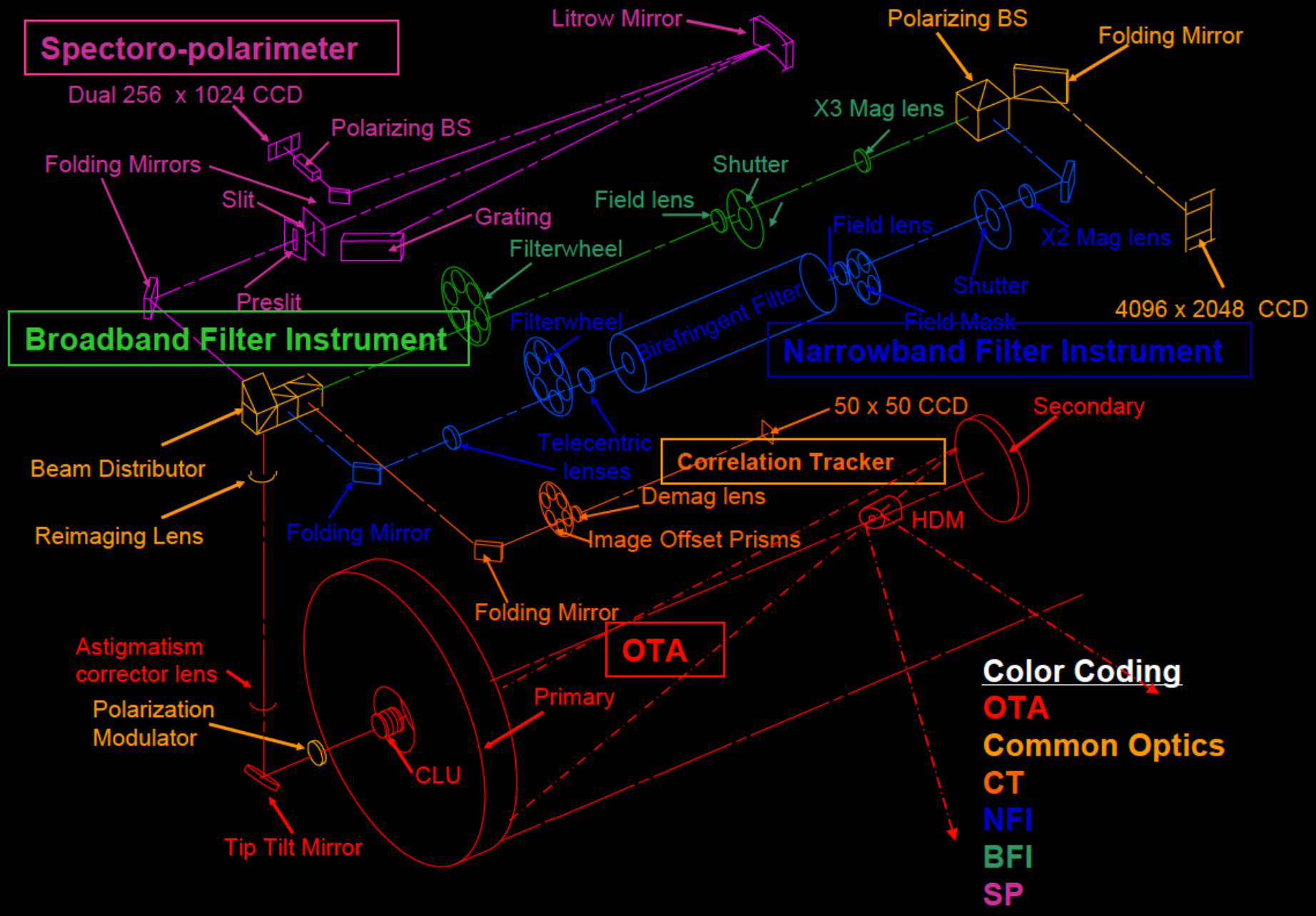

Filter Polarimetry with SOT/NFI

- **Capable of both longitudinal and vector polarimetry**
- **Photospheric fields from FeI lines at 5250, 6302 Å**
- **"Chromospheric" magnetograms in Na D1 5173 Å and Mg b1 5896 Å**
- **"Shuttered" magnetograms: shutter controls magnetogram exposures**
- **"Shutterless" magnetograms: Filter wheel mask creates frame store area on CCD, rapid parallel shift of CCD columns**
- **Valuable tool for evolution of photospheric field**

Three issues with Narrowband Filter instrument:

- **"Bubbles"**
- **Degradation of filters**
- **Camera failure, February 2016, no longer operative**

Flux Emergence and Active region Evolution with SOT/NFI

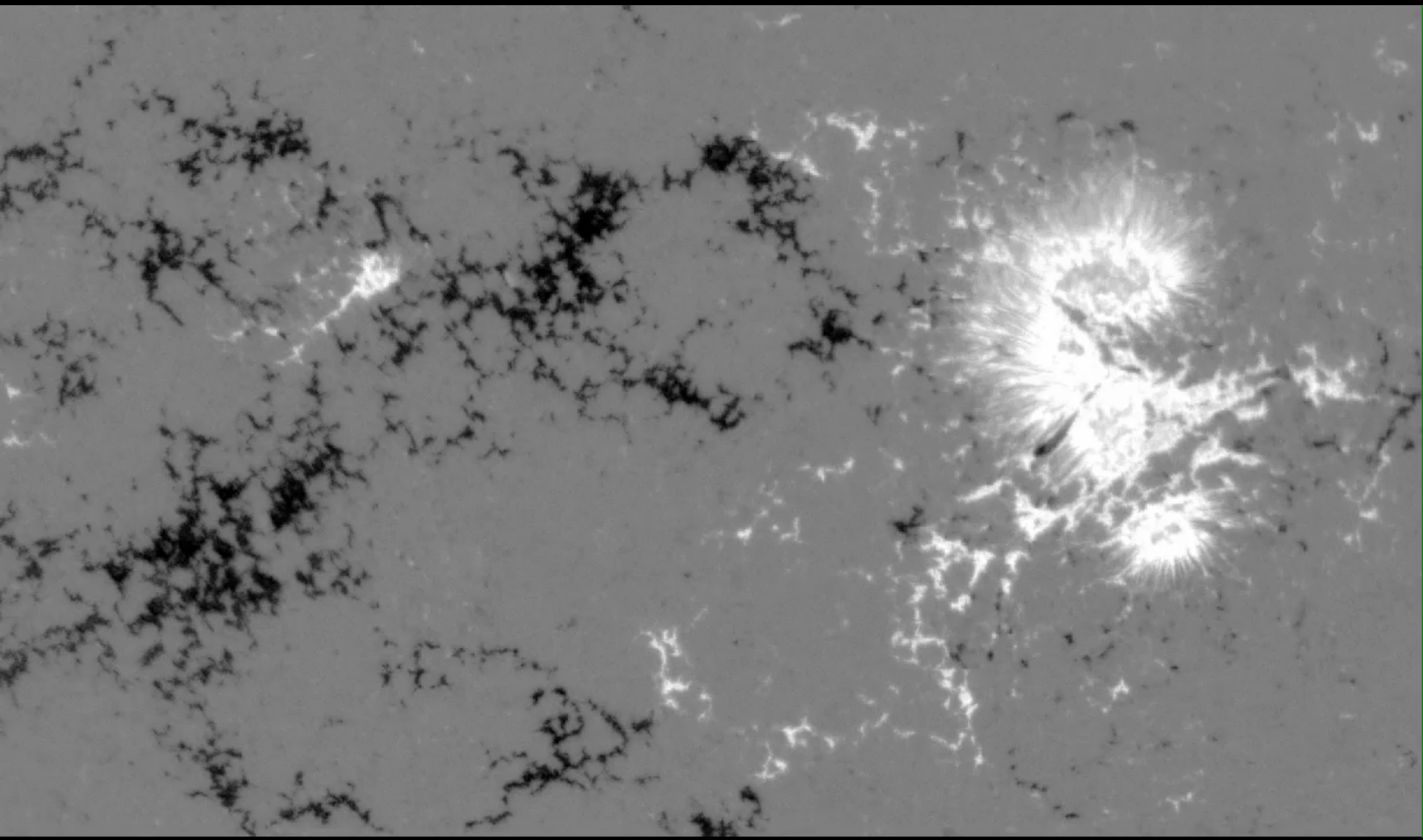

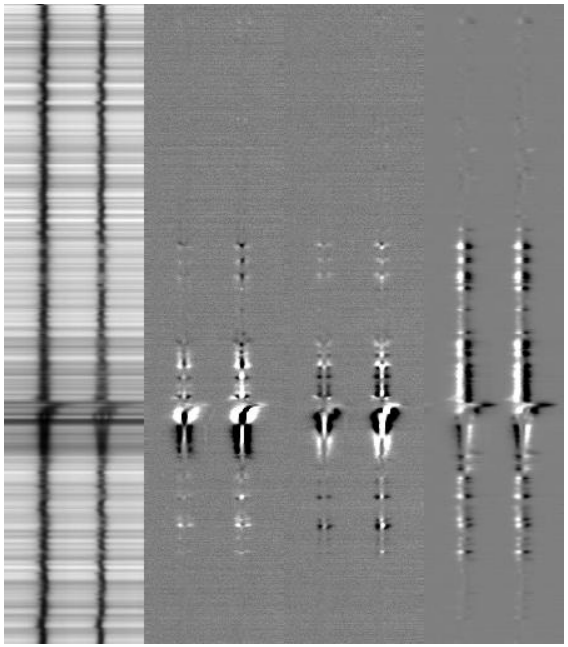

SOT SP (Spectro-Polarimeter)

- Fe I 6301.5 and 6302.5 Å
- Obtain spectra at 16 angular positions of polarization modulator
- 83min for 160" wide scan

Field of view along slit	**164" (north-south direction)**
Spatial scan range	**±164"**
Slit width	**0.16"**
Spectral coverage	**6300.8 – 6303.2 Å**
Spectral resolution	**27mÅ with 21.53 mÅ sampling**
Measurement of polarization	**Stokes I,Q,U,V simultaneously with dual beams (orthogonal linear components)**
Polarization signal to noise	**10^3 (with normal mapping)**

Optical layout of SOT

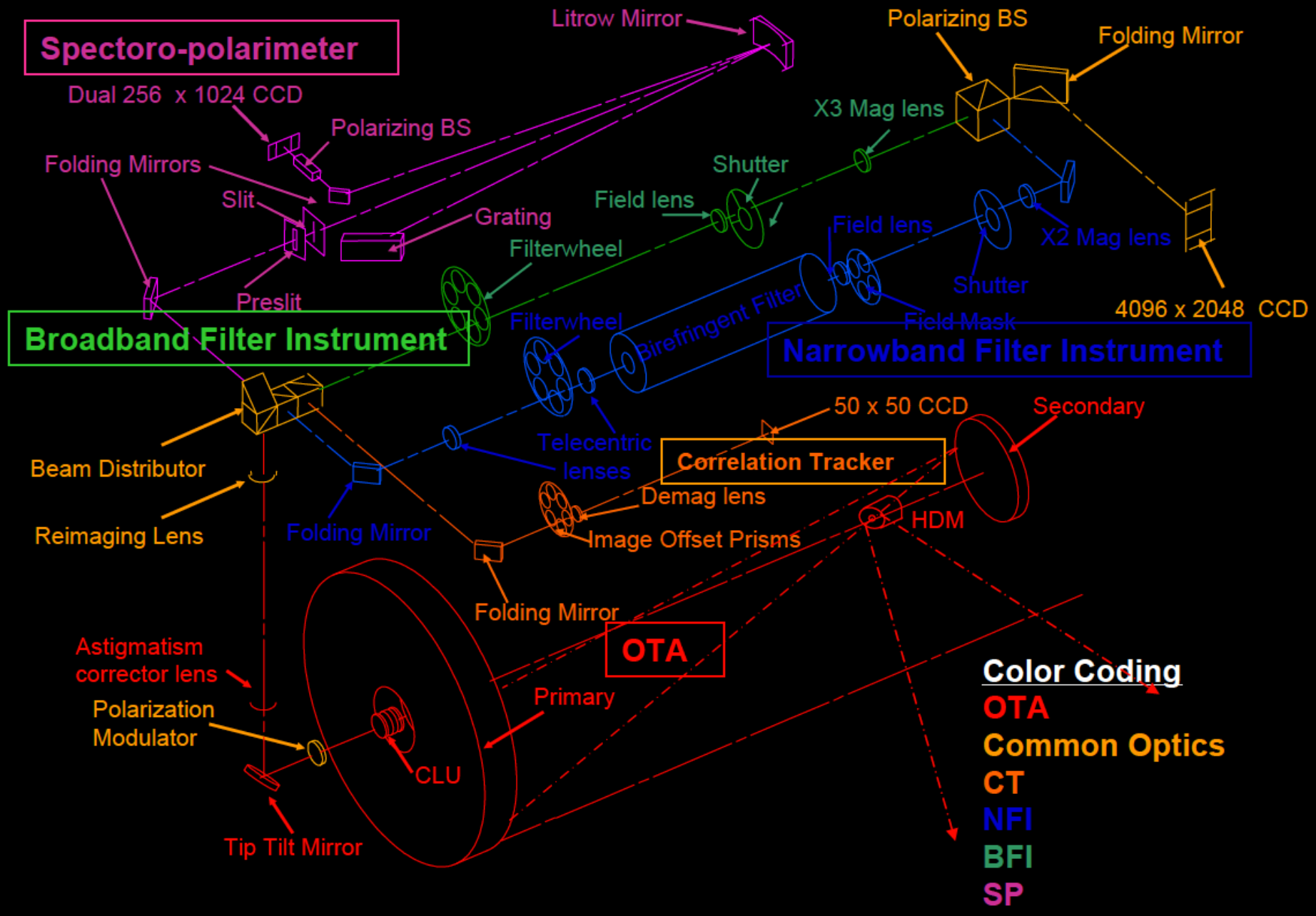

SP CCD Architecture

Custom Spectro-Polarimeter CCD

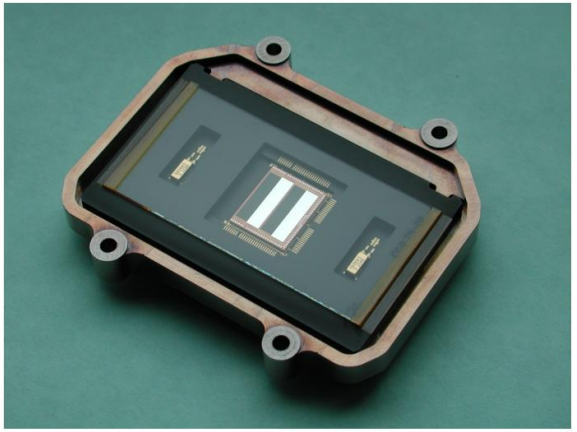

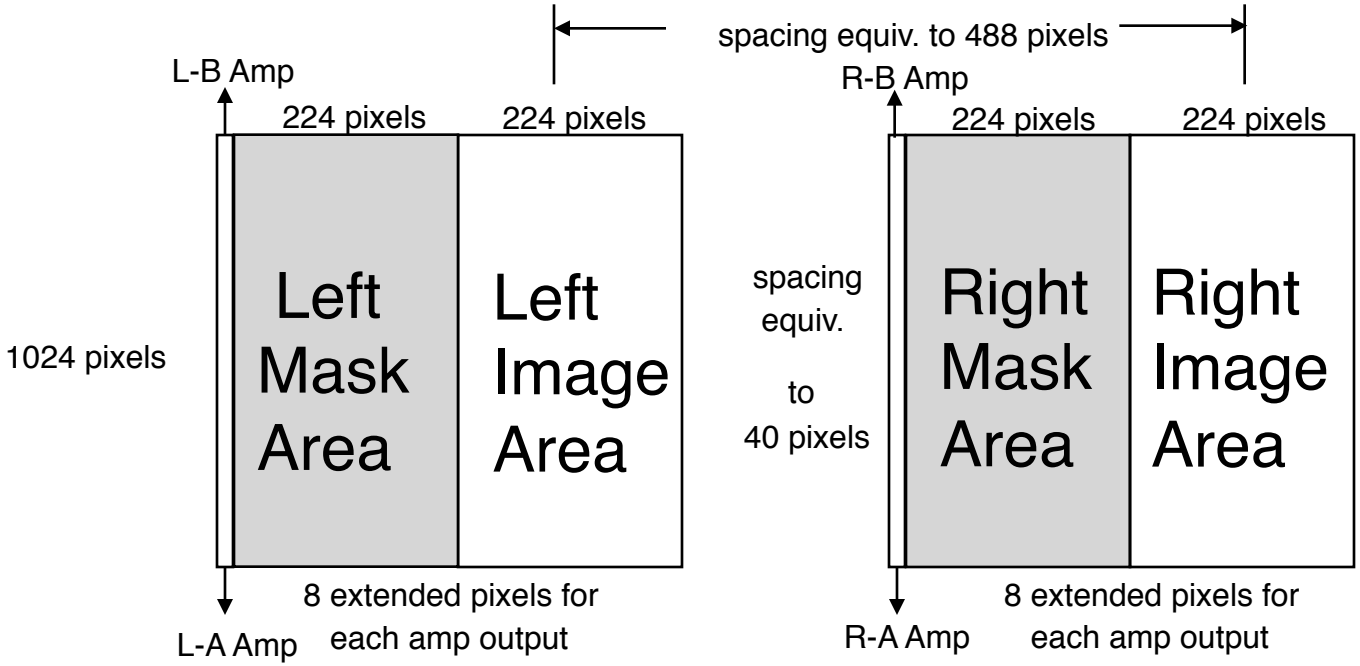

- **10 Hz fixed frame transfer rate**
- **Onboard "smart memory" for demodulation of Stokes signals**
- **Typically use only central 112 pixels in wavelength**

Dual-Beam Polarimetry

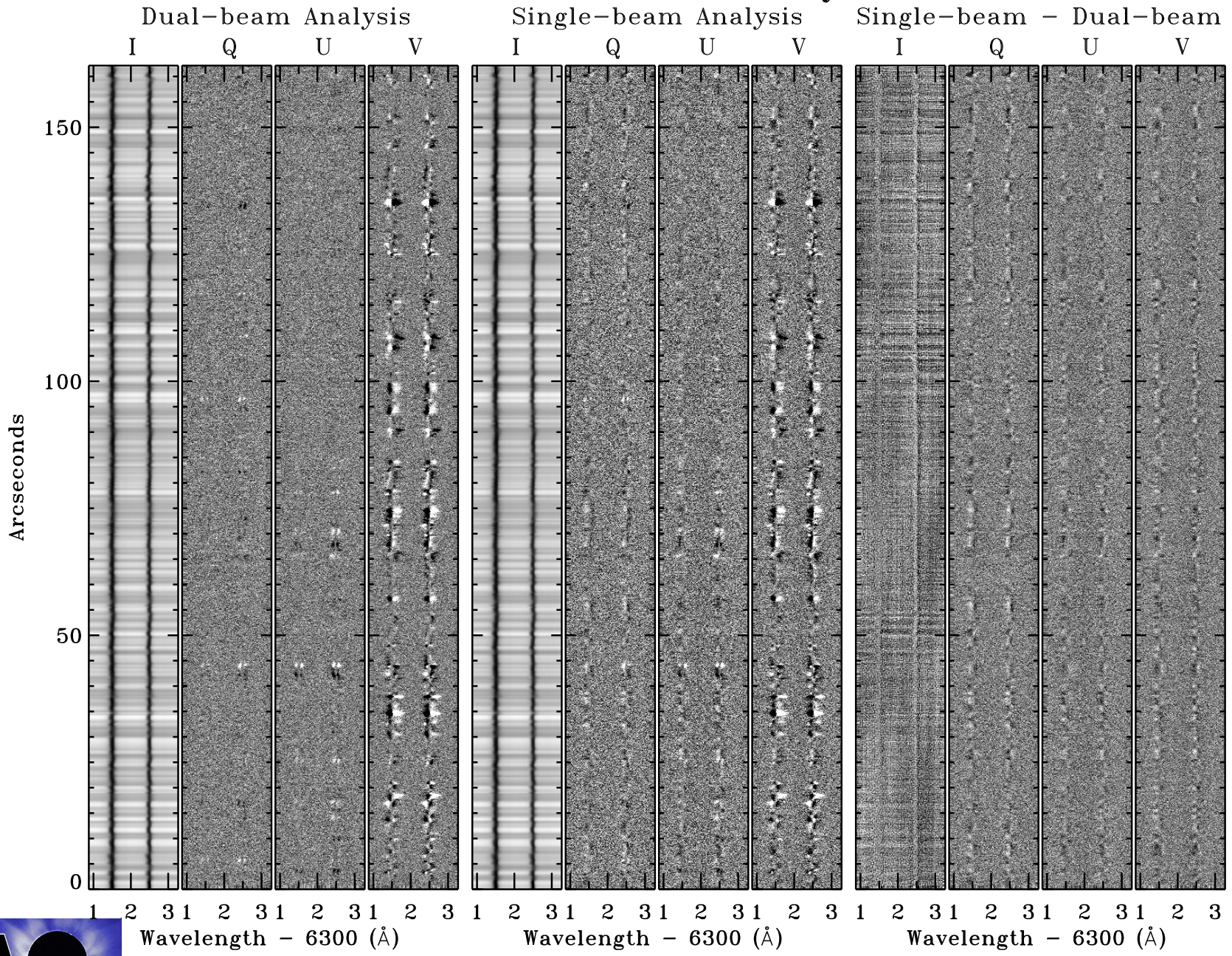

rms fluctuations, dual – single beam analysis

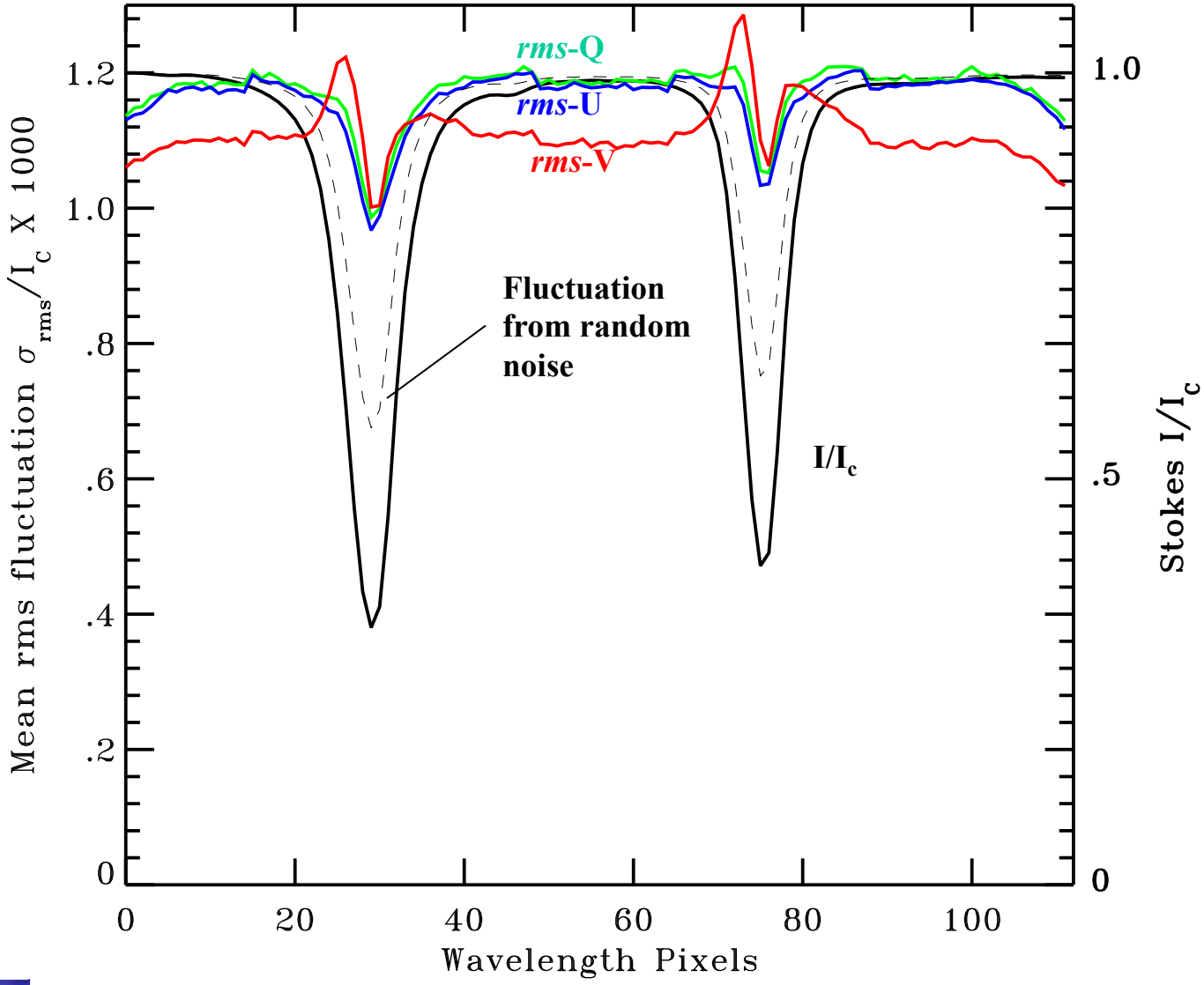

Hinode/SOT Irradiance Program

- **Performed once per month since 2008**
- **SP samples continuously from pole-to-pole**
- **Accompanied by SOT filtergrams**

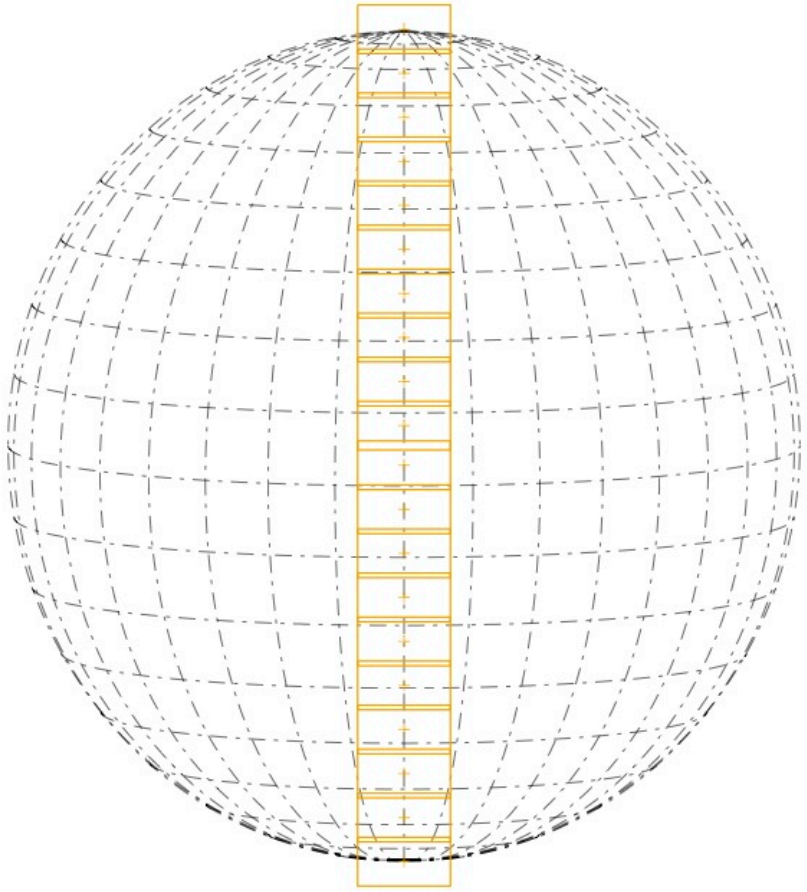

Solar Cycle Dependence of the Weakest Flux – Lites et al. 2014

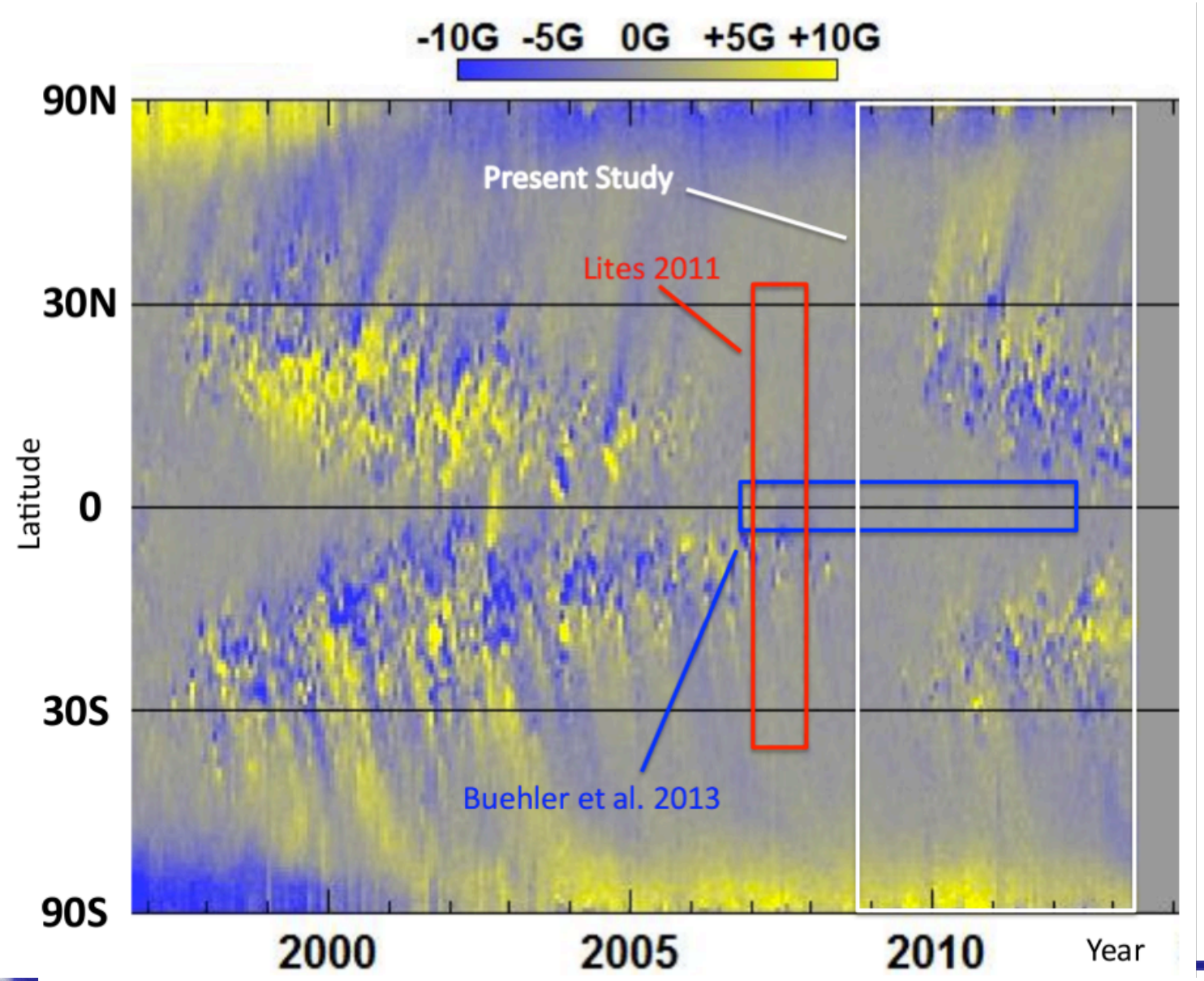

- *Hinode* "Irradiance" monthy observing program
- Isolate weak internetwork (IN) flux elements above noise
- Examine behavior from 2008 – 2013 (solar minimum to past maximum)
- Annual fluctuation due to changing solar B_0 angle
- No obvious signature of the global solar cycle in the weakest IN flux
- Results consistent with the operation of a small-scale solar dynamo

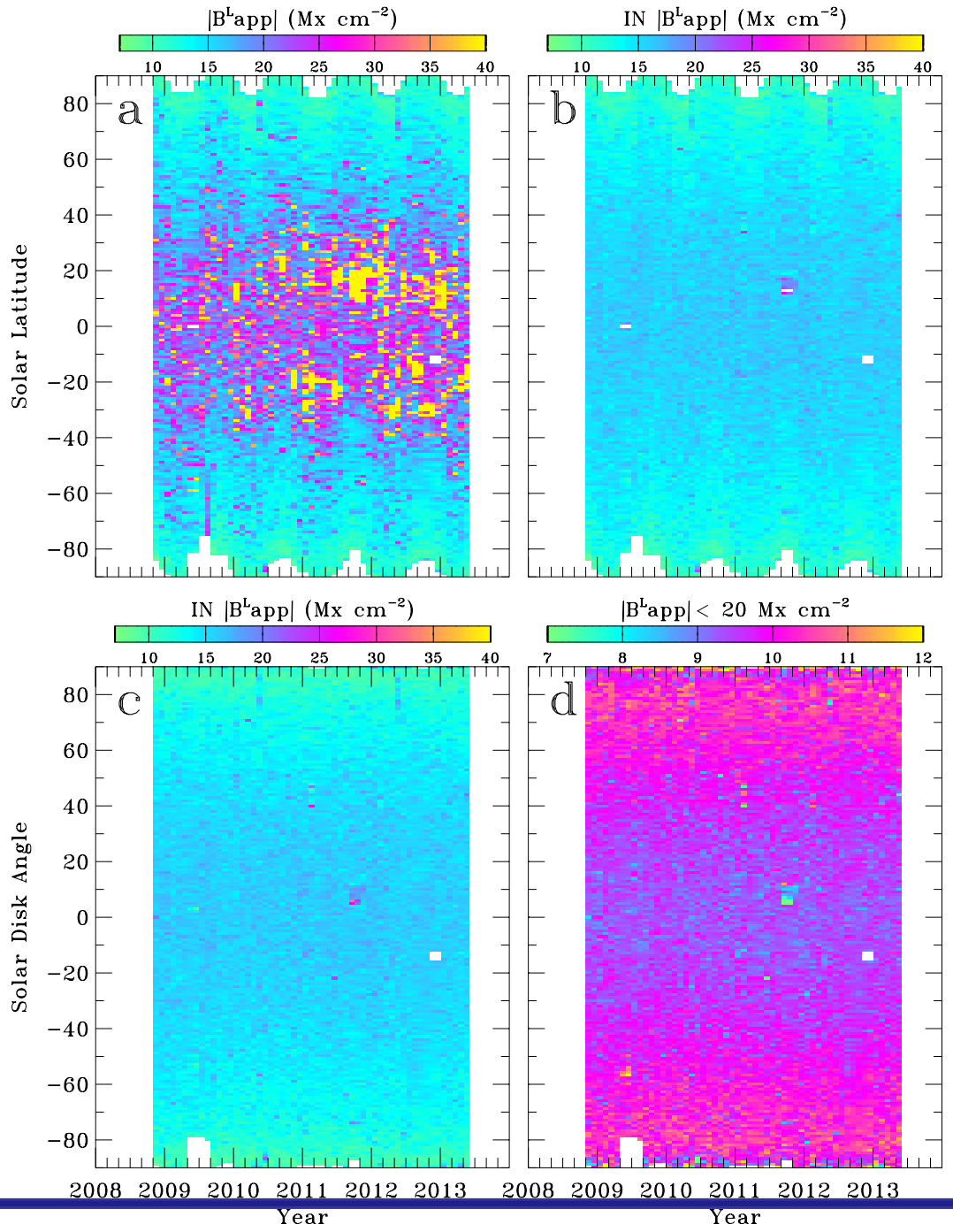

Hinode/SOT status:

- **SOT/NFI inoperative since February 2016 due to camera failure**
- **SOT/SP operating nominally with slight throughput degradation**
- **Both instruments suffer from failed high-speed X-band downlink since December 2007 – But routine operations continue with S-band downlink**

Hinode SOT/SP Advantages/Limitations:

- **SOT/SP continues to provide resolved spectral Stokes *IQUV* profiles simultaneously with high spectral resolution and good S/N**
- **Resolved profiles allow detailed analysis ➔ extraction of information along line-of-sight**
- **Dual-beam polarimetry ➔ minimize crosstalk**
- **Two spectral lines simultaneously ➔ more accurate field determination**
- **Full λ coverage of lines plus continuum ➔ capture high-velocity events**
- **SOT/SP is scanning spectrograph: slow coverage of solar image in one dimension**

3. The *Sunrise*/IMaX instrument (June 2009, June 2013)

- **Sunrise is a high-altitude balloon mission: like space mission in that there is negligible atmospheric seeing**
- **Very high angular resolution with 1-m telescope: < 0.2 arcsec**
- **Tunable double-pass Fabry-Perot filter instrument, 65 mÅ FWHM spectral resolution at 5250 Å**
- **Dual-beam polarimetry**
- **Phase diversity to correct for slowly-varying aberrations**
- **Full Stokes polarimetry allows vector field measurements**
- **Up to 11 wavelengths in line, plus continuum**

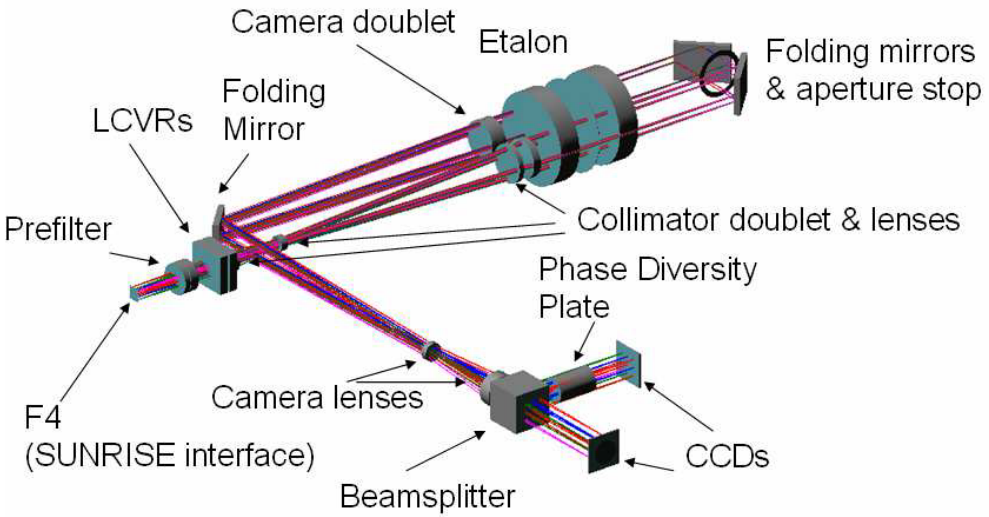

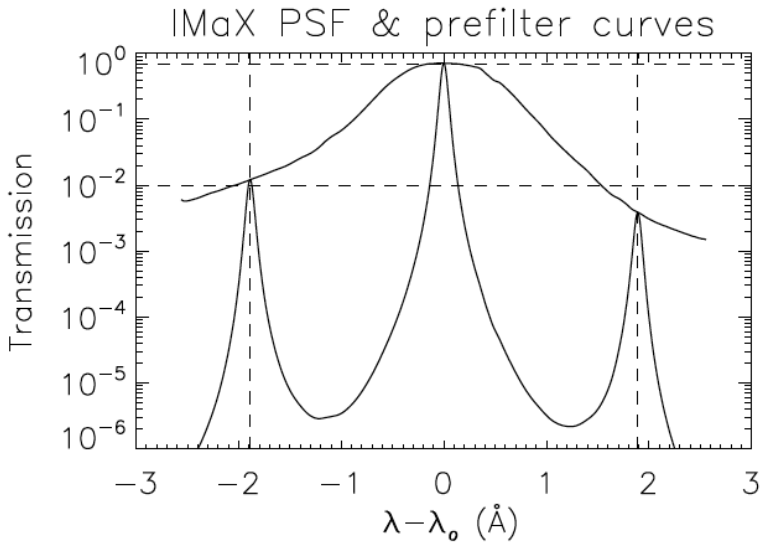

Sunrise/IMaX Observations of "Dead Calm" Areas in Quiet Sun - Martínez González et al. 2012

- Examine polarization signals over sequences 22, 31 minutes
- Identify small-scale loops in internetwork region (dipolar in B_{los} with B_{trans} between)
- Internetwork flux emergence is not uniform, thus generating mechanism is not strictly local in the upper layers of granulation

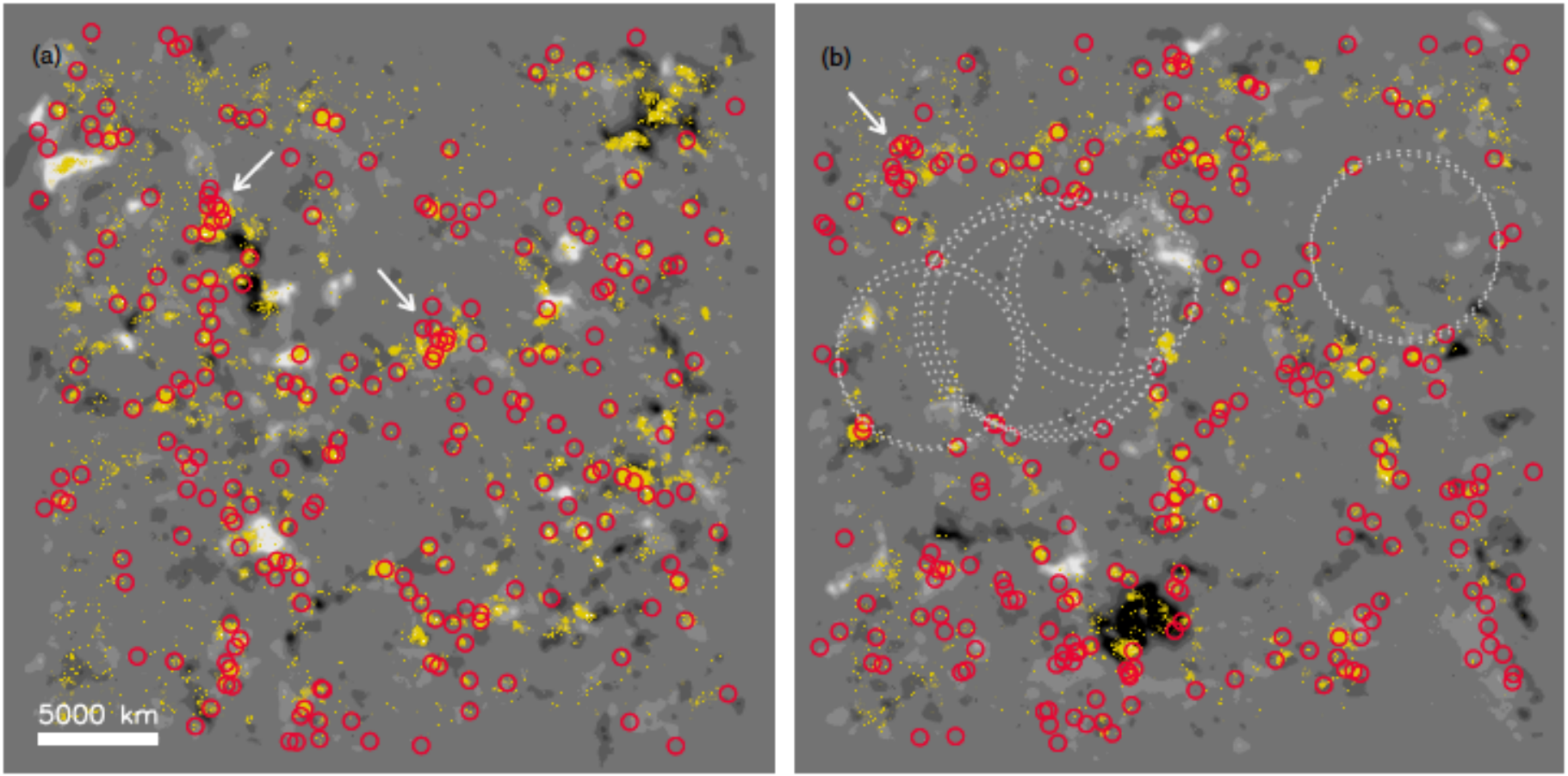

Sunrise/IMaX Advantages for Magnetic Field Measurement:

- Large 1-m aperture yields high resolution
- Improved filtergraph vector magnetic field diagnostics:
  - Dual-beam polarimetry
  - narrow filter width
  - Fine sampling of line

Sunrise/IMaX Limitations for Magnetic Field Measurement:

- Short duration flights (several days)
- Some instrumental issues compromised the first two missions
- Limited field-of-view (50 arcsec^2): cannot cover typical active region

4. The *SDO*/HMI instrument (February 2010 - Present)

- **Optical system very similar to *SoHO*/MDI – Michelson interferometers**
- **Spectral line differs from MDI line – better suited to magnetic field measurement**
- **Higher angular resolution than MDI 1.0 arcsec (0.5 arcsec pixels)**
- **Routine vector magnetometry**
- **Two cameras, but NOT for dual-beam polarimetry (one for Doppler velocity/longitudinal magnetograms, the other for full Stokes polarimetry)**
- **Geo-synchronous orbit (higher orbital velocity excursions than *SoHO*)**

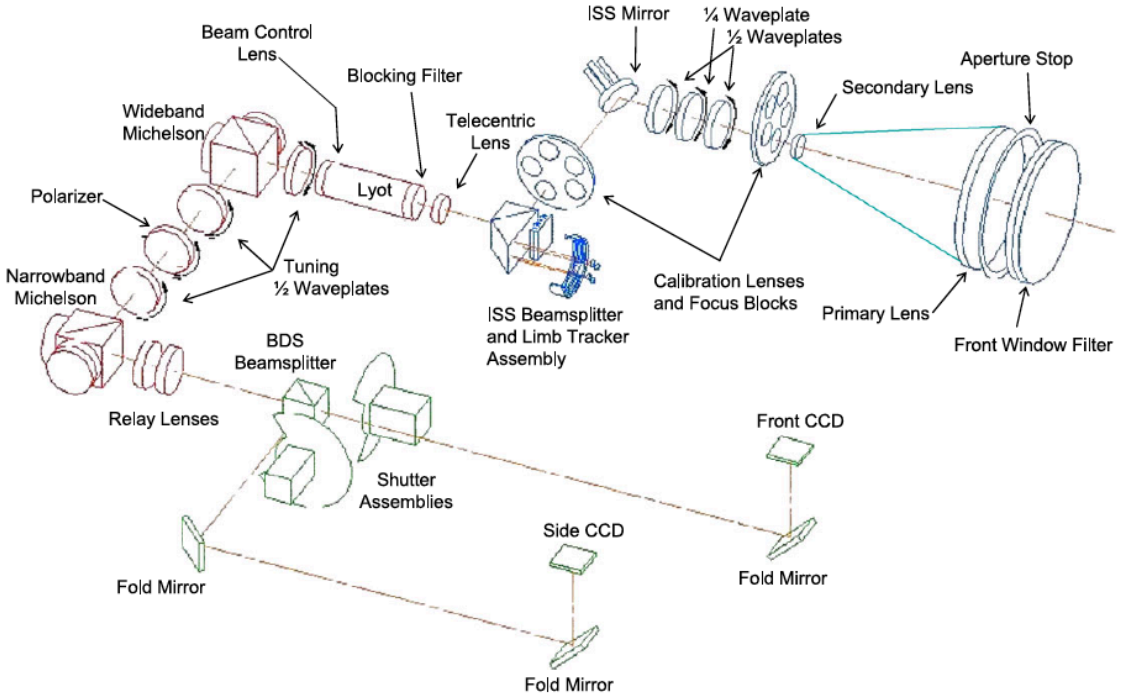

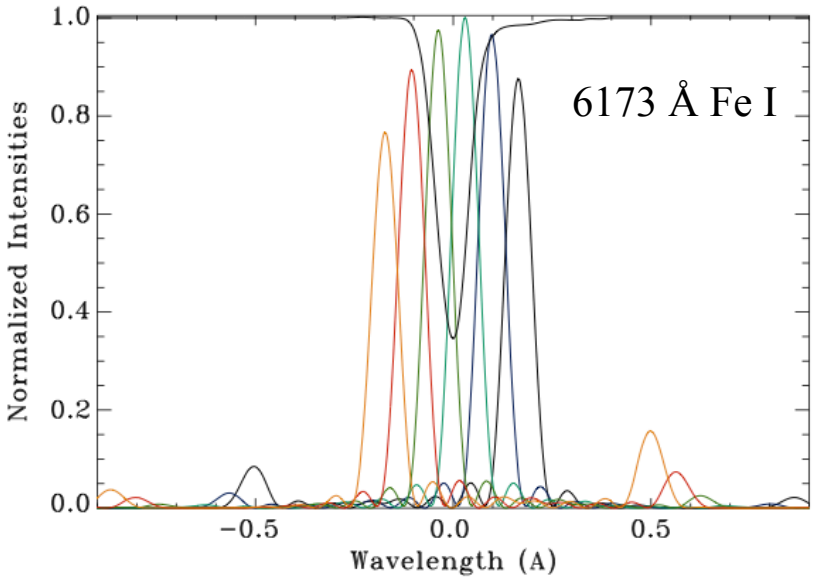

Full disk HMI LOS Magnetogram – AZAM disambiguation

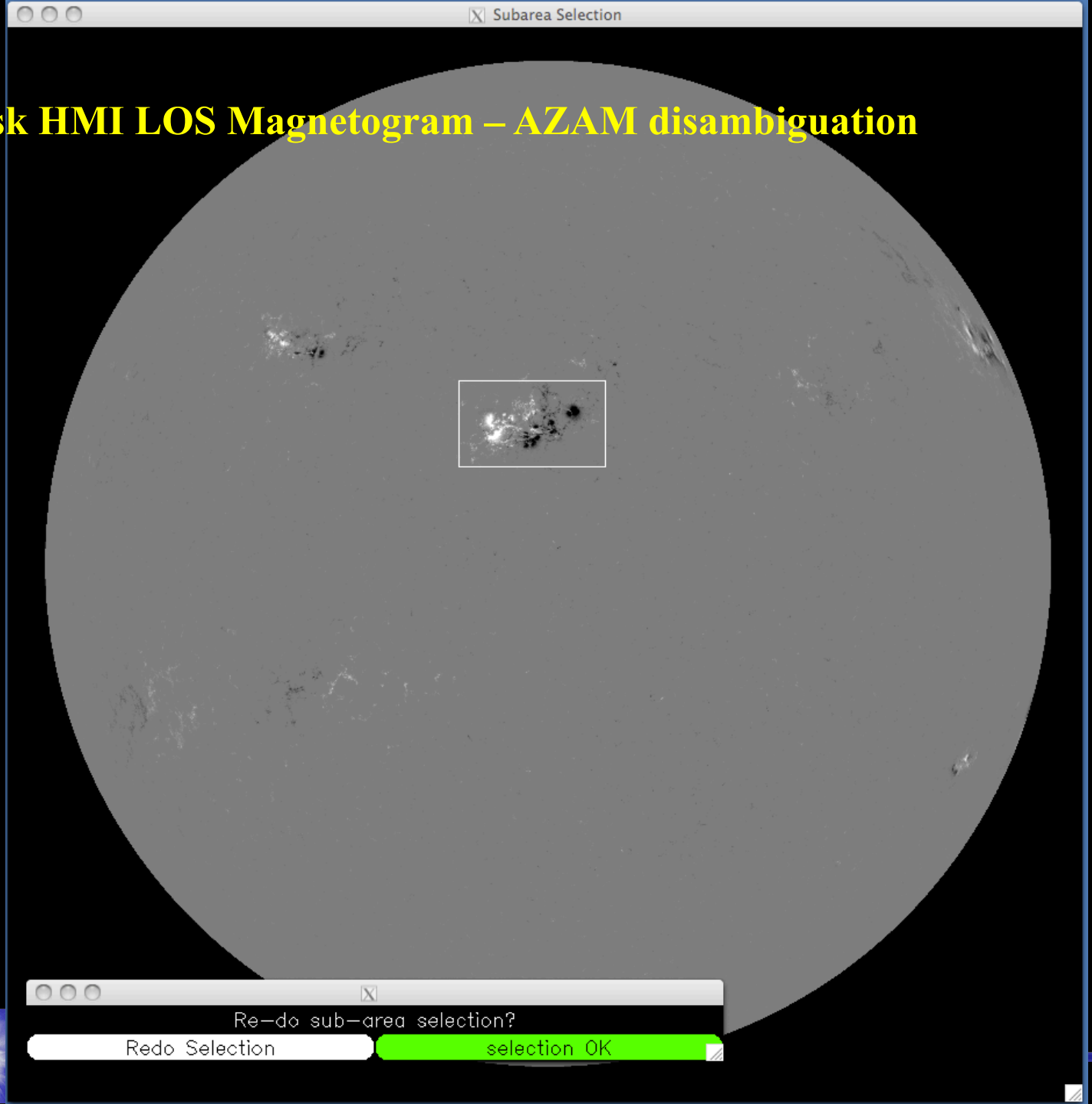

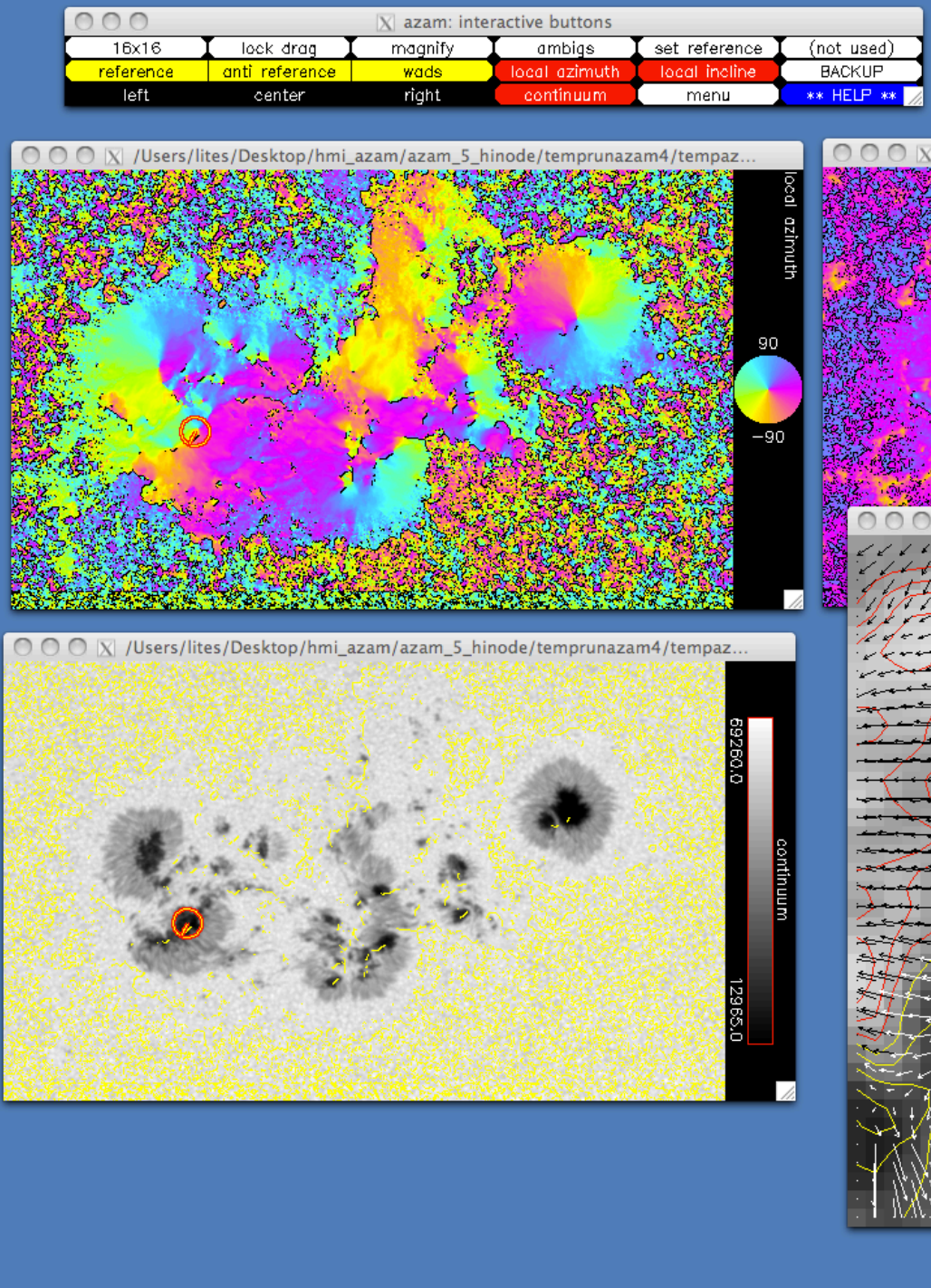
azam: interactive buttons
16x16
lock drag
magnify
ambigs
set reference
(not used)
reference
anti reference
wads
local azimuth
local incline
BACKUP
left
center
right
continuum
menu
** HELP **
/Users/lites/Desktop/hmi_azam/azam_5_hinode/temprunazam4/tempaz...
local azimuth
90
−90
/Users/lites/Desktop/hmi_azam/azam_5_hinode/temprunazam4/tempaz...
local incline
0
180
/Users/lites/Desktop/hmi_azam/azam_5_hinode/temprunazam4/tempaz...
69260.0
continuum
12965.0
/Users/lites/Desktop/hmi_azam/azam_5_hinode/temprunaza...
azam: data at cursor
continuum 21149.0
field 2191.1
Doppler 1482.3750
1−fill 1.0000
a__pip 0.117383
a__mu 0.960767 ambig
flux 2165.1 1827.0
Jz 0.0 0.0
azimuth 131.52 −48.48
incline 14.47
zenith_azimuth −114.73 −61.86
zenith_angle 8.85 33.51
(141,136)(1863,2544)(51.67,50.14)Mm

Hemispheric Twist Preference from HMI – Liu et al. 2014

- Use B_z^2-weighted force-free parameter α, integrated over active region, as a measure of twist
- 151 active regions analyzed
- Confirm earlier results based on lower quality data

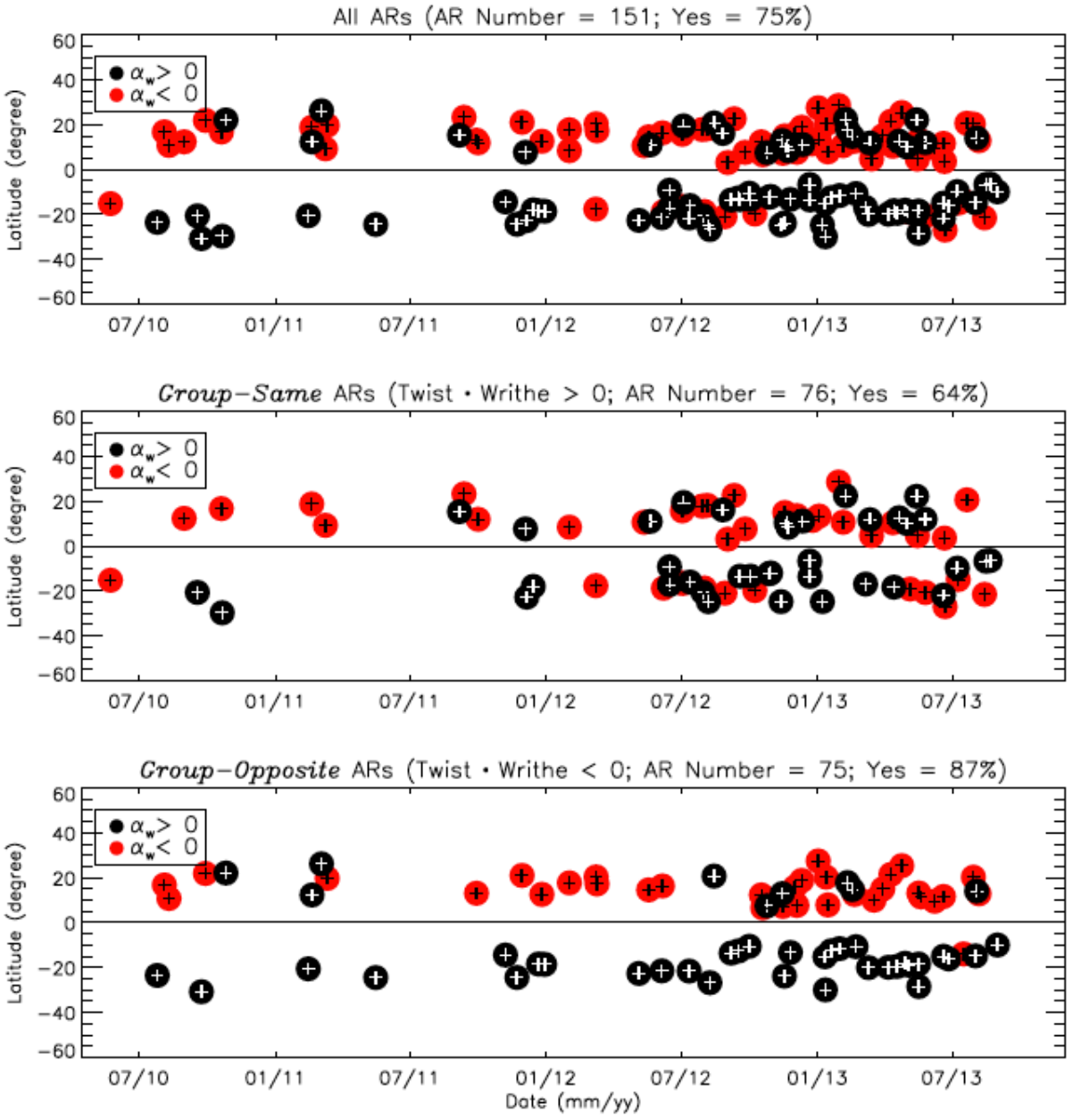

SDO/HMI Limitations for Polarimetry:

- Single-beam polarimetry
- Slow sequential measurement of polarization states
- Limited S/N
- Filter bandpass: 76 mÅ FWHM
- Only 5 samples of line + continuum
- Single-line observations
- Typical analysis: no compensation for magnetic fill fractors

Implications:

- Quiet Sun fields (especially transverse fields) out-of-reach
- High-precision polarimetry hampered by S/N, motion-induced crosstalk
- Accuracy of inferences compromised by limited spectral resolution and sampling
- 1 arcsec resolution insufficient for true high-resolution Studies

BUT:

- Active region vector field is well-represented by HMI data

Comparison: *SDO*/HMI and *Hinode* SOT/SP – Sainz Dalda et al. 2013

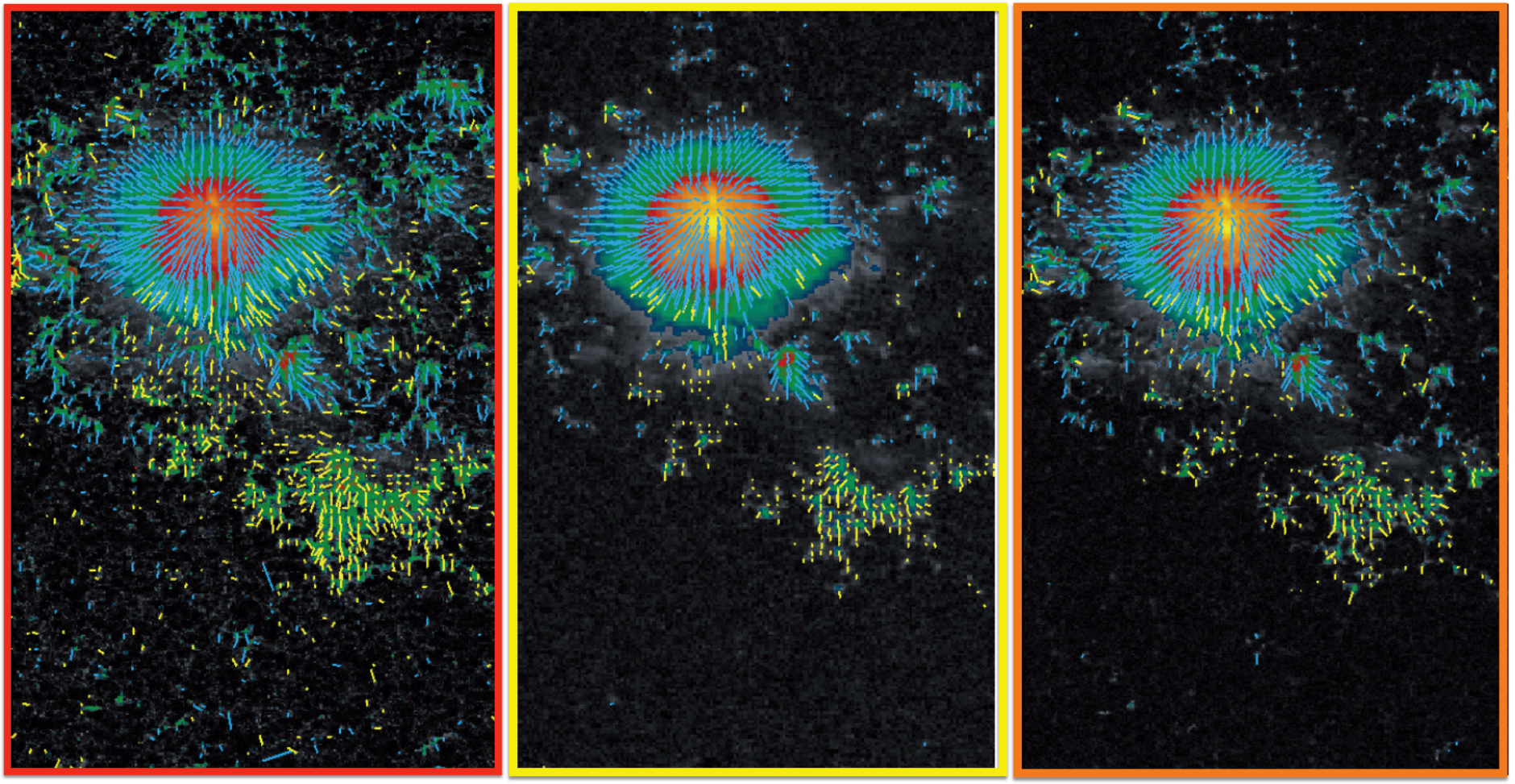

Hinode **SOT/SP** | ***SDO/*****HMI** | **HMI-like SOT/SP**

Comparison: *SDO*/HMI and *Hinode* SOT/SP – Sainz Dalda et al. 2013

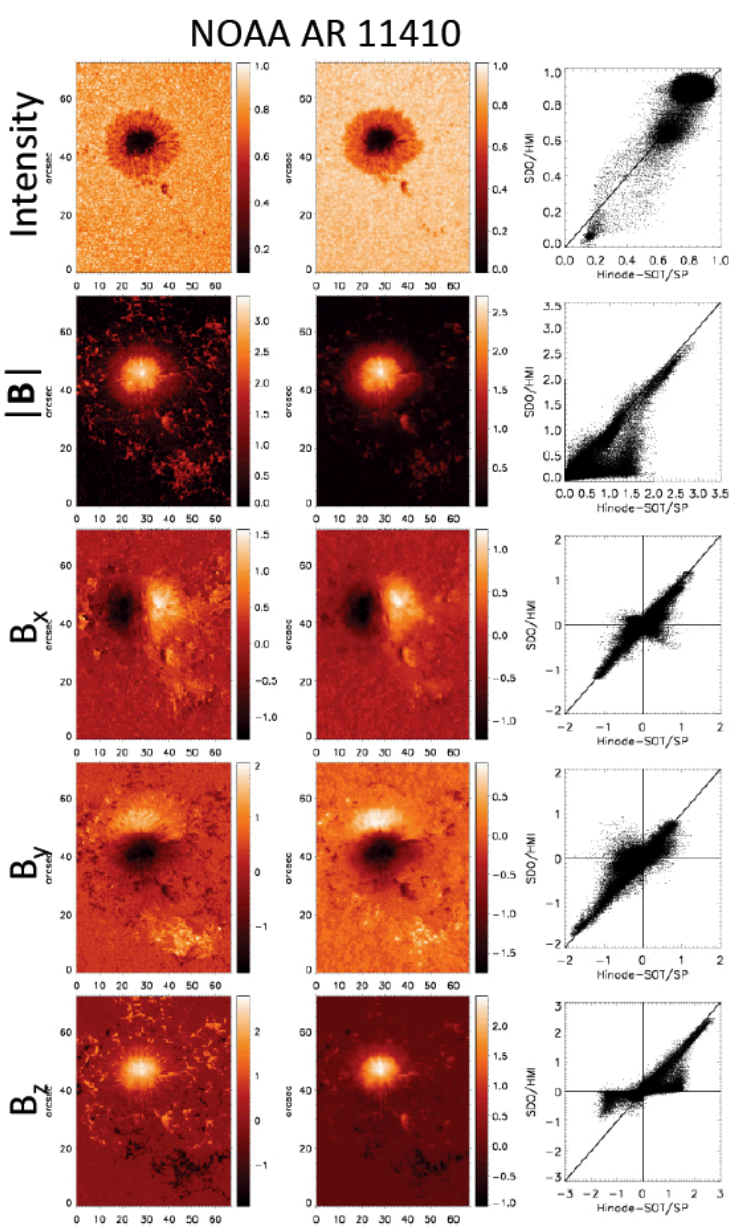

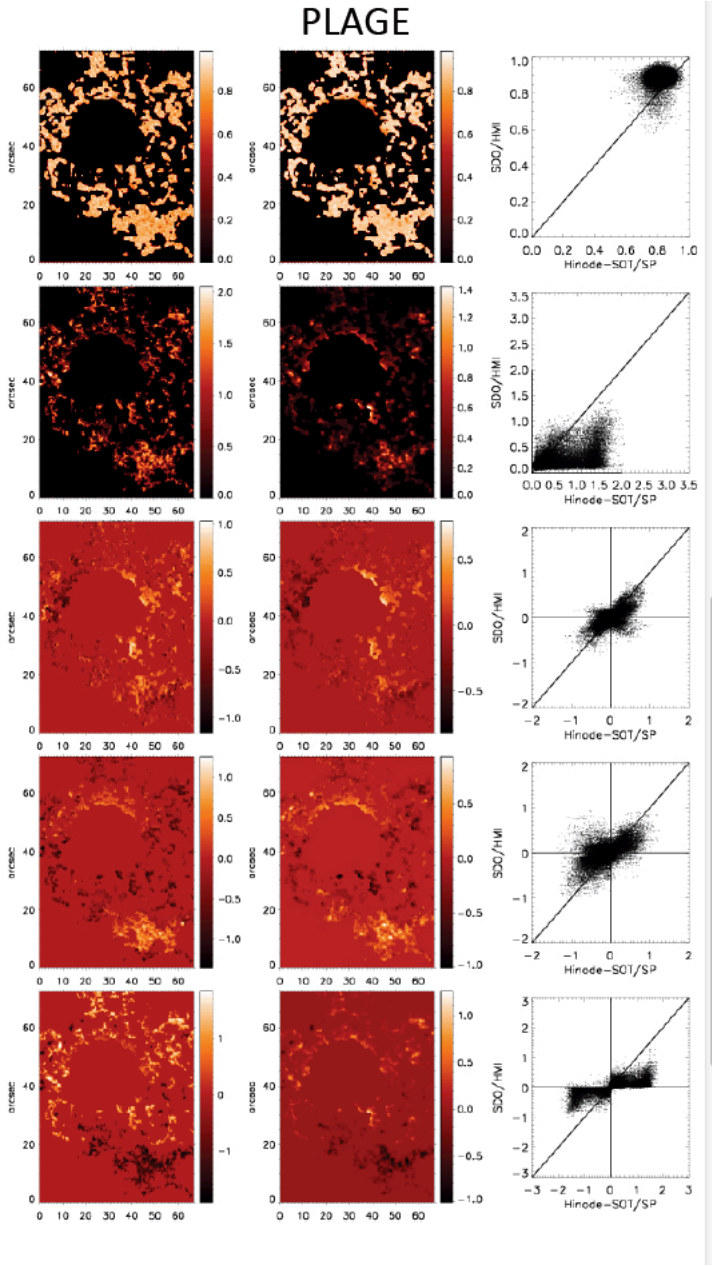

Entire AR

Plage Only

The Future of Space Measurements of Photospheric Magnetic Fields

Personal View: Frontier of solar magnetic field studies lies higher in the atmosphere – chromosphere and corona. Little is to be gained by additional space missions *ONLY* emphasizing photospheric field measurements.

Some aspects of photospheric magnetism not yet understood:

- **What is the distribution of field strength in the quiet internetwork?**

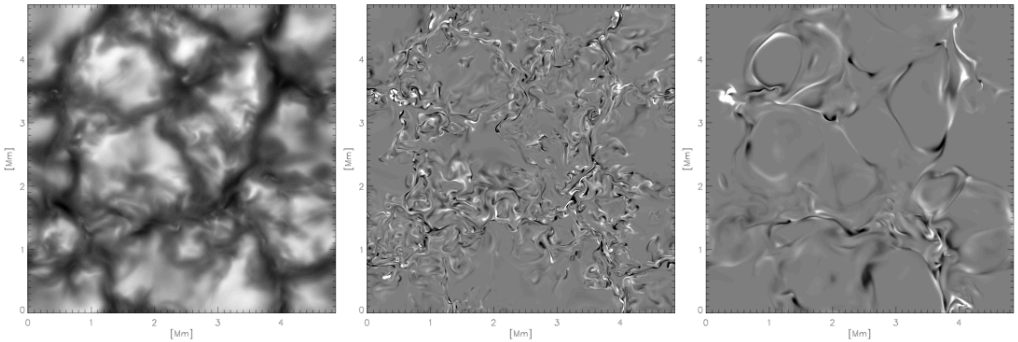

- **How (quantitatively) does the Sun remove active region fields from photosphere?**
- **What is the evolution and dynamics of the chromosphere and corona in response to changes of the field at and through the photosphere?**
- **Do the *Hinode* SOT/SP results accurately reflect the state of fields near the poles?**

Future Directions in Science

- **Highest angular resolution: use ground-based with adaptive optics**
  - **A/O capabilities improving**
  - **Large telescopes in space very expensive – is the science important enough to justify the cost?**
  - **May never fully resolve fine-scale structure of intergranular fields, even with interferometry, due to scattering within the photosphere**

- **Plenty still to learn about active region evolution, especially with respect to layers above the photosphere**
  - **Cotemporaneous observations almost necessitate space-based measurements**
  - ***SDO*/HMI, with *Hinode* SOT/SP, remain under-utilized for evolutionary studies of the magnetic field in active regions**
  - **Future missions will require access to high-resolution, precision measures of the field vector in the photosphere as data ancillary to studies of the upper atmosphere**

Simultaneous Vector Field Measurements in Chromosphere and Photosphere: Kuckein et al. 2012

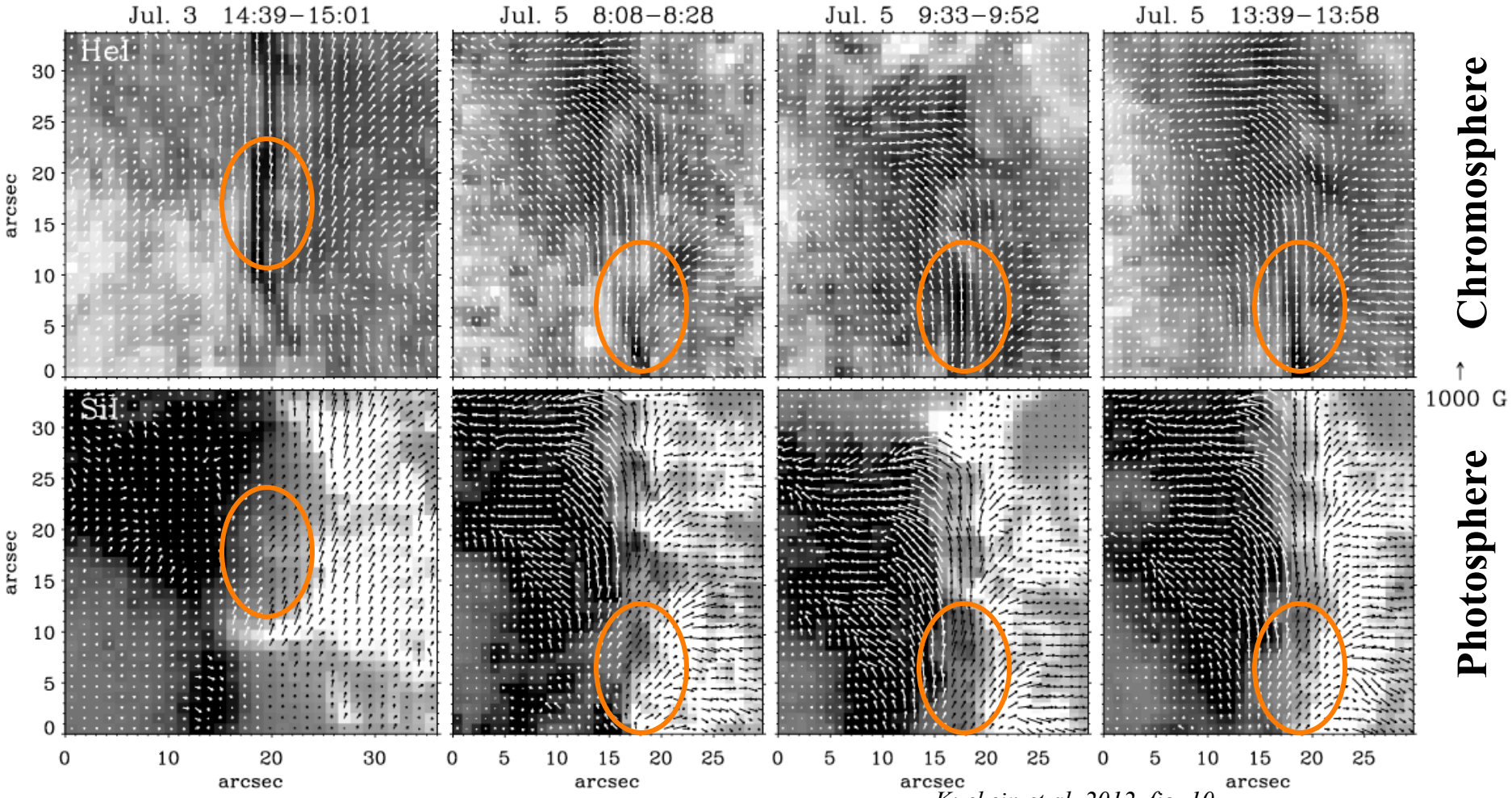

Kuckein et al. 2012, fig. 10

Planned and In-Development Space Missions to Measure Photospheric Fields

Solar Orbiter (In Development)

- Polarimetric and Helioseismic Imager (PHI) will observe polar fields at high resolution

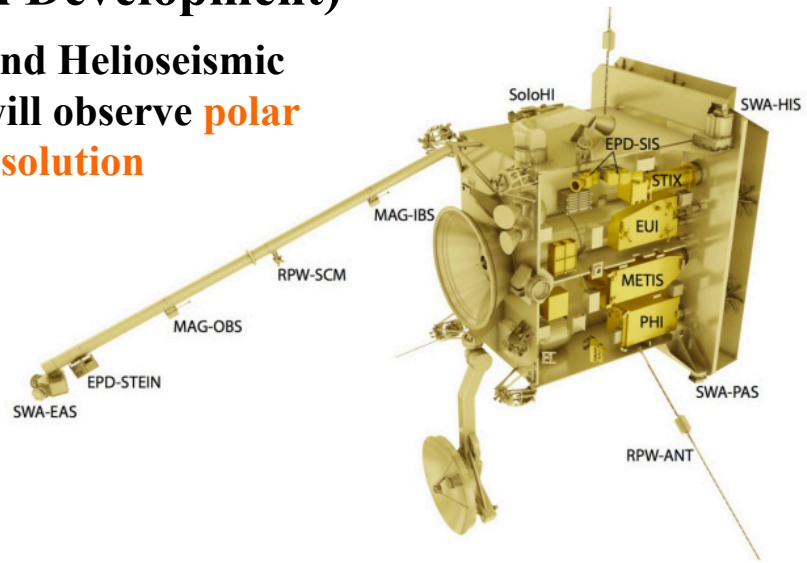

Solar-C (Proposed)

- Solar UV-IR-Visible Telescope (SUVIT) will accomplish photospheric field measurements to complement its prime objective of magnetism of the chromosphere and corona

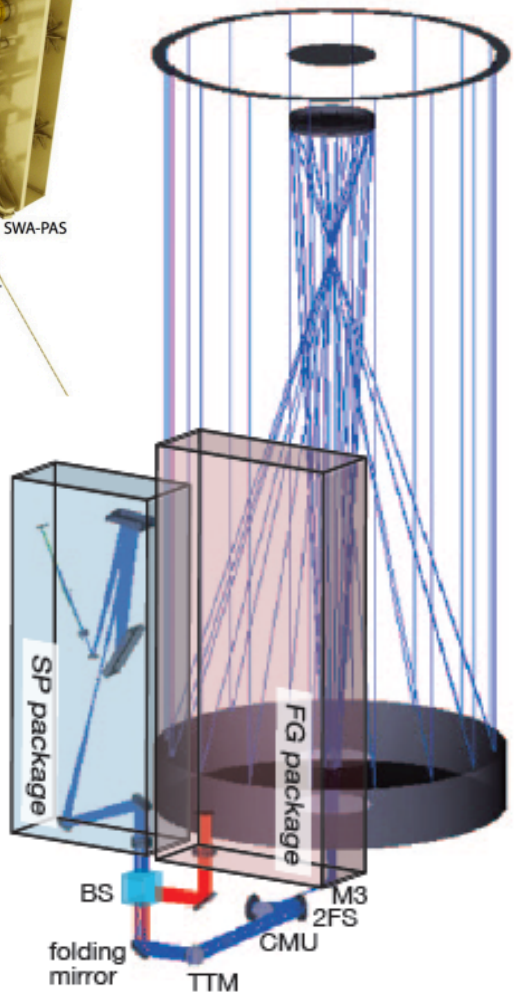

Beyond missions in the planning stage, what might future space instrumentation look like?

- **The ideal: some form of three-dimensional imaging [x,y,λ]**
  - **Retain simultaneity of spectral information for more than just a single slit position**
    - **Image slicers**
    - **Fiber optic spectrographs**
  - **Hybrid spectrographic/imaging devices blend spatial scanning and wavelength**
    - **TUNIS (Tunable Narrowband Universal Imaging Spectrograph, López Ariste et al. 2011)**
    - **Stereoscopic spectroscopy (DeForest 2004)**

Beyond missions in the planning stage, what might future space instrumentation look like?

- **Avoid image motion induced crosstalk: rapid modulation/demodulation**
  - **Rapid readout of detectors:**
    - **Readout rates of hundreds of Hz desirable**
    - **High readout rate at low noise requires lots of power, cooling**
    - **Large arrays ➔ many readout channels ➔ high power/cooling requirement**

Beyond missions in the planning stage, what might future space instrumentation look like?

- **Avoid image motion induced crosstalk: rapid modulation/demodulation**
  - **ZIMPOL (Zurich Imaging POLarimeter) method: shuffle charge horizontally on chip**

Beyond missions in the planning stage, what might future space instrumentation look like?

- **Avoid image motion induced crosstalk: rapid modulation/demodulation**
  - **ZIMPOL (Zurich Imaging POLarimeter) method: shuffle charge horizontally on chip**
  - **On-chip demodulation: shuffle charge wells vertically instead of horizontally**

Outlook

Current situation:

- Theoretical understanding of mechanisms for polarization is now in place
- Observational diagnostics are understood
  - Polarimetry in He I lines
  - Photospheric vector field measurements of filaments on disk
  - Ancillary intensity diagnostics
- Ground-based observational capability exists, but soon will be enhanced
  - TIP, GRIS at GREGOR on Tenerife for filaments,
  - ProMag for prominences
  - ViSP
- Data analysis tools are mature (pattern recognition techniques)
- Finally! Systematic maps of magnetic vector in prominences/filaments are being produced, but
- Not many systematic observations of prominence fields have yet been achieved

Needed Developments:

- More study of resolution of various ambiguities is needed
- *New instrumentation is needed to increase angular resolution, sensitivity*
  - Prominences: Large-aperture ground-based coronagraphs! (COSMO,….)
  - Large aperture ground-based solar telescopes! (NST, GREGOR, DKIST, EST….)
  - Solar-C!

Angular Resolution– 2: Tradeoff with Speed

- $S/N = \sigma^{-1} \sim F^{1/2}$
- Chromosphere demands somewhat lower spatial resolution, much quicker observations
- Significant difference in F at different wavelengths
- Large aperture telescopes (4m) will permit measurements of very small structures (0.07") at high speed (0.8 sec) for the chromosphere

Red pairs for chromospheric Alfvén speed

time scales vs. spatial resolution

- photosphere (blue): 7 km s^{-1}
- chromosphere (red): 35 km s^{-1}
  (v_A(B=100 G, z=1 Mm) = 100 km s^{-1})

Solutions

1. stay away from diffraction limit → collect photons
2. very fast measurements → "feature averaging"

(Note: solar evolution intrduces crosstalk in polarimetry → modulation much faster → FSP)

A. Feller, FSP

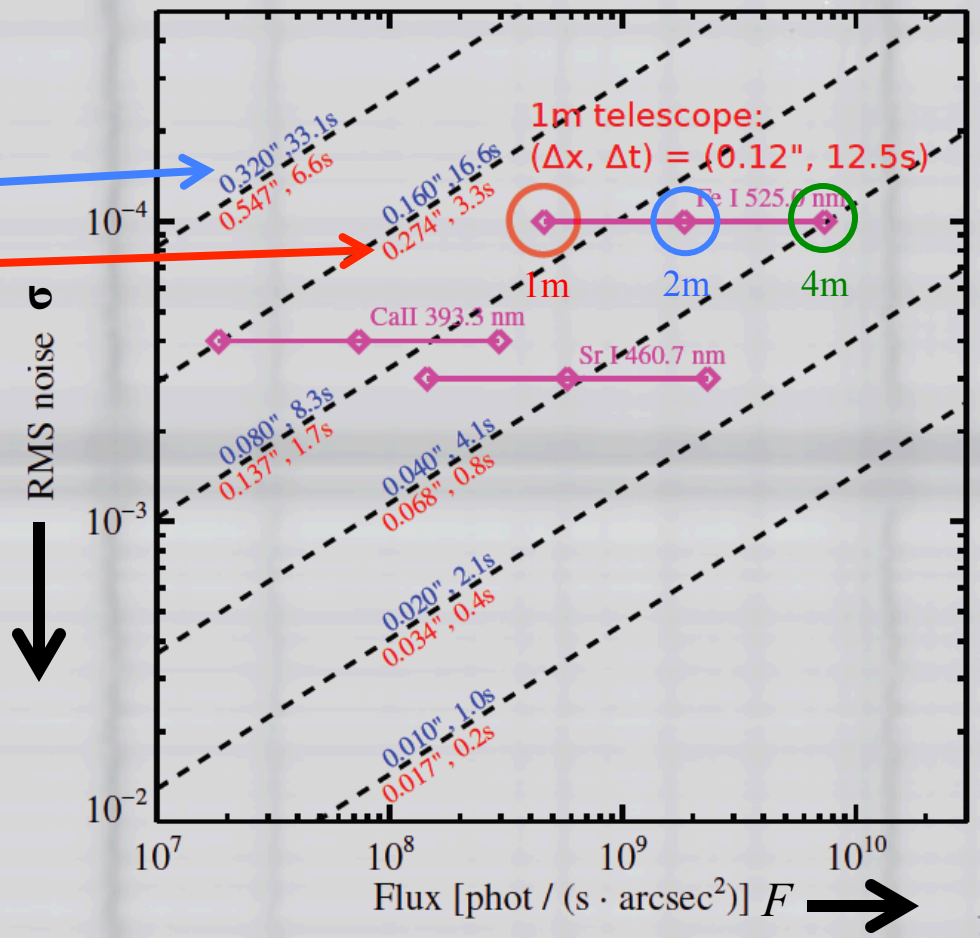

Illustration courtesy of A. Feller (MPS) via A. Lagg (MPS)